



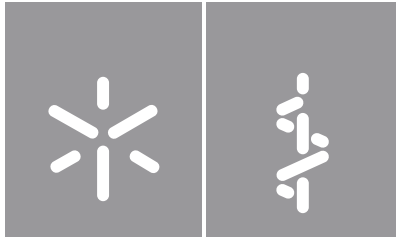
Inês Morais Mesquita

**Crosslinking Immunity and Metabolism  
during *Leishmania* Infection**

**Universidade do Minho**  
Escola de Medicina







Universidade do Minho  
Escola de Ciências da Saúde

Inês Morais Mesquita

## Crosslinking Immunity and Metabolism during *Leishmania* Infection

Tese de Doutoramento  
Doutoramento em Ciências da Saúde

Trabalho efectuado sob a orientação do  
**Doutor Ricardo Jorge Leal Silvestre**  
**e Professor Doutor António Gil Pereira Castro**

## DECLARAÇÃO

Nome: Inês Morais Mesquita

Endereço eletrónico: [id7024@alunos.uminho.pt](mailto:id7024@alunos.uminho.pt); [nesmesquita@gmail.com](mailto:nesmesquita@gmail.com)

Telefone: +351 963204190

Cartão de Cidadão: 13944933

### **Título da tese:**

Crosslinking Immunity and Metabolism during *Leishmania* Infection

### **Orientadores:**

Doutor Ricardo Jorge Leal Silvestre

Doutor António Gil Pereira Castro

Ano de conclusão: 2020

Designação do Doutoramento: Doutoramento em Ciências da Saúde

É AUTORIZADA A REPRODUÇÃO INTEGRAL DESTA TESE APENAS PARA EFEITOS DE INVESTIGAÇÃO, MEDIANTE DECLARAÇÃO ESCRITA DO INTERESSADO, QUE A TAL SE COMPROMETE

Universidade do Minho, 30 de Dezembro de 2020

Assinatura:

## AGRADECIMENTOS

Em primeiro lugar, quero agradecer ao meu orientador Ricardo. Obrigada por me teres acolhido desde o início, por me teres guiado e mostrado o que é a ciência e por todos estes (longos) anos. Foi um prazer aprender contigo e tenho a certeza de que levarei comigo tudo o que me ensinaste! Agradeço ao meu orientador, professor Gil, por ter acreditado que eu era a pessoa certa para começar um projecto novo. Obrigada pelas horas de discussão científica e pelo apoio ao longo deste caminho. To Jérôme, that was always there for me when I needed help and motivation. Thank you for accepting me as your student and for all the scientific input. Your contribution to my scientific career has been irreplaceable.

Agradeço aos MIRD, por me terem acolhido antes de ter iniciado o meu doutoramento. Em particular, gostaria de agradecer ao Fernando, à Belém, ao Agostinho e à Cristina, por toda a ajuda prestada neste período. Gostaria também de agradecer à Cláudia Nóbrega e à Alice Miranda pela ajuda e por terem estado presente quando precisei de ajuda. À Alex, Catarina, Margarida e João, por terem estado comigo desde o início, nos bons e nos maus momentos, e por toda a amizade que fomos construindo e que vou certamente levar comigo. À Carolina, que partilhou comigo esta viagem e que me acompanhou neste percurso, sempre com um sorriso e palavras de motivação.

Agradeço à Diana que sempre me acompanhou ao longo deste percurso e que tornou a ciência muito mais interessante e estimulante. Obrigada por me teres inspirado e teres contribuído para o que sou. Gostaria também de agradecer à Patocha e à Daniela, com quem iniciei a minha *vida* científica, e à Renata, por me ter inspirado a ser criativa durante a escrita desta tese.

À Belinha, que ao longo deste tempo todo foi um dos meus pilares e que sempre me deu uma amizade insubstituível, e à Joana e à Patrícia, que estiveram presentes e me mostraram que a amizade não pode ser medida em tempo. Aos meus tios, primos e à minha avó, que sempre compreenderam e apoiaram as minhas motivações (e ausências). Ao meu avô, que sempre acreditou em mim e que apesar de longe, esteve este tempo todo comigo.

Por fim, aos meus pais, que sempre acreditaram no que eu era e no que eu queria ser e que me apoiaram incondicionalmente ao longo deste tempo. Obrigada por me ajudarem a crescer, pessoalmente e profissionalmente, e por me terem amparado sempre que precisei. Ao Nuno, que partilhou comigo as minhas vitórias e as minhas derrotas. Obrigada por toda a dedicação e amor e por me ajudares a ultrapassar todas as dificuldades que fui encontrando. Vocês foram essenciais para eu conseguir completar esta etapa.

The work presented in this thesis was performed in the Life and Health Sciences Research Institute (ICVS), Minho University. Financial support was provided by grants from Foundation of Science and Technology (FCT) through the Individual Fellowship SFRH/BD/120127/2016, Infect-Era (project INLEISH), the European Society of Clinical Microbiology and Infectious Diseases (ESCMID Research Grant 2019) and the ICVS Scientific Microscopy Platform, member of the national infrastructure PPBI - Portuguese Platform of Bioimaging (PPBI-POCI-01-0145-FEDER-022122; by National funds, through the Foundation for Science and Technology (FCT) - project UIDB/50026/2020 and UIDP/50026/2020; and by the projects NORTE-01-0145-FEDER-000013 and NORTE-01-0145-FEDER-000023, supported by Norte Portugal Regional Operational Programme (NORTE 2020), under the PORTUGAL 2020 Partnership Agreement, through the European Regional Development Fund (ERDF).



The work presented in this dissertation was developed at:

Microbiology and Infection Research Domain,  
Life and Health Sciences Research Institute (ICVS), School of Medicine, University of Minho,  
Braga, Portugal



Universidade do Minho  
Escola de Medicina

## STATEMENT OF INTEGRITY

I hereby declare having conducted my thesis with integrity. I confirm that I have not used plagiarism or any form of falsification of results in the process of the thesis elaboration.

I further declare that I have fully acknowledged the Code of Ethical Conduct of the University of Minho.

University of Minho, December 30th, 2020

Full name: Inês Morais Mesquita

Signature:

## RESUMO

### Estudo da interação entre imunidade e metabolismo durante infecção por *Leishmania*

As escolhas metabólicas condicionam a função das células imunes e o decorrer da infecção. Os agentes patogênicos evoluíram com os hospedeiros, desenvolvendo estratégias para aumentar a sobrevivência através do bloqueio das capacidades microbicidas do hospedeiro: através do sequestro do metabolismo do hospedeiro e controlo da polarização de células imunes.

Observou-se que na ausência do fator HIF-1 $\alpha$  ocorria um aumento da lipogénese em células mielóides infetadas com *Leishmania donovani*, através do eixo BNIP3/mTOR/SREBP-1c, que levou a um aumento de suscetibilidade a estes parasitas. A perda de função decorrente do polimorfismo no gene *HIF1A* recapitulou as observações anteriores, uma vez que macrófagos de indivíduos com o genótipo CT/TT acumularam mais lípidos e revelaram-se mais suscetíveis. Esta suscetibilidade foi revertida através do bloqueio da lipogénese, realçando a importância da acumulação de lípidos para a infecção. A susceptibilidade de ratinhos mHIF-1 $\alpha$ <sup>-/-</sup> cronicamente infetados deriva da exaustão de linfócitos T. Observou-se um aumento de expressão do recetor TIM-3 em linfócitos T no baço de ratinhos mHIF-1 $\alpha$ <sup>-/-</sup> infetados, assim como perda da produção de citocinas efetoras. Observou-se, igualmente, um aumento do número de células mielóides produtoras de IL-10, sugerindo que um ambiente imunossupressor poderá contribuir para a exaustão de células T. Estes resultados sugerem que abordagens imunoterapêuticas poderão revitalizar os linfócitos T durante a cronicidade e contribuir para a eliminação do parasita. Uma vez a IL-10 foi associada a imunossupressão, decidiu-se estudar o impacto desta citocina em diferentes etapas da infecção. Induziu-se a expressão de IL-10 na etapa inicial e tardia de infecção por *L. donovani*, usando ratinhos pMT-10. Observou-se que a expressão de IL-10 nas etapas iniciais culminaram num aumento da carga parasitária no baço e fígado, assim como na perda de linfócitos T multifuncionais e diminuição do ratio IFN- $\gamma$ /IL-10, indicativo de menor proteção contra a infecção. Finalmente, foi proposto dissecar o papel do tecido adiposo branco como reservatório de *L. donovani*. Estes resultados demonstram que os parasitas são capazes de acumular no tecido adiposo branco, especialmente em ratinhos com excesso de peso, sugerindo um novo reservatório que pode alterar a resposta do hospedeiro às terapias antiparasíticas.

Este trabalho realça a importância das redes imunometabólicas durante a infecção, enfatizando a complexidade das interações patógeno-hospedeiro. Estudando esta interface dinâmica, demonstrou-se como este conhecimento pode ajudar a desenvolver novas terapias.

Palavras-chave: *Leishmania*; Imunometabolismo; Macrófagos; interação hospedeiro-patógeno



## ABSTRACT

### Crosslinking immunity and metabolism during *Leishmania* infection

It is now accepted that metabolic choices condition immune cell function and the outcome of infection. Pathogens have evolved closely with their hosts, thus developing strategies to optimize and enhance their survival by hindering host's microbicidal capacity. Pathogens actively hijack host metabolism to fulfill their bioenergetic and biosynthetic needs and control immune cell polarization.

We showed that genetic deficiency of HIF-1 $\alpha$  increased lipogenesis in *Leishmania donovani*-infected myeloid cells through the BNIP3/mTOR/SREBP-1c axis, which contributed to increased susceptibility, both *in vitro* and *in vivo*. A loss-of-function SNP in the human *HIF1A* gene recapitulated previous findings, as macrophages from individuals with the CT/TT genotype accumulated more lipids and were more susceptible to infection. This susceptibility was reversed through blockade of lipogenesis, highlighting the importance of lipid accumulation during infection. During chronicity, myeloid-restricted HIF-1 $\alpha$ <sup>-/-</sup> mice (mHIF-1 $\alpha$ <sup>-/-</sup>) susceptibility associated with T cell exhaustion. We found increased expression of TIM-3 in T cells from the spleen of infected mHIF-1 $\alpha$ <sup>-/-</sup> mice, as well as loss of effector cytokine production. Higher levels of IL-10-producing myeloid cells were also found, suggesting an immunosuppressive environment that may contribute to T cell exhaustion. This suggests that immunotherapeutic approaches may reinvigorate T cells during chronic infection and contribute to pathogen clearance. As IL-10 has been vastly associated to immunosuppression, we sought to study its impact in different stages of *Leishmania* infection. We induced IL-10 overexpression both at early and late stages of *L. donovani* infection, using the pMT-10 mouse model. IL-10 overexpression early after infection increased parasite burden in both the spleen and liver and led to loss of multifunctional CD4 T cells and decreased IFN- $\gamma$ /IL-10 ratios, indicative of lower protection against infection. Finally, we proposed to dissect the role of white adipose tissue as a reservoir during leishmaniasis, as we showed that lipid-rich environments are permissive niches. Our data demonstrates that these parasites are capable of accumulating in the white adipose tissue. This was particularly evident in overweighted mice, suggesting the existence of a new, undiscovered reservoir that can alter host response to antileishmanial therapies.

The work here presented highlights the importance of the immunometabolic network during *Leishmania* infection, while emphasizing the complexity inherent to host-pathogen interactions. By tackling different cornerstones of this dynamic interface, we demonstrated how this knowledge can be translated into the development of innovative antileishmanial therapies.

**Keywords:** *Leishmania*; Immunometabolism; Macrophages; Host-pathogen interaction.

## TABLE OF CONTENTS

RESUMO .....	V
ABSTRACT .....	VI
LIST OF FIGURES .....	IX
LIST OF ABBREVIATIONS.....	X
<b>CHAPTER I    CROSSLINKING IMMUNITY AND METABOLISM.....</b>	<b>1</b>
<b>1.    Cellular metabolism at a glance– an overview of metabolic pathways.....</b>	<b>2</b>
1.1    Glycolysis and the Pentose Phosphate Pathway.....	4
1.2    The Tricarboxilic Acid Cycle and Oxidative Phosphorylation.....	4
1.3    Fatty acids: synthesis and metabolism .....	5
1.3.1    Fatty acid synthesis .....	6
1.3.2    Fatty acid oxidation.....	7
1.4    Amino acid metabolism and function .....	8
<b>2.    Regulation of cell metabolism: the role of metabolic sensors.....</b>	<b>9</b>
2.1    mTOR – an amino acid sensor that regulates whole-cell metabolism .....	10
2.2    HIF-1 $\alpha$ – the impact of oxygen sensing in cell metabolism .....	11
2.3    AMPK – an energy sensor for cellular homeostasis .....	12
<b>3.    Immunometabolism – metabolism as a unique driver of immunity.....</b>	<b>13</b>
3.1    Innate immune cells.....	13
3.1.1    Macrophages .....	13
3.1.2    Dendritic cells .....	16
3.1.3    Neutrophils .....	17
3.2    Adaptive immune cells.....	18
3.2.1    T cells.....	18
3.2.1.1    Metabolic regulation of T cell exhaustion .....	18
<b>CHAPTER II    THE INTRICATE RELATION BETWEEN <i>LEISHMANIA</i> PARASITES AND HOST ...</b>	<b>21</b>
<b>1.    <i>Leishmania</i> parasites – the etiological agents of leishmaniasis.....</b>	<b>22</b>
1.1 <i>Leishmania</i> life cycle .....	22
1.2    Leishmaniasis – a neglected tropical disease .....	23
<b>2.    Treatment for visceral leishmaniasis.....</b>	<b>24</b>

3.	<i>Leishmania</i> biology and metabolism.....	25
4.	Parasite-host interaction.....	26
4.1	Immune response on VL.....	27
4.1.1	Impact of T cell exhaustion on leishmaniasis.....	30
4.2	Nutritional microenvironment during infection .....	31
4.3	Adipose tissue: an (un)expected reservoir? .....	35
<b>CHAPTER III AIMS AND RESULTS .....</b>		<b>39</b>
<b>AIMS .....</b>		<b>40</b>
<b>RESULTS.....</b>		<b>43</b>
	The Absence of HIF-1 $\alpha$ Increases Susceptibility to <i>Leishmania donovani</i> Infection via Activation of BNIP3/mTOR/SREBP-1c Axis.....	43
	Defective anti- <i>Leishmania</i> T cell effector response in the absence of myeloid HIF-1 $\alpha$ .....	81
	The impact of IL-10 dynamic modulation on host immune response against visceral leishmaniasis .....	93
	Feeding immunity: development of new nutraceuticals for visceral leishmaniasis .....	101
<b>CHAPTER IV DISCUSSION .....</b>		<b>111</b>
1.	<b>Parasite-host immunometabolic crosstalk: how lipids condition the biology of <i>Leishmania</i> infection .....</b>	<b>112</b>
1.1	HIF-1 $\alpha$ mediates cellular reprogramming of lipid metabolism .....	112
1.2	Intracellular lipids as major hubs in <i>Leishmania</i> -host interaction .....	113
1.3	Targeting lipids: new avenues in antileishmanial therapy? .....	114
1.4	Immunometabolic-related gene polymorphisms in <i>Leishmania</i> infection.....	116
2.	<b>Adaptive immunity during <i>Leishmania</i> infection: Prospects for immunotherapy .....</b>	<b>118</b>
2.1	Immune cells and associated mediators during antileishmanial T cell responses.....	118
2.2	Immunotherapy in the treatment of leishmaniasis .....	120
3.	<b>The adipose tissue as a reservoir for <i>Leishmania</i> parasites .....</b>	<b>122</b>
4.	<b>Concluding remarks.....</b>	<b>124</b>
<b>CHAPTER V FUTURE PERSPECTIVES.....</b>		<b>125</b>
<b>REFERENCES 129</b>		

## LIST OF FIGURES

<b>Figure 1</b> Cellular Metabolic Pathways At a Glance.....	3
<b>Figure 2</b> Lipid metabolism pathways.....	6
<b>Figure 3</b> Metabolic Sensors and Related Pathways. ....	9
<b>Figure 4</b> Macrophage Polarization: Metabolism and Function.....	16
<b>Figure 5</b> Causes and consequences of T cell exhaustion.....	20
<b>Figure 6</b> <i>Leishmania</i> life cycle and visceral immune response. ....	23
<b>Figure 7</b> Immunotherapy for <i>Leishmania</i> infection.....	31
<b>Figure 8</b> The impact of lipid-rich environments in <i>Leishmania</i> infection. ....	35
<b>Figure 9</b> The Adipose Tissue as a Reservoir of <i>Leishmania</i> Parasites. ....	37

## LIST OF ABBREVIATIONS

<b>2-DG</b>	2-deoxyglucose
<b>ACC</b>	Acetyl-Coenzyme A Carboxylase
<b>ADP</b>	Adenosine Diphosphate
<b>ALT</b>	Alanine Aminotransferase
<b>AMP</b>	Adenosine Monophosphate
<b>AMPK</b>	AMP-activated Protein Kinase
<b>APC</b>	Antigen Presenting Cell
<b>ARNT</b>	Aryl Hydrocarbon Receptor Nuclear Translocator
<b>AST</b>	Aspartate Aminotransferase
<b>ATM</b>	Adipose Tissue Macrophage
<b>ATP</b>	Adenosine Triphosphate
<b>BCAA</b>	Branched Chain Amino Acids
<b>BMDC</b>	Bone Marrow-Derived Dendritic Cells
<b>BNIP3</b>	BCL2/Adenovirus E1B 19 kDa Protein-Interacting Protein 3
<b>CAMKK<math>\beta</math></b>	Calcium/Calmodulin-Dependent Protein Kinase Kinase 2
<b>cDC</b>	Conventional Dendritic Cell
<b>CL</b>	Cutaneous Leishmaniasis
<b>CoA</b>	Coenzyme A
<b>CPT</b>	Carnitine Palmitoyltransferase
<b>CTLA-4</b>	Cytotoxic T-Lymphocyte-Associated Protein 4
<b>DC</b>	Dendritic Cell
<b>ER</b>	Endoplasmic Reticulum
<b>ETC</b>	Electron Transport Chain
<b>FA</b>	Fatty acid
<b>FAD</b>	Flavin Adenine Dinucleotide
<b>FAO</b>	Fatty Acid $\beta$ -Oxidation
<b>FASN</b>	Fatty Acid Synthase
<b>FAS</b>	Fatty Acid Synthesis
<b>FLT3L</b>	FMS-Like Tyrosine Kinase 3 Ligand
<b>G6PD</b>	Glucose-6-Phosphate Dehydrogenase
<b>GM-CSF</b>	Granulocyte-Macrophage Colony-Stimulating Factor

<b>GTP</b>	Guanosine Triphosphate
<b>HBV</b>	Hepatitis B Virus
<b>HFD</b>	High Fat Diet
<b>HIF-1<math>\alpha</math></b>	Hypoxia-Inducible Factor 1 Alpha
<b>HIG2</b>	Hypoxia-Inducible Protein 2
<b>HK</b>	Hexokinase
<b>HMG</b>	3-hydroxy-3-methylglutaryl
<b>HSL</b>	Hormone-Sensitive Lipase
<b>IDO</b>	Indoleamine 2,3-Dioxygenase
<b>IFN-<math>\gamma</math></b>	Interferon gamma
<b>IL</b>	Interleukin
<b>iNOS</b>	Inducible Nitric Oxide Synthase
<b>LAG3</b>	Lymphocyte-Activation Gene 3
<b>LCMV</b>	Lymphocytic Choriomeningitis Virus
<b>LD</b>	Lipid Droplet
<b>LKB1</b>	Liver Kinase B1
<b>LPG</b>	Lipophosphoglycan
<b>LPS</b>	Lipopolysaccharide
<b>LysM</b>	Lysozyme M
<b>M-CSF</b>	Macrophage Colony-Stimulating Factor
<b>MCL</b>	Mucocutaneous Leishmaniasis
<b>MHC</b>	Major Histocompatibility Complex
<b>moDC</b>	Monocytic Dendritic Cell
<b>mTOR</b>	Mammalian Target of Rapamycin
<b>NAD</b>	Nicotinamide Adenine Dinucleotide
<b>NADP</b>	Nicotinamide Adenine Dinucleotide Phosphate
<b>NET</b>	Neutrophil Extracellular Traps
<b>NF-KB</b>	Nuclear Factor Kappa-light-chain-enhancer of Activated B cells
<b>NO</b>	Nitric Oxide
<b>NOX</b>	NADPH Oxidase
<b>NPC1</b>	Niemann–Pick C1 protein
<b>OXPHOS</b>	Oxidative Phosphorylation

<b>PBMC</b>	Peripheral Blood Mononuclear Cell
<b>PD-1</b>	Programmed Cell Death Protein 1
<b>PD-L1</b>	Programmed Death Ligand 1
<b>pDC</b>	Plasmacytoid Dendritic Cell
<b>PDH</b>	Pyruvate Dehydrogenase
<b>PDK1</b>	Pyruvate Dehydrogenase Kinase 1
<b>PG</b>	Prostaglandin
<b>PGC-1<math>\alpha</math></b>	Peroxisome Proliferator-Activated Receptor-gamma Coactivator 1 alpha
<b>PKDL</b>	Post-Kala-azar Dermal Leishmaniasis
<b>PMN</b>	Polimorphonuclear
<b>PPP</b>	Pentose Phosphate Pathway
<b>PV</b>	Parasitophorous Vacuole
<b>REDD1</b>	Regulated in Development and DNA damage Responses 1
<b>ROS</b>	Reactive Oxygen Species
<b>S6K</b>	Ribosomal Protein S6 Kinase
<b>SFD</b>	Standard Fat Diet
<b>SIRT</b>	Sirtuin
<b>SNP</b>	Single Nucleotide Polymorphism
<b>SREBP-1</b>	Sterol Regulatory-Element Binding Proteins
<b>SVF</b>	Stromal Vascular Fraction
<b>TCA</b>	Tricarboxilic Acid Cycle
<b>Tex</b>	Exhausted T cell
<b>TGF</b>	Transforming Growth Factor
<b>Th</b>	T helper
<b>TIM-3</b>	T-cell immunoglobulin mucin-3
<b>TLR</b>	Toll-Like Receptor
<b>TNF</b>	Tumor Necrosis Factor
<b>UCP</b>	Uncoupling Protein
<b>VEGF-A</b>	Vascular Endothelial Growth Factor
<b>VL</b>	Visceral Leishmaniasis
<b>WAT</b>	White Adipose Tissue
<b>WT</b>	Wild type

# CHAPTER I      CROSSLINKING IMMUNITY AND METABOLISM



The overall function of our immune systems is to protect us against internal and external threats, regardless of whether these are vicious pathogens or aggressive tumors. When this complex and intricate system is activated, it aims at eliminating all possible threats to homeostasis and health, in order to prevent pathology and disease progression. The immune system is broadly divided (but not compartmentalized) in two interactive sections, the innate and the adaptive immune systems. Briefly, innate immunity is a fast, immediate response led by innate immune cells (as monocytes/macrophages, dendritic cells, neutrophils, natural killer cells and innate lymphoid cells) and several associated molecules (as cytokines, chemokines, the complement system and others). Although it has initially been thought to be unspecific, this paradigm has been recently challenged. The concept of trained immunity arose from studies showing that both epigenetic and metabolism play a crucial role in the development of innate immune memory (Cheng et al., 2014; Netea et al., 2016). The adaptive immune response consists in the production of antigen-specific reactions that involve both B and T lymphocytes, which clonally expand upon activation. It generally takes place a few days after the initial challenge (upon antigen processing and presentation by innate cells) and has been characterized by antigen specificity and establishment of memory.

In the past decades, technological advances have helped us to achieve a greater understanding on how cellular bioenergetic status dictate function, as well as the contribution of specific metabolites and distinct metabolic fluxes to the development of an effector response. As such, the complexity of the immune response became even greater and, simultaneously, increasingly interesting due to the relentless identification of new players. In this section, we will obtain an overview of cellular metabolism and acknowledge the importance of distinct metabolic pathways/metabolites for immune cells function.

### **1. Cellular metabolism at a glance– an overview of metabolic pathways**

Metabolism is a highly coordinated component of the cellular activity that involves sequential chemical transformations, within a so-called metabolic network. This allows the acquisition of energy and biosynthetic precursors to maintain cellular homeostasis and function (Mesquita and Rodrigues, 2018). In recent years, we have appreciated a rediscovery of metabolism through the identification of metabolic intermediaries that act as key players on differentiation, proliferation, and function of immune cells. This recent acknowledgement of the impact of

metabolism in the overall immune response originated the groundbreaking field of immunometabolism, which will be addressed further on.

Metabolism relies on energy interconversion within the adenylate system, composed by adenosine triphosphate, diphosphate and monophosphate (ATP, ADP and AMP, respectively), and/or oxidation–reduction reactions where electrons are transiently stored within the nicotinamide adenine dinucleotide (NAD), flavin adenine dinucleotide (FAD) systems and nicotinamide adenine dinucleotide phosphate (NADP). A schematic representation of cellular metabolic pathways is presented in figure 1.

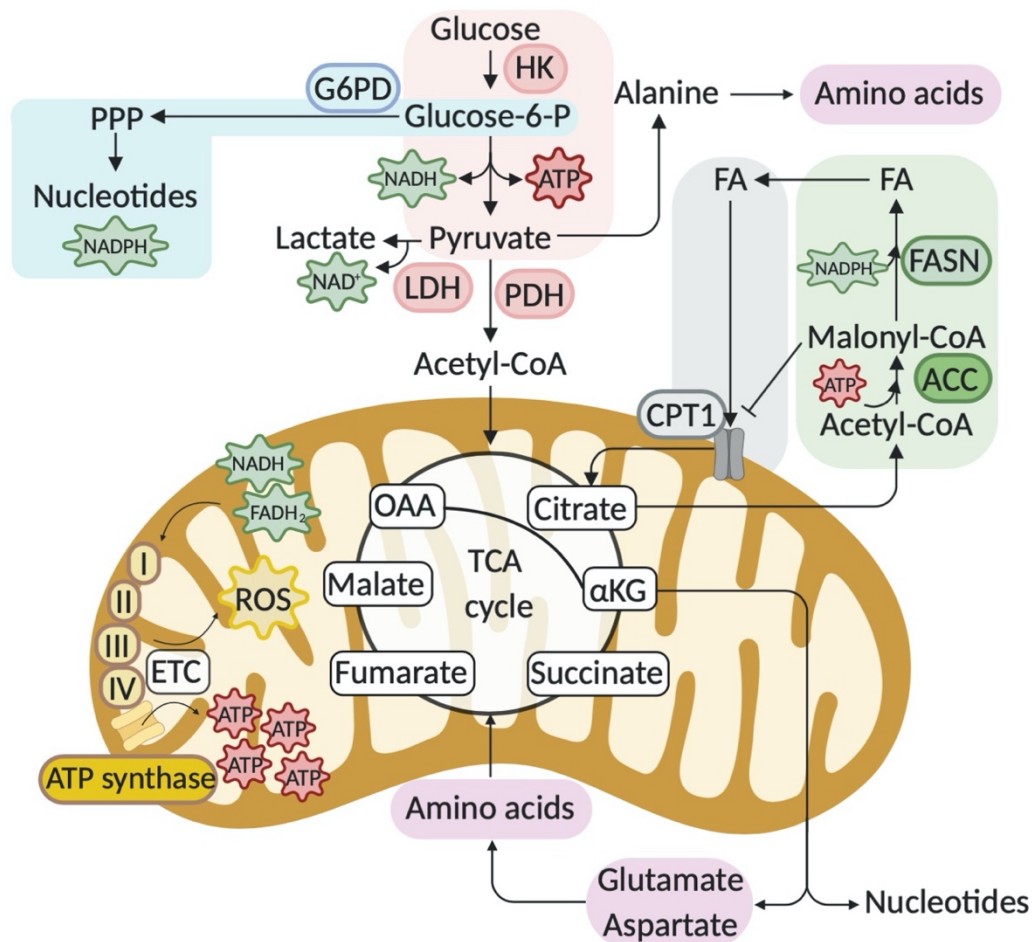


**Figure 1. Cellular Metabolic Pathways At a Glance.** Glycolysis (red) initiates with the conversion of glucose in glucose-6-P by HK. Through a series of reactions, glucose-6-P is converted in pyruvate and free energy is released in the form of NADH and ATP. The PPP (blue) branches from glucose-6-P through the initial action of G6PD. This pathway is important for nucleotide and NADPH synthesis. Pyruvate may be fermented in lactate through LDH and, in this reaction, NAD<sup>+</sup> is regenerated. Pyruvate may also be converted in alanine, providing a direct link between carbohydrate and amino acid metabolism. Finally, PDH may catalyse the irreversible decarboxylation of pyruvate in acetyl-CoA, which may then enter the mitochondria. In the TCA cycle, organic carbon fuels are either completely oxidized to H<sub>2</sub>O and CO<sub>2</sub> or extracted for macromolecule biosynthesis. For example, αKG and oxaloacetate may be extracted to yield glutamate and aspartate (to synthesize other amino acids) or to build nucleotides. During this cycle, NADH and FADH<sub>2</sub> are produced and used as substrates for the ETC (yellow). In here, an electrochemical proton gradient is created along the internal mitochondrial membrane, which is further used for ATP production in ATP synthase and also leads to ROS production. Citrate may be extracted from the TCA cycle to fuel FAS (green), which leads to carboxylation of acetyl-CoA into malonyl-CoA at the expense of ATP, via ACC. Further steps catalysed by FASN culminate in FA production. These FA can be uptaken by the mitochondria (through CPT1 if their length is 14-20 carbons) and further oxidized by FAO (grey). Amino acids (pink) may fuel the TCA cycle. Created with BioRender. Adapted from Buck, 2015.

### 1.1 Glycolysis and the Pentose Phosphate Pathway

Glycolysis was the first identified and better studied metabolic pathway. In this process, present in the cytosol of every cell, one molecule of glucose is enzymatically broken in two molecules of pyruvate, with the release of two molecules of ATP and two NADH. The cellular rate for glucose metabolism depends mainly on the major cellular metabolic fluxes, as cellular requirement for ATP or building blocks for anabolism.

Glycolysis is tightly regulated by specific players, namely by hexokinase (HK) that regulates the initial phosphorylation of glucose in glucose-6-phosphate and pyruvate kinase that converts phosphoenolpyruvate in the end-product pyruvate. The pentose phosphate pathway (PPP), which branches from the production of glucose-6-phosphate, is a major glycolytic-divergent pathway that produces precursors for nucleotide and amino acid synthesis as well as the reducing co-factor NADPH (Berg et al., 2002). NADPH is a cofactor for the biosynthesis of fatty acids and sterols and has a vital role in countering oxidative stress. Pyruvate may then be further metabolized via two major catabolic pathways: it is either oxidized in the mitochondria, thus yielding acetyl-Coenzyme A (CoA) to sustain the Tricarboxylic Acid (TCA) cycle or fermented in lactate with consequent replenishment of NAD<sup>+</sup> pool. This latter has been initially identified as the Warburg Effect, in which glucose is fermented in lactate in normoxic conditions (Potter et al., 2016). This phenomenon has been coined by Otto Warburg, as he observed that cancer cells displayed a unique metabolism, characterized by glucose fermentation in the presence of oxygen.

### 1.2 The Tricarboxylic Acid Cycle and Oxidative Phosphorylation

The TCA cycle is the universal aerobic pathway that occurs in the mitochondrial matrix. It is an amphibolic pathway used for the complete oxidation of several macromolecules, including glucose, fatty acids, and some amino acid (Akram, 2014; Kornberg, 2000), as well as the production of building blocks for macromolecule synthesis.

Briefly, macromolecules are oxidized to acetyl-CoA, which feeds the TCA cycle and releases energy in the form of NADH, FADH<sub>2</sub> and guanosine triphosphate (GTP). However, biosynthetic precursors may be withdrawn from the TCA cycle (cataplerosis) at the cost of reduction of the oxidative capacity. For instance, oxaloacetate and  $\alpha$ -ketoglutarate may contribute for aspartate and glutamate synthesis, as well as the synthesis of pyrimidines and purines (Lane and Fan, 2015),

while citrate has an important role in fatty acid synthesis (Williams and O'Neill, 2018). The high-energy reduced molecules that are released from the TCA cycle are used as substrates for the electron transport chain (ETC), which culminates with the reduction of molecular oxygen to H<sub>2</sub>O. A proton gradient is established along the internal mitochondrial membrane, allowing for ATP production via ATP synthase.

### 1.3 Fatty acids: synthesis and metabolism

Fatty acids (FA) are composed of long hydrocarbon chains and a terminal carboxylate group. These macromolecules have three major biological roles: (a) phospholipids and glycolipid synthesis, which compose cellular membranes; (b) posttranslational modifications of proteins, as lipoproteins; and (c) synthesis of neutral lipids (as triglycerides) for energy storage, mostly within lipid droplets (LDs). An overview of the anabolic and catabolic metabolism of fatty acids is presented on figure 2.

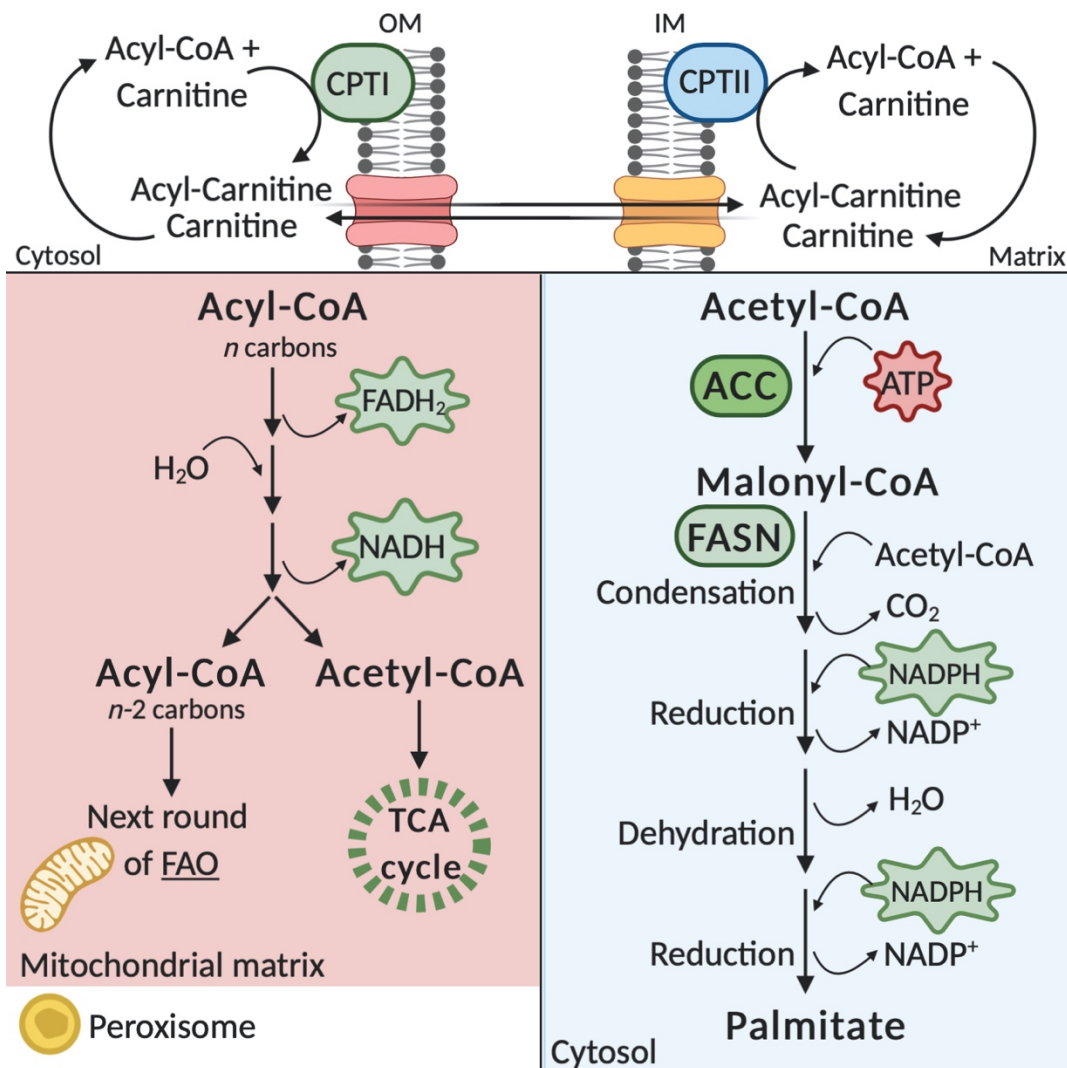


**Figure 2 Lipid metabolism pathways.** Depending on the size of the fatty acid, carnitine shuttles may be required for transport into the mitochondria. Long and branched-chain fatty acids may suffer peroxisomal FAO. After activation (attachment of carnitine to acyl-CoA molecule) by CPTI on the outer membrane (OM), the acylcarnitine is transported into the mitochondria by a translocase. Once inside the matrix, CPTII on the inner membrane (IM) releases the carnitine for recycling and the acyl-CoA for further FAO (red). Briefly, in each round of FAO, the acyl-CoA is shortened by two carbons, in a 4-step reaction that produces  $\text{FADH}_2$  and NADH. The resulting acetyl-CoA is directed towards the TCA cycle, while the resulting shorter acyl-CoA ( $n-2$ ) undergoes another round of FAO. FAS (blue) takes place in the cytosol and relies on NADPH consumption. Following acetyl-CoA carboxylation into malonyl-CoA (via ACC), a 4-step sequence catalysed by FASN originates palmitate, which is further incorporated in triglycerides or double-layer phospholipidic membranes. Created with BioRender.

### 1.3.1 Fatty acid synthesis

Fatty acid synthesis (FAS) occurs in the cytosol and is dependent on the reducing equivalent NADPH (figure 2, blue section). The first step of FAS consists of the carboxylation of the cytosolic acetyl-CoA into malonyl-CoA. The major source of cytosolic acetyl-CoA is citrate that is synthesized from oxaloacetate and acetyl-CoA within the mitochondria. The formation of malonyl-CoA is mediated by acetyl-CoA carboxylase (ACC) at the expense of energy. Malonyl-CoA plays a crucial role in controlling the rate of FAS and fatty acid oxidation (FAO), as it is able to inhibit carnitine palmitoyltransferase I (CPTI) and, therefore, translocation of fatty acids into the mitochondria. Additionally, intracellular levels of other molecules involved in fatty acid anabolism and catabolism, as citrate, AMP, and palmitoyl-CoA, also dictate the flux of degradation versus synthesis. These negative feedback regulatory mechanisms are particularly important since they clearly represent the global status of cellular metabolic needs. Cytosolic citrate is a two-carbon biosynthetic precursor for fatty acid synthesis. Consequently, in the presence of high intracellular citrate, the cells are primed to initiate anabolic programs that culminate in increased lipid content. Furthermore, citrate is an allosteric activator of ACC and inhibitor of the glycolytic enzyme phosphofructokinase-1. This diverts cellular metabolism from the catabolism of organic fuels to the storage of fatty acids and glycogen by promoting increased levels of glucose-6-phosphate and phosphoglucomutase, respectively. Likewise, the presence of higher levels of palmitoyl-CoA inhibits the activity of ACC. Palmitoyl-CoA is also responsible for inhibiting the transport of citrate to the cytosol, as well as glucose-6-phosphate dehydrogenase that provides NADPH for fatty acid synthesis. ACC activity can also be regulated by covalent modifications, as phosphorylation, mainly via AMP-associated protein kinase (AMPK) activation (Hardie and Pan, 2002; O'Neill et al., 2013), which will be further addressed in section 2.3. Following malonyl-CoA synthesis, the elongation of acyl chains and consequent formation of fatty acids occur in a four-step sequence (condensation,

reduction, dehydration, and reduction). As stated previously, in opposition to FAO, which uses  $\text{NAD}^+$  and  $\text{FAD}^+$  as electron acceptors in fatty acid synthesis, one molecule of NADPH is oxidized to  $\text{NADP}^+$  in each of the two reduction steps. Fatty acid synthase (FASN) is a multienzyme complex, which includes seven differentially functional catalytic sites. This complex is responsible for the catalysis of the final steps of the anabolic process originating palmitate. The synthesis of each molecule of palmitate requires eight molecules of acetyl-CoA as the primary biosynthetic precursor, as well as 14 molecules of NADPH and seven molecules of ATP. Most of the newly synthesized fatty acids are either incorporated in triglycerides or double-layer phospholipidic membranes. The chosen fate relies on cellular requirements: in dividing cells, new membranes have to be promptly synthesized, so fatty acids are converted in phospholipids (Yao et al., 2016); in quiescent and naïve cells, fatty acids accumulate in the form of LDs, which may constitute an energetic reservoir, passible of degradation (Knobloch et al., 2017; Lee et al., 2015).

### 1.3.2 Fatty acid oxidation

In terms of metabolism, FA can be synthesized or degraded through FAO (figure 2, red section). Triglycerides are constituted by three FA and a glycerol molecule (Houten and Wanders, 2010). Through the activity of a lipase, glycerol and free FAs are released from triglycerides. Following release of FAs, those with twelve or fewer carbons enter freely in the mitochondria where they are activated to acyl-CoA. Those with more than 14 and less than 20 carbon are activated in the cytosol, which consists in the attachment of a CoA group to the fatty acid carboxyl group, in a process mediated by acyl-CoA synthase. After activation, CPTI promotes an exchange of the CoA group of the acyl with a carnitine, giving rise to an acyl-carnitine. The acyl-carnitine is consequently transported into the mitochondrial matrix by the carnitine/acylcarnitine antiport system (translocase). Once inside the matrix, the CoA group is conjugated with the acyl group, through the activity of CPTII, giving rise to carnitine that fuels translocase for recycling in the cytosol. Inside the mitochondrial matrix, FA are committed to FAO. Overall, each round of oxidation consists of four reactions (oxidation, hydration, oxidation, and thiolysis) and culminates in the shortening of the acyl chain by two carbons, as well as the generation of  $\text{FADH}_2$ , NADH, and acetyl-CoA. In terms of energy production, each molecule of palmitate, the prototype sixteen-carbon FA, yields eight molecules of acetyl-CoA and several reducing equivalents for ATP production.

#### 1.4 Amino acid metabolism and function

Amino acids are the building blocks of proteins and can be divided in essential, nonessential, and conditionally essential amino acids, depending on whether or not they are synthesized by the organism. Amino acids are transformed into carbon skeletons and can either be converted to glucose, enter the TCA cycle or fuel fatty acid synthesis.

Glutamine, initially described in 1953 by Hans Krebs, is the most abundant amino acid in the body (Newsholme et al., 2003). This amino acid is known to fuel distinct immune cells, as well as malignant ones: glutamine can be used as a nitrogen donor for synthesis of essential amino acids and nucleotides and as a precursor of  $\alpha$ -ketoglutarate, which fuels the TCA cycle for energy production. Arginine and branched chain amino acid (BCAA) sensors have been identified as positive regulators of the mammalian target of rapamycin (mTOR) complex 1 (mTORC1) pathway, responsible for the regulation of cell growth, metabolism and other crucial biological processes (Wolfson and Sabatini, 2017). Additionally, arginine has a dual role in macrophage polarization, which will be addressed in section 3.1.1. High levels of arginine have been shown to promote a shift from glycolysis to oxidative metabolism in activated T cells, which prompted the generation of anti-tumor memory T cells (Geiger et al., 2016). Further, Rodriguez and colleagues showed that arginine competition between anti-inflammatory macrophages and T cells results in T cell dysfunction by hampering its proliferation (Rodriguez et al., 2003), which may have a crucial importance in cancer and infection settings. Similar results were obtained with tryptophan, which was shown to be catabolized by macrophages, thus suppressing T cell proliferation (Munn et al., 1999). Dietary L-tryptophan is initially catabolized by indoleamine 2,3-dioxygenase 1 (IDO1), an interferon gamma (IFN- $\gamma$ )-induced enzyme, which indicates that this step is critically regulated by immune responses. Further, this amino acid is the principal precursor of *de novo* biosynthesis of NAD<sup>+</sup>, highlighting its importance in cellular homeostasis, redox state, host defense and cell survival (Mesquita *et al.*, 2016; Mesquita, Vergnes and Silvestre, 2018). Despite these short examples, the role of amino acids in the modulation of immune system has already been vastly addressed (Li et al., 2007).

## 2. Regulation of cell metabolism: the role of metabolic sensors

The metabolic choices that regulate immune cell function are governed by the modulation of specific key players that act as metabolic sensors and nutrient-sensing molecules, which will be addressed in this section (figure 3).

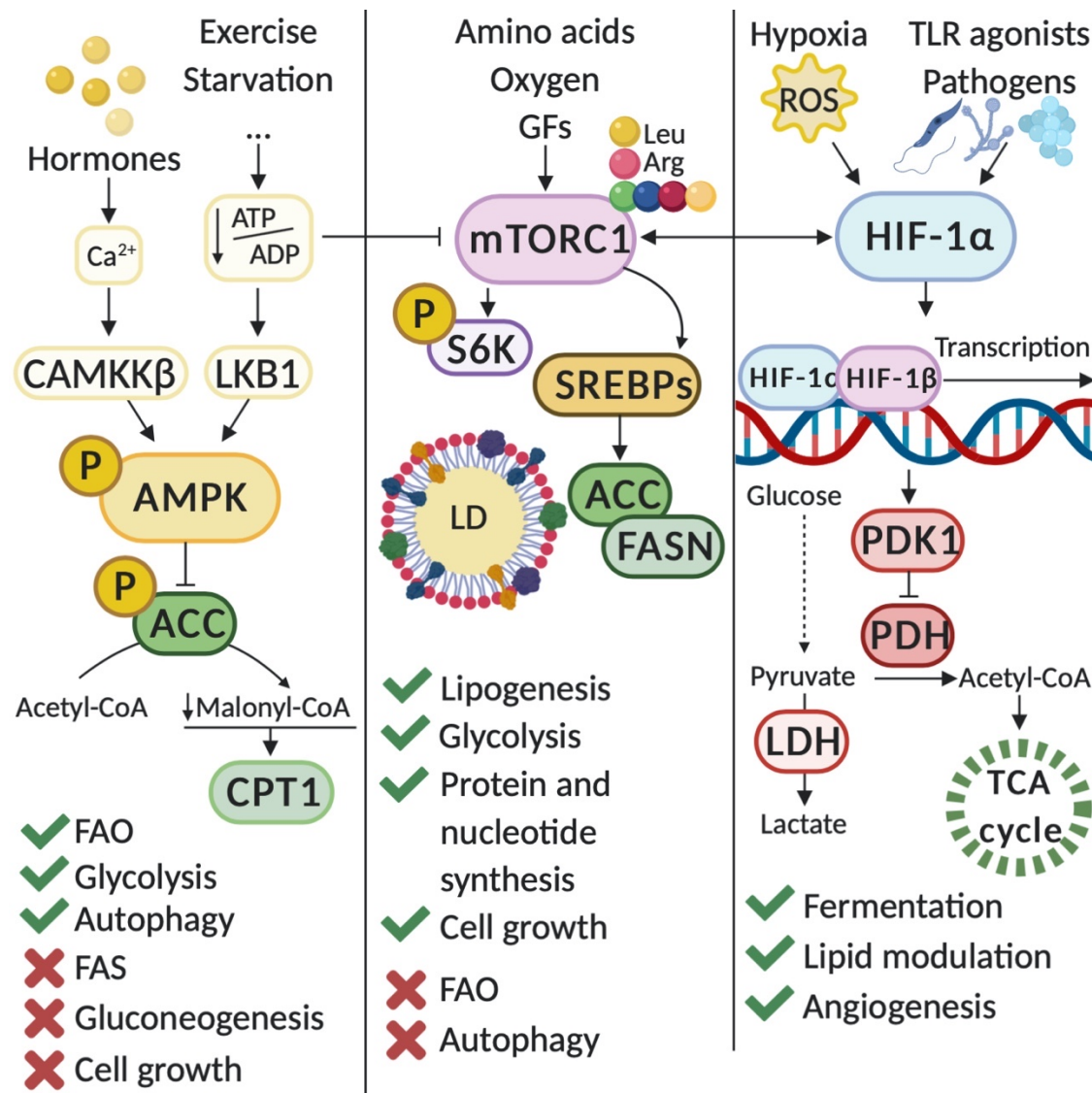


**Figure 3 Metabolic Sensors and Related Pathways.** AMPK may be activated by upstream CAMKK $\beta$  due to alterations in calcium signalling, mainly driven by hormones. AMPK may also be activated by upstream LKB1, which responds to low ratios ATP:ADP, induced by exercise, starvation and other factors. Upon AMPK phosphorylation (and consequent activation), ACC is the primary AMPK target that, upon phosphorylation, decreases carboxylation of acetyl-CoA to malonyl-CoA. Intracellular malonyl-CoA levels decrease and CPT1 is unleashed, thus promoting FAO. Other outcomes of AMPK activation include induction of glycolysis and autophagy, while FAS, gluconeogenesis and cell growth are restrained. mTORC1 can be activated by amino acids (namely leucine and arginine), oxygen levels and growth factors. During energy stress (low ATP:ADP levels), mTORC1 is repressed by AMPK. However, during activation, mTORC1 phosphorylates its main target S6K, responsible for initiating protein translation. mTORC1 also activates SREBPs, which in turn activate lipogenic enzymes as ACC and FASN, contributing to LD accumulation. Other outcomes of mTORC1 activation include increased glycolysis and cell growth, whilst FAO and autophagy are inhibited. The transcription factor HIF-1 $\alpha$  may be activated by hypoxia, ROS and TLR signalling (via TLR agonists or pathogenic agents). Upon activation, HIF-1 $\alpha$  dimerizes with HIF-1 $\beta$  and initiates a cascade of transcription. Glucose fermentation is induced and HIF-1 $\alpha$  is responsible for activating PDK1, which in turn inhibits PDH and, consequently, conversion of pyruvate to acetyl-CoA and TCA cycle entry. Pyruvate is then converted in lactate through LDH. Other outcomes of HIF-1 $\alpha$  activation include lipid modulation and angiogenesis. Created with BioRender.



## 2.1 mTOR – an amino acid sensor that regulates whole-cell metabolism

The mTOR integrates both intracellular and extracellular signals that regulate metabolism, growth and survival. The mTOR protein is composed by two multi-protein complexes, mTORC1 and mTORC2 that display non-redundant functions. mTORC1 is the most well studied component, regulated by lysosomal-bound GTPase Rheb. It is known to be modulated by growth factors, oxygen tension, amino acid levels and cellular energy status. Interestingly, upon intracellular energy depletion, which corresponds to a low ATP:ADP ratio, mTORC1 activation is repressed by AMPK through phosphorylation of the subunits TSC2 (Inoki et al., 2003) and Raptor (Gwinn et al., 2008). Rag GTPases are critical components of the mTORC1 pathway that explain the strong impact of amino acids in mTORC1 activation: during nutrient scarcity, the Rag complex is inactivated and mTORC1 is dispersed; however, during nutrient abundance (high amino acid levels), Rag GTPases display an active Rag complex, which anchors mTORC1 to the lysosome, where Rheb is located (Nguyen et al., 2017; Sancak et al., 2008). It is now clear that mTORC1 senses both intralysosomal and cytosolic amino acids, as leucine, arginine and glutamine, through different mechanisms (Saxton et al., 2016; Wang et al., 2015; Zoncu et al., 2011). Hypoxia has also been shown to inhibit mTORC1 either through reduction of ATP levels (which activated AMPK) or through activation of TSC1/2-induced transcription of DNA damage response 1 (REDD1), which blocks mTORC1 signaling (Brugarolas et al., 2004). The outcomes of mTORC1 activation include upregulation of protein synthesis via activation of translation activator S6 kinase (S6K) (Magnuson et al., 2012), which is required for cell growth, blockage of autophagy, regulation of mitochondrial metabolism and biogenesis and modulation of lipid synthesis (Laplante and Sabatini, 2009). mTORC1 was found to positively regulate lipid sensor sterol regulatory element-binding protein 1 (SREBP-1) at different levels, both *in vitro* and *in vivo* (Bakan and Laplante, 2012; Porstmann et al., 2008), which provides a direct link between mTORC1 activation and lipogenesis.

A causal link between mTORC1 and hypoxia-inducible factor-1 $\alpha$  (HIF-1 $\alpha$ ) has already been established by several groups. Through Rheb overexpression, Land and Tee demonstrated that potent mTOR activation enhanced HIF-1 $\alpha$  transcriptional activity, which required interaction with Raptor (Land and Tee, 2007). Harada *et al.* showed an increase in Akt and S6K phosphorylation in HeLa cells upon reoxygenation and glucose treatment, which accelerated intratumoral HIF-1 $\alpha$  translation (Harada et al., 2009). In addition, mTORC1 was found to mediate vascular endothelial growth factor A (VEGF-A) activity via HIF-1 $\alpha$ -dependent interaction (Dodd et al., 2015). It has also been demonstrated that, in opposition, HIF-1 $\alpha$  is able to modulate mTORC1 activity (Marhold *et*

*al.*, 2015). This molecular association between mTORC1 and HIF-1 $\alpha$  is of great importance when considering the impact of these players in several biological processes, as the regulation of metabolism, angiogenesis and vascularization. Interestingly, a recent study showed that mTORC1-induced metabolic reprogramming depends on mTORC1-driven hypophosphorylation of the transcription factor forkhead/winged helix family k1(Foxk1), which regulates HIF-1 $\alpha$ -driven gene expression (He et al., 2018).

## 2.2 HIF-1 $\alpha$ – the impact of oxygen sensing in cell metabolism

HIF is a basic helix-loop-helix transcription factor that mediates adaptation to low oxygen availability and, as such, accumulates during hypoxic conditions, as observed in sites of inflammation or in solid tumors. HIF is a ubiquitously expressed, heterodimeric protein composed of two subunits, the  $\alpha$ -subunit and the  $\beta$ -subunit, also known as aryl hydrocarbon receptor nuclear translocator (ARNT). Alterations on HIF-1 $\alpha$  expression rely on oxygen-dependent ubiquitination and proteosomal degradation, which takes place in normoxia (Salceda and Caro, 1997). In addition to low oxygen tensions, HIF-1 $\alpha$  is activated by distinct pathogens or Toll-like receptor (TLR) stimulation (Nishi et al., 2008; Spirig et al., 2010; Werth et al., 2010), as well as reactive oxygen species (ROS) (Galanis et al., 2008; Jung et al., 2008). Upon activation, HIF-1 $\alpha$  induces a transcriptional program responsible for the regulation of metabolism, oxygen delivery and cell survival. The first evidences that HIF-1 $\alpha$  regulates glucose metabolism came from cancer research: in hypoxic conditions, as in solid tumors, a shutdown of oxidative metabolism gives a biological advantage to cancer cells (Papandreou et al., 2006). This is accompanied by an increase of the glycolytic machinery, which generates energy via glucose fermentation. However, intensive investigations in several fields shown that distinct cell types are able to use glucose fermentation as a major metabolic pathway, regardless of the surrounding oxygen tension (Cheng et al., 2014; Rey et al., 2011; Del Rey et al., 2017; Wang et al., 2017). This transcription factor is responsible for upregulating several genes of the glycolytic pathway, including HK and enolase. Additionally, HIF-1 $\alpha$  directly activates pyruvate dehydrogenase 1 (PDK1), which inhibits the pyruvate dehydrogenase (PDH) enzyme complex, responsible for the conversion of pyruvate to acetyl-CoA. Consequently, upon HIF-1 $\alpha$ /PDK1 activation, pyruvate metabolism through the TCA cycle is impaired, mitochondrial respiration is attenuated and glucose metabolism is shifted towards lactate production (Kim et al., 2006). HIF-1 $\alpha$  has also been shown to have a role in lipid metabolism and storage, although HIF-2 has also been implied in lipid modulation (Mylonis et al., 2019; Rankin et al., 2009). It was demonstrated

that HIF-2 promoted the expression of PLIN2 protein, which in turn increased lipid accumulation in xenograft tumors and allowed the sustainment of endoplasmic reticulum (ER) homeostasis (Qiu et al., 2016). Gimm and colleagues showed that hypoxia-inducible protein 2 (HIG2) is a direct target of HIF-1 $\alpha$  (and not HIF-2) and, in normoxic conditions, HIG2 is expressed in the hemimembrane of LDs and contributes to accumulation of neutral lipids (Gimm et al., 2010). Further, Furuta *et al.* demonstrated that the *FASN* gene is upregulated in human breast cancer cell lines during hypoxia through HIF1-dependent activation of SREBP-1, a major transcriptional regulator of FAS (Furuta et al., 2008). Similarly, both HIF-1 $\alpha$  and HIF-2 $\alpha$  were shown to be involved in hypoxia-induced lipid accumulation, as deletion of these factors in hepatocytes abrogated the reduction of proliferator-activated receptor- $\gamma$  coactivator-1 $\alpha$  (PGC-1 $\alpha$ ) protein levels, critically involved in FAO (Liu et al., 2014). Nonetheless, the impact of HIF-1 $\alpha$  in lipid accumulation appears to be context-specific. Nishiyama and colleagues elucidated the role of HIF-1 $\alpha$  in the suppression of hepatic lipid accumulation in alcoholic fatty liver disease, as SREBP-1c and ACC were found to be greatly increased in diseased hepatocyte-specific HIF-1 $\alpha$ -null mice (Nishiyama et al., 2012).

### 2.3 AMPK – an energy sensor for cellular homeostasis

AMPK is trimeric complex with one catalytic ( $\alpha$ ) and two regulatory subunits ( $\beta$  and  $\gamma$ ). This energy sensor can be broadly activated through distinct upstream factors: a) when intracellular ATP levels decrease (and consequently, ADP and/or AMP levels increase), which can be induced by starvation, exercise, ischemia or mitochondrial inhibitors. This leads to activation of serine/threonine liver-kinase-B1 (LKB1), which responds to energy stress and phosphorylates Thr172, thus activating AMPK (Shaw et al., 2004; Woods et al., 2003); b) through non-canonical Thr172 phosphorylation via calcium/calmodulin-dependent kinase kinase 2 (CAMKK $\beta$ ) (Hawley et al., 2005), which is activated through hormone-dependent Ca<sup>2+</sup> levels; c) other factors, described elsewhere (Garcia and Shaw, 2017). AMPK has been shown to display a conserved function throughout several species and it plays a general role in cellular growth and homeostatic adaptation to low energy states. As a signal of cellular energetic stress, AMPK activation blocks anabolic pathways (as FAS and gluconeogenesis), while switching on nutrient catabolism (as FAO and glycolysis), to restore intracellular ATP levels (Hardie and Pan, 2002). Among the vast myriad of targets, AMPK directly phosphorylates and inhibits ACC and 3-hidroxi-3-methyl-glutaril (HMG)-CoA reductase, which are rate-limiting enzymes of the fatty acid and cholesterol synthesis, respectively (Carling et al., 1987). This results in decreased levels of malonyl-CoA, which unleash CPT-I and

initiates FAO. Consistently, in basal conditions, AMPK phosphorylates desnutrin and hormone-sensitive lipase (HSL) in the adipose tissue, thus activating lipolysis (Kim et al., 2016). Furthermore, AMPK activation augments glucose uptake by controlling translocation of glucose transporters GLUT1 and GLUT4 to cell surface (Wu et al., 2013; Yamaguchi et al., 2005). The role of AMPK in immune cell function in different tissues/organisms has been vastly studied due to the development of genetic models and pharmacological inhibitors.

### **3. Immunometabolism – metabolism as a unique driver of immunity**

The state of activation, challenge and function of a certain cell dictates its metabolic choices, in order to fulfill the necessary requirements of energy and biosynthetic precursors. This implies that the same cell may shift between different metabolic programs depending on the challenges it faces. Further, immune cells with different functions may display different metabolic requirements, adjusted to its microenvironment. In here, we will highlight innate immune cell immunometabolism and adaptive immune cell metabolism will be briefly addressed.

#### **3.1 Innate immune cells**

##### **3.1.1 Macrophages**

Macrophages are vastly involved in host defense and tissue homeostasis and repair, fulfilling basic yet essential functions as phagocytosis, microbial killing and cytokine production (figure 4). To accommodate these extreme and quite heterogeneous functions, commonly known as polarization phenotypes, macrophages adopt a range of metabolic pathways, which are tightly regulated. Initially, macrophage polarization was divided into classically (M1) and alternatively (M2) activated macrophages, referring to the *in vitro* stimuli required for such differentiation. Additionally, M1 macrophages were associated with the promotion of T helper (Th) 1 responses, while M2 macrophages induced type 2 responses. In terms of function, while pro-inflammatory macrophages are associated with tumor suppression and clearance of intracellular infections, anti-inflammatory macrophages fulfil immunosuppressive and tissue repair functions (Viola et al., 2019). As such, the term M1 referred to macrophages classically activated with lipopolysaccharide (LPS) and IFN- $\gamma$ , while M2 macrophages were alternatively activated with interleukin (IL)-4 (and later on with IL-13) (Martinez and Gordon, 2014; Mills et al., 2000; Stein et al., 1992). However, such

nomenclature fell into disuse, as a panoply of other players and mixed phenotypes appear in *in vitro* and *in vivo* settings. Further, for *in vitro* studies, the type of precursors and differentiation growth factors used greatly conditions the phenotype and basal state of the obtained naïve macrophages. Murine bone marrow-derived macrophages can be obtained by culture of precursors with macrophage colony-stimulating factor (M-CSF) or granulocyte-macrophage colony-stimulating factor (GM-CSF), with distinct populations being generated during these differentiation processes. While M-CSF is required for maintenance of tissue homeostasis and resolution of inflammation, GM-CSF is present in inflammatory settings. In fact, a groundbreaking study by Lacey and colleagues showed that M-CSF-induced differentiation generated anti-inflammatory macrophages, while GM-CSF induced the production of pro-inflammatory, M1-like macrophages (Lacey et al., 2012). Another problematic relies on isolation procedures for obtaining *ex vivo* macrophage cultures, as well as differences on the target tissue and the marker combination used to address macrophage activation (Murray et al., 2014). Further complexity arises upon translation of these findings to cultures of human macrophages, which highlights the importance of standardize macrophage nomenclature throughout the field.

Altered amino acid metabolism was the first differential finding that allowed the characterization of pro- and anti-inflammatory macrophages (Munder et al., 1998). While inflammatory macrophages convert arginine into nitric oxide (NO) through inducible NO synthase (iNOS) activity, anti-inflammatory macrophages shift arginine towards polyamine production via arginase-1 (Bronte and Zanovello, 2005; Rath et al., 2014). The production of NO is a hallmark of pro-inflammatory macrophages, as it associates with higher microbicidal capacity (Nathan and Hibbs, 1991). Although macrophages are known to be *plastic* cells, NO has been shown to prevent repolarization to an IL-4-driven phenotype. Upon LPS+IFN- $\gamma$  treatment, NO production inhibited mitochondrial respiration, which is required for polarization towards an anti-inflammatory phenotype (Van den Bossche et al., 2016). Inflammatory macrophages display an upregulation of glucose fermentation, which is mainly orchestrated by HIF-1 $\alpha$ . This metabolic player regulates ATP production via glucose fermentation, as energy generation is dramatically impaired in both macrophage and neutrophil HIF-1 $\alpha$  null mutants (Cramer et al., 2003). In terms of bioenergetics, although ATP yield is higher during oxidative phosphorylation, this process is much slower than glycolysis, which is swiftly activated in immune cells (Nagy and Haschemi, 2015). Further, activation of glycolysis also produces important intermediates that enter the pentose phosphate pathway. This allows for the sustainment of inflammatory responses due to the generation of ROS

via NADPH oxidase (NOX), as well as amino acids and ribose for protein and nucleic acid synthesis, respectively. Although ROS production is critical for pro-inflammatory macrophage function, recent evidences have suggested that low levels of ROS are essential for polarization towards the anti-inflammatory state (Griess et al., 2020). Anti-inflammatory macrophages rely mostly on AMPK-driven mitochondrial metabolism, with metabolites being incorporated in the TCA cycle and oxidative phosphorylation (OXPHOS). Further, these cells are also characterized by an upregulation of fatty acid uptake and oxidation (Hamers and Pillai, 2018; Wang et al., 2018). Sag and colleagues showed that naïve macrophages primed with anti-inflammatory cytokines as IL-10 and transforming growth factor (TGF)- $\beta$  quickly activate AMPK, while LPS stimulation led to kinase dephosphorylation and deactivation. Further, inhibition of AMPK $\alpha$  increased transcription of pro-inflammatory cytokines, as IL-6 and tumor necrosis factor (TNF)- $\alpha$ , in LPS-stimulated macrophages (Sag et al., 2008).

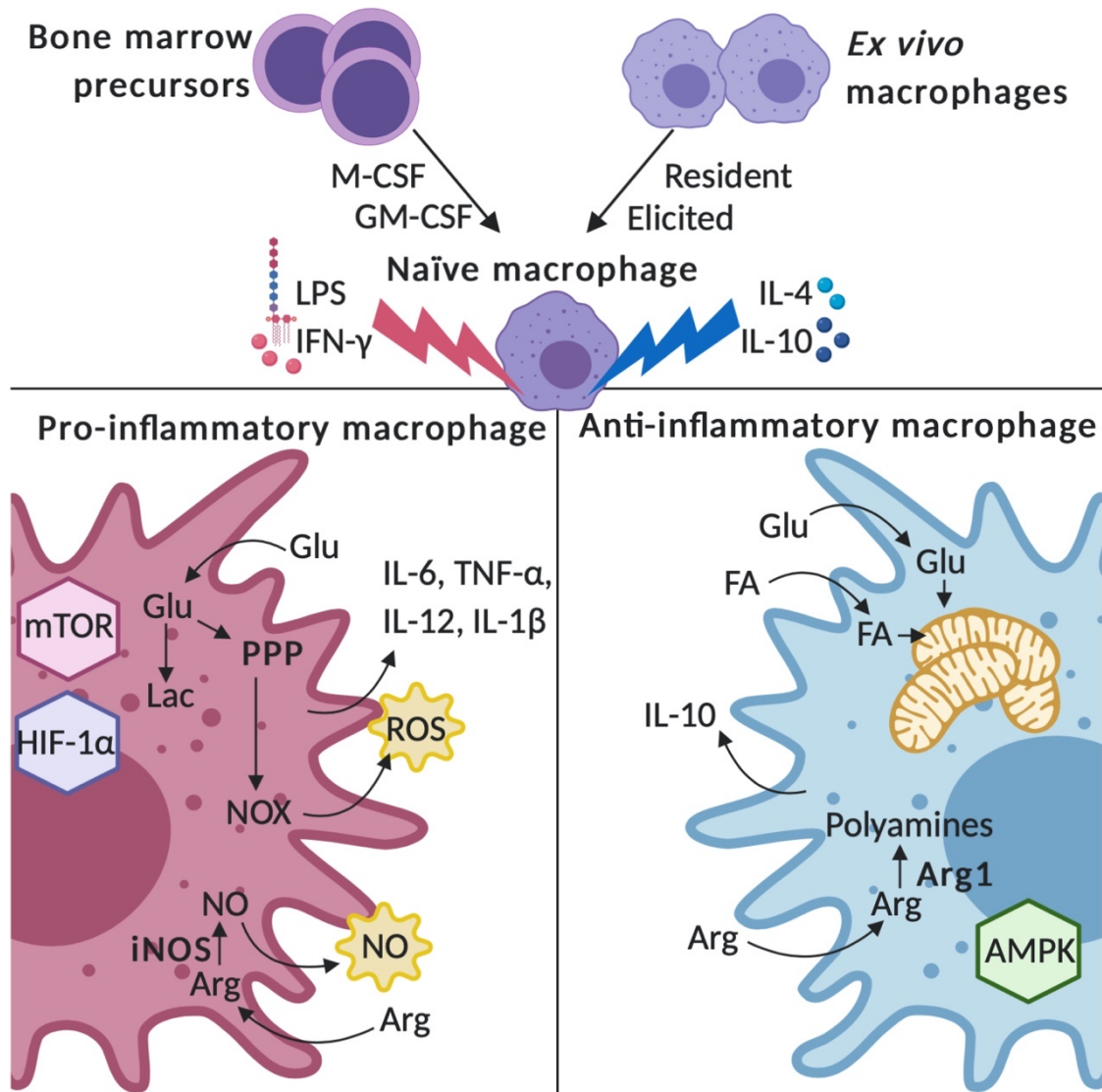


**Figure 4 Macrophage Polarization: Metabolism and Function.** Cultured macrophages can be obtained *in vitro* from bone marrow precursors, differentiated with either M-CSF or GM-CSF. *Ex vivo* macrophages can also be obtained from tissues, either by recruiting them or by extracting resident ones. Naïve macrophages can be further polarized into a pro-inflammatory profile (pink), through LPS-induced TLR stimulation and IFN- $\gamma$ . On the opposite, macrophages may be polarized towards an anti-inflammatory phenotype (blue) by stimulation with IL-4 and IL-10. Pro-inflammatory macrophages, mainly governed by mTOR and HIF-1 $\alpha$ , uptake large quantities of glucose, which is fermented in lactate and feeds the PPP. Consequently, NOX is activated and leads to ROS production. Arg is shifted towards NO production via iNOS activity. These macrophages are responsible for secreting pro-inflammatory cytokines, as IL-6, TNF- $\alpha$ , IL-12 and IL-1 $\beta$ . Anti-inflammatory macrophages rely on glucose oxidation and FAO in the mitochondria, a process that is driven by AMPK activation. IL-10 is a major anti-inflammatory molecule produced. These cells are also responsible for producing high amounts of other immunosuppressive molecules. Arg is converted in polyamines through the action of Arg1. Created with BioRender.

AMPK $\alpha$  has also been shown to be crucial for the induction of IL-10-driven STAT3-mediated anti-inflammatory pathways during macrophage polarization (Zhu et al., 2015).

### 3.1.2 Dendritic cells

Dendritic cells (DC) are innate immune cells that bridge the innate and adaptive immune response, as these cells directly influence T cell priming and Th cell differentiation upon migration to draining lymph nodes. These *bona fide* antigen-presenting cells (APCs) have a pivotal role in the orchestration of antimicrobial and antitumoral immune responses.

Similarly to macrophages, DC metabolism depends on DC subset, as well as whether these cells are actively resting or activated. In the peripheral blood, it is possible to find conventional DCs (subdivided in cDC1 and cDC2), plasmacytoid DC (pDC) and monocyte-derived DC (moDC). Further, tissues are also populated by specialized DCs, as Langerhans cells, tissue cDC1 and cDC2, intestinal DCs and inflammatory DCs, depending on the location (Mildner and Jung, 2014; Rhodes et al., 2019).

Culture systems are far from being perfect, although several efforts have been made to standardize DC generation. Widely used protocols involve the utilization of GM-CSF to obtain murine bone marrow-derived DCs (BMDCs). However, Helft and colleagues have shown that GM-CSF-driven differentiation originates both DCs and macrophages, with quite heterogeneous responses to stimuli (Helft et al., 2015). Currently, bone marrow progenitors can be differentiated in DCs through culture with GM-CSF and FMS-like tyrosine kinase 3 ligand (FLT3L), which is required *in vivo* for DC differentiation from common DC progenitors and DC precursors (Mayer et al., 2014; Wculek et al., 2019). It is crucial to acknowledge these differences in the culture system, as they will greatly change the phenotype and metabolism of the obtained cells.

Resting DCs engage in fatty acid oxidation and glutaminolysis, in order to fuel ATP production as well as to face the low anabolic demands inherent to their state. This is regulated by AMPK, which was shown to antagonize TLR-induced glycolytic metabolism (Krawczyk et al., 2010). Upon stimulation by TLR agonists, an up-regulation of glucose fermentation is observed (Jantsch et al., 2008), similarly to what happens with pro-inflammatory macrophages. This early induction of glycolysis relies on activation of key metabolic sensors AKT, mTOR and HIF-1 $\alpha$ . Glycolysis inhibition with 2-deoxyglucose (2-DG) impairs DC motility and DC migration to the draining lymph nodes (Guak et al., 2018). Further, Thwe and colleagues showed that intracellular glycogen storages can be mobilized upon DC activation with LPS. However, the authors shown that glycogen-driven carbons are responsible not only for fueling glycolysis, but also mitochondrial respiration in LPS-activated DCs (Thwe et al., 2017). Despite the clear importance of metabolic choices in different DC states (resting vs. activated), it is important to acknowledge that these findings are also context- and DC subset-dependent.

### 3.1.3 Neutrophils

Neutrophils, the most common blood leukocytes, play a central role in the early response to acute inflammation. Neutrophils retain the capacity of phagocytize invading pathogens and other foreign bodies. Additionally, neutrophils are responsible for the oxidative burst and production of microbicidal neutrophil extracellular traps (NETs) to kill and prevent microbe dissemination.

Neutrophil metabolism is far less studied than its innate counterparts, macrophages and DCs. Studies on human neutrophils have shown that phagocytosis is dependent on glucose fermentation, while glycogen is the main energy source used in the absence of glucose (Borreagaard and Herlin, 1982). It was also shown that autophagy-mediated lipolysis is critical for neutrophils development from bone marrow precursors, as it liberates fatty acids from lipid droplets, which in turn fuel mitochondrial respiration (Riffelmacher et al., 2017). The production of NETs was demonstrated to be dependent on glucose and, to a lesser extent, glutamine (Rodríguez-Espinosa et al., 2015). Additionally, reprogramming towards PPP is required as glucose-6-phosphate dehydrogenase (G6PD) fuels NOX, essential for superoxide-driven NET induction (Azevedo et al., 2015). As neutrophils migrate to inflammatory sites, it is likely that an adaptation to the available nutrients and conditions is required for the development of effective functions.



## 3.2 Adaptive immune cells

### 3.2.1 T cells

Naïve T cells are maintained in a state of quiescence, characterized by low metabolic requirements. In the lymph nodes, upon antigen presentation and priming by APCs, T cells undergo clonal expansion and effector differentiation. Following this, contraction of antigen-specific T cells takes place and a memory pool is maintained, which allows for a fast and effective response upon antigen reencounter. CD4 T cells recognize major histocompatibility complex (MHC)-II molecules presented by APCs. These lymphocytes can be polarized in different subsets, characterized by different cytokine secretion and distinct transcriptional programs. So far, several subsets have been identified (Th1, Th2, Th17, Treg, Th22, Tfh) but its impact on different pathologies remains to be identified for the most of them. CD8 T lymphocytes are cytotoxic cells that recognize MHC-I molecules and that possess crucial host defense mechanisms against intracellular pathogens and tumors, including massive production of IFN- $\gamma$  and TNF- $\alpha$ , secretion of cytotoxic granules (perforin and granzyme) and destruction of target cells via Fas/FasL interactions.

Considering that different T cell subsets reflect different metabolic requirements, it is no surprise that specific metabolic programs govern the function of specific subsets. Upon activation, the function of T cells is dramatically dependent on increased consumption of extracellular nutrients, which dynamically change according with T cell subset and state. Importantly, T cell dysfunction has been associated with metabolic dysregulation, which may contribute to T cell exhaustion (figure 5).

#### 3.2.1.1 Metabolic regulation of T cell exhaustion

T cell exhaustion is a rather complex phenomenon that is characterized by the loss of effector functions (as loss of IFN- $\gamma$ , TNF and IL-2 production), decreased proliferative potential and the persistent expression of inhibitory receptors, as programmed cell death protein 1 (PD-1), T-cell immunoglobulin and mucin-domain containing-3 (TIM-3) and lymphocyte activation gene 3 (LAG3), among others. During chronicity, as the infection persists, the immunosuppressive environment (rich in cytokines as IL-10 and TGF- $\beta$ ) and the increased antigen load constantly stimulates T cells, leading them to a state of unresponsiveness (Wherry, 2011). Recent evidences have also tried to establish a causal link between T cell exhaustion and inadequate nutrient supply and energy

production (Saeidi et al., 2018). Several studies in both cancer and infectious diseases have started to unveil how alterations on cellular metabolic fitness may impact T cell exhaustion and, consequently, host protective responses (Lim et al., 2020; Saeidi et al., 2018; Zhang and Romero, 2018). Bengsch and colleagues demonstrated that during chronic lymphocytic choriomeningitis virus (LCMV) infection, CD8 T cells display an early defect in the uptake and catabolism of glucose, in spite of a persistent mTOR signaling. Further, PD-1 was shown to repress PGC-1 $\alpha$ , thus impairing mitochondrial metabolism (Bengsch et al., 2016). Hepatitis B virus (HBV)-specific PD-1<sup>hi</sup> T cells displayed increased glucose uptake via GLUT1 expression, which was associated with an inability to switch towards an oxidative phenotype and with mitochondrial defects (Schurich et al., 2016). Staron *et al.* showed that LCMV infection originates impaired Akt and mTOR activation in antiviral lymphocytes. Further, blockade of PD-1 increases mTOR activity in LCMV-specific cytotoxic T cells, while rapamycin reverts these therapeutic effects (Staron et al., 2014). A critical understanding of T cell exhaustion is required to further apply this knowledge to forge new therapies and approaches for targeting chronic diseases.

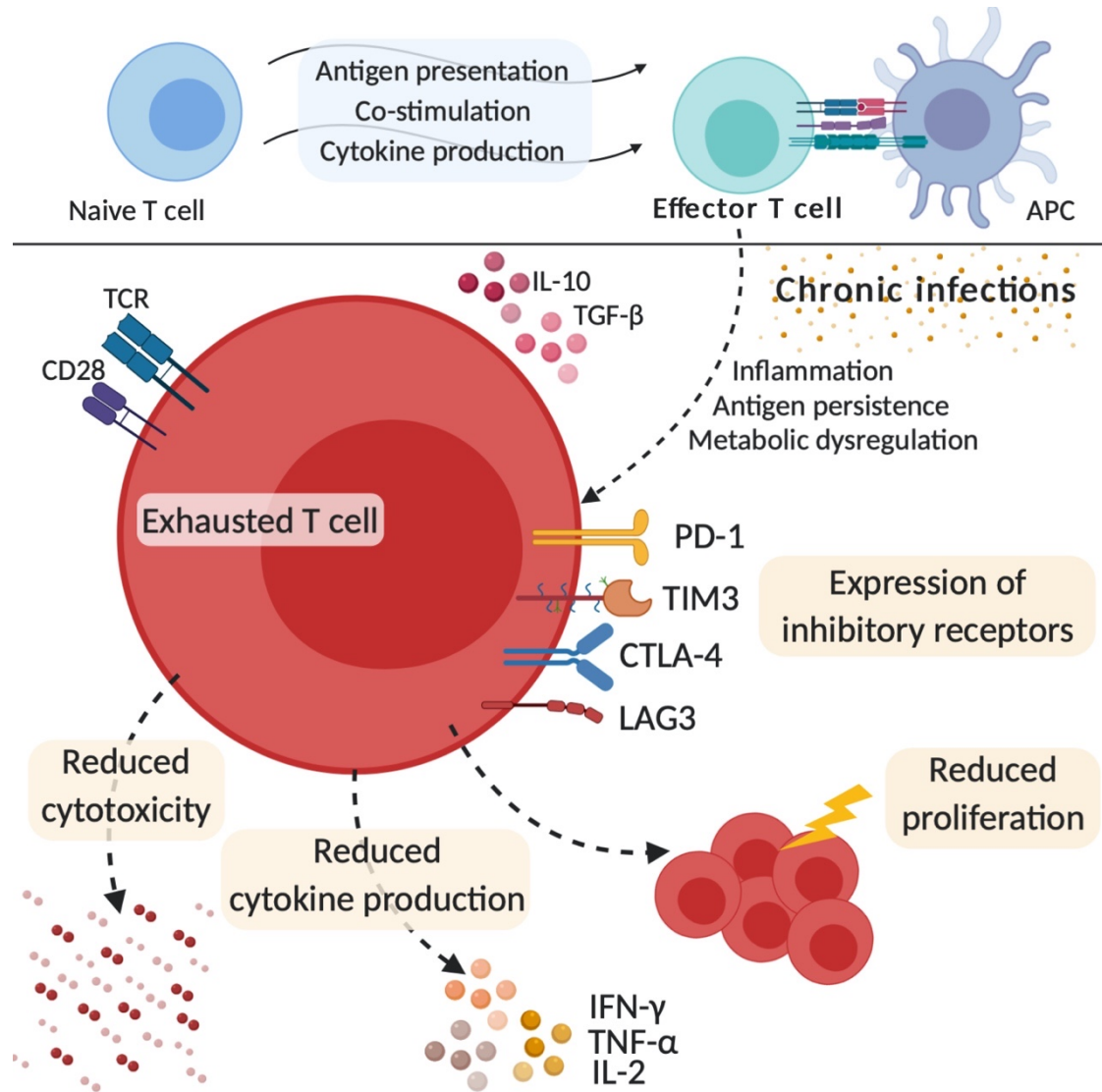


**Figure 5 Causes and consequences of T cell exhaustion.** Upon antigen presentation, engagement of co-stimulatory molecules and adequate cytokine production, a naive T cell originates an effector T cell. However, in the context of chronic infections, with high degrees of inflammation, antigen persistence and metabolic dysregulation, an immunosuppressive environment (via IL-10 and TGF- $\beta$ ) is created and T cells may become exhausted. This leads to upregulation of inhibitory receptors (as PD-1, TIM-3, LAG3 and CTLA-4), reduced proliferation, decreased cytokine production and reduced cytotoxicity. Created with BioRender.

**CHAPTER II**    THE INTRICATE RELATION  
BETWEEN *LEISHMANIA*  
PARASITES AND HOST

## 1. *Leishmania* parasites – the etiological agents of leishmaniasis

*Leishmania* parasites are protozoan parasites that belong to the family Trypanosomatidae and the genus *Leishmania*. These digenic parasites are obligate intracellular pathogens and shift between two major morphologies: the promastigote and the amastigote forms. There are 18 different species of *Leishmania* that are pathogenic for humans and they cause different sub-types of leishmaniasis (Steverding, 2017). The severity of the disease relies not only on some characteristics of the infecting parasite (specie, strain, virulence, etc), but also on host-intrinsic factors (immune status, nutritional status, genetics, etc), which will be addressed further on.

### 1.1 *Leishmania* life cycle

*Leishmania* parasites are the causative agents of leishmaniasis, which is a vector-borne disease transmitted by the bite of an infected phlebotomine sandfly (Arenas et al., 2017). During the bloodmeal, flagellated and motile promastigotes that are located behind the stomodeal valve on the sandfly are regurgitated on the dermis of the mammalian host. Once there, these parasites infect a wide range of hematopoietic cells, as macrophages, dendritic cells and neutrophils. Inside host cells, *Leishmania* parasites differentiate into the amastigote form, which possesses an internal flagellum and is immotile. Amastigotes undergo multiplication within the phagolysosomal compartment and eventually burst host cells and proceed to infect new ones. The cycle is closed when a sandfly takes a bloodmeal from an infected mammalian host and ingests free amastigotes or infected cells (figure 6).

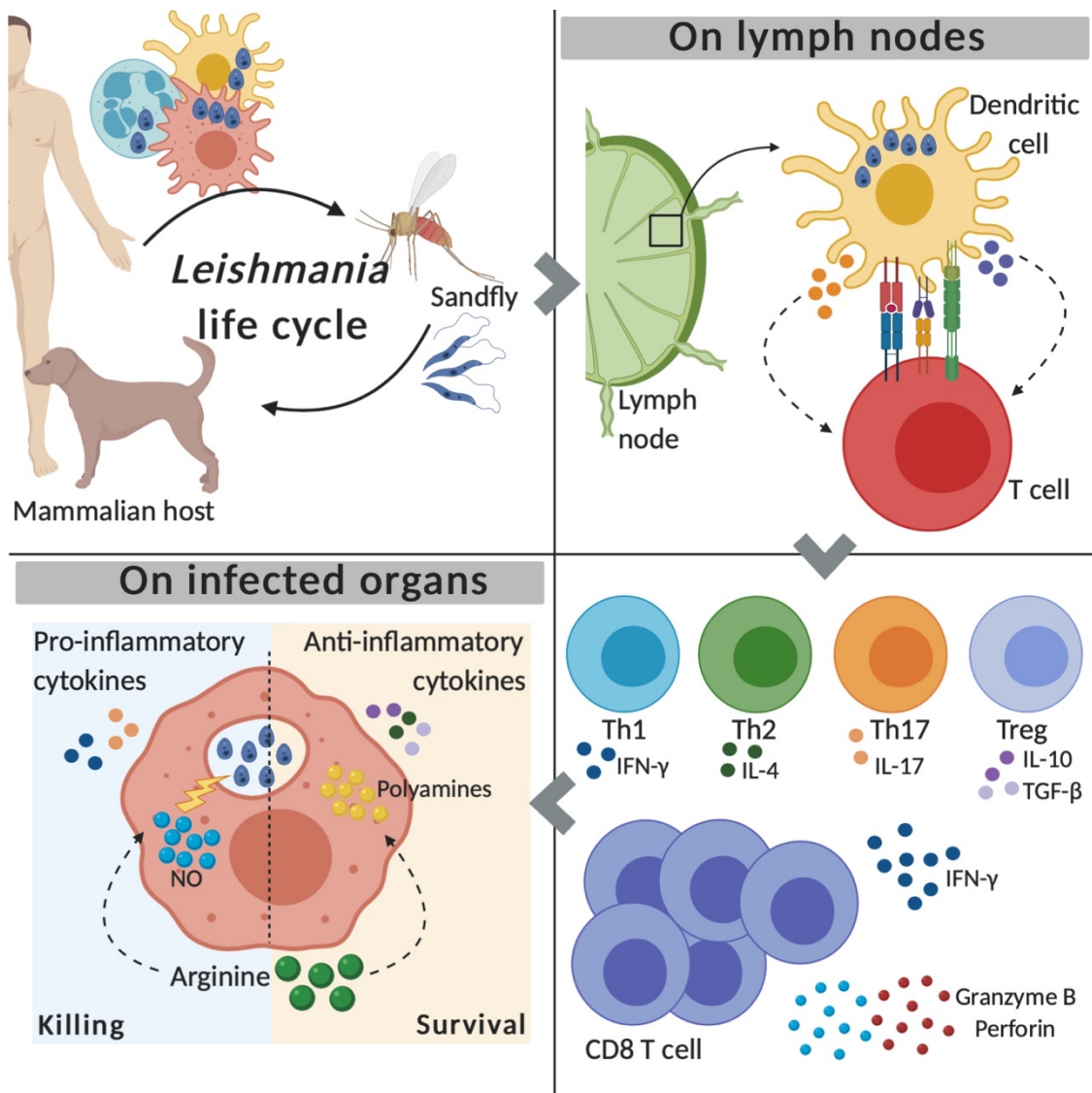


**Figure 6** *Leishmania* life cycle and visceral immune response. *Leishmania* promastigotes are inoculated on the dermis of a mammalian host through the bite of an infected sandfly. Within the host, promastigotes infect mainly phagocytes and are converted into intracellular amastigotes. Infected APCs, as DCs, migrate to the lymph nodes and activate naïve T cells, through MHC-TCR interactions, co-stimulatory molecule signalling and cytokine production. This leads to T cell expansion and production of antigen-specific clones. CD4 T cells may then be polarized in different Th subsets, responsible for differential cytokine production, while cytotoxic CD8 T cells produce large amounts of IFN- $\gamma$ , as well as granzyme and perforin. On infected organs, *Leishmania* amastigotes subvert host response, in order to create a suitable niche for survival, which is characterized by production of anti-inflammatory cytokines and polyamines. On the contrary, pro-inflammatory macrophages may produce microbicidal molecules, as NO, aimed at parasite killing. The phenotype of resident cells is likely to influence adaptive immune response. Created with BioRender.

## 1.2 Leishmaniasis – a neglected tropical disease

Leishmaniasis is currently endemic in over 50 countries from the regions of East Africa, Southeast Asia and Latin America. This disease comprises three major clinical presentations, which

range from a self-healing disease to a potentially fatal one (Burza et al., 2018; Kone et al., 2019). Cutaneous leishmaniasis (CL) is the most common form of the disease, in which small self-healing skin lesions or ulcers may show on exposed body parts. CL is usually caused by some species of the subgenus *Viannia*, but also by *L. major* and *L. tropica*. Mucocutaneous leishmaniasis (MCL) results from the appearance of lesions on mucosal surfaces, as the nose, mouth and throat and can lead to mutilating and debilitating lesions. It typically appears after infection with *Leishmania* parasites from the subgenus *Viannia*. Visceral leishmaniasis (VL), also known as kala-azar, is the most severe manifestation of the disease, caused mainly by *L. donovani* and *L. infantum* (= *chagas*) (Dantas-Torres et al., 2006). It is characterized by episodes of fever, weight loss, hepatosplenomegaly and anemia. Post-kala-azar dermal leishmaniasis (PKDL) is a complication that may appear in *Leishmania donovani*-infected patients, characterized by nodular rashes that appear after apparent cure.

## 2. Treatment for visceral leishmaniasis

Treatment of leishmaniasis should be strictly performed after diagnosis and identification of the infecting *Leishmania* species. Accordingly to WHO guidelines, antileishmanial medicines include: pentavalent antimonials (meglumine antimoniate and sodium stibogluconate), amphotericin B deoxycholate, lipid formulations of amphotericin B, paromomycin, pentamidine isethionate and miltefosine. First-line therapy for VL includes pentavalent antimonials and liposomal amphotericin B, while amphotericin B and pentamidine have been used as second-line drugs (WHO, 2010, 2012). Despite this therapeutic arsenal, some concerns have arisen regarding leishmaniasis treatment. Most drugs are very expensive, highly toxic, presenting severe side effects that include nephrotoxicity and hepatotoxicity. To overcome this, lipid formulations of amphotericin B (as liposomal amphotericin B, amphotericin B lipid complex and amphotericin B cholesterol dispersion) were developed and, while displaying the same efficacy when compared to amphotericin B deoxycholate, show lower kidney toxicity (Shirzadi, 2019; Sundar and Jaya, 2010). A further concern is the fact that the majority of the available medicines must be administered using intramuscular or intravenous route, which requires adequate public health services mostly absence in leishmaniasis endemic regions. Although miltefosine is the only available oral drug, the onset of severe side effects, as teratogenicity, may hinder its broad utilization. In addition to this,

the emergence of resistance to antileishmanial drugs poses an enormous threat, as it culminates in therapy failure (Hefnawy et al., 2017; Ponte-Sucre et al., 2017).

### 3. *Leishmania* biology and metabolism

*Leishmania* promastigotes attach to the surface of mononuclear phagocytes, which leads to their internalization and conversion to amastigotes. This implies that virtually every cell that expresses adequate phagocytosis-associated receptors is prone to harbor *Leishmania* parasites. However, professional phagocytes, such as macrophages, dendritic cells and neutrophils are the most common and well-studied hosts, with macrophages being the preferred ones. Once within these cells, parasites have to adapt to the increased temperature and to the highly acidic, phagolysosome-like structure where they reside, the parasitophorous vacuole (PV) (Rittig and Bogdan, 2000). Additionally, these parasites also have to couple their metabolic requirements with nutrient availability on the host cell. As such, parasites ultimately rely on host cells to scavenge some nutrients that are limiting but essential. Consistently, it has been shown that these parasites are auxotrophic for purines, vitamins, heme and several amino acids, which are hijacked from host's lysosome (McConville et al., 2015; Naderer and McConville, 2008).

Besides their clear morphological differences, *Leishmania* promastigotes and amastigotes also possess quite distinct metabolic requirements. This is due to the fact that both forms have to endure and adapt to different stimuli and challenges that are driven by the intrinsic difference between its hosts. *Leishmania* promastigotes display high rates of glucose and non-essential amino acid uptake and catabolism, as well as fatty acid uptake to fuel the need for membrane synthesis. Upon entering host cells, the parasites face a harsh and hostile environment, characterized by a rise of temperature (from 27°C in the insect to 37°C in the mammalian host) and an increased acidification. Once inside the PV, amastigotes suffer a rewiring of central carbon metabolism, mainly characterized by the utilization of glucose as a carbon source, uptake of amino acids for protein synthesis and fatty acid catabolism for fueling the TCA cycle (McConville and Naderer, 2011; McConville et al., 2007, 2015). At this stage, the activation of a stringent response that leaves amastigotes in a state of quiescence may be presented as a strategy to: a) overcome nutrient overload on the PV, which, although displaying reduced bioavailability of some nutrients, is highly



rich in glucose; b) adequately adapt to the environmental changes, as the increase in temperature and pH.

#### 4. Parasite-host interaction

Parasitism is defined as a relationship between two organisms, in which one (the parasite) benefits from exploiting the other (the host). Once inside the host, parasites become intrinsically dependent of host metabolism and develop strategies to hijack essential and limiting nutrients. To ensure the successful thrive of infection, parasites try to subvert host defense mechanisms and to access host's nutritional pool, while the host delivers microbicidal molecules and limits nutrient availability. The outcome of this competition between host and parasite implies a dynamic interaction and the establishment of a delicate balance, at the end of which the host either succumbs, eliminates the infectious agent or co-exists in homeostasis.

Trypanosomatid parasites, as *Leishmania* spp. and *Trypanosoma cruzi* have already been shown to target specific host metabolic checkpoints, as AMPK, HIF-1 $\alpha$  and mTOR (Caradonna et al., 2013; Jaramillo et al., 2011; Kumar et al., 2018; Libisch et al., 2018; Moreira et al., 2018). Kumar and colleagues demonstrated recently that *L. donovani* induced mTOR activation shifts macrophage polarization towards an anti-inflammatory state, characterized by lower accumulation of ROS and NO and higher production of IL-10 and TGF- $\beta$ . Inhibition of mTOR with rapamycin culminated in increased nuclear factor kappa-light-chain-enhancer of activated B cells (NF- $\kappa$ B) nuclear translocation and lower *L. donovani* viability (Kumar et al., 2018). Furthermore, mTORC1 activation has also been linked to the modulation of *in vivo* immune response to VL. Up-regulation of chemokine CXCL16 upon *L. donovani* infection is dependent on activation of AKT/mTOR pathway and increased chemotaxis of CXCR6-expressing cells, which suggests that the modulation of these players may greatly impact the pathogenesis of VL (Chaparro et al., 2019). The utilization of mTOR inhibitors as adjuvants in antileishmanial therapy has already been suggested, due to their potent anti-parasitic properties (Khadir et al., 2018). Conversely, it has been shown that mTORC1 inactivation by GP63-mediated cleavage and consequent activation of host translational repressor 4E-BP1 is essential for *L. major* survival (Jaramillo et al., 2011). Different studies on *T. cruzi* have also demonstrated that, upon infection, perturbations on the mTORC1 pathway are linked to the establishment of a *metabolically* permissive niche for parasite growth in macrophages (Libisch et al., 2018; Márquez et al., 2018) and HeLa cells (Caradonna et al., 2013). Moreira and

colleagues have shown that host AMPK is activated upon *L. infantum* infection via the axis LKB1/sirtuin (SIRT) 1, which shifts the early fermentative metabolism towards a late mitochondrial one (Moreira et al., 2015). This strategy of host subversion allows the creation of an adequate intracellular microenvironment prone for parasite survival. On the contrary, silencing of genes encoding for AMPK subunits establishes a favorable growth environment for *T. cruzi* (Caradonna et al., 2013). Alongside with this, Nagajothi and colleagues suggest a *pathogen*-beneficial role for AMPK impairment and decreased adiponectin production in infected *T. cruzi*-infected adipocytes (Nagajothi et al., 2008). Additional perspectives on the role of AMPK and mTOR during parasitic infections can be found elsewhere (Brunton et al., 2013; Mesquita et al., 2016b; Moreira et al., 2018).

The most drastic outcome of parasite-induced hijacking of host metabolic sensors is the modulation of the metabolic environment and consequent alteration of cellular function. As described previously, nutrient availability and the triggered metabolic pathways are crucial for defining host immune function and response towards the invading agent. As such, during infection, the modulation of these pathways will allow the scavenge of essential nutrients, which fuel parasite persistence and, eventually, fragilize host cells and weaken antiparasitic immune response, thus favoring parasite survival and proliferation.

#### 4.1 Immune response on VL

As a consequence of its mandatory intracellular stage, *Leishmania* parasites have evolved closely within host cells, which comprise mainly innate immune cells. In order to acquire survival advantage, these parasites were forced to develop strategies of immune evasion, to avoid elimination and infection clearance. At an organismal level, the complex immune response in infected organs (mainly liver, spleen and bone marrow), as well as the cellular and molecular events that culminate in an effective innate and adaptive antileishmanial response dictate the outcome of infection (figure 6).

In the initial stage, promastigotes rapidly infect resident and chemoattracted phagocytes that are elicited due to the pro-inflammatory properties of sandfly saliva (Hall and Titus, 1995; Lestinova et al., 2017; Teixeira et al., 2014). The first wave of host defense is led by polymorphonuclear neutrophil granulocytes (PMNs). Although the half-life of circulating PMNs is considerably low (~6-10 hours), it has been shown that *Leishmania* parasites delay neutrophil

apoptosis for their own advantage, both *in vitro* and *in vivo* (Aga et al., 2002). Once neutrophils start to die (~2-3 days after infection), apoptotic vesicles containing parasites are ingested by the immune system cleaners, macrophages (Aga et al., 2002; van Zandbergen et al., 2004). This promotes a silent (and anti-inflammatory) uptake of intracellular *Leishmania* by professional phagocytes, which has been coined as the Trojan horse hypothesis (Laskay et al., 2003). However, parasites may escape dying neutrophils and then directly infect macrophages, which has been known as the Trojan rabbit hypothesis. Upon the establishment of a long-lasting infection, *Leishmania* parasites face a second trial: the anti-*Leishmania* response is activated and evasion strategies to prevent parasite killing are required. Over the last decades, several immune evasion techniques adopted by *Leishmania* parasites have been reported. Briefly, these include: a) decreasing microbicidal ROS production, which has been shown to be mediated by lipophosphoglycan (LPG), one of the major dominant surface macromolecules of the promastigote stage, which inhibits NOX complex assembly (Lodge et al., 2006); b) decreasing antileishmanial NO production through upregulation of host arginase, which shifts arginine towards polyamine production – this has a dual beneficial effect, as parasites also feed on the produced byproducts (Rogers et al., 2009); c) creating an anti-inflammatory niche, characterized by heightened production of IL-10 and TGF- $\beta$  and reduced IL-12 (Carrera et al., 1996; Reiner et al., 1994); d) interfering with macrophagic phagosome maturation, as delaying phagosome acidification favors parasite survival in this hostile environment (Moradin and Descoteaux, 2012; Winberg et al., 2009); e) decreasing antigen presentation by APC (Contreras et al., 2014; Meier et al., 2003).

DCs have a crucial role during *Leishmania* infection, as they bridge innate and adaptive immune response: upon recognition of invading pathogens, DCs migrate to lymphoid tissues where naïve T cells wait for activation to unleash full killing potential (Sher et al., 2003). Disruption of DC migration was shown to increase susceptibility towards *L. donovani* infection (Ato et al., 2002, 2006). As such, an adequate DCs response regulates the antileishmanial adaptive immune response and, consequently, the outcome of infection. Belkaid and colleagues demonstrated that low-dose *L. major* infection of the dermis was followed by a *silent* phase (~4-5 weeks), which was shown to be crucial for the establishment of infection and the consequent increase in parasite load, as no inflammatory response was elicited. The late detection of IL-12<sup>+</sup> DCs in the dermis (4 weeks post-infection) preceded the development of a Th1 response, responsible for infection clearance (Belkaid et al., 2000). However, the role of DCs during *Leishmania* infection is not always beneficial for the host. Resende and colleagues showed that infected MHC-II<sup>high</sup> DCs polarize T cells into a

pathogenic, nonprotective role, characterized by the expansion of T-bet<sup>+</sup>IFN- $\gamma$ <sup>+</sup>IL-10<sup>-</sup> CD4 T cells. In opposition, bystander, uninfected DCs induced a protective phenotype with increased levels of IL-12p40 (Resende et al., 2013). Additionally, a study by Owens and colleagues showed that IL-27-producing CD11c<sup>hi</sup> dendritic cells promote further production of IL-10 by effector Th1 cells, thus contributing to pathology and disease progression (Owens et al., 2012).

Initial studies on the field identified the Th1/Th2 dichotomy as an important regulator of susceptibility/resistance to cutaneous leishmaniasis following *L. major* infection. In mice models, it is widely accepted that Th1 responses, characterized by IFN- $\gamma$  production and consequent antileishmanial NO production are protective (Cunningham, 2002; Scharon-Kersten et al., 1995), whilst deleterious IL-4-producing Th2 cells are present in nonhealing animals (Heinzel et al., 1989; Sacks and Noben-Trauth, 2002). However, although protective immunity in VL relies on the IL-12/IFN- $\gamma$  axis, the role of type 2 cytokines is controversial (Satoskar et al., 1995; Stäger et al., 2003). McFarlane and colleagues showed that, in opposition to what was shown using global IL-4R $\alpha$ <sup>-/-</sup> mice, CD4<sup>+</sup> T cell specific IL-4R $\alpha$ <sup>-/-</sup> mice were more resistant to *L. donovani* infection when compared to littermate controls (McFarlane et al., 2019). This suggests a protective role of this cytokine during VL, although a mechanistic explanation still needs to be found.

The utilization of different mice strains with different susceptibilities to leishmaniasis (Balb/c as susceptible and C57BL/6 as resistant to leishmaniasis) allowed for a deeper understanding of the cellular events that govern infection pathology (Roberts, 2005). In human CL, expansion of IFN- $\gamma$ <sup>+</sup> CD4 T cells indicate protection, while IL-4 and IL-10 levels were found to associate with pathology and disease progression (KEMP et al., 2008; Louzir et al., 1998). Further, secretion of Th2-related cytokines, as IL-4, IL-5 and IL-10, were found to be higher in peripheral blood mononuclear cells (PBMCs) from individuals with non-healing lesions, while Th1 cytokines, as IL-12 and IFN- $\gamma$  were increased in patients with healing lesions (Shahi et al., 2013). PBMCs from VL patients exposed to *Leishmania* antigens fail to proliferate and upregulate IFN- $\gamma$ . This phenotype was shown to be reverted upon blockage of IL-10 receptor, suggesting a role for IL-10 in suppressing T cell responses during active disease (Ghalib et al., 1993). However, PBMCs from patients bearing active lesions have been shown to produce both IFN- $\gamma$  and IL-10 upon antigen stimulation (Castellano et al., 2009). Similarly, high levels of both cytokines were found in patients with active VL, while IL-10 was shown to markedly decrease during resolution (Karp et al., 1993). It has been shown that persistence of parasites in the dermis is driven by expansion of CD4<sup>+</sup> CD25<sup>+</sup> regulatory T cells. Further, IL-10-producing CD4 and CD8 T cells were found in the chronic sites of

*L. major* infection, while treatment of chronically infected C57BL/6 mice with anti-IL-10 receptor antibody allowed the achievement of sterile cure (Belkaid et al., 2001, 2002). Darrah and colleagues have shown that multifunctional Th1 cells are critical players against *L. major*, as the degree of protection is dependent on CD4 T cell ability to produce IFN- $\gamma$ , IL-2 and TNF- $\alpha$  (Darrah et al., 2007a).

The role of CD8 T cells during leishmaniasis still remains to be fully acknowledged. In experimental VL, CD8 T cells have been associated with parasite control and resistance to infection due to their cytotoxic potential (Stern et al., 1988). This cytotoxic activity is mainly mediated by IFN- $\gamma$  and TNF- $\alpha$  production, as well as perforin secretion and activation of the Fas/FasL pathway (Tsagozis et al., 2003). Conversely, in a self-healing *L. infantum*-cutaneous model of infection, CD8 T cells do not appear to be essential for parasite control. The authors showed that beta2-microglobulin deficient C57BL/6 mice, which do not produce functional CD8 T cells, have similar burden to WT counterparts, thus indicating a negligible role for these cells in this context (Tsagozis et al., 2005). As in other chronic, persistent infections, CD8 T cells may become dysfunctional during leishmaniasis, which is further described below.

#### 4.1.1 Impact of T cell exhaustion on leishmaniasis

Little is known about the impact of CD4 and CD8 T cell exhaustion during VL. It has already been shown that CD8 T cells are driven towards an exhaustive phenotype during human VL. CD8 T cells isolated from patients' blood showed increased levels of *IL10* transcripts and exhaustion markers cytotoxic T-lymphocyte antigen 4 (CTLA-4) and PD-1, while transcription levels of *IFNG* were shown to be decreased (Gautam et al., 2014). Esch and colleagues showed that T cell exhaustion also represents a major clinical challenge, as the loss of antigen-specific cells and IFN- $\gamma$  production associate with increased VL symptomatology. Interestingly, blockage of PD-1 with B7.H1 restored both CD4 and CD8 T cell functions, while increasing ROS-derived parasite killing by monocytes (Esch et al., 2013). Anti-PD-1 and anti-PD-L1 have also been suggested as potent therapies for T cell reinvigoration in *L. amazonensis*-infected mice, as smaller lesions and lower parasite burden were observed in treated animals (da Fonseca-Martins et al., 2019). Studies on the impact of T cell exhaustion in leishmaniasis, as well as on the impact of metabolism in T cell dysfunction may open new avenues for developing more effective antileishmanial strategies (figure 7).

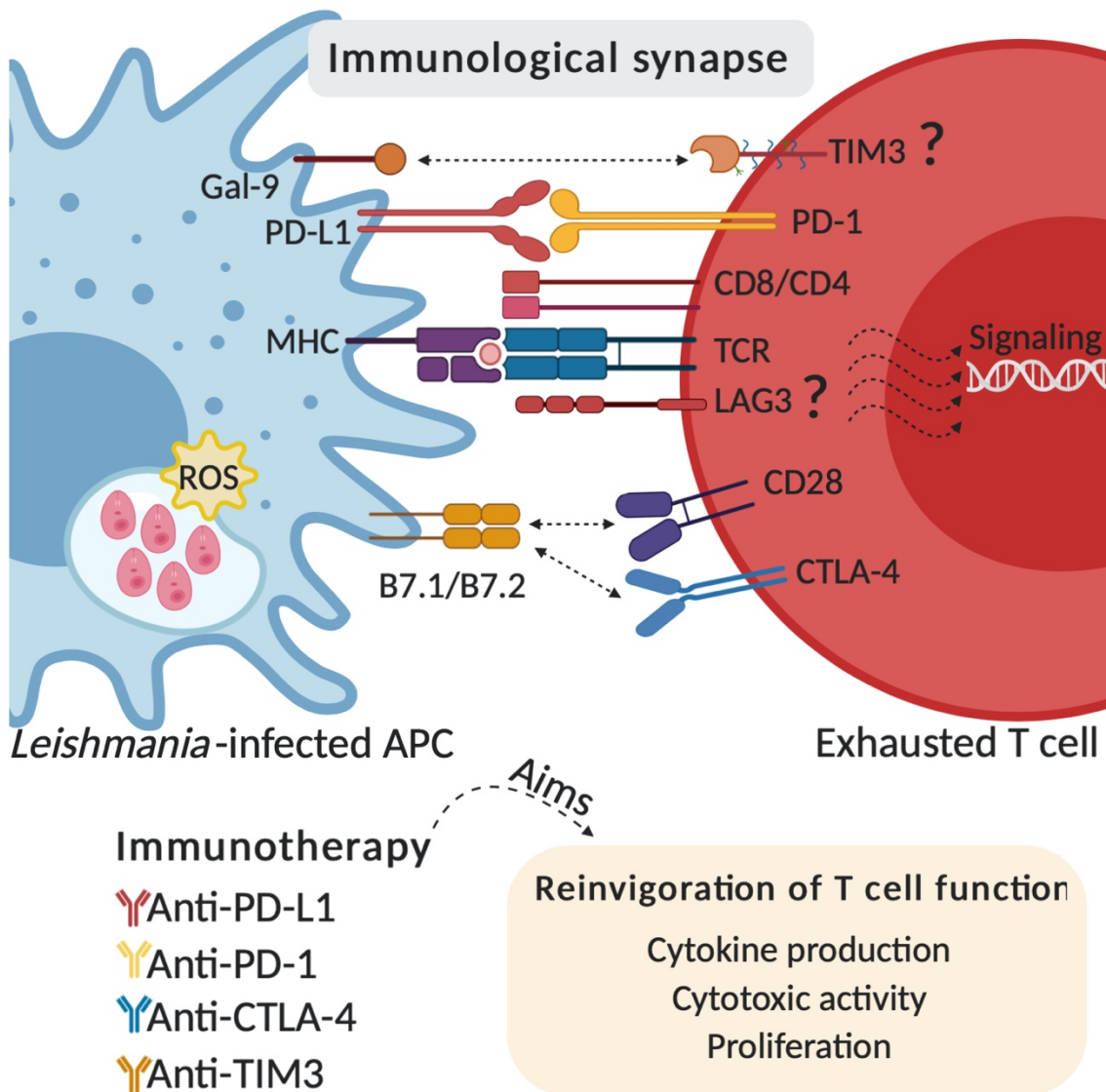


**Figure 7 Immunotherapy for *Leishmania* infection.** During chronic *Leishmania* infection, exhausted T cells express several inhibitory molecules, which bind to counterpart receptors at the surface of the infected APC and contribute to decreased activation and increased inhibitory signalling. Immunotherapy (which includes antibodies against inhibitory receptors expressed by both APC and T cells) aims at reverting this phenotype through the reinvigoration of T cell function, which ideally culminates in enhanced cytokine production and restoration of cytotoxic and proliferative abilities. Created with BioRender.

#### 4.2 Nutritional microenvironment during infection

One of the hallmarks of a successful parasitic infection is the modulation of host intracellular milieu. This is important because this modulation a) fuels parasite survival due to the scavange of essential nutrients, for which parasites are auxotrophs; b) fulfils parasite metabolic needs, thus permitting their growth and proliferation; c) depletes host nutritional reserves and, consequently, hampers immune response. Interestingly, this link between the metabolic microenvironment and immune response has shed light on the importance of nutrition during

infections. As immune cells are influenced by the circulating nutrients acquired in the diet (Alwarawrah et al., 2018; Cohen et al., 2017; Smith, 2007), it is expectable that changes in the host nutritional status impact infection outcome. Similarly, upon nutritional alterations, the reshaping of the immune system may define the influence host permissiveness towards the pathogen. As nutritional diseases increase in prevalence worldwide, distinct pathogens exploit the decrease in host immune fitness to thrive and persist (Karlsson et al., 2010; Wieland et al., 2005).

Digenic parasites, as *Leishmania* species, must adapt to different niches, as they shift between the insect stage and the mammalian host. During bloodmeal and parasite injection in the dermis of the mammalian host, promastigotes are forced to adapt their metabolism, as host microenvironment and nutrient composition is quite different from the one found in the sandfly gut. This suggests that nutritional pressure exerted by each stage (insect versus mammalian) dictates not only parasite morphology, but also metabolism.

This section will focus on the importance of lipid modulation and metabolism during infection, as the scavenging of host lipids is transversal to different parasites (Ginger, 2006; Moreira et al., 2018) and *Leishmania* parasites are no exception. Several reports have elucidated the importance of lipids in the course of *Leishmania* infection. The modulation of cholesterol during *Leishmania* infection is one of the most well studied examples on how these parasites take advantage of host lipids. Semini *et al.* demonstrated an upregulation of the genetic machinery responsible for cholesterol synthesis in *L. mexicana*-infected macrophages. Consistently, reduced levels of Niemann–Pick C1 (NPC1) protein, responsible for cholesterol efflux, were found early after infection, as well as an accumulation of this protein near *L. mexicana* PV, which indicates cholesterol retention (Semini et al., 2017). Also, Pucadyil and colleagues showed that cholesterol depletion from macrophage membranes reduces the kinetics in host-parasite interaction, which is normalized upon its replenishment (Pucadyil et al., 2004). Due to the importance of cholesterol for membrane fluidity, chronic statin-induced cholesterol depletion reduced the attachment of promastigotes to macrophage membrane, as well as intracellular amastigote load (Kumar et al., 2016). Mukherjee and colleagues showed that *L. donovani* infection induced SREBP-2 stabilization and consequent increased incorporation of cholesterol in the membrane, which culminated in delayed phagosomal acidification. Additionally, mitochondrial ROS production was shown to be impaired due to SREBP-2-induced upregulation of uncoupling protein (UCP) 2, which benefits parasite survival (Mukherjee et al., 2014). It has also been shown that during phagocytosis LPG co-localizes with lipid rafts on the membrane of infected macrophages and this hinders phagosomal

maturation, which is crucial for parasite survival (Winberg et al., 2009). Additionally, disruption of membrane rafts in infected antigen-presenting cells increases membrane fluidity and impairs antileishmanial T cell response (Chakraborty et al., 2005; Ghosh et al., 2014), due to altered conformation of MHC-II and dissociation from the cognate peptide (Roy et al., 2016). During transition of promastigotes to amastigotes, lipid classes greatly change, in terms of quantity and composition. While promastigotes show elevated levels of phospholipids, amastigotes display increased levels of cholesterol, which may derive from host cell membranes (Bouazizi-Ben Messaoud et al., 2017).

LDs are ubiquitous, cytoplasmic organelles, initially thought to be solely used for energy storage. However, recent evidences suggest that LDs have important roles in protein and lipid handling, as well as an impact on cellular stress and infection outcome. These organelles are composed by a core of intracellular neutral lipids, as triglycerides and cholesterol acids, surrounded by a lipid monolayer (Welte and Gould, 2017). Rabhi and colleagues showed that lipid droplets accumulate in the cytoplasm of *Leishmania*-infected macrophages. These organelles are located in the vicinity and even inside the PV (Rabhi et al., 2016; Rodríguez et al., 2017), suggesting that *Leishmania* amastigotes may take advantage of this high-energy source. Further, axenic *L. infantum* (= *chagasi*) amastigotes and metacyclic promastigotes were also shown to possess intracellular LDs, indicating that lipid accumulation may not be exclusively host derived (Araújo-Santos et al., 2014). LDs are a known source of eicosanoids, as both precursors and enzymes are present in these organelles (Bozza et al., 2011). The generation of prostaglandin (PG) E<sub>2</sub> in infected macrophages has been shown to contribute towards susceptibility (Bhattacharjee et al., 2016; Matte et al., 2001; Saha et al., 2014; Saini et al., 2020). Additionally, LB-driven PGF<sub>2</sub>α production was shown to facilitate macrophage infection (Araújo-Santos et al., 2014). Interestingly, a recent study showed that overexpression of PGF<sub>2</sub> synthase in *L. braziliensis* led to increased *in vitro* infectivity, highlighting a potential role for lipid mediators in disease progression and pathogenesis (Alves-Ferreira et al., 2020).

Another remarkable characteristic of LD is the ability of limiting cellular damage caused by ROS (Bailey et al., 2015a), which we can hypothesize to be extendable in the context of infections. *Leishmania* parasites may take shelter within lipid-laden macrophages, thus preventing the potentially damaging action of host microbicidal mechanisms. As such, considering the importance of these microbicidal molecules in the control of parasitic infections, it could be noteworthy to investigate possible parasite-induced manipulations of these organelles as evasion strategies.



The cellular and molecular events associated to alterations in lipid accumulation/metabolism and related pathways during *Leishmania* infection largely reproduce the findings obtained using animal models of leishmaniasis and infected patients. The majority of studies show a pronounced hypocholesterolemia and hypertriglyceridemia in VL patients (Liberopoulos et al., 2002; Seçmeer et al., 2006), suggesting the observed systemic lipid alteration as potent diagnostic and prognostic tools of VL (Lal et al., 2010; Mohapatra et al., 2014). Ghosh and colleagues have shown that gp63, present in *L. donovani* exosomes, cleaves DICER1, which in turn downregulates miRNP-122 production in infected hepatocytes and, consequently, cholesterol synthesis (Ghosh et al., 2013). Furthermore, hyperlipidemia was shown to protect against VL pathogenesis, through modulation of antileishmanial immune response (Ghosh et al., 2012). However, as this phenotype was induced through diet supplementation with cholesterol (1.25%), the role of other lipid families in disease progression remain to be addressed. A summary of the impact of lipids during *Leishmania* infection is presented in figure 8.

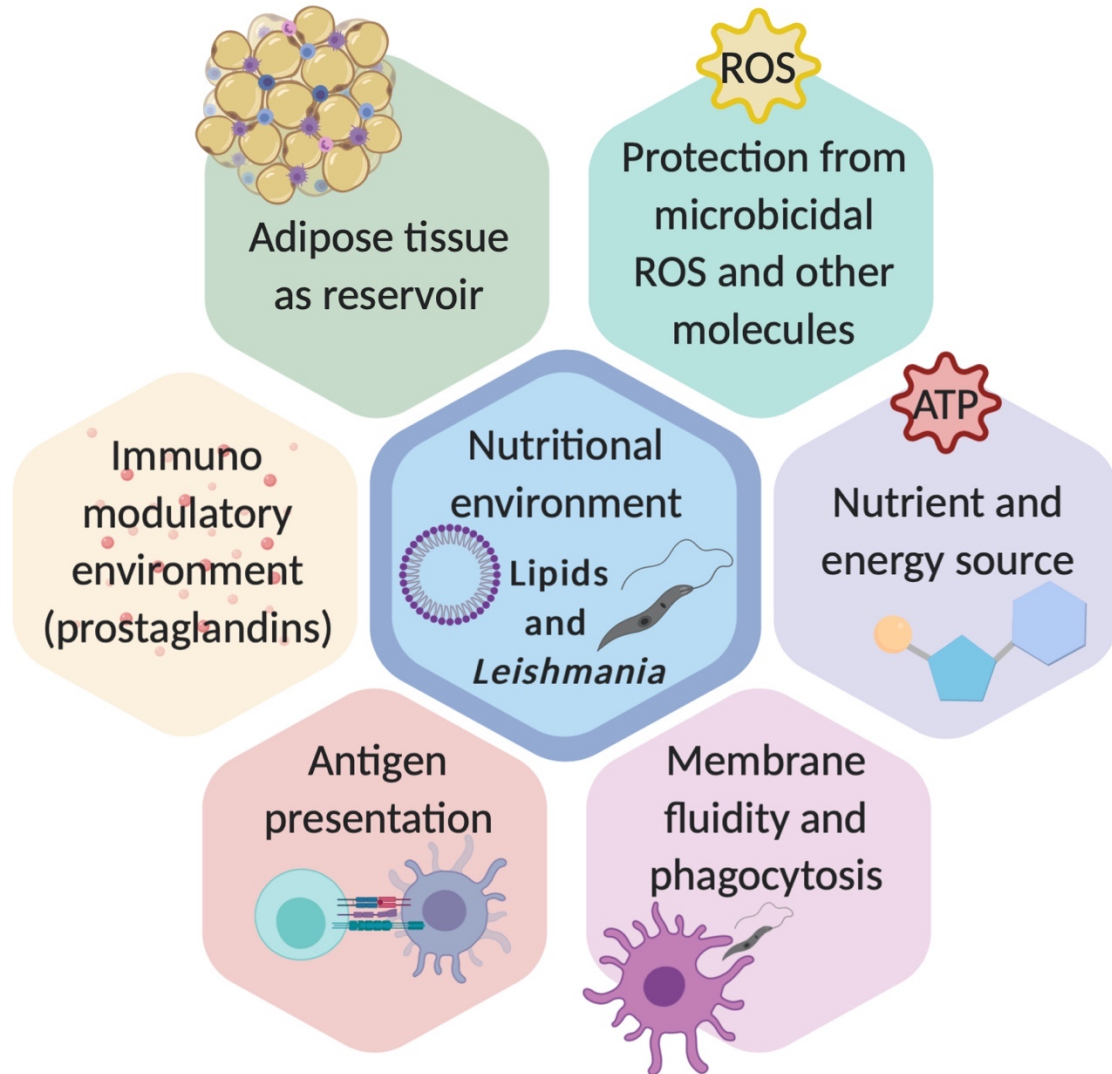


**Figure 8 The impact of lipid-rich environments in *Leishmania* infection.** Lipids may condition immune response and further impact *Leishmania* infection in distinct ways. Lipids may be used by *Leishmania* parasites as shields from host microbicidal mechanisms, while serving to fulfil parasites' metabolic needs. Further, lipids may impact membrane fluidity and, consequently phagocytosis, as well as antigen presentation by APCs. Specific lipid families, as the prostaglandins, may equally contribute to an immunomodulatory environment, permissive to *Leishmania* parasites. Additionally, the adipose tissue appears to have a crucial role as parasite reservoir. Created with BioRender.

#### 4.3 Adipose tissue: an (un)expected reservoir?

Long known as an energy storage tissue, the adipose tissue is populated by distinct immune cells and produces several cytokines and chemokines, which indicates that it may have a crucial role during infections (Ferrante, 2013a; Grant and Dixit, 2015). Furthermore, considering adipocytes as major hubs of lipid accumulation, it is interesting to hypothesize that parasites

infecting immune cells within the adipose tissue may gain access and hijack different types of nutrients (figure 9). In addition to this, the adipose tissue may serve as a reservoir, as the pharmacokinetics of antileishmanial drugs may impair their ability to reach certain tissues due to their lipophilicity. Our group has shown that *L. donovani*-infected fat-laden macrophages are insensitive to amphotericin B, which fails to produce the desired therapeutic outcome. Further, during a treatment regimen of overweighted mice with amphotericin B, we observed that *Leishmania* parasites may evade and *hide* in the adipose tissue as amphotericin B cannot fully penetrate this lipophilic environment (Moreira *et al.*, unpublished). Lipids have also been shown to have a protective role against ROS by preventing lipid peroxidation (Bailey *et al.*, 2015b). In accordance with this, we have seen an increase in peroxidation in lipid-enriched organs from *L. donovani*-infected mice (Mesquita *et al.*, unpublished).

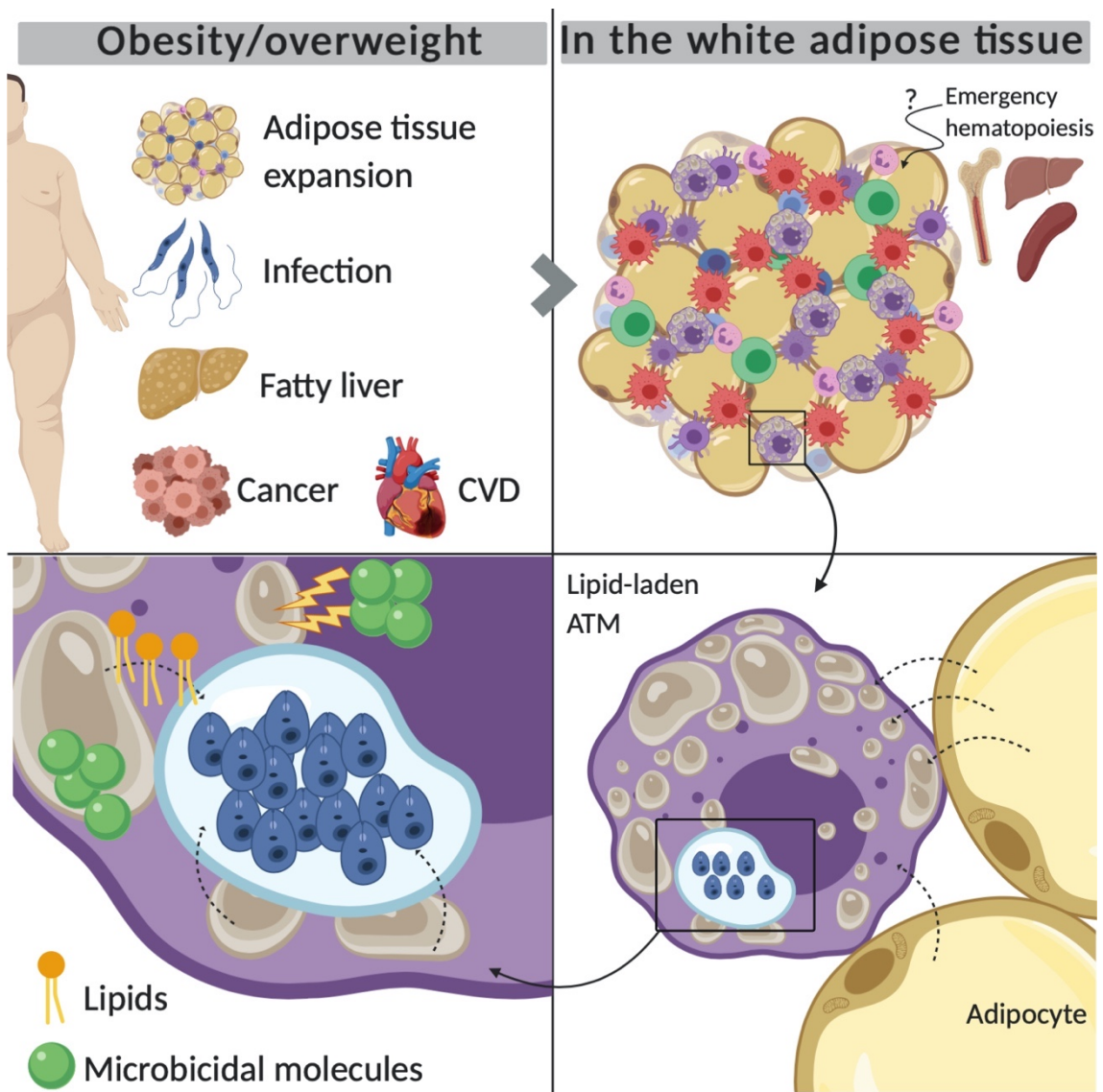


**Figure 9 The Adipose Tissue as a Reservoir of *Leishmania* Parasites.** Obesity and states of overweight originate adipose tissue expansion and increased susceptibility to infection, fatty liver disease, cancer and cardiovascular diseases. The adipose tissue becomes populated with a high proportion of immune cells, possibly driven from emergency hematopoiesis. In here, macrophages and other innate cells, possible of being infected by *Leishmania* parasites, accumulate lipids (possibly by uptaking them from dying adipocytes). Once inside the ATMs, these lipids may be scavenged by the parasites, contributing to their proliferation and survival (working as a carbon and energy source), whilst protecting the parasites from host-driven microbial molecules by forming a shield around the parasitophorous vacuole that prevents parasite killing. Created with BioRender.

Although there are scarce reports on the importance of the adipose tissue during infection, it seems that it can be protective or harmful for the host, depending on the infectious agent. In fact, protection against *Staphylococcus aureus* infection of the skin is dependent on the production of antimicrobial peptides by adipocytes, which expand shortly after infection (Zhang et al., 2015). Additionally, the adipose tissue may also constitute a reservoir of immune cells, prone to respond quickly and fight infections. Han and colleagues showed that the white adipose tissue represents a major hub of memory CD8 T cells, which expand and proliferate in order to protect the host against lethal pathogen challenge (Han et al., 2017). In opposition, diet-induced expansion and activation of adipose tissue memory T cells upon LCMV re-challenge culminates in fat necrosis, pancreatitis and eventually death (Misumi et al., 2019). The intracellular protozoan *Neospora caninum* was found in the adipose tissue, 7 days post-infection. Its presence on this tissue dysregulated immune populations, as seen by the increased numbers of macrophages, Tregs and T-bet<sup>+</sup> cells in distinct adipose tissues (Teixeira et al., 2015).

Considering the handful of advantages that parasites may acquire in lipid-rich environments, it is interesting to hypothesize that they may actively invade the adipose tissue. This is true for some parasites, as *Trypanosoma brucei*, *T. cruzi* and *Plasmodium* spp. Although only *T. cruzi* is known to directly infect adipocytes, *T. brucei* has been found on the interstitial spaces that exist between adipocytes, while *Plasmodium* parasites infect red blood cells present in the microvasculature that irrigates this tissue (Tanowitz et al., 2017). Martins and colleagues showed that obese mice infected with *L. major* present complex lesions with a higher parasite burden, when compared to standard chow-fed mice (Silva et al., 2018). A similar susceptibility phenotype was obtained upon infection of obese mice with *L. infantum*, which presented higher TNF- $\alpha$  and IL-6 and lower IL-10 levels in the gonadal adipose tissue (Sarnágua et al., 2016). However, whether these parasites infect the adipose tissue immune cells or if infected phagocytes migrate and accumulate in this tissue is still unknown.

As previously mentioned, F4/80<sup>+</sup> CD11c<sup>+</sup> macrophages infiltrate in the obese adipose tissue (Lumeng et al., 2007). Considering *Leishmania* parasites' host preference, one would expect

that adipose tissue macrophages (ATMs) and other innate populations could be infected. This would imply that either free amastigotes or infected phagocytes migrate and accumulate in the adipose tissue. This is interesting when considering that *Leishmania* infection promotes emergency hematopoiesis and skews hematopoietic stem cells towards a more permissive niche (Abidin et al., 2017). Further, it is theoretically possible that infected precursors leave the bone marrow and relocate on distinct sites, as the adipose tissue. However, how this occurs and what are the players involved remains to be elucidated and, at this point, the questions outnumber the answers.

## CHAPTER III AIMS AND RESULTS

## AIMS

In order for an immune cell to eliminate the eminent threat by conducting its *bona fide* function, the metabolic needs of such cell must be fulfilled. This implies the existence of a rich and permissive microenvironment, where nutrients are available *ad libitum*, and the unbiased implementation of suitable metabolic programs. However, when a pathogen invades an organism, the emergence of inflammation conditions dually the local microenvironment: in one hand, pathogens may subvert host cells with the aim of improving its own survival odds; on the other, local inflammation greatly changes the quality/quantities of several important intermediates, including cytokines, chemokines and metabolites, in an attempt to increase the success of pathogen elimination. In this scenario, immune cells may adopt unconventional behaviors that can derive from alterations on metabolite availability and altered balance of pro-/anti-inflammatory mediators. Further, infected cells will suffer pronounced alterations on its metabolic requirements, which may reveal pathogens' needs, while having to compete with other cells for scarce nutrients.

In this work, we propose to:

1. Study the modulation of innate immune cell metabolism and function during *Leishmania* infection:

Previous work has shown that *Leishmania* parasites hijack macrophagic energy sensors SIRT1 and AMPK, in order to promote a switch from glucose fermentation towards mitochondrial metabolism and the development of a permissive niche (Moreira et al., 2015). Interestingly, accumulation of intracellular lipids appears to condition greatly parasite proliferation and survival, disease outcome and progression, as these parasites may exploit LDs in their own advantage (Rabhi et al., 2016; Rodríguez et al., 2017). In the extreme of AMPK-induced macrophage polarization, the transcription factor HIF-1 $\alpha$  has been associated with inflammation and rewiring of distinct metabolic pathways. As such, we propose to address the role of this factor during visceral *Leishmania* infection. In this published work, we demonstrated that genetic deficiency of HIF-1 $\alpha$  in the myeloid compartment, which targets mainly macrophages, promotes lipogenesis via modulation of BNIP3/mTOR/SREBP-1c axis. Furthermore, susceptibility to *Leishmania donovani* can be reverted both *in vitro* and *in vivo* through inhibition of fatty acid synthesis, which restores antileishmanial functions (Mesquita et al., 2020).

## 2. Understand the impact of T cell exhaustion and immunosuppression during chronic VL:

During visceral leishmaniasis, T cells have a very important role in the development of a protective response that culminates in pathogen clearance. However, it has been shown that disease progression in humans drives CD8 T cell exhaustion, thus hampering their cytotoxic function (Gautam et al., 2014). T cell exhaustion represents a state of T cell dysfunction, mainly characterized by loss of effector functions and expression of inhibitory receptors. Exhaustion prevents optimal control of both infections and tumors and reversion of this state represents a desired therapeutic avenue (Wherry, 2011). We hypothesize that the susceptibility previously observed in myeloid-deficient HIF-1 $\alpha$  (mHIF1 $\alpha$ <sup>-/-</sup>) mice (Mesquita et al., 2020) could be partially due to an impairment of T cell function in infected organs, possibly representing a phenomenon of T cell exhaustion. We showed that chronically infected mHIF1 $\alpha$ <sup>-/-</sup> mice display lymphocyte infiltration in the spleen and liver, which is consistent with increased frequency and number of CD4 and CD8 T cells. However, these cells do not appear to have fully functional anti-leishmanial functions, as they express high levels of inhibitory marker TIM-3, as well as impaired cytokine production. Further, an increased number of IL-10-producing cells, within the myeloid population, is observed, when compared to WT counterparts. This may suggest that the absence of HIF-1 $\alpha$  in the myeloid compartment dysregulates T cell responses, thus promoting the progression of disease (Mesquita *et al.*, unpublished work).

Considering the current evidences that highlight T cell function in infection outcome, we also decided to address the dynamic impact of IL-10, a major immunosuppressive cytokine, in visceral leishmaniasis and T cell dysfunction. In this published work, we took advantage of the pMT-10 mouse model, in which IL-10 was induced by zinc sulfate administration. Using this model, we unveiled the crucial impact of IL-10 overexpression in the early steps of infection, which conditioned the late expansion of multifunctional CD4 T cells and contributed to the observed susceptibility (Mesquita et al., 2018b).



3. Unveil the role of the adipose tissue as a central hub for parasite survival and disease progression:

We have recently showed that macrophages with higher lipid accumulation are more susceptible to *Leishmania* infection (Mesquita et al., 2020). Moreover, previous work from our group has demonstrated that treatment with amphotericin B is less efficient in promoting parasite elimination both *in vitro*, using infected fat-laden macrophages, and *in vivo*, using a model of diet-induced overweight (Moreira *et al.*, unpublished data). This suggests a major role of the adipose tissue in the therapeutic response of antileishmanial drugs and highlights potential alterations in tissue immunity that contribute to susceptibility towards infection.

As such, we propose to address the role of adipose tissue during *Leishmania* infection, as we have already observed that these parasites are capable of accumulating in the white adipose tissue.

## RESULTS

### **The Absence of HIF-1 $\alpha$ Increases Susceptibility to *Leishmania donovani* Infection via Activation of BNIP3/mTOR/SREBP-1c Axis.**

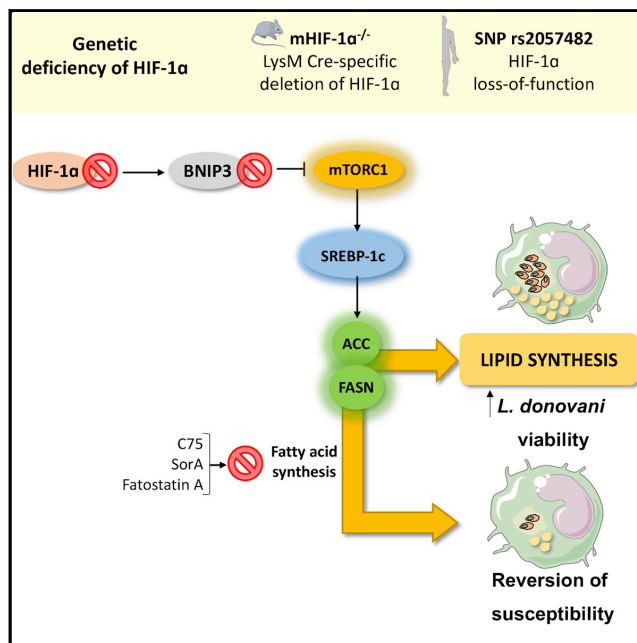
Inês Mesquita, Carolina Ferreira, Diana Moreira, George Eduardo Gabriel Kluck,  
Ana Margarida Barbosa, Egídio Torrado, Ricardo Jorge Dinis-Oliveira, Luís Gafeira Gonçalves,  
Charles-Joly Beuparlant, Arnaud Droit, Luciana Berod, Tim Sparwasser, Neelam Bodhale,  
Bhaskar Saha, Fernando Rodrigues, Cristina Cunha, Agostinho Carvalho, António Gil Castro,  
Jérôme Estaquier and Ricardo Silvestre

Published in *Cell Reports*, 30(12), pp. 4052-4064.e7. doi: 10.1016/j.celrep.2020.02.098

# Cell Reports

## The Absence of HIF-1 $\alpha$ Increases Susceptibility to *Leishmania donovani* Infection via Activation of BNIP3/mTOR/SREBP-1c Axis

### Graphical Abstract



### Authors

Inês Mesquita, Carolina Ferreira, Diana Moreira, ..., António Gil Castro, Jérôme Estaquier, Ricardo Silvestre

### Correspondence

estaquier@yahoo.fr (J.E.), ricardosilvestre@med.uminho.pt (R.S.)

### In Brief

Mesquita et al. show that genetic deficiency of HIF-1 $\alpha$  in the myeloid compartment promotes *de novo* lipogenesis through the BNIP3/mTOR/SREBP-1c axis. This is associated with higher susceptibility to *Leishmania donovani* infection, which is reduced upon pharmacological inhibition of fatty acid synthesis.

### Highlights

- HIF-1 $\alpha$  is a protective factor against *Leishmania donovani* infection
- In absence of HIF-1 $\alpha$ , lipogenesis is induced via BNIP3/mTOR/SREBP-1c modulation
- Blockage of lipogenesis reverts HIF-1 $\alpha$ -associated *Leishmania* susceptibility
- *HIF1A* polymorphism correlates with susceptibility to infection



Mesquita et al., 2020, Cell Reports 30, 4052–4064  
March 24, 2020 © 2020 The Authors.  
<https://doi.org/10.1016/j.celrep.2020.02.098>

CellPress

# The Absence of HIF-1 $\alpha$ Increases Susceptibility to *Leishmania donovani* Infection via Activation of BNIP3/mTOR/SREBP-1c Axis

Inês Mesquita,<sup>1,2</sup> Carolina Ferreira,<sup>1,2</sup> Diana Moreira,<sup>1,2,16</sup> George Eduardo Gabriel Kluck,<sup>1,2,3,17</sup> Ana Margarida Barbosa,<sup>1,2</sup> Egidio Torrado,<sup>1,2</sup> Ricardo Jorge Dinis-Oliveira,<sup>4,5,6</sup> Luís Gafeira Gonçalves,<sup>7</sup> Charles-Joly Beauparlant,<sup>8,9</sup> Arnaud Droit,<sup>8,9</sup> Luciana Berod,<sup>10</sup> Tim Sparwasser,<sup>11</sup> Neelam Bodhale,<sup>12</sup> Bhaskar Saha,<sup>12,13,14</sup> Fernando Rodrigues,<sup>1,2</sup> Cristina Cunha,<sup>1,2</sup> Agostinho Carvalho,<sup>1,2</sup> António Gil Castro,<sup>1,2</sup> Jérôme Estaquier,<sup>9,15,\*</sup> and Ricardo Silvestre<sup>1,2,18,\*</sup>

<sup>1</sup>Microbiology and Infection Research Domain (MIRD), Life and Health Sciences Research Institute (ICVS), School of Medicine, University of Minho, 4710-057 Braga, Portugal

<sup>2</sup>ICVS/3B's-PT Government Associate Laboratory, Braga/Guimarães, Portugal

<sup>3</sup>Laboratory of Lipid and Lipoprotein Biochemistry, Medical Biochemistry Institute, Federal University of Rio de Janeiro, 21941-901 Rio de Janeiro, Brazil

<sup>4</sup>Department of Public Health and Forensic Sciences, and Medical Education, Faculty of Medicine, University of Porto, 4200-319 Porto, Portugal

<sup>5</sup>Department of Sciences, IINFACTS-Institute of Research and Advanced Training in Health Sciences and Technologies, University Institute of Health Sciences (IUCS), CESPU, CRL, 4585-116 Gandra, Portugal

<sup>6</sup>UCIBIO-REQUIMTE, Laboratory of Toxicology, Department of Biological Sciences, Faculty of Pharmacy, University of Porto, 4050-313 Porto, Portugal

<sup>7</sup>Instituto de Tecnologia Química e Biológica António Xavier, Universidade Nova de Lisboa, 2780-157 Oeiras, Portugal

<sup>8</sup>Département de Médecine Moléculaire-Faculté de Médecine, Université Laval, Québec, QC G1V 0A6, Canada

<sup>9</sup>Centre de Recherche du CHU de Québec-Université Laval, Québec, QC G1V 4G2, Canada

<sup>10</sup>Institute of Infection Immunology, TWINCORE, Centre for Experimental and Clinical Infection Research, A Joint Venture between the Medical School Hannover (MHH) and the Helmholtz Centre for Infection Research (HZI), Hannover, Niedersachsen 30625, Germany

<sup>11</sup>Department of Medical Microbiology and Hygiene, Medical Center of the Johannes Gutenberg-University of Mainz, Obere Zahlbacherstrasse, 6755131 Mainz, Germany

<sup>12</sup>National Centre for Cell Science, 411007 Pune, India

<sup>13</sup>Case Western Reserve University, Cleveland, OH 44106, USA

<sup>14</sup>Trident Academy of Creative Technology, 751024 Bhubaneswar, Odisha, India

<sup>15</sup>INSERM U1124, Université de Paris, 75006 Paris, France

<sup>16</sup>Present address: School of Biochemistry and Immunology, Trinity Biomedical Sciences Institute, Trinity College Dublin, 152-160 Pearse Street, Dublin 2, Ireland

<sup>17</sup>Present address: Department of Biochemistry and Biomedical Sciences, Thrombosis and Atherosclerosis Research Institute (TaARI), David Braley Cardiac, Vascular and Stroke Research Institute, McMaster University, Hamilton General Hospital Campus, Hamilton Health Sciences, 237 Barton St. E., Hamilton, ON L8L 2X2, Canada

<sup>18</sup>Lead Contact

\*Correspondence: [estaquier@yahoo.fr](mailto:estaquier@yahoo.fr) (J.E.), [ricardosilvestre@med.uminho.pt](mailto:ricardosilvestre@med.uminho.pt) (R.S.)

<https://doi.org/10.1016/j.celrep.2020.02.098>

## SUMMARY

Hypoxia-inducible factor-1 alpha (HIF-1 $\alpha$ ) is considered a global regulator of cellular metabolism and innate immune cell functions. Intracellular pathogens such as *Leishmania* have been reported to manipulate host cell metabolism. Herein, we demonstrate that myeloid cells from myeloid-restricted HIF-1 $\alpha$ -deficient mice and individuals with loss-of-function *HIF1A* gene polymorphisms are more susceptible to *L. donovani* infection through increased lipogenesis. Absence of HIF-1 $\alpha$  leads to a defect in BNIP3 expression, resulting in the activation of mTOR and nuclear translocation of SREBP-1c. We observed the induction of lipogenic gene transcripts, such as FASN, and lipid accumulation in infected HIF-1 $\alpha$ <sup>-/-</sup> macrophages. *L. donovani*-infected HIF-1 $\alpha$ -deficient

mice develop hypertriglyceridemia and lipid accumulation in splenic and hepatic myeloid cells. Most importantly, our data demonstrate that manipulating FASN or SREBP-1c using pharmacological inhibitors significantly reduced parasite burden. As such, genetic deficiency of HIF-1 $\alpha$  is associated with increased lipid accumulation, which results in impaired host-protective anti-leishmanial functions of myeloid cells.

## INTRODUCTION

Pathogen-induced hijacking of host cell metabolism results in the dampening of host defense mechanisms and is therefore considered an important host-pathogen interface (Naderer and McConville, 2008; McConville, 2016). Carbohydrate metabolism was initially proposed to play a central role in providing a



nutrient-rich niche for pathogen multiplication and survival, as demonstrated in *Trypanosoma cruzi*, *T. brucei*, *Toxoplasma gondii*, and *Leishmania donovani* infections (Caradonna et al., 2013; Blume et al., 2015; Ghosh et al., 2015; Smith et al., 2017). Other carbon sources, such as lipids, have also been proposed to contribute to the outcome of infection (Bozza et al., 2009). Dysregulated lipid metabolism poses a social health problem worldwide due to the high prevalence of intertwined pathologies such as obesity, coronary heart disease, nonalcoholic fatty liver disease, and diabetes. In the past few years, these pathologies have been gaining relevance in developing countries burdened by infectious diseases. These recently found nutritional alterations may favor pathogen dissemination, which poses a new challenge in the clinics.

Hypoxia-inducible factor 1 alpha (HIF-1 $\alpha$ ) was initially identified as an oxygen-sensitive transcription factor involved in the regulation of the homeostatic response to hypoxia (Weidemann and Johnson, 2008; Thompson, 2016; Choudhry and Harris, 2018). In innate immune cells, HIF-1 $\alpha$  activation in response to pathogen-associated molecular patterns (PAMPs) (Peyssonnaud et al., 2007; Spirig et al., 2010; Cheng et al., 2014) or pathogenic agents (Werth et al., 2010) reprograms both carbohydrate and lipid metabolism and establishes an inflammatory phenotype (Palazon et al., 2014). We and others previously reported that in *Leishmania*-infected macrophages, metabolism of carbohydrate and lipid is altered (Rabhi et al., 2012; Moreira et al., 2015) and HIF-1 $\alpha$  expression is upregulated (Degrossoli et al., 2007; Singh et al., 2012; Alonso et al., 2019). Despite the implications for the metabolic networks in the immune functions of macrophages (Na et al., 2016), the impact of HIF-1 $\alpha$  in the immune-metabolic regulation of macrophages, as modeled here with *Leishmania donovani* infection, remains elusive.

Herein, we demonstrate that HIF-1 $\alpha$  is a resistance factor against experimental visceral leishmaniasis (VL) caused by *Leishmania donovani*. The analysis of three distinct mouse strains with disparate susceptibility to the infection demonstrated that HIF-1 $\alpha$  expression is positively associated with the capacity to resist VL. To further dissect the role of this transcription factor, a murine model of myeloid HIF-1 $\alpha$  deficiency (*mHIF-1 $\alpha$ <sup>-/-</sup>* mice) was used to explore the association between HIF-1 $\alpha$  expression and infection outcome. Among the few genes altered between infected *HIF-1 $\alpha$ <sup>-/-</sup>* and wild-type (WT) myeloid cells, the absence of HIF-1 $\alpha$  prevented BCL2-interacting protein 3 (BNIP3) upregulation, resulting in mammalian target of rapamycin (mTOR) activation. Consequently, sterol regulatory element-binding protein-1c (SREBP-1c) is activated leading to the upregulation of key lipogenic enzymes, acetyl-CoA carboxylase (ACC) and fatty acid synthase (FASN), thus contributing to fatty acid synthesis. *L. donovani*-infected *mHIF-1 $\alpha$ <sup>-/-</sup>* mice developed a dysregulated lipid metabolism leading to lipid accumulation in both liver and spleen, thus favoring parasite multiplication. Pharmacological inhibition of FASN and SREBP-1c significantly reduced the susceptibility to infection and lipid dysregulation, demonstrating the causal relationship between HIF-1 $\alpha$ , lipid accumulation, and *L. donovani* susceptibility. Furthermore, by associating the single-nucleotide polymorphism (SNP) rs2057482 in human *HIF1A* gene with lower levels of HIF-1 $\alpha$ , we demonstrated the clinical relevance of this SNP during a protozoan infection.

## RESULTS

### HIF-1 $\alpha$ Expression Is Associated with Increased Resistance against *Leishmania donovani* Infection

Because HIF-1 $\alpha$ <sup>-/-</sup> macrophages are more susceptible to *Leishmania major* infection (Schatz et al., 2016), we first evaluated HIF-1 $\alpha$  transcription levels during *in vivo* *L. donovani* infection of three mouse strains with distinct outcomes to visceral leishmaniasis (VL): BALB/c as susceptible, 129/Sv as resistant, and C57BL/6 as intermediate resistant hosts (Bodhale et al., 2018). Splenic HIF-1 $\alpha$  transcription levels positively correlated with increased resistance to infection: the resistant 129/Sv mice had the highest levels of HIF-1 $\alpha$  transcription, whereas C57BL/6 mice had less HIF-1 $\alpha$  transcripts and BALB/c mice had the lowest HIF-1 $\alpha$  levels (Figure 1A). To further dissect the role of this transcription factor during infection, we took advantage of myeloid-restricted *HIF-1 $\alpha$ <sup>-/-</sup>* mice (*mHIF-1 $\alpha$ <sup>-/-</sup>*), in which LysM Cre-specific deletion affects mostly monocytes, mature macrophages, and neutrophils (Abram et al., 2014). Although *L. donovani*-infected peritoneal macrophages from both WT and *mHIF-1 $\alpha$ <sup>-/-</sup>* mice displayed a similar level of phagocytosis (Figure 1B), we observed at 5 days post-infection that parasite viability increases in *HIF-1 $\alpha$ <sup>-/-</sup>* macrophages when compared with WT counterparts (Figure 1C). As expected, HIF-1 $\alpha$  activation with iron-chelating agent deferoxamine (DFX) resulted in lower parasite viability in WT macrophages and no alteration in *mHIF-1 $\alpha$ <sup>-/-</sup>* macrophages. We observed similar results with a distinct *L. donovani* strain or using a second visceral *Leishmania* species, *L. infantum* (Figure S1A). To determine whether *L. donovani* parasites display preferential tropism toward WT or *HIF-1 $\alpha$ <sup>-/-</sup>* macrophages, which could explain alterations in parasite viability, we co-cultured CD45.1 WT and CD45.2 *HIF-1 $\alpha$ <sup>-/-</sup>* macrophages and infected them with carboxyfluorescein succinimidyl ester (CFSE)-labeled promastigotes. No differences were found in the percentage of phagocytosis between WT and *HIF-1 $\alpha$ <sup>-/-</sup>* macrophages (Figure S1B), indicating that both macrophages comparably internalize the parasites. However, higher parasite viability was observed in *HIF-1 $\alpha$ <sup>-/-</sup>* macrophages (Figure 1D), suggesting HIF-1 $\alpha$  as a host-protective factor against infection. The analysis of prototypical M1-like (*Cxcl9* and *Nos2*) and M2-like (*Arg1* and *Fizz1*) genes (Murray et al., 2014) showed that the absence of HIF-1 $\alpha$  drives infected macrophages toward an anti-inflammatory phenotype, as shown by decreased *Cxcl9* and increased *Fizz1* transcriptional levels (Figure 1E). Furthermore, infected *HIF-1 $\alpha$ <sup>-/-</sup>* macrophages display an imbalance in inflammation with lower levels of interleukin 6 (IL-6) and tumor necrosis factor alpha (TNF- $\alpha$ ) and higher levels of IL-10 (Figure 1F). Altogether, our results indicate that HIF-1 $\alpha$  levels inversely associate with *Leishmania* infection.

### *L. donovani*-Infected *HIF-1 $\alpha$ <sup>-/-</sup>* Macrophages Failed to Upregulate BNIP3, Leading to the Activation of the mTOR Signaling Pathway

To further dissect the role of HIF-1 $\alpha$ , we analyzed macrophage transcriptome through RNA sequencing at 6 h post-infection. We only found 41 differentially regulated genes when comparing infected *mHIF-1 $\alpha$ <sup>-/-</sup>* and WT myeloid cells, with 27 downregulated and 14 upregulated in *HIF-1 $\alpha$ <sup>-/-</sup>* macrophages (Figure 2A).

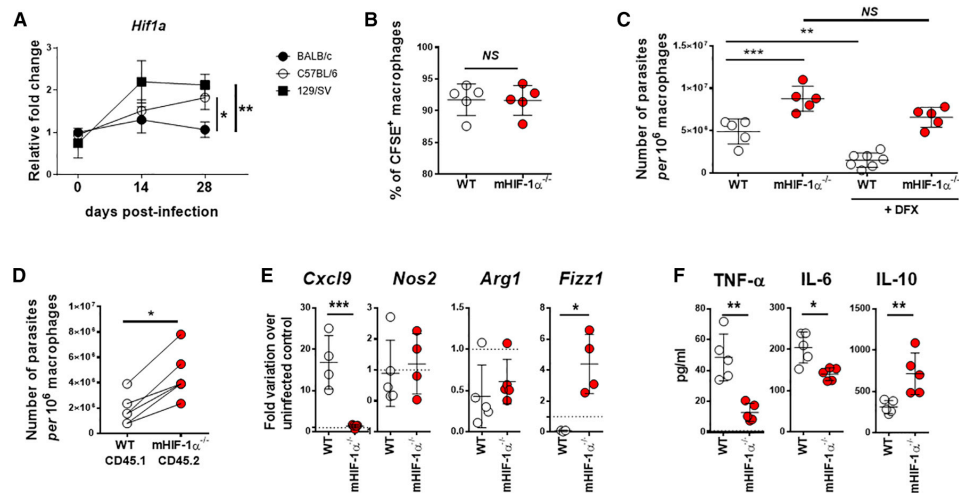


**Figure 1. HIF-1 $\alpha$  Expression Is Associated with Increased Resistance against *Leishmania donovani* Infection**

(A) The *Hif1a* transcription levels were quantified on splenic extracts of uninfected and 14- and 28-day *L. donovani*-infected BALB/c, C57BL/6, and 129/SV mice. (B) Peritoneal macrophages from WT and *mHIF-1 $\alpha$* <sup>-/-</sup> mice were infected with CFSE-labeled promastigotes. Phagocytosis was assessed 4 h post-infection by flow cytometry. (C) Peritoneal macrophages from WT and *mHIF-1 $\alpha$* <sup>-/-</sup> were infected and parasite burden was evaluated by quantifying *L. donovani* viability at 5 days post-infection. Deferoxamine (DFX) treatment was performed 24 h post-infection. (D) An equal amount of WT CD45.1 and *HIF-1 $\alpha$* <sup>-/-</sup> CD45.2 macrophages were co-cultured and infected with *L. donovani*. Parasite viability was determined. Lines represent the cells cultured in the same well. (E) qPCR analysis of the transcriptional levels of *Cxcl9*, *Nos2*, *Arg1*, and *Fizz1* 24 h post-infection. (F) Cytokines (TNF- $\alpha$ , IL-6, and IL-10) were quantified on the supernatant of both WT and *HIF-1 $\alpha$* <sup>-/-</sup> by ELISA. Data are shown as mean  $\pm$  SD; n = 5–7 mice/group. \*p < 0.05; \*\*p < 0.01; \*\*\*p < 0.001; NS, not significant.

No major changes were observed between uninfected macrophages, suggesting that HIF-1 $\alpha$  plays a minor role in macrophage basal phenotype (Figure S2). Given that HIF-1 $\alpha$  is a transcription factor, we focused on the genes and pathways downregulated in *L. donovani*-infected *mHIF-1 $\alpha$* <sup>-/-</sup> compared to WT. We found seven downregulated pathways in the absence of HIF-1 $\alpha$ , mostly related to cell response to hypoxia as expected (Figure 2B). Among the gene transcripts, we found that BCL2/adenovirus E1B 19-kDa-interacting protein 3 (BNIP3) was distinctively expressed in infected WT and *HIF-1 $\alpha$* <sup>-/-</sup> macrophages (Figure 2C). A quantitative PCR analysis confirmed that *Bnip3* transcriptional levels reach a maximum at 6 to 8 h post-infection with viable *L. donovani* in WT macrophages, while *Bnip3* fails to be expressed in the absence of HIF-1 $\alpha$  (Figure 2D). Furthermore, by western blot, lower BNIP3 levels were found in *HIF-1 $\alpha$* <sup>-/-</sup> macrophages when compared to WT macrophages 10 h post-infection (Figure 2E).

Because BNIP3 has been shown to contribute for the repression of mTOR via interaction with Ras-related GTPase Rheb (Li et al., 2007), we investigated whether the absence of HIF-1 $\alpha$  was associated with the activation of p70 S6 kinase, a downstream target of mTOR. For that, we evaluated by western blot the phosphorylation status of p70 S6 kinase. We observed an increase in p70 S6K phosphorylation in *HIF-1 $\alpha$* <sup>-/-</sup> macrophages, 10 h post-infection (Figure 2F), indicating that the mTOR pathway is activated in the absence of HIF-1 $\alpha$ . Furthermore, a

time dependency on mTOR activation was observed in *L. donovani*-infected *HIF-1 $\alpha$* <sup>-/-</sup> macrophages, as increased phosphorylation of p70 S6 kinase is not observed prior to 10 h and is maintained until 24 h post-infection (Figure S3A). Next, we sought to understand whether BNIP3 was responsible for controlling mTOR activation. Small interfering RNA (siRNA) against BNIP3 (Figure 2G) induces p70 S6K phosphorylation in WT macrophages infected with *L. donovani* (Figure 2H), demonstrating that BNIP3 represses the mTOR pathway in *L. donovani*-infected macrophages. Thus, our results support the idea that the absence of HIF-1 $\alpha$  by impairing BNIP3 expression induces the activation of mTOR during *L. donovani* infection.

#### **SREBP1c Activation in *HIF-1 $\alpha$* <sup>-/-</sup> Macrophages Is Responsible for De Novo Lipogenesis and Increased In Vitro Susceptibility to *L. donovani* Infection**

Previous works have showed that activation of the mTOR pathway positively regulates the activity of the SREBP-1c transcription factor (Porstmann et al., 2008; Düvel et al., 2010). SREBP-1c is well known to bind to the promoter regions of lipogenic genes, thus inducing lipid synthesis (Figure S3B). Although no differences were found in the transcriptional levels of the *Srebp1c* gene between infected WT and *HIF-1 $\alpha$* <sup>-/-</sup> macrophages (Figure S3C), we observed a significantly increased nuclear localization of this protein in infected *HIF-1 $\alpha$* <sup>-/-</sup> macrophages compared to WT (Figures 3A, S3D, and S3E). Because

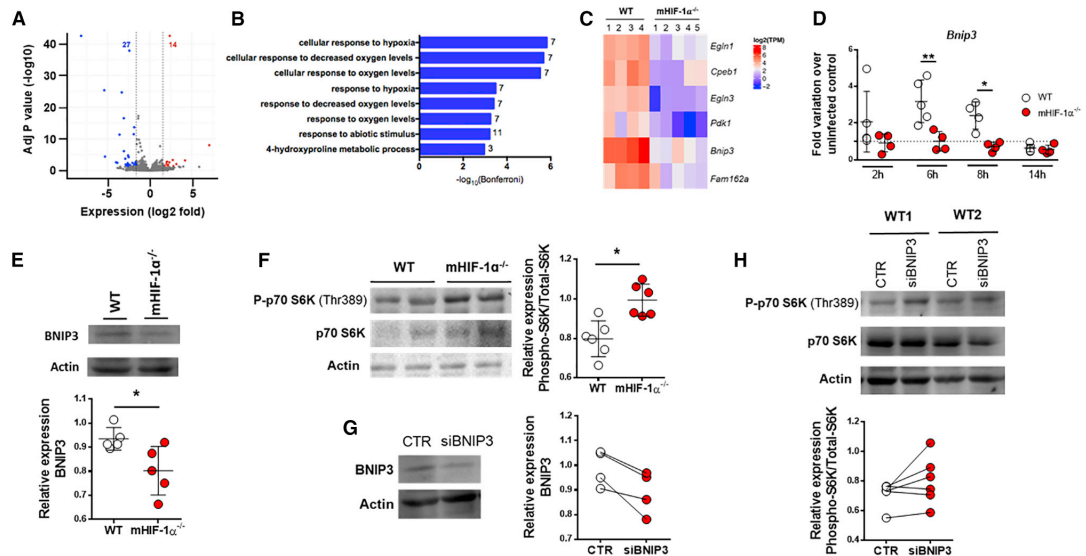


**Figure 2. *L. donovani*-infected *HIF-1 $\alpha$* <sup>-/-</sup> Macrophages Failed to Upregulate BNIP3, Leading to the Activation of the mTOR Signaling Pathway**

(A) Genome-wide transcriptome analysis of murine WT and *HIF-1 $\alpha$* <sup>-/-</sup> macrophages infected with *L. donovani* for 6 h. Expression values (log<sub>2</sub> fold) were plotted against the adjusted p value ( $-\log_{10}$ ) for the difference in expression. Annotated numbers indicate genes with significant differential expression: upregulated (red = 14) or downregulated (blue = 27), 1.5-fold or more in infected *HIF-1 $\alpha$* <sup>-/-</sup> macrophages relative to infected WT cells.

(B) Pathway analysis of significantly downregulated genes. The genes were divided into the top eight most represented pathways. The number of differentially expressed genes in each pathway is annotated in each bar.

(C) Genome-wide transcriptional profiles of murine WT and *HIF-1 $\alpha$* <sup>-/-</sup> macrophages infected with *L. donovani* (n = 4–5). Expression of genes (right margins) is presented as centered and “scaled” log<sub>2</sub> fluorescence intensity.

(D) qPCR analysis of the transcriptional levels of *Bnip3* 2, 6, 8, and 14 h post-infection.

(E) Western blot analysis and densitometry of BNIP3 and beta-actin.

(F) Western blot analysis and densitometry of phospho-p70 S6K, total p70 S6K, and beta-actin.

(G) Western blot analysis and densitometry of BNIP3 and beta-actin, after siBNIP3 transfection.

(H) Western blot analysis and densitometry phospho-p70 S6K, total p70 S6K, and beta-actin, after siBNIP3 transfection.

Data are shown as mean  $\pm$  SD; n = 4–5 mice/group. \*p < 0.05; \*\*p < 0.01.

SREBP-1c activation is associated with increased lipid synthesis (Chang et al., 2006; Sone et al., 2002), we started by assessing any potential lipid accumulation during infection. A semiquantitative analysis by high-performance thin layer chromatography (HPTLC) showed a significant increase of distinct lipid families, such as free fatty acids and triacylglycerol, in infected *HIF-1 $\alpha$* <sup>-/-</sup> macrophages (Figures S4A and S4B), suggesting a *Leishmania*-driven lipid accumulation in the absence HIF-1 $\alpha$ . In opposition, activation of HIF-1 $\alpha$  in WT macrophages using deferoxamine (DXF) led to reduced lipid accumulation (Figure S4C). Corroboratively, infected *HIF-1 $\alpha$* <sup>-/-</sup> macrophages had increased intracellular neutral lipids, even in co-culture with WT macrophages (Figures 3B–3D). Overall, acetyl-CoA is a convergent metabolite from different carbon sources in metabolism, namely glucose, glutamine, acetate, and lactate, that can fuel lipid synthesis. Interestingly, we observed a significantly increased acetate concentration in *L. donovani*-infected *HIF-1 $\alpha$* <sup>-/-</sup> macrophages, which is reduced in the presence of the SREBP-1c inhibitor fatostatin A (Figures 3E and 3F). Nuclear magnetic resonance (NMR)

analysis confirmed increased uptake of 2-<sup>13</sup>C-labeled acetate and its incorporation on the lipid fraction of infected *HIF-1 $\alpha$* <sup>-/-</sup> macrophages (Figures 3G, S5A, and S5B), suggesting acetate uptake as a result of enhanced fatty acid synthesis in infected *HIF-1 $\alpha$* <sup>-/-</sup> macrophages. Additionally, increased transcriptional levels of *Slc16a3* gene that codes for monocarboxylate transporter 4 (MCT4), were observed in infected *HIF-1 $\alpha$* <sup>-/-</sup> macrophages, which is in accordance with a higher acetate uptake in the absence of HIF-1 $\alpha$  (Figure 3H). To further confirm that extracellular acetate is an additional source for lipid synthesis, macrophages were cultured in a medium supplemented with dialyzed fetal bovine serum (dFBS), which is deprived of acetate (Figure 3I). A significant reduction of intracellular neutral lipids was observed in *L. donovani*-infected *HIF-1 $\alpha$* <sup>-/-</sup> macrophages cultured in acetate deprivation (Figure 3J). Medium supplementation with acetate (5 mM) led to a significant neutral lipid accumulation in both WT and *HIF-1 $\alpha$* <sup>-/-</sup> and macrophages (Figure 3J), providing a causal link between acetate consumption and lipid accumulation in macrophages infected with *L. donovani*.

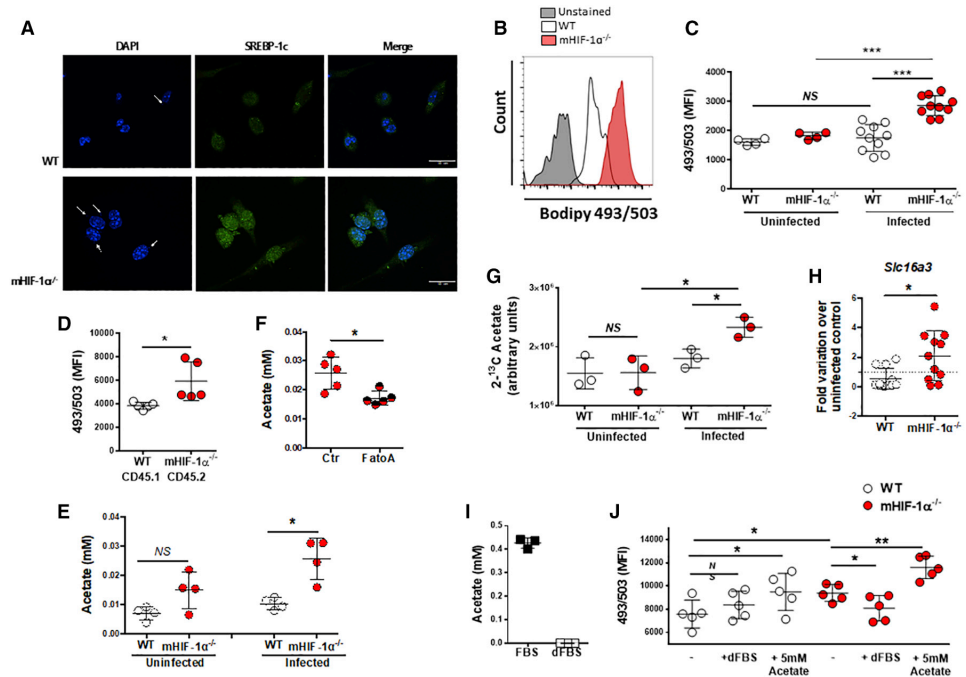


**Figure 3. SREBP1c Activation in *mHIF-1 $\alpha$ <sup>-/-</sup>* Is Responsible for Acetate-Driven *De Novo* Lipid Accumulation and Susceptibility to Infection**  
 (A) Immunofluorescence confocal microscopy of *Leishmania*-infected WT or *HIF-1 $\alpha$ <sup>-/-</sup>* macrophages. At 24 h post-infection, macrophages were fixed and probed with an anti-SREBP1c antibody; green, SREBP1c; blue, DNA (DAPI). The white arrows point to *L. donovani* nucleus. Scale 10  $\mu$ m.  
 (B) Representative histogram of Bodipy 493/503 staining by flow cytometry at 5 days post-infection.  
 (C) Intracellular neutral lipids in infected and uninfected WT and *HIF-1 $\alpha$ <sup>-/-</sup>* macrophages.  
 (D) Intracellular neutral lipids in infected co-cultured WT CD45.1 and *HIF-1 $\alpha$ <sup>-/-</sup>* CD45.2 macrophages.  
 (E) Acetate quantification in intracellular extracts from infected WT and *HIF-1 $\alpha$ <sup>-/-</sup>* macrophages, 5 days post-infection.  
 (F) Acetate quantification in intracellular extracts from infected *HIF-1 $\alpha$ <sup>-/-</sup>* macrophages in the absence or presence of fatostatin A.  
 (G) Intracellular accumulation of the <sup>13</sup>C label that was incorporated in 2-<sup>13</sup>C-labeled acetate was determined in lysates from uninfected and *L. donovani*-infected WT or *HIF-1 $\alpha$ <sup>-/-</sup>* peritoneal macrophages upon 24 h by NMR.  
 (H) qPCR analysis of the transcriptional levels of *Slc16a3* 24 h post-infection.  
 (I) Acetate concentration in RPMI media, supplemented with regular fetal bovine serum (FBS) or dialyzed FBS (dFBS).  
 (J) WT or *HIF-1 $\alpha$ <sup>-/-</sup>* macrophages cultured in standard conditions (–), with dialyzed FBS (+ Dial. FBS), or in the presence of 5 mM acetate (+5 mM acetate) were infected with *L. donovani*. Intracellular neutral lipids were quantified as abovementioned. Data are shown as mean  $\pm$  SD; n = 4–11 mice/group. \*p < 0.05; \*\*p < 0.01; \*\*\*p < 0.001.

Following the hypothesis that lipogenesis is occurring in *L. donovani*-infected *HIF-1 $\alpha$ <sup>-/-</sup>* macrophages, we analyzed the levels of fatty acid synthase (*Fasn*) and acetyl-CoA carboxylase (*Acaca*), which are two key enzymes from the *de novo* fatty acid synthesis (Figure S4D). These two genes were found to be increased in infected *HIF-1 $\alpha$ <sup>-/-</sup>* macrophages (Figure 4A). Inhibition of upstream players mTOR and SREBP-1c, with rapamycin and fatostatin A, respectively, abolished the induction of *Fasn* and *Acaca* transcription observed in infected *HIF-1 $\alpha$ <sup>-/-</sup>* macrophages (Figure 4A). The protein levels of FASN were consistently increased in infected *HIF-1 $\alpha$ <sup>-/-</sup>* macrophages (Figure 4B). Moreover, flow-cytometric analyses of palmitate internalization revealed no difference between WT and *HIF-1 $\alpha$ <sup>-/-</sup>* macrophages, corroborating lipogenesis as the main source of lipid accumulation (Figure S4E). To address

the causal relationship between lipogenesis and increased parasite growth and survival, we inhibited FASN and ACC with C75 and Sorafen A (SorA), respectively. Both treatments led to a reduction in parasite viability observed in *HIF-1 $\alpha$ <sup>-/-</sup>* cells (Figure 4C), along with a decrease of approximately 25% of total intracellular lipids (Figure S4F). Moreover, fatostatin A significantly reduced the parasite viability in *HIF-1 $\alpha$ <sup>-/-</sup>* macrophages (Figure 4D), indicating that lipid biogenesis is likely associated to an upstream activation of FASN by SREBP-1c and leading to the establishment of a permissive niche for parasite proliferation and survival. Of note, although lipid storage and metabolism have been associated with HIF-2 activation (Rankin et al., 2009; Liu et al., 2014), we observed a negligible role for HIF-2 in lipid metabolism in infected macrophages (data not shown). These data demonstrate that



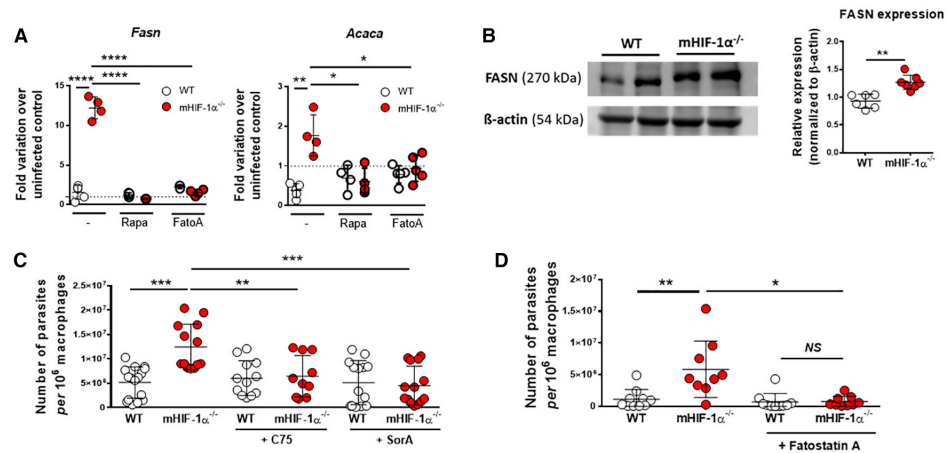


**Figure 4. Increased Susceptibility to *Leishmania donovani* Infection in the Absence of HIF-1 $\alpha$  Is Associated with *De Novo* Lipid Accumulation**  
 (A) qPCR analysis of the transcriptional levels of *Acaca* and *Fasn* 24 h post-infection.  
 (B) Western blot analysis and densitometry of FASN and beta-actin 24 h post-infection.  
 (C) *L. donovani* viability was assessed 5 days post-infection, upon C75 and sorafenin A (SorA) treatment.  
 (D) *L. donovani* viability was assessed 5 days post-infection, after fatostatin A treatment.  
 Data are shown as mean  $\pm$  SD; n = 4–15 mice/group. \*p < 0.05; \*\*p < 0.01; \*\*\*p < 0.001.

*Leishmania* infection of *HIF-1α*<sup>-/-</sup> macrophages *in vitro* is associated with lipogenesis that contributes to parasite growth.

#### HIF-1 $\alpha$ Deficiency in the Myeloid Compartment Correlates with *In Vivo* Lipid Accumulation and Higher *L. donovani* Burdens

To determine the *in vivo* impact of HIF-1 $\alpha$  on parasite growth and lipid metabolism, we infected *mHIF-1α*<sup>-/-</sup> mice with *L. donovani*. Assessment of parasite load at the indicated time points revealed that *mHIF-1α*<sup>-/-</sup> mice exhibited higher parasite burdens in the spleen and in the liver, compared to WT mice (Figure 5A). Splenic and hepatic myeloid cells (gated on CD11b<sup>+</sup>Ly6C<sup>+</sup>) of infected *mHIF-1α*<sup>-/-</sup> mice displayed higher intracellular neutral lipids (Figure 5B). A similar phenotype regarding parasite burden and lipid accumulation in parasitized organs was observed using a 10-fold lower *L. donovani* inoculum (Figures S6A and S6B), demonstrating that the observed phenotype is independent of the initial inoculum. We also observed a positive correlation between splenic intracellular lipid content and parasite burden in 2-week-infected *mHIF-1α*<sup>-/-</sup> mice (Figure 5C). Corroborating our *in vitro* observations, spleen homogenates from infected *mHIF-1α*<sup>-/-</sup> mice showed significantly higher transcriptional levels of *Fasn* and *Acaca* (Figure 5D). We observed a pronounced Oil Red O staining in frozen liver sections from infected *mHIF-1α*<sup>-/-</sup> mice, indicating generalized lipid accumulation (Figure 5E). Two weeks post-infection, higher levels of cholesterol and triglycerides were detected in the serum of *mHIF-1α*<sup>-/-</sup> mice (Figure 5F). The levels of HDL were decreased in infected *mHIF-1α*<sup>-/-</sup> mice, while LDL levels remained unaltered (Figure S6C). Similar observations regarding lipid accumulation in the serum were made at 8 weeks post-infection (data not shown). Because lipid dysregulation may be a consequence of liver damage, we analyzed the levels of

aspartate and alanine transaminase (AST and ALT, respectively) as biomarkers for hepatic injury. Both were significantly elevated in infected *mHIF-1α*<sup>-/-</sup> mice at 2 weeks post-infection (Figure 5G). Altogether, these results suggest that the absence of HIF-1 $\alpha$  facilitates parasite growth through lipid accumulation and dysregulation of its metabolism.

#### Targeting Lipid Biosynthesis *In Vivo* Reverts *mHIF-1α*<sup>-/-</sup>-Associated Susceptibility

As lipids accumulated during experimental infection of *mHIF-1α*<sup>-/-</sup> mice, we then hypothesized that the blockade of lipid synthesis would modulate the susceptibility phenotype and improve the outcome of the infection. We infected both WT and *mHIF-1α*<sup>-/-</sup> mice and treated the animals with FASN or SREBP-1c inhibitors C75 and fatostatin A, respectively (Figure 6A). We observed that the FASN or SREBP-1c blockade reverted the observed susceptibility in *mHIF-1α*<sup>-/-</sup> mice, as parasite burden was significantly reduced in both spleen and liver (Figure 6B). *L. donovani*-infected and treated *mHIF-1α*<sup>-/-</sup> mice displayed lower levels of cholesterol and triglycerides in the serum, compared to the infected mice on placebo (Figure 6C). The levels of ALT, AST, creatine, and urea in the serum remained unchanged upon drug treatment, suggesting that acute treatment with C75 and fatostatin A is not associated with liver or kidney toxicity (Figures S6D and S6E). Our data suggest that lipid biosynthesis occurring in infected *mHIF-1α*<sup>-/-</sup> mice contributes for the increased susceptibility toward *L. donovani* infection.

#### Genetic Variation in Human *HIF1A* Promotes Increased Parasite Viability and Lipid Accumulation

Genetic variations in human *HIF1A* have been reported to influence several diseases (Hlatky et al., 2007; Kim et al., 2008;

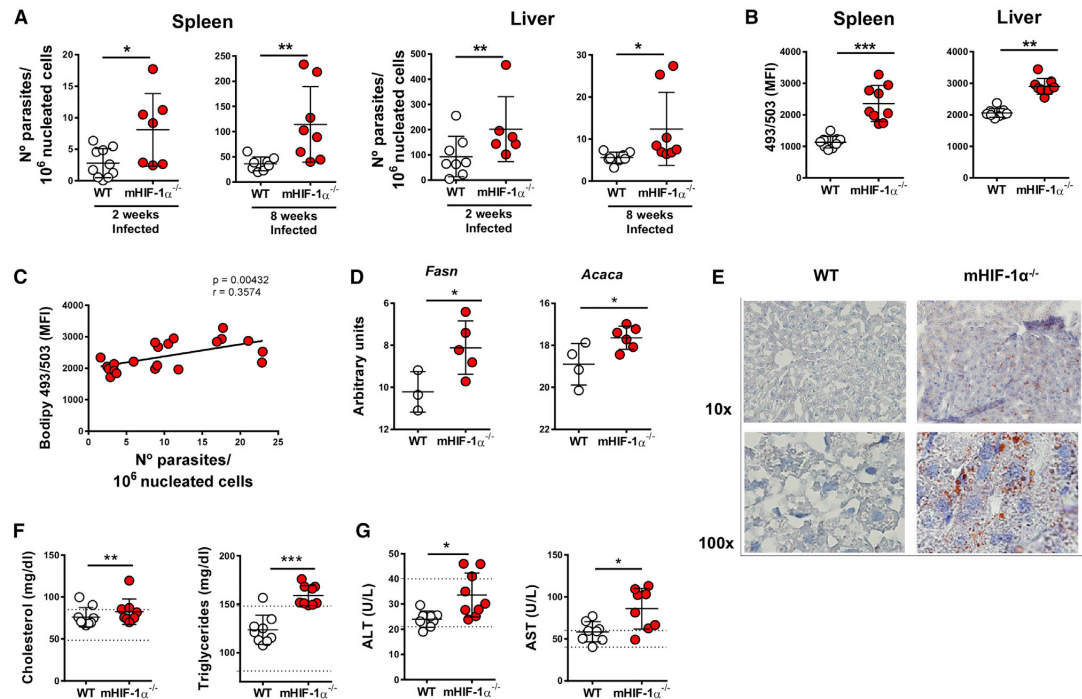


**Figure 5. HIF-1 $\alpha$  Deficiency in the Myeloid Compartment Correlates with Higher *L. donovani* Burdens and Systemic Lipid Dysregulation**

(A) Parasite burden in the spleen and liver of WT and *mHIF-1 $\alpha$ <sup>-/-</sup>* 2 and 8 weeks post-infection. (B) Quantification of intracellular neutral lipids by flow cytometry using Bodipy 493/503, on gated splenic and hepatic CD11b<sup>+</sup> cells. (C) Correlation between intracellular neutral lipids on CD11b<sup>+</sup> cells and parasite burden in the spleen of *mHIF-1 $\alpha$ <sup>-/-</sup>* mice. (D) qPCR analysis of the transcriptional levels of *Acaca* and *Fasn* in spleen homogenates. (E) Liver sections with Oil Red O staining and H&E counterstaining. (F and G) Cholesterol and triglycerides (F) and ALT and AST levels (G) on the spleen and liver extracts. All data from (B) to (G) were obtained with samples from WT and/or *mHIF-1 $\alpha$ <sup>-/-</sup>* 2 weeks post-infection. Data are shown as mean  $\pm$  SD; n = 3–10 mice/group. \*p < 0.05; \*\*p < 0.01; \*\*\*p < 0.001.

Guo et al., 2015; Wang et al., 2016). It has been described that the mRNA expression level of *HIF1A* is lower in individuals carrying CT/TT genotypes at rs2057482 compared to CC carriers. This SNP is localized in the 3'-UTR region of *HIF1A* and close to two predicted microRNA binding sites (hsa-miR-199a/b-5p and hsa-miR-340) (Guo et al., 2015; Wang et al., 2016). Therefore, we decided to assess whether human monocyte-derived macrophages from healthy donors carrying different genotypes displayed distinct *L. donovani* infection outcomes. First and consistent with a previous report (Wang et al., 2016), we observed that the transcription levels of *HIF1A* gene were decreased in macrophages with the CT/TT genotype, when compared to cells from CC carriers (Figure 7A). Furthermore, our results showed an increase in parasite viability in CT/TT macrophages, associated with lower levels of *HIF1A* (Figure 7B). We also demonstrated that *HIF1A* levels were inversely correlated with parasite viability (Figure 7C; p = 0.0362; r = -0.3777) and intracellular neutral lipids (Figure 7D; p = 0.0057; r = -0.4777), while parasite viability correlated positively with intracellular

neutral lipids (Figure 7E; p = 0.0150; r = 0.3929). Treatment of infected macrophages from CT/TT donors with C75 led to a significant decrease in parasite viability, in contrast to what occurs with CC macrophages (Figures 7F and 7G). These results unveil a major breakthrough in our understanding of human susceptibility to parasite infection associated with a genetic variation in human *HIF1A* expression that can be reverted by inhibiting lipid accumulation through FASN blockage.

## DISCUSSION

A growing body of evidence suggests that the metabolic status of a host cell has pivotal importance for building up an adequate immune response. However, successful pathogens have in turn evolved and acquired complex and efficient methods to subvert and evade immune responses by manipulating host cell metabolism. Whereas several groups have proposed a role for HIF-1 $\alpha$  in regulating protozoan infections (Degrossoli et al., 2007; Singh et al., 2012; McGettrick et al., 2016; Schatz et al.,

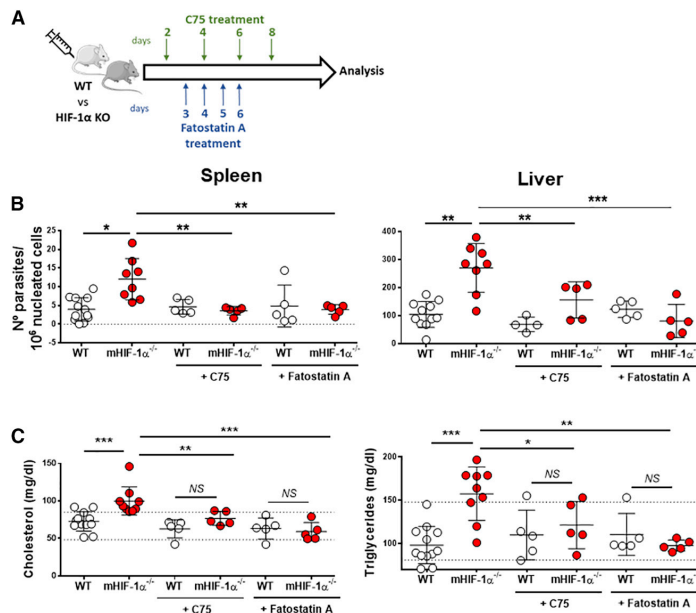


**Figure 6. Targeting Lipid Anabolism Reverts *mHIF-1 $\alpha$* <sup>-/-</sup> Associated Susceptibility**

(A) Treatment scheme with C75 and fatostatin A (further detailed in STAR Methods). Mice were euthanized 10 days post-infection.

(B) Parasite burden in the spleen and liver of C75 and fatostatin A-treated and untreated WT and *mHIF-1 $\alpha$* <sup>-/-</sup>.

(C) Cholesterol and triglycerides levels on the serum of C75 and fatostatin A-treated and untreated WT and *mHIF-1 $\alpha$* <sup>-/-</sup>.

Data are shown as mean  $\pm$  SD; n = 4–12 mice/group. \*p < 0.05; \*\*p < 0.01; \*\*\*p < 0.001.

with this, we observed that infected, susceptible BALB/c mice display constant levels of HIF-1 $\alpha$  through the course of infection. In opposition, resistant mouse strains, such as 129/SV and C57BL/6, exhibit an induction of HIF-1 $\alpha$  transcription, suggesting that HIF-1 $\alpha$  expression and activation is relevant for the establishment of an effective anti-*Leishmania* responses (Figure 1A). Therefore, the levels of HIF-1 $\alpha$  may dictate host susceptibility or resistance, as the absence of this factor in CD11b<sup>+</sup> population during *L. donovani* infection results in a

2016; Alonso et al., 2019), the mechanisms behind it remain elusive. In this study, we demonstrate the contributing role of myeloid HIF-1 $\alpha$  in the modulation of lipid metabolism during *L. donovani* infection. We show that the absence of myeloid HIF-1 $\alpha$  dysregulates lipid metabolism via BNIP3/mTOR/SREBP-1c axis upon *L. donovani* infection. This survival advantage to the parasite is reverted by the blockade of lipid synthesis. Finally, we demonstrate that individuals carrying a *HIF1A* SNP (rs2057482) display lower transcript levels of *HIF1A* in macrophages and are more susceptible to *L. donovani* infection, which positively correlates with increased lipogenesis.

HIF-1 $\alpha$  was initially described as a master transcriptional factor in response to hypoxia and a key mediator of glycolysis (Lu et al., 2002; Lee et al., 2004; Marín-Hernández et al., 2009). Recent evidence suggests that this factor is also essential in regulating the production of inflammatory cytokines and chemo-attractive factors by macrophages and endothelial cells (Imtiyaz and Simon, 2010; Palazon et al., 2014). PAMPs, including Toll-like receptor (TLR) agonists, induce an HIF-1 $\alpha$ -dependent production of inflammatory cytokines in pro-inflammatory macrophages (Cramer et al., 2003; Rius et al., 2008; Nicholas and Sumbayev, 2009; Palsson-McDermott et al., 2015). By contrast, anti-inflammatory macrophages display a more oxidative metabolic profile, characterized by the utilization of oxidative phosphorylation and fatty acid oxidation (FAO), for which HIF-1 $\alpha$  has a minor role (Vats et al., 2006; Nomura et al., 2016). The absence of HIF-1 $\alpha$  could hypothetically drive macrophage polarization toward an anti-inflammatory and permissive profile, characterized by lower levels of nitric oxide (NO) and reactive oxygen species (ROS), which weakens the anti-*Leishmania* response (Rodrigues et al., 2016; Schatz et al., 2016). In accordance

higher number of intracellular parasites (Figure 1C). Accordingly, we observed a decreased NO production on infected HIF-1 $\alpha$ <sup>-/-</sup> macrophages when compared to WT counterpart (Figure S7A), demonstrating that the absence of this factor leads to reduced host microbicidal mechanisms, as previously reported (Schatz et al., 2016). The observed susceptibility phenotype contrasts with a previous work in which the absence of HIF1 $\alpha$  in CD11c<sup>+</sup> cells (C57BL/6 Cd11c-Cre<sup>-/-</sup>) rendered a protective phenotype (Hammami et al., 2017). We assume that the differences observed are mainly related to the type of cells deficient for HIF1 $\alpha$ .

In addition to this, a shift in the literature-based prototype transcript markers toward an anti-inflammatory phenotype, as well as a dysregulated balance between pro- and anti-inflammatory cytokines was observed in the absence of HIF-1 $\alpha$  (Figures 1E and 1F). However, additional host-driven mechanisms are thought to be implied in the observed susceptibility in the absence of HIF-1 $\alpha$ . Considering the importance of an adequate metabolic environment for the correct development of immune responses, we hypothesized that HIF-1 $\alpha$  deficiency in the CD11b compartment could severely influence host metabolism with a consequent impact on infection outcome. Although seminal works in cancer metabolism have elucidated the role of HIF-1 $\alpha$  in glycolysis, a quite controversial role for this factor in lipid metabolism has been established for distinct models of pathogenesis. While a positive association between lipid accumulation and HIF-1 $\alpha$  activation has been explored (Nath et al., 2011; Bensaad et al., 2014; Du et al., 2017), this process appears to be cell- and context-specific, as other studies have demonstrated the opposite (Zhang et al., 2010; Nishiyama et al., 2012; Rahtu-Korpela et al., 2014, 2016). In our work, we found

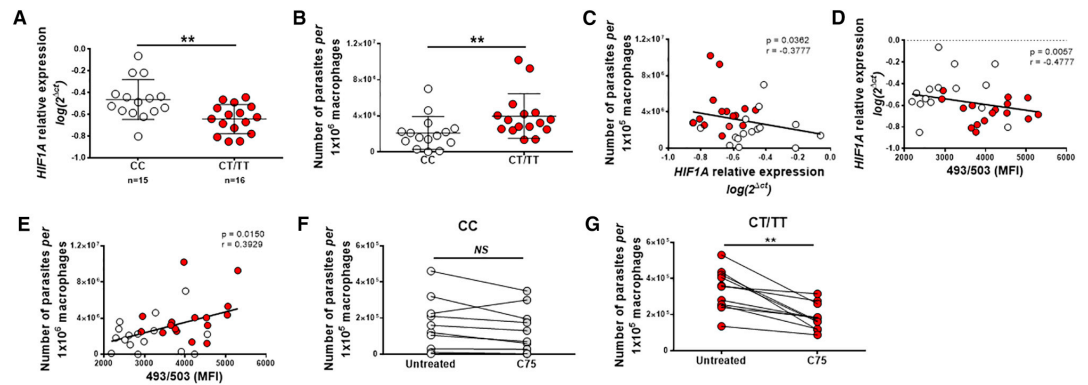


**Figure 7. Genetic Variation in Human *HIF1A* Promotes Increased Parasite Viability and Lipid Accumulation**

(A) qPCR analysis of the transcriptional levels of *HIF1A* in human macrophages from donors with the CC and CT/TT genotype at rs2057482.

(B) *L. donovani* viability 5 days post-infection.

(C–E) Correlation between parasite viability and *HIF1A* transcriptional levels (C), *HIF1A* transcriptional levels and intracellular neutral lipids (D), and parasite viability and intracellular neutral lipids (E).

(F and G) *L. donovani* viability after C75 treatment in macrophages with the CC (F) and CT/TT (G) genotype, respectively.

Data are shown as mean  $\pm$  SD; \*\* $p < 0.01$ .

that the absence of HIF-1 $\alpha$  during *L. donovani* infection is associated with an increased lipogenesis driven by an upregulation of ACC and FASN (Figures 3 and 4). We ascribed the increased growth of *L. donovani* to a higher lipogenesis, as pharmacological inhibition of this pathway reverted the observed phenotype and reduced parasite growth (Figures 4C and 6B). The blockage of fatty acid synthesis has already been explored as a therapeutic approach in several diseases. Indeed, blockade of FASN with C75 has been explored in the context of sepsis (Idrovo et al., 2016), hemorrhagic shock (Kuncewitch et al., 2016), colitis (Matsuo et al., 2014), and cancer (Kuhajda et al., 2000; Flavin et al., 2010), while the ACC inhibitor soraphen A was shown to have an impact in experimental autoimmune encephalomyelitis (Berod et al., 2014) and graft-versus-host disease (Raha et al., 2016). Therefore, these molecules could be included in the therapeutics arsenal against VL.

Given that HIF-1 $\alpha$  is a transcriptional factor, we performed an RNA-sequencing approach of infected WT and *HIF-1 $\alpha$ <sup>-/-</sup>* gene expression profile to ascertain the mechanism behind the observed phenotype. Our results show that, in the absence of HIF-1 $\alpha$ , infected macrophages downregulate several pathways associated with hypoxia (Figure 2B). Interestingly, we observed that *Bnip3* was the most significantly altered gene, which was upregulated in infected WT macrophages, while no transcriptional changes were observed in *HIF-1 $\alpha$ <sup>-/-</sup>* macrophages (Figure 2C). This gene has a promoter region that is a direct target of transcriptional activation via HIF-1 $\alpha$ , which is steadily induced in hypoxia (Chinnadurai et al., 2008). Alongside with this, BNIP3 has been shown to repress mTORC1 activation via interaction with Rheb GTPase (Li et al., 2007), which suggests that BNIP3 directly interferes with cellular metabolism through the modulation of mTOR function. Accordingly, our results show that in the absence of HIF-1 $\alpha$ , BNIP3 expression is maintained at basal levels, and consequently, mTOR is activated,

as observed by the increased phosphorylation status of mTOR direct target S6 kinase (Figure 2F). Of note, even though BNIP3 is a pro-apoptotic protein, we found no differences on the levels of autophagy or cell death between *L. donovani*-infected WT and *HIF-1 $\alpha$ <sup>-/-</sup>* macrophages (data not shown). One of the most important functions regulated by mTOR is the activation of SREBP-driven lipid synthesis, which is crucial for the maintenance and establishment of cell growth programs (Laplante and Sabatini, 2009; Caron et al., 2015; Mao and Zhang, 2018). SREBP-1c is a master promoter of lipogenesis via activation of a specific transcriptional program (Horton et al., 2002; Joseph et al., 2002; Eberlé et al., 2004; Xiao and Song, 2013). Consistently, we demonstrated that the activation of fatty acid synthesis is driven by mTOR/SREBP-1c activation as blockage of these factors with rapamycin or fatostatin A reverts lipid accumulation and, consequently, the increased susceptibility of *mHIF-1 $\alpha$ <sup>-/-</sup>* mice (Figures 4A and 6B). Therefore, this represents a different avenue in our understanding of host-pathogen interaction in which BNIP3 may play a major role in the susceptibility of parasite infection.

We observed that acetate was used as an additional carbon source for the lipid synthesis and accumulation in *HIF-1 $\alpha$ <sup>-/-</sup>* macrophages, which is consistent with an increased acetate uptake in infected *HIF-1 $\alpha$ <sup>-/-</sup>* macrophages. The role of acetate in promoting lipid biogenesis as well as its incorporation in lipid droplets in both mammalian cells and pathogenic agents has already been described in certain experimental conditions (Howard, 1977; Rivière et al., 2009; Liu et al., 2016). The synthesis of acetyl-CoA from acetate is known to be induced via SREBP-1c activation, which indicates a role for acetate in lipogenesis. Consistently, isotope-labeling experiments using sodium acetate-2-<sup>13</sup>C showed that infected *mHIF-1 $\alpha$ <sup>-/-</sup>* macrophages have an increased uptake of acetate and incorporation in the lipid fraction (Figures 3G, S5A, and S5B), explaining the

increased lipogenic flux in these cells. We also observed an increased expression of MCT4 that has been shown to uptake lactate, pyruvate, or acetate. Conversely to acetate, pyruvate and lactate supplementation did not lead to increased lipid accumulation in *HIF-1 $\alpha$* <sup>-/-</sup>-infected macrophages (Figure 3J; data not shown). Furthermore, although we observed a decrease in lipid accumulation in infected *HIF-1 $\alpha$* <sup>-/-</sup> macrophages cultured in the absence of acetate (Figure 3J), we cannot exclude the contribution of other sources for the observed phenotype.

Rabhi et al. (2012, 2016) demonstrated that *Leishmania* parasites co-localize with intracellular lipid droplets. However, whether lipids are used as a high-energy source to feed amastigotes (De Cicco et al., 2012) or as a shield to protect them from host microbicidal mechanisms (Bailey et al., 2015) remains to be addressed. Our preliminary data show that infected *HIF-1 $\alpha$* <sup>-/-</sup> macrophages display higher levels of lipid peroxidation (data not shown), suggesting a role for lipids in protecting *L. donovani* parasites from killing by host cells. The mechanistic events that explain how the absence of HIF-1 $\alpha$  results in the increased activation of these lipogenic factors remain to be deciphered. One hypothesis could be that an initial peak of ROS production by infected *HIF-1 $\alpha$* <sup>-/-</sup> macrophages could trigger SREBP-1c activation and consequent lipid production (Liu et al., 2015). No major alterations were observed in peroxynitrite and superoxide anion accumulation in infected macrophages early after infection (data not shown), although other sources, such as mitochondrial ROS production, remain to be addressed. Alternatively, HIF-1 $\alpha$  may induce lipogenesis due to activation of upstream TLR2 and TLR4, which are triggered upon *Leishmania* infection (Becker et al., 2003; Kropf et al., 2004; Tuon et al., 2008; Silvestre et al., 2009) and have been associated to macrophage lipid accumulation (Feingold et al., 2012). Indeed, TLR2 and TLR4 activation with Pam3CSK4 and LPS, respectively, increases intracellular neutral lipids in the absence of HIF-1 $\alpha$  (Figure S7B). Thus, HIF-1 $\alpha$  may restrict lipid accumulation through alterations of TLR signaling, although this hypothesis requires further studies.

Genetic variations in human *HIF1A* have been reported to influence the developing risk and prognosis of many types of human malignancies, such as cancer and coronary artery disease (Hlatky et al., 2007; Kim et al., 2008; Guo et al., 2015; Wang et al., 2016). Among *HIF1A* polymorphisms, rs2057482 has been associated with a lower expression of HIF-1 $\alpha$ . This SNP is localized in the 3'-UTR region of the *HIF1A* gene, a site that has been demonstrated to be under the control of miR-199a, capable of repressing HIF-1 $\alpha$  transcription (Wang et al., 2016). Our results demonstrated that genetic variation in *HIF1A* may contribute to regulate parasite growth in macrophages. Thus, in macrophages from individuals with the CT/TT genotype at rs2057482, in which HIF-1 $\alpha$  expression is lower, parasite growth is higher than the observed in macrophages from CC carriers. Moreover, we observed that lower levels of HIF-1 $\alpha$  are positively correlated with higher levels of lipids (Figure 7). High frequencies of the rs2057482 SNP in regions with a high number of VL cases (Asia, ~34.88%, and sub-Saharan Africa, ~46.02%; available on <https://www.ncbi.nlm.nih.gov/snp>) may identify HIF-1 $\alpha$  as a major host factor that regulates resistance and susceptibility to VL. Therefore, it would be of interest to perform clinical studies assessing the impact of such polymorphism in patients.

In conclusion, our data identified HIF-1 $\alpha$  as a host-protective factor against *L. donovani* infection. Absence of HIF-1 $\alpha$  results in elevated lipogenesis, creating an intracellular milieu conducive for parasite growth and survival, thus supporting the hypothesis that lipid accumulation is important for *Leishmania* survival within host cells (Rabhi et al., 2016; Rodríguez et al., 2017; Semini et al., 2017). Our demonstration that pharmacological compounds targeting lipid synthesis modulate susceptibility to parasite infection that may aid the development of therapies for VL cure.

## STAR★METHODS

Detailed methods are provided in the online version of this paper and include the following:

- KEY RESOURCES TABLE
- LEAD CONTACT AND MATERIALS AVAILABILITY
- EXPERIMENTAL MODEL AND SUBJECT DETAILS
  - Mice
  - Parasite culture and staining
  - Macrophage culture and *in vitro* infections
- METHOD DETAILS
  - Parasite viability
  - SNP selection and genotyping
  - Experimental *Leishmania* infection
  - Oil Red O staining
  - Flow cytometry
  - High performance liquid chromatography
  - Lipid extraction and HPTLC analysis
  - Quantitative PCR analysis
  - Western blot
  - Enzyme-linked Immunosorbent Assay
  - Macrophage transfection
  - Immunofluorescence
  - Nuclear Magnetic Resonance
  - Cell sorting
  - RNA sequencing
- QUANTIFICATION AND STATISTICAL ANALYSIS
- DATA AND CODE AVAILABILITY

## SUPPLEMENTAL INFORMATION

Supplemental Information can be found online at <https://doi.org/10.1016/j.celrep.2020.02.098>.

## ACKNOWLEDGMENTS

This work was supported by the Northern Portugal Regional Operational Programme (NORTE 2020), under the Portugal 2020 Partnership Agreement, through the European Regional Development Fund (FEDER) (NORTE-01-0145-FEDER-000013), Project LISBOA-01-0145-FEDER-007660 (Microbiologia Molecular, Estrutural e Celular) funded by FEDER funds through COMPETE2020—Programa Operacional Competitividade e Internacionalização (POCI) and the Fundação para a Ciência e Tecnologia (FCT) (Contracts SFRH/BD/120127/2016 to I.M., PD/BDE/127830/2016 to C.F., SFRH/BD/120371/2016 to A.M.B., IF/01147/2013 to R.J.D.-O., SFRH/BPD/111100/2015 to L.G.G., IF/01390/2014 to E.T., IF/00735/2014 to A.C., SFRH/BPD/96176/2013 to C.C., and IF/00021/2014 to R.S.) and Infect-Era (Project INLEISH). J.E. also thanks the Canada Research Chair program for financial assistance. B.S. thanks CWRU/UH Centre for AIDS Research (NIH Grant P30 AI036219) and DBT (BT/In/Infect-eRA/33/BS/2016-2017). The

NMR data were acquired at CERMAX, ITQB-NOVA, Oeiras, Portugal, with equipment funded by FCT, Project AAC 01/SAICT/2016. We thank Dr. Cláudia Nobrega and Dr. Margarida Correia Neves for providing the Ly5.1 mice and Dr. Nuno Alves for the cell sorting.

#### AUTHOR CONTRIBUTIONS

Conceptualization and Methodology, I.M., D.M., B.S., F.R., C.C., A.C., A.G.C., J.E., and R.S.; Investigation, I.M., C.F., D.M., G.E.G.K., A.M.B., R.J.D.-O., L.G.G., N.B., C.C., and R.S.; Formal Analysis, I.M., C.F., D.M., G.E.G.K., E.T., R.J.D.-O., L.G.G., N.B., A.D., C.-J.B., J.E., and R.S.; Visualization, I.M., B.S., J.E., and R.S.; Writing – Original Draft, I.M., B.S., J.E., and R.S.; Supervision, J.E. and R.S.; Resources, T.S., L.B., B.S., J.E., and R.S.; Funding Acquisition, B.S., J.E., and R.S.

#### DECLARATION OF INTERESTS

The authors declare no competing interests.

Received: September 2, 2019

Revised: January 14, 2020

Accepted: February 26, 2020

Published: March 24, 2020

#### REFERENCES

- Abram, C.L., Roberge, G.L., Hu, Y., and Lowell, C.A. (2014). Comparative analysis of the efficiency and specificity of myeloid-Cre deleting strains using ROSA-EYFP reporter mice. *J. Immunol. Methods* **408**, 89–100.
- Alonso, D., Serrano, E., Bermejo, F.J., and Corral, R.S. (2019). HIF-1 $\alpha$ -regulated MIF activation and Nox2-dependent ROS generation promote *Leishmania amazonensis* killing by macrophages under hypoxia. *Cell. Immunol.* **335**, 15–21.
- Bailey, A.P., Koster, G., Guillermier, C., Hirst, E.M., MacRae, J.I., Lechene, C.P., Postle, A.D., and Gould, A.P. (2015). Antioxidant role for lipid droplets in a stem cell niche of *Drosophila*. *Cell* **163**, 340–353.
- Becker, I., Salaiza, N., Aguirre, M., Delgado, J., Carrillo-Carrasco, N., Kobeh, L.G., Ruiz, A., Cervantes, R., Torres, A.P., Cabrera, N., et al. (2003). *Leishmania* lipophosphoglycan (LPG) activates NK cells through Toll-like receptor-2. *Mol. Biochem. Parasitol.* **130**, 65–74.
- Bensaad, K., Favaro, E., Lewis, C.A., Peck, B., Lord, S., Collins, J.M., Pinnick, K.E., Wigfield, S., Buffa, F.M., Li, J.L., et al. (2014). Fatty acid uptake and lipid storage induced by HIF-1 $\alpha$  contribute to cell growth and survival after hypoxia-reoxygenation. *Cell Rep.* **9**, 349–365.
- Berod, L., Friedrich, C., Nandan, A., Freitag, J., Hagemann, S., Harmrolfs, K., Sandouk, A., Hesse, C., Castro, C.N., Bähre, H., et al. (2014). De novo fatty acid synthesis controls the fate between regulatory T and T helper 17 cells. *Nat. Med.* **20**, 1327–1333.
- Bligh, E.G., and Dyer, W.J. (1959). A Rapid Method of Total Lipid Extraction and Purification. *Canadian J. Biochem. Physiology*. <https://www.nrcresearchpress.com/doi/pdf/10.1139/o59-099>.
- Blume, M., Nitzsche, R., Sternberg, U., Gerlic, M., Masters, S.L., Gupta, N., and McConville, M.J. (2015). A *Toxoplasma gondii* gluconeogenic enzyme contributes to robust central carbon metabolism and is essential for replication and virulence. *Cell Host Microbe* **18**, 210–220.
- Bodhale, N.P., Pal, S., Kumar, S., Chattopadhyay, D., Saha, B., Chattopadhyay, N., and Bhattacharyya, M. (2018). Inbred mouse strains differentially susceptible to *Leishmania donovani* infection differ in their immune cell metabolism. *Cytokine* **112**, 12–15.
- Bozza, P.T., et al. (2009). Lipid droplets in host-pathogen interactions. *Clin. Lipidol.* **4**, 791–807.
- Caradonna, K.L., Engel, J.C., Jacobi, D., Lee, C.H., and Burleigh, B.A. (2013). Host metabolism regulates intracellular growth of *Trypanosoma cruzi*. *Cell Host Microbe* **13**, 108–117.

Caron, A., Richard, D., and Laplante, M. (2015). The roles of mTOR complexes in lipid metabolism. *Annu. Rev. Nutr.* **35**, 321–348.

Chang, Y., Edeen, K., Lu, X., De Leon, M., and Mason, R.J. (2006). Keratinocyte growth factor induces lipogenesis in alveolar type II cells through a sterol regulatory element binding protein-1c-dependent pathway. *Am. J. Respir. Cell Mol. Biol.* **35**, 268–274.

Cheng, S.-C., Quintin, J., Cramer, R.A., Shepardson, K.M., Saeed, S., Kumar, V., Giamarellos-Bourboulis, E.J., Martens, J.H., Rao, N.A., Aghajani-Refah, A., et al. (2014). mTOR- and HIF-1 $\alpha$ -mediated aerobic glycolysis as metabolic basis for trained immunity. *Science* **345**, 1250684–1250684.

Chinnadurai, G., Vijayalingam, S., and Gibson, S.B. (2008). BNIP3 subfamily BH3-only proteins: mitochondrial stress sensors in normal and pathological functions. *Oncogene* **27** (Suppl 1), S114–S127.

Choudhry, H., and Harris, A.L. (2018). Advances in hypoxia-inducible factor biology. *Cell Metab.* **27**, 281–298.

Cramer, T., Yamanishi, Y., Clausen, B.E., Förster, I., Pawlinski, R., Mackman, N., Haase, V.H., Jaenisch, R., Corr, M., Nizet, V., et al. (2003). HIF-1 $\alpha$  is essential for myeloid cell-mediated inflammation. *Cell* **112**, 645–657.

De Cicco, N.N.T., Pereira, M.G., Corrêa, J.R., Andrade-Neto, V.V., Saraiva, F.B., Chagas-Lima, A.C., Gondim, K.C., Torres-Santos, E.C., Folly, E., Saraiva, E.M., et al. (2012). LDL uptake by *Leishmania amazonensis*: involvement of membrane lipid microdomains. *Exp. Parasitol.* **130**, 330–340.

Degrossoli, A., Bosetto, M.C., Lima, C.B., and Giorgio, S. (2007). Expression of hypoxia-inducible factor 1 $\alpha$  in mononuclear phagocytes infected with *Leishmania amazonensis*. *Immunol. Lett.* **114**, 119–125.

Du, W., Zhang, L., Brett-Morris, A., Aguila, B., Kerner, J., Hoppel, C.L., Puchowicz, M., Serra, D., Herrero, L., Rini, B.I., et al. (2017). HIF drives lipid deposition and cancer in ccRCC via repression of fatty acid metabolism. *Nat. Commun.* **8**, 1769.

Düvel, K., Yecies, J.L., Menon, S., Raman, P., Lipovsky, A.I., Souza, A.L., Triantafellow, E., Ma, Q., Gorski, R., Cleaver, S., et al. (2010). Activation of a metabolic gene regulatory network downstream of mTOR complex 1. *Mol. Cell* **39**, 171–183.

Eberlé, D., Hegarty, B., Bossard, P., Ferré, P., and Foufelle, F. (2004). SREBP transcription factors: master regulators of lipid homeostasis. *Biochimie* **86**, 839–848.

Feingold, K.R., Shigenaga, J.K., Kazemi, M.R., McDonald, C.M., Patzek, S.M., Cross, A.S., Moser, A., and Grunfeld, C. (2012). Mechanisms of triglyceride accumulation in activated macrophages. *J. Leukoc. Biol.* **92**, 829–839.

Flavin, R., Peluso, S., Nguyen, P.L., and Loda, M. (2010). Fatty acid synthase as a potential therapeutic target in cancer. *Future Oncol.* **6**, 551–562.

Ghosh, A.K., Sardar, A.H., Mandal, A., Saini, S., Abhishek, K., Kumar, A., Purkait, B., Singh, R., Das, S., Mukhopadhyay, R., et al. (2015). Metabolic reconfiguration of the central glucose metabolism: a crucial strategy of *Leishmania donovani* for its survival during oxidative stress. *FASEB J.* **29**, 2081–2098.

Guo, X., Li, D., Chen, Y., An, J., Wang, K., Xu, Z., Chen, Z., and Xing, J. (2015). SNP rs2057482 in HIF1A gene predicts clinical outcome of aggressive hepatocellular carcinoma patients after surgery. *Sci. Rep.* **5**, 11846.

Hammami, A., Abidin, B.M., Charpentier, T., Fabié, A., Duguay, A.P., Heinonen, K.M., and Stäger, S. (2017). HIF-1 $\alpha$  is a key regulator in potentiating suppressor activity and limiting the microbicidal capacity of MDSC-like cells during visceral leishmaniasis. *PLoS Pathog.* **13**, e1006616.

Hlatky, M.A., Quertermous, T., Boothroyd, D.B., Priest, J.R., Glassford, A.J., Myers, R.M., Fortmann, S.P., Iribarren, C., Tabor, H.K., Assimes, T.L., et al. (2007). Polymorphisms in hypoxia inducible factor 1 and the initial clinical presentation of coronary disease. *Am. Heart J.* **154**, 1035–1042.

Horton, J.D., Goldstein, J.L., and Brown, M.S. (2002). SREBPs: activators of the complete program of cholesterol and fatty acid synthesis in the liver. *J. Clin. Invest.* **109**, 1125–1131.

Howard, B.V. (1977). Acetate as a carbon source for lipid synthesis in cultured cells. *Biochim. Biophys. Acta* **488**, 145–151.

- Idrovo, J.P., Yang, W.L., Jacob, A., Corbo, L., Nicastro, J., Coppa, G.F., and Wang, P. (2016). Inhibition of lipogenesis reduces inflammation and organ injury in sepsis. *J. Surg. Res.* 200, 242–249.
- Imtiyaz, H.Z., and Simon, M.C. (2010). Hypoxia-inducible factors as essential regulators of inflammation. *Curr. Top. Microbiol. Immunol.* 345, 105–120.
- Jain, S.K., Sahu, R., Walker, L.A., and Tekwani, B.L. (2012). A parasite rescue and transformation assay for antileishmanial screening against intracellular *Leishmania donovani* amastigotes in THP1 human acute monocytic leukemia cell line. *J. Vis. Exp.* (70), 4054.
- Joseph, S.B., Laffitte, B.A., Patel, P.H., Watson, M.A., Matsukuma, K.E., Walczak, R., Collins, J.L., Osborne, T.F., and Tontonoz, P. (2002). Direct and indirect mechanisms for regulation of fatty acid synthase gene expression by liver X receptors. *J. Biol. Chem.* 277, 11019–11025.
- Kim, H.O., Jo, Y.H., Lee, J., Lee, S.S., and Yoon, K.S. (2008). The C1772T genetic polymorphism in human HIF-1 $\alpha$  gene associates with expression of HIF-1 $\alpha$  protein in breast cancer. *Oncol. Rep.* 20, 1181–1187.
- Kropf, P., Freudenberg, M.A., Modolell, M., Price, H.P., Herath, S., Antoniazzi, S., Galanos, C., Smith, D.F., and Müller, I. (2004). Toll-like receptor 4 contributes to efficient control of infection with the protozoan parasite *Leishmania major*. *Infect. Immun.* 72, 1920–1928.
- Kuhajda, F.P., Pizer, E.S., Li, J.N., Mani, N.S., Frehywot, G.L., and Townsend, C.A. (2000). Synthesis and antitumor activity of an inhibitor of fatty acid synthase. *Proc. Natl. Acad. Sci. USA* 97, 3450–3454.
- Kuncewitch, M., Yang, W.L., Jacob, A., Khader, A., Giangola, M., Nicastro, J., Coppa, G.F., and Wang, P. (2016). Inhibition of fatty acid synthase with C75 decreases organ injury after hemorrhagic shock. *Surgery* 159, 570–579.
- Laplante, M., and Sabatini, D.M. (2009). An emerging role of mTOR in lipid biosynthesis. *Curr. Biol.* 19, R1046–R1052.
- Lee, J.-W., Bae, S.H., Jeong, J.W., Kim, S.H., and Kim, K.W. (2004). Hypoxia-inducible factor (HIF-1) $\alpha$ : its protein stability and biological functions. *Exp. Mol. Med.* 36, 1–12.
- Li, Y., Wang, Y., Kim, E., Beemiller, P., Wang, C.Y., Swanson, J., You, M., and Guan, K.L. (2007). Bnip3 mediates the hypoxia-induced inhibition on mammalian target of rapamycin by interacting with Rheb. *J. Biol. Chem.* 282, 35803–35813.
- Liu, Y., Ma, Z., Zhao, C., Wang, Y., Wu, G., Xiao, J., McClain, C.J., Li, X., and Feng, W. (2014). HIF-1 $\alpha$  and HIF-2 $\alpha$  are critically involved in hypoxia-induced lipid accumulation in hepatocytes through reducing PGC-1 $\alpha$ -mediated fatty acid  $\beta$ -oxidation. *Toxicol. Lett.* 226, 117–123.
- Liu, L., Zhang, K., Sandoval, H., Yamamoto, S., Jaiswal, M., Sanz, E., Li, Z., Hui, J., Graham, B.H., Quintana, A., and Bellen, H.J. (2015). Glial lipid droplets and ROS induced by mitochondrial defects promote neurodegeneration. *Cell* 160, 177–190.
- Liu, N., Qiao, K., and Stephanopoulos, G. (2016). <sup>13</sup>C metabolic flux analysis of acetate conversion to lipids by *Yarrowia lipolytica*. *Metab. Eng.* 38, 86–97.
- Lu, H., Forbes, R.A., and Verma, A. (2002). Hypoxia-inducible factor 1 activation by aerobic glycolysis implicates the Warburg effect in carcinogenesis. *J. Biol. Chem.* 277, 23111–23115.
- Mao, Z., and Zhang, W. (2018). Role of mTOR in glucose and lipid metabolism. *Int. J. Mol. Sci.* 19, E2043.
- Marín-Hernández, A., Gallardo-Pérez, J.C., Ralph, S.J., Rodríguez-Enríquez, S., and Moreno-Sánchez, R. (2009). HIF-1 $\alpha$  modulates energy metabolism in cancer cells by inducing over-expression of specific glycolytic isoforms. *Mini Rev. Med. Chem.* 9, 1084–1101.
- Matsuo, S., Yang, W.L., Aziz, M., Kameoka, S., and Wang, P. (2014). Fatty acid synthase inhibitor C75 ameliorates experimental colitis. *Mol. Med.* 20, 1–9.
- McConville, M.J. (2016). Metabolic crosstalk between Leishmania and the macrophage host. *Trends Parasitol.* 32, 666–668.
- McGettrick, A.F., Corcoran, S.E., Barry, P.J., McFarland, J., Crès, C., Curtis, A.M., Franklin, E., Corr, S.C., Mok, K.H., Cummins, E.P., et al. (2016). *Trypanosoma brucei* metabolite indolepyruvate decreases HIF-1 $\alpha$  and glycolysis in macrophages as a mechanism of innate immune evasion. *Proc. Natl. Acad. Sci. USA* 113, E7778–E7787.
- Moreira, D., Rodrigues, V., Abengozar, M., Rivas, L., Rial, E., Laforge, M., Li, X., Foretz, M., Viollet, B., Estaqueir, J., et al. (2015). *Leishmania infantum* modulates host macrophage mitochondrial metabolism by hijacking the SIRT1-AMPK axis. *PLoS Pathog.* 11, e1004684.
- Murray, P.J., Allen, J.E., Biswas, S.K., Fisher, E.A., Gilroy, D.W., Goerdt, S., Gordon, S., Hamilton, J.A., Ivashkiv, L.B., Lawrence, T., et al. (2014). Macrophage activation and polarization: nomenclature and experimental guidelines. *Immunity* 41, 14–20.
- Na, Y.R., Gu, G.J., Jung, D., Kim, Y.W., Na, J., Woo, J.S., Cho, J.Y., Youn, H., and Seok, S.H. (2016). GM-CSF induces inflammatory macrophages by regulating glycolysis and lipid metabolism. *J. Immunol.* 197, 4101–4109.
- Naderer, T., and McConville, M.J. (2008). The *Leishmania*-macrophage interaction: a metabolic perspective. *Cell. Microbiol.* 10, 301–308.
- Nath, B., Levin, I., Csak, T., Petrasek, J., Mueller, C., Kodys, K., Catalano, D., Mandrekar, P., and Szabo, G. (2011). Hepatocyte-specific hypoxia-inducible factor-1 $\alpha$  is a determinant of lipid accumulation and liver injury in alcohol-induced steatosis in mice. *Hepatology* 53, 1526–1537.
- Nicholas, S.A., and Sumbayev, V.V. (2009). The involvement of hypoxia-inducible factor 1 $\alpha$  in Toll-like receptor 7/8-mediated inflammatory response. *Cell Res.* 19, 973–983.
- Nishiyama, Y., Goda, N., Kanai, M., Niwa, D., Osanai, K., Yamamoto, Y., Senoo-Matsuda, N., Johnson, R.S., Miura, S., Kabe, Y., and Suematsu, M. (2012). HIF-1 $\alpha$  induction suppresses excessive lipid accumulation in alcoholic fatty liver in mice. *J. Hepatol.* 56, 441–447.
- Nomura, M., Liu, J., Rovira, I.L., Gonzalez-Hurtado, E., Lee, J., Wolfgang, M.J., and Finkel, T. (2016). Fatty acid oxidation in macrophage polarization. *Nat. Immunol.* 17, 216–217.
- Palazon, A., Goldrath, A.W., Nizet, V., and Johnson, R.S. (2014). HIF transcription factors, inflammation, and immunity. *Immunity* 41, 518–528.
- Palsson-McDermott, E.M., Curtis, A.M., Goel, G., Lauterbach, M.A., Sheedy, F.J., Gleeson, L.E., van den Bosch, M.W., Quinn, S.R., Domingo-Fernandez, R., Johnston, D.G., et al. (2015). Pyruvate kinase M2 regulates Hif-1 $\alpha$  activity and IL-1 $\beta$  induction and is a critical determinant of the Warburg effect in LPS-activated macrophages. *Cell Metab.* 21, 65–80.
- Peyssonnaud, C., Cejudo-Martin, P., Doedens, A., Zinkernagel, A.S., Johnson, R.S., and Nizet, V. (2007). Cutting edge: essential role of hypoxia inducible factor-1 $\alpha$  in development of lipopolysaccharide-induced sepsis. *J. Immunol.* 178, 7516–7519.
- Porstmann, T., Santos, C.R., Griffiths, B., Cully, M., Wu, M., Leevers, S., Griffiths, J.R., Chung, Y.L., and Schulze, A. (2008). SREBP activity is regulated by mTORC1 and contributes to Akt-dependent cell growth. *Cell Metab.* 8, 224–236.
- Rabhi, I., Rabhi, S., Ben-Othman, R., Rasche, A., Daskalaki, A., Trentin, B., Piquemal, D., Regnault, B., Descoteaux, A., and Guizani-Tabbane, L.; Sysco Consortium (2012). Transcriptomic signature of *Leishmania* infected mice macrophages: a metabolic point of view. *PLoS Negl. Trop. Dis.* 6, e1763.
- Rabhi, S., Rabhi, I., Trentin, B., Piquemal, D., Regnault, B., Goyard, S., Lang, T., Descoteaux, A., Enninga, J., and Guizani-Tabbane, L. (2016). Lipid droplet formation, their localization and dynamics during *Leishmania major* macrophage infection. *PLoS ONE* 11, e0148640.
- Raha, S., Raud, B., Oberdörfer, L., Castro, C.N., Schreder, A., Freitag, J., Lonerich, T., Lochner, M., Sparwasser, T., Berod, L., et al. (2016). Disruption of de novo fatty acid synthesis via acetyl-CoA carboxylase 1 inhibition prevents acute graft-versus-host disease. *Eur. J. Immunol.* 46, 2233–2238.
- Rahtu-Korpela, L., Karsikas, S., Hökkö, S., Blanco Sequeiros, R., Lammintausta, E., Mäkelä, K.A., Herzig, K.H., Walkinshaw, G., Kivirikko, K.I., Myllyharju, J., et al. (2014). HIF prolyl 4-hydroxylase-2 inhibition improves glucose and lipid metabolism and protects against obesity and metabolic dysfunction. *Diabetes* 63, 3324–3333.
- Rahtu-Korpela, L., Määttä, J., Dimova, E.Y., Hökkö, S., Gylling, H., Walkinshaw, G., Hakkola, J., Kivirikko, K.I., Myllyharju, J., Serpi, R., and Koivunen, P. (2016). Hypoxia-inducible factor prolyl 4-hydroxylase-2 inhibition protects

- against development of atherosclerosis. *Arterioscler. Thromb. Vasc. Biol.* **36**, 608–617.
- Rankin, E.B., Rha, J., Selak, M.A., Unger, T.L., Keith, B., Liu, Q., and Haase, V.H. (2009). Hypoxia-inducible factor 2 regulates hepatic lipid metabolism. *Mol. Cell. Biol.* **29**, 4527–4538.
- Rius, J., Guma, M., Schachtrup, C., Akassoglou, K., Zinkernagel, A.S., Nizet, V., Johnson, R.S., Haddad, G.G., and Karin, M. (2008). NF- $\kappa$ B links innate immunity to the hypoxic response through transcriptional regulation of HIF-1 $\alpha$ . *Nature* **453**, 807–811.
- Rivière, L., Moreau, P., Allmann, S., Hahn, M., Biran, M., Plazolles, N., Franconi, J.M., Boshart, M., and Bringaud, F. (2009). Acetate produced in the mitochondrion is the essential precursor for lipid biosynthesis in procyclic trypanosomes. *Proc. Natl. Acad. Sci. USA* **106**, 12694–12699.
- Rodrigues, V., Cordeiro-da-Silva, A., Laforge, M., Silvestre, R., and Estaquier, J. (2016). Regulation of immunity during visceral *Leishmania* infection. *Parasit. Vectors* **9**, 118.
- Rodríguez, N.E., Lockard, R.D., Turcotte, E.A., Araújo-Santos, T., Bozza, P.T., Borges, V.M., and Wilson, M.E. (2017). Lipid bodies accumulation in *Leishmania infantum*-infected C57BL/6 macrophages. *Parasite Immunol.* **39**.
- Schatz, V., Strüssmann, Y., Mahnke, A., Schley, G., Waldner, M., Ritter, U., Wild, J., Willam, C., Dehne, N., Brüne, B., et al. (2016). Myeloid cell-derived HIF-1 $\alpha$  promotes control of *Leishmania major*. *J. Immunol.* **197**, 4034–4041.
- Semini, G., Paape, D., Paterou, A., Schroeder, J., Barrios-Llerena, M., and Aebischer, T. (2017). Changes to cholesterol trafficking in macrophages by *Leishmania* parasites infection. *MicrobiologyOpen* **6**, e00469.
- Silvestre, R., et al. (2009). Recognition of *Leishmania* parasites by innate immunity. *Immunol. Endocr. Metab. Agents Med. Chem.* **9**, 106–127.
- Singh, A.K., Mukhopadhyay, C., Biswas, S., Singh, V.K., and Mukhopadhyay, C.K. (2012). Intracellular pathogen *Leishmania donovani* activates hypoxia inducible factor-1 by dual mechanism for survival advantage within macrophage. *PLoS ONE* **7**, e38489.
- Smith, T.K., Bringaud, F., Nolan, D.P., and Figueiredo, L.M. (2017). Metabolic reprogramming during the *Trypanosoma brucei* life cycle. *F1000Res.* **6**, 683.
- Sone, H., Shimano, H., Sakakura, Y., Inoue, N., Amemiya-Kudo, M., Yahagi, N., Osawa, M., Suzuki, H., Yokoo, T., Takahashi, A., et al. (2002). Acetyl-coenzyme A synthetase is a lipogenic enzyme controlled by SREBP-1 and energy status. *Am. J. Physiol. Endocrinol. Metab.* **282**, E222–E230.
- Spirig, R., Djafarzadeh, S., Regueira, T., Shaw, S.G., von Garnier, C., Takala, J., Jakob, S.M., Rieben, R., and Lepper, P.M. (2010). Effects of TLR agonists on the hypoxia-regulated transcription factor HIF-1 $\alpha$  and dendritic cell maturation under normoxic conditions. *PLoS ONE* **5**, e0010983.
- Thompson, C.B. (2016). Into thin air: How we sense and respond to hypoxia. *Cell* **167**, 9–11.
- Tuon, F.F., Amato, V.S., Bacha, H.A., Almusawi, T., Duarte, M.I., and Amato Neto, V. (2008). Toll-like receptors and leishmaniasis. *Infect. Immun.* **76**, 866–872.
- Vats, D., Mukundan, L., Odegaard, J.I., Zhang, L., Smith, K.L., Morel, C.R., Wagner, R.A., Greaves, D.R., Murray, P.J., and Chawla, A. (2006). Oxidative metabolism and PGC-1 $\beta$  attenuate macrophage-mediated inflammation. *Cell Metab.* **4**, 13–24.
- Wang, X., Ren, H., Zhao, T., Ma, W., Dong, J., Zhang, S., Xin, W., Yang, S., Jia, L., and Hao, J. (2016). Single nucleotide polymorphism in the microRNA-199a binding site of HIF1A gene is associated with pancreatic ductal adenocarcinoma risk and worse clinical outcomes. *Oncotarget* **7**, 13717–13729.
- Weidemann, A., and Johnson, R.S. (2008). Biology of HIF-1 $\alpha$ . *Cell Death Differ.* **15**, 621–627.
- Werth, N., Beerlage, C., Rosenberger, C., Yazdi, A.S., Edelmann, M., Amr, A., Bernhardt, W., von Eiff, C., Becker, K., Schäfer, A., et al. (2010). Activation of hypoxia inducible factor 1 is a general phenomenon in infections with human pathogens. *PLoS ONE* **5**, e11576.
- Xiao, X., and Song, B.L. (2013). SREBP: a novel therapeutic target. *Acta Biochim. Biophys. Sin. (Shanghai)* **45**, 2–10.
- Zhang, X., Lam, K.S., Ye, H., Chung, S.K., Zhou, M., Wang, Y., and Xu, A. (2010). Adipose tissue-specific inhibition of hypoxia-inducible factor 1 $\alpha$  induces obesity and glucose intolerance by impeding energy expenditure in mice. *J. Biol. Chem.* **285**, 32869–32877.



## STAR★METHODS

## KEY RESOURCES TABLE

REAGENT or RESOURCE	SOURCE	IDENTIFIER
<b>Antibodies</b>		
Brilliant Violet 785 anti-mouse NK-1.1 (clone PK136)	Biolegend	Cat#: 108749; RRID:AB_2564304
APC anti-mouse I-A/I-E (clone M5/114.15.2)	Biolegend	Cat#: 107614; RRID:AB_313329
Brilliant Violet 605 anti-mouse CD11c (clone N418)	Biolegend	Cat#: 117334; RRID:AB_2562415
PE/Cy7 anti-mouse CD11b (clone M1/70)	Biolegend	Cat#: 101216; RRID:AB_312799
Brilliant Violet 711 anti-mouse Ly-6G (clone 1A8)	Biolegend	Cat#: 127643; RRID:AB_2565971
PerCP/Cy5.5 anti-mouse Ly-6C (clone HK14)	Biolegend	Cat#: 128012; RRID:AB_1659241
APC anti-mouse CD45.2 (clone 104)	Biolegend	Cat#: 109814; RRID:AB_389211
PE anti-mouse CD45.1 (clone A20)	Biolegend	Cat#: 110708; RRID:AB_313497
Mouse monoclonal anti-fatty acid synthase (G-11)	Santa Cruz Biotechnology	Cat#: Sc-48357; RRID:AB_627584
Rabbit monoclonal anti-beta-actin (N-21)	Santa Cruz Biotechnology	Cat#: Sc-130656; RRID:AB_2223228
Peroxidase AffiniPure Goat Anti-Rabbit IgG (H+L)	Jackson ImmunoResearch	Cat#: 111-035-144; RRID:AB_2307391
Peroxidase AffiniPure Goat Anti-Mouse IgG (H+L)	Jackson ImmunoResearch	Cat#: 115-035-003; RRID:AB_10015289
SREBP1 antibody	Novus Biologicals	Cat#: NB100-2215SS; RRID:AB_922504
Alexa Fluor 488 goat anti-rabbit IgG (H+L)	ThermoFisher Technologies	Cat#: A11008; RRID:AB_143165
BNIP3 Antibody (BH3 Domain Specific)	Antibodies Online	Cat#: ABIN388117
P70 S6 Kinase Antibody	Cell Signaling Technologies	Cat#: 9202S; RRID:AB_331676
Phospho-p70 S6 Kinase (Thr389) Antibody	Cell Signaling Technologies	Cat#: 9205S; RRID:AB_330944
HIF-1 $\alpha$ Antibody	Cell Signaling Technologies	Cat#: 14179S; RRID:AB_2622225
<b>Chemicals, Peptides, and Recombinant Proteins</b>		
Dulbecco's Modified Eagle Medium (DMEM)	ThermoFisher Technologies	Cat#: 10938025
RPMI medium 1640	ThermoFisher Technologies	Cat#: 31870025
L-glutamine (200 mM)	ThermoFisher Technologies	Cat#: 25030081
HEPES buffer solution (1M)	ThermoFisher Technologies	Cat#: 15630056
Penicillin-Streptomycin (10 000U/ml)	ThermoFisher Technologies	Cat#: 15140122
Phosphate Buffered Saline (PBS) pH 7.4 (10x)	ThermoFisher Technologies	Cat#: 70011044
UltraPure Distilled Water Dnase/Rnase free	ThermoFisher Technologies	Cat#: 10977035
Oil Red O	Sigma-Aldrich	Cat#: O0625
Recombinant human M-CSF	Peptotech	Cat#: 300-25
Recombinant murine M-CSF	Peptotech	Cat#: 315-02
C 75	Tocris	Cat#: 2489
Fatostatin A	Tocris	Cat#: 4444
Deferoxamine Mesylate Salt	Sigma-Aldrich	Cat#: D9533
Sorafenib A	Dr. Tim Sparwasser and Dr. Luciana Berod (TWINCORE)	N/A

(Continued on next page)

<b>Continued</b>		
REAGENT or RESOURCE	SOURCE	IDENTIFIER
Lipopolysaccharide from <i>Escherichia coli</i> O26:B6	Sigma-Aldrich	Cat#: L-8274
Pam3CSK4	Invivogen	Cat#: 112208-00-1
TRI reagent	Sigma-Aldrich	Cat#: T9424
Tissue-Tek O.C.T. compound	Sakura Finetek, VWR	Cat#: 4583
Complete EDTA-free Protease Inhibitor Cocktail Tablets	Roche	Cat#: 11873580001
Halt Protease and Phosphatase Inhibitor Cocktail (100x)	ThermoFisher Scientific	Cat#:78440
SuperSignal West Femto Maximum Sensitivity Substrate	ThermoFisher Scientific	Cat#: 34094
HiMark Pre-stained Protein Standard	ThermoFisher Scientific	Cat#: LC5699
PageRuler Prestained Protein Ladder, 10 to 180 kDa	ThermoFisher Scientific	Cat#: 26616
Phenol:Chloroform:Isoamyl Alcohol 25:24:1, Saturated with 10mM Tris, pH 8.0, 1mM	Sigma-Aldrich	Cat#: P3803
Formalin solution, neutral buffered, 10%	Sigma-Aldrich	Cat#: HT501128
Percoll	GE HealthCare	Cat#: 17-0891-01
Histopaque-1077	Sigma-Aldrich	Cat#: 10771
Chloroform	Carlo Erba Reagents	Cat#: 438603
Methanol	Sigma-Aldrich	Cat#: 34885-M
Hexane	Sigma-Aldrich	Cat#: 296090
Acetic acid glacial	Carlo Erba Reagents	Cat#: 401424
Diethyl ether	Sigma-Aldrich	Cat#: 676845
Paraformaldehyde	Sigma-Aldrich	Cat#: P6148
Sulfuric acid 96%	PanReac AppliChem	Cat#: 131058.1212
Copper (II) sulfate pentahydrate	Sigma-Aldrich	Cat#: C7631
Sodium phosphate dibasic dihydrate	Carlo Erba Reagents	Cat#: 480227
Corn Oil, delivery for fat-soluble compounds	Sigma-Aldrich	Cat#: C8267
Dimethyl sulfoxide	Sigma-Aldrich	Cat#: 276855
Albumin from bovine serum	Sigma-Aldrich	Cat#: A7906
Fetal Bovine Serum	ThermoFisher Scientific	Cat#: 10270106
Fetal Bovine Serum, dialyzed, US origin	ThermoFisher Scientific	Cat#: 26400044
Sodium acetate-2- <sup>13</sup> C	Cortecnet	Cat#: CC3395P
Sodium pyruvate (100 mM)	ThermoFisher Scientific	Cat#: 11360070
Sodium acetate	Sigma-Aldrich	Cat#: S-2889
Sodium DL-lactate	Sigma-Aldrich	Cat#: 71720-25G
Opti-MEM Reduced Serum Media	ThermoFisher Scientific	Cat#: 31985047
Lipofectamine RNAiMAX Transfection Reagent	ThermoFisher Scientific	Cat#: 13778075
<b>Critical Commercial Assays</b>		
SensiFAST cDNA Synthesis Kit	Bioline	Cat#: BIO-65054
SensiFAST Sybr Hi-ROX kit	Bioline	Cat#: BIO-92005
DC protein Assay Kit II	Bio-rad	Cat#: 5000111
CellTrace CFSE Cell Proliferation Kit	ThermoFisher Scientific	Cat#: C34570
Trans-Blot Turbo Mini Nitrocellulose Transfer Packs	Bio-rad	Cat#: 1704158
Maxima Probe/ROX qPCR Master Mix (2x)	ThermoFischer Scientific	Cat#: K0231

(Continued on next page)

**Continued**

REAGENT or RESOURCE	SOURCE	IDENTIFIER
Kit for Creatinine detection	Spinreact	Cat#: 1001113
Kit for GOT/AST detection	Spinreact	Cat#: 1001162
Kit for GPT/ALT detection	Spinreact	Cat#: 41282
Kit for Cholesterol detection	Spinreact	Cat#: 1001093
Kit for HDL detection	Spinreact	Cat#: 1001098
Kit for LDL detection	Spinreact	Cat#: 41023
Kit for Urea detection	Spinreact	Cat#: 41043
Kit for Triglycerides detection	Spinreact	Cat#: 1001314
Kit for Acetic Acid detection (ACS Analyzer Format)	Megazyme	Cat#: K-ACETAF
KASP V4.0 2X Mastermix 96/384, Low Rox	LGC Group	Cat#: KBS-1016-002
KASP by Design (KBD) Primer Mix (for <i>HIF1A</i> rs2057482 and <i>HIF1A</i> rs11519465)	LGC Group	<a href="https://www.biosearchtech.com/products/pcr-kits-and-reagents/genotyping-assays/kasp-genotyping-chemistry/kasp-on-design-kbd">https://www.biosearchtech.com/products/pcr-kits-and-reagents/genotyping-assays/kasp-genotyping-chemistry/kasp-on-design-kbd</a>
TNF alpha Mouse Uncoated ELISA Kit with Plates	Invitrogen	Cat#: 88-7324-22
IL-6 Mouse Uncoated ELISA Kit with Plates	Invitrogen	Cat#: 88-7064-22
IL-10 Mouse Uncoated ELISA Kit with Plates	Invitrogen	Cat#: 88-7105-22
Silencer Select <i>Bnip3</i> siRNA	ThermoFisher Scientific	Cat#: 4390771
Experimental Models: Organisms/Strains		
C57BL/6J mice	Jackson Laboratories	Cat#: 000664
C57BL/6-Ly5.1 mice	Dr. Cláudia Nóbrega and Dr. Margarida Correia-Neves (ICVS, Braga)	N/A
BALB/c mice	Dr. Bhaskar Saha (NCCS, Pune)	N/A
129/Sv mice	Dr. Bhaskar Saha (NCCS, Pune)	N/A
mHIF-1 $\alpha$ <sup>-/-</sup> mice	Prof. Rui Appelberg (IBMC, Porto)	N/A
<i>Leishmania donovani</i> MHOM/IN/82/Patra1	Dr. Baptiste Vergnes (IRD, Montpellier)	N/A
<i>Leishmania infantum</i> ITMAP 263	Dr. Baptiste Vergnes (IRD, Montpellier)	N/A
<i>Leishmania donovani</i> MHOM/IN/83/AG83	Dr. Bhaskar Saha (NCCS, Pune)	N/A
Oligonucleotides		
Oligonucleotides		Table S1
Software and Algorithms		
GraphPad Prism v6	GraphPad Software	<a href="https://www.graphpad.com">https://www.graphpad.com</a>
FlowJo	FlowJo LLC	<a href="https://www.flowjo.com">https://www.flowjo.com</a>
CFX Manager	Bio-rad	<a href="https://www.bio-rad.com/en-pt/product/cfx-manager-software?ID=aed9803d-cb4d-4ecb-9263-3efc9e650edb">https://www.bio-rad.com/en-pt/product/cfx-manager-software?ID=aed9803d-cb4d-4ecb-9263-3efc9e650edb</a>
Fiji	ImageJ	<a href="https://fiji.sc">https://fiji.sc</a>
Other		
CD14 Microbeads, human	MACS Miltenyi Biotec	Cat#: 130-097-052
MS columns	MACS Miltenyi Biotec	Cat#: 130-041-301
BODIPY 493/503	ThermoFisher Scientific	Cat#: D3922
BODIPY FL C16	ThermoFisher Scientific	Cat#: D3821
DAF-FM Diacetate	ThermoFisher Scientific	Cat#: D23844
DAPI (4',6-Diamidino-2-Phenylindole, Dihydrochloride)	ThermoFisher Scientific	Cat#: D1306

(Continued on next page)

**Continued**

REAGENT or RESOURCE	SOURCE	IDENTIFIER
Lab Vision PermaFluor Aqueous Mounting Medium	ThermoFisher Scientific	Cat#: TA-030-FM
HPTLC silica gel 60 (25 aluminum sheets)	Merck	Cat#: 1.05547.0001
MicroAmp Fast Optical 96-well reaction plate	Applied Biosystems by Life Technologies	Cat#: 4346906
Multiplate PCR Plates 96-well, clear	Bio-rad	Cat#: MLL9601

**LEAD CONTACT AND MATERIALS AVAILABILITY**

Further information and requests for resources and reagents should be directed to and will be fulfilled by the Lead Contact, Ricardo Silvestre ([ricardosilvestre@med.uminho.pt](mailto:ricardosilvestre@med.uminho.pt)). This study did not generate new unique reagents. There are no restrictions to the availability of data generated in this study.

**EXPERIMENTAL MODEL AND SUBJECT DETAILS****Mice**

Wild-type (WT) C57BL/6 were purchased from Charles River Laboratories and *Hif1 $\alpha$ <sup>fl $\alpha$ /fl $\alpha$</sup>*  mice crossed with lysozyme M-driven Cre (*LysM<sup>Cre</sup>*)-transgenic mice on a C57BL/6 background, here identified as myeloid-restricted HIF-1 $\alpha$  deficient mice (mHIF-1 $\alpha$ <sup>-/-</sup>), were kindly provided by Dr. Rui Appelberg (I3S; Porto, Portugal). C57BL/6 WT, mHIF-1 $\alpha$ <sup>-/-</sup> mice, BALB/c and 129/SV were bred and maintained in accredited animal facilities at the Life and Health Sciences Research Institute (ICVS). Mice were housed in groups of 3-6, in HEPA filter-bearing cages, under 12-h light/dark cycles. Autoclaved chow and water were provided *ad libitum* and cages were enriched with nesting materials (paper towels). Males and females with 8-12 weeks were used. Due to colony management and animal availability, all the *in vitro* experiments were performed with males while *in vivo* infection experiments were performed with mixed-gender groups (Tables S2 and S3). Experimental animal procedures agreed with the European Council Directive (2010/63/EU) guidelines that were transposed into Portuguese law (Decree-Law n.º 113/2013, August 7th). Experiments were conducted with the approval of the UMinho Ethical Committee (process no. SECVS 074/2016) and complied with the guidelines of the Committee and National Council of Ethics for the Life Sciences (CNECV). RS has an accreditation for animal research given from Portuguese Veterinary Direction (Ministerial Directive 1005/92).

**Parasite culture and staining**

Cloned lines of virulent *Leishmania donovani* (MHOM/IN/82/Patra1 and MHOM/IN/83/AG83) and *L. infantum* (ITMAP 263) were maintained with weekly subpassages at 27°C in complete RPMI 1640 medium, supplemented with 10% heat-inactivated fetal bovine serum, 2 mM L-glutamine, 100 U/ml penicillin plus 100 mg/ml streptomycin and 20 mM HEPES buffer. Only parasites under ten passages were used in the experimental work. *L. donovani* promastigotes were stained with carboxyfluorescein succinimidyl ester (CFSE). Briefly, parasites were centrifuged and washed with warm phosphate-buffered saline (PBS) twice and then labeled with 5  $\mu$ M CFSE (10  $\times$  10<sup>6</sup> parasites/ml of PBS) for 10 minutes, at 37°C. The parasites were subsequently washed twice with PBS to quench the excess of fluorescence and suspended in complete RPMI.

**Macrophage culture and in vitro infections**

For peritoneal macrophages, peritoneal exudate was recovered after injection of ice-cold PBS in the peritoneal cavity. Cells were washed, resuspended in complete RPMI and plated at a density of 1  $\times$  10<sup>6</sup>/ml. Non-adherent cells were removed through washing 4 hours after plating.

Bone marrow precursors from WT and HIF-1 $\alpha$ <sup>-/-</sup> mice were recovered and differentiated in macrophages using recombinant M-CSF. Precursors were plated at 0.5  $\times$  10<sup>6</sup> cells/ml with 20 ng/ml of M-CSF. Growth factor was renewed at day 4 post-differentiation. The macrophages were used 7 days after differentiation.

Peripheral blood mononuclear cells (PBMCs) were enriched from blood from healthy volunteers using a density gradient with Histopaque 1077. The mononuclear phase was recovered and washed with PBS. Next, cells were labeled with magnetic CD14 MicroBeads and CD14<sup>+</sup> monocytes were positively separated using an MS column. Human CD14<sup>+</sup> monocytes were differentiated in macrophages using recombinant M-CSF. Briefly, monocytes were plated at 1  $\times$  10<sup>6</sup> cells/ml with 20 ng/ml of M-CSF. Growth factor was renewed at day 4 post-differentiation. The macrophages were used 7 days after differentiation.

Macrophages were infected with *L. donovani* promastigotes at a 1:10 ratio. After 4 hours of incubation, non-phagocytosed parasites were removed, and cells were recovered. Macrophages were treated with C75 (40  $\mu$ M), sorA (500 nM) or deferoxamine (DFX; 500  $\mu$ M), 24 hours post-infection, for two hours, or left untreated as control. Following drug treatment, macrophages were left in culture for 4 days. Fatostatin A (10  $\mu$ M) was added 24 hours post-infection and left until analysis at day 5 post-infection. To assess if these drugs have a direct effect on the parasites, axenic promastigotes (starting with 1  $\times$  10<sup>6</sup> parasites/ml) were treated with

C75, fatostatin A and sorA and cultured until stationary phase. Parasites were fixated with 2% PFA and counted daily, for 4 days, using a Neubauer chamber. No major alterations were found, suggesting that the used drugs do not impact on parasite biology (Figure S7C).

## METHOD DETAILS

### Parasite viability

Five days post-infection, the parasite viability was performed by adapting the Parasite Rescue Transformation Assay (Jain et al., 2012). Briefly, culture media was renewed, and the plates were further sealed and placed in an incubator at 27°C to allow the conversion of amastigotes in promastigotes. The parasites were counted as above-mentioned upon 7 days of incubation at 27°C. Similar results were obtained in parallel by following the rescue protocol (Jain et al., 2012) and giemsa staining counting.

### SNP selection and genotyping

The rs2057482 single nucleotide polymorphism (SNP) analyzed was selected based on their putative functional consequences. Genomic DNA was isolated from whole blood using the QIAcube automated system. Genotyping was performed using KASPar assays in an Applied Biosystems 7500 Fast Real-Time PCR system. Quality control for the genotyping results was achieved with negative controls and randomly selected samples with known genotypes.

### Experimental Leishmania infection

Mice were infected with  $10 \times 10^6$  (intravenous route) or  $100 \times 10^6$  (intraperitoneal route) stationary *L. donovani* promastigotes. Weight and general well-being were monitored during the infection. FASN inhibitor C75 was administered via intraperitoneal route, at days 2, 4, 6 and 8 post-infection (10 mg/kg). Control animals were equally injected with vehicle (sterile PBS with 5% DMSO). Fatostatin A was administered via intraperitoneal route at days 3, 4, 5 and 6 post-infection (15 mg/kg). Control animals were equally injected with vehicle (sterile corn oil with 5% DMSO). Mice were anesthetized with volatile isoflurane and blood was withdrawn by cardiac puncture. Euthanasia by cervical dislocation was performed following this procedure. The bone marrow, liver and spleen were recovered for further analysis. The bone marrow was flushed from the femurs and tibias and precursors were washed with PBS and frozen for DNA extraction. The liver and spleen were mechanically resuspended and cells were recovered for flow cytometry and DNA extraction. Liver cell suspensions were subjected to a Percoll gradient (40/80) to isolate hepatic leukocytes. DNA was extracted using the phenol-chloroform-isoamyl alcohol method. Briefly, an aqueous suspension with approximately  $1 \times 10^6$  cells was mixed with a mixture of phenol-chloroform-isoamyl alcohol (25:24:1). After centrifugation, the aqueous phase was recovered and incubated overnight with 3M sodium acetate and absolute ethanol. The DNA pellet was washed twice with 70% ethanol and resuspended in RNase/DNase-free water. Parasite burden was assessed, using a TaqMan-based qPCR assay for detection and quantification of *L. donovani* kinetoplastid DNA. Total cholesterol, triglycerides, LDL, HDL, acetate, creatine, urea, ALT and AST levels were quantified in the serum using an AutoAnalyzer, using reagents from the same provider.

### Oil Red O staining

The liver was perfused with saline solution (portal vein perfusion) and fixed overnight with 10% (w/v) formalin. The samples were then embedded in Tissue-Tek O.C.T. compound and frozen in liquid nitrogen. After sample section on the cryostat (8  $\mu$ m), the slides were stained with Oil Red O solution and bright field images were acquired on a BX6 microscope.

### Flow cytometry

Bodipy 493/503 (3  $\mu$ g/ml) and Bodipy FL C16 (1  $\mu$ M) were diluted in complete media and add to adherent cells for 30 minutes at 37°C. DAF-FM (2  $\mu$ g/ml) was diluted in PBS and incubated for 30 minutes at 37°C. The cells were then washed with PBS, detached and analyzed. Before analysis, cells stained with DAF-FM were left to rest for 20 minutes, to complete de-esterification of intracellular diacetates. Surface staining was performed with the following antibodies: BV605 anti-mouse CD11c, clone N418; APC anti-mouse I-A/I-E, clone M5/114.15.2; BV785 anti-mouse NK1.1, clone PK136; PE/Cy7 anti-mouse CD11b, clone M1/70; BV711 anti-mouse Ly6G, clone 1A8; PerCP/Cy5.5 anti-mouse Ly6C, clone HK14. Samples were acquired on a LSRII flow cytometer (BD Biosciences) and data analyzed using FlowJo software. The gating strategy for myeloid cells is depicted on Figure S7D.

### High performance liquid chromatography

Glucose and lactate were quantified in cell culture supernatant using HPLC technology (Gilson bomb system); HyperREZ XP Carbohydrate H<sup>+</sup> 8 $\mu$ M. Samples were filtered with a 0.2  $\mu$ m filter and the mobile phase (0.0025M H<sub>2</sub>SO<sub>4</sub>) was similarly filtered and degassed for 30 minutes. Each sample was analyzed using the following running protocols (sensitivity 8): 15 minutes at a constant flux of 0.7 ml/min at 54°C for glucose and lactate detection. The peaks were detected in a refractive index detector (IOTA 2, Reagents) and integration was performed using Gilson Uniprot Software, version 5.11.

### Lipid extraction and HPTLC analysis

Lipid extraction was performed using a modified Bligh and Dyer, 1959 methodology. Macrophages were lysed in ice-cold lysis buffer containing 50 mM Tris, pH 7.4, 1% Triton X-100, 150 mM NaCl, 10% glycerol, 50 mM NaF, 5 mM sodium pyrophosphate, 1 mM

$\text{Na}_3\text{VO}_4$ , 25 mM sodium- $\beta$ -glycerophosphate, 1 mM DTT, 0.5 mM PMSF and protease inhibitors. A chloroform-methanol-water solution (2:1:0.8 v/v) was added to the lysates (70  $\mu\text{g}$ ), which were left in intermittent shaking for two hours. The initial phases were separated by centrifugation (730 g, 20 min at 4°C) and the supernatant was collected. A water-chloroform solution (1:1) was added to the supernatant and the organic phase was collected after centrifugation (730 g, 20 min at 4°C). The extracted lipids were analyzed by high performance thin layer chromatography (HPTLC) using hexane-diethyl ether-acetic acid solvent (60:40:1 v/v). For detection, the plates were sprayed in a carbonization solution with 8%  $\text{CuSO}_4$  and 10%  $\text{H}_3\text{PO}_4$  and heated at 110°C for 20 minutes. The lipid bands were then analyzed by densitometry using the Fiji software.

#### Quantitative PCR analysis

Total RNA was isolated from cells with TRI reagent, according to the manufacturer instructions. RNA concentration was determined by OD260 measurement using a NanoDrop spectrophotometer. Total RNA (10–200 ng) was reverse-transcribed using the SensiFAST cDNA Synthesis Kit. Real-Time quantitative PCR (qRT-PCR) reactions were run for each sample on a Bio-Rad CFX96 Real-Time System C1000 Thermal Cycler. Primer sequences were obtained from Alfagene and thoroughly tested. The RT product was expanded using the SensiFAST SYBR Hi-ROX kit and the results were normalized to the expression of the housekeeping gene 18 s. After amplification, cycle threshold-values (Ct-values) were calculated for all samples and gene expression changes were analyzed in the CFX Manager Software.

#### Western blot

Approximately  $1\text{--}4 \times 10^6$  macrophages were lysed in ice-cold lysis buffer containing 50 mM Tris, 0.25 M NaCl, 2 mM EDTA, 1% NP-40, 10% glycerol, complemented with protease/phosphatase cocktail inhibitor. The samples were left resting on ice for 30 minutes and then sonicated in an ultrasonic bath for additional 30 minutes. Following centrifugation (13,000 g, 30 minutes, at 4°C), the lysates (ten to twenty-five micrograms of protein) were subjected to SDS-PAGE electrophoresis and the proteins were transferred to mini nitrocellulose membranes by the Trans Blot Turbo Transfer System. The membranes were then incubated with primary antibodies (1/1000 for each primary antibody) and with horseradish peroxidase-coupled secondary reagents. Detection was made with SuperSignal West Femto Maximum Sensitivity Substrate. Primary antibodies were directed against BNIP3, Phospho-p70 S6k kinase (Thr389), p70 S6 kinase, FASN and  $\beta$ -actin.

#### Enzyme-linked Immunosorbent Assay

The levels of cytokines were determined in the supernatant of WT and HIF-1 $\alpha^{-/-}$  macrophages, 5 days post-infection, using TNF- $\alpha$ , IL-6 and IL-10 Mouse ELISA, following manufacturer's instructions.

#### Macrophage transfection

Bone marrow-derived macrophages were differentiated, as previously described. At the 7<sup>th</sup> day of differentiation, BNIP3 silencing was induced, using small interfering RNA (siRNA) technology. Briefly, a lipid-based transfection was performed with Lipofectamine RNAiMAX Transfection Reagent. The siRNA/lipid complexes were added to macrophage culture during 4h, in Opti-MEM Reduced Serum Media. Then, the complexes were removed and cells were left resting in complete RPMI for 14 hours. Cell viability was unaltered in BNIP3-silenced conditions, when compared to scramble control and untransfected cells. Macrophage infection was performed as already described and samples were stored for western blot and quantitative PCR, 10 and 24 hours post-infection, respectively.

#### Immunofluorescence

Peritoneal macrophages were cultured and infected in coverslips, as abovementioned. Upon 24 hours of infection, cells were fixed during 30 minutes with 10% formalin, at room temperature. Next, ice-cold methanol was added for ten minutes and cells were washed three times with PBS. To block non-specific antibody binding, the coverslips were incubated for one hour with 10% bovine serum albumin, at room temperature. The primary rabbit anti-SREBP-1c antibody was incubated at room temperature for two hours (1/200). The coverslips were washed three times with PBS. The secondary Alexa Fluor 488-labeled goat anti-rabbit IgG (H+L) antibody was incubated during one hour at room temperature. Following three washes with PBS, the nuclei were stained with DAPI during 10 minutes. The coverslips were mounted in Permafluor Mountant and appropriately sealed. Images were acquired on an Olympus FluoView FV1000 confocal laser scanning microscope.

#### Nuclear Magnetic Resonance

Bone marrow-derived macrophages from WT and mHIF-1 $\alpha^{-/-}$  mice were cultured in the presence of 5 mM sodium acetate-2- $^{13}\text{C}$  for 24 hours, 3 days post-infection. The cells were recovered and washed twice with PBS. After centrifugation, the pellet was resuspended in methanol (4 ml/g of cells) and water (0.85 ml/g of cells) and left on ice for 10 minutes. Chloroform (4 ml/g of cells) and water (2 ml/g of cells) were then added, followed by an additional 10 minutes on ice. The organic and aqueous phases were separated by centrifugation and stored at  $-80^\circ\text{C}$ . After solvent evaporation in a speed-vacuum concentrator, the aqueous phases were suspended in 600  $\mu\text{L}$   $\text{D}_2\text{O}$  containing 2 mM  $\text{NaN}_3$  and 0.29 mM TSP. All NMR experiments were performed at 25°C in a Bruker Avance II+ spectrometer, operating at a frequency of 800.33 MHz for  $^1\text{H}$ , equipped with a 5 mm three channel probe (TXI-Z H/C/N-D). For all

samples were acquired: an  $^1\text{H}$ -NMR spectra (*noesygppr1d* pulse program, with 64 k points, 96 scans, using a spectral window of 20.55 ppm, 4 s relaxation delay and 10 ms mixing time) and a  $^1\text{H}$ - $^{13}\text{C}$  Heteronuclear Single Quantum Coherence spectra (*hsqcetg-psisp2* pulse program, with 512 points in F1 and 2048 points in F2, 128 scans, using a sweep width of 165 ppm in F1 and 16 ppm in F2 and 1.5 s relaxation delay). Spectra processing was performed using Topspin3.2 software and the resonances volumes on the  $^1\text{H}$ - $^{13}\text{C}$ -HSQC spectra were determined using the same software.

#### Cell sorting

Peritoneal macrophages from Ly5.1 WT and mHIF-1 $\alpha$ <sup>-/-</sup> mice were co-cultured for two hours (1:1 ratio) and infected with *L. donovani*, as previously described. At the fifth day of infection, macrophages were recovered by detachment with a solution of 10 mM ethylenediaminetetraacetic acid (EDTA). Surface staining with PE anti-mouse CD45.1, clone A20 and APC anti-mouse CD45.2, clone 104 was performed and cells were sorted using BD FACSAria II. A similar number of purified WT and HIF-1 $\alpha$ <sup>-/-</sup> macrophages were used to assess parasite viability.

#### RNA sequencing

Reads were trimmed using Trimmomatic v0.36 with the following options: TRAILING:30, SLIDINGWINDOW:4:20 and MINLEN:30. All other options used the default values. Quality check was performed on raw and trimmed data to ensure the quality of the reads using FastQC v0.11.5 and MultiQC v1.5. The quantification was performed with Kallisto v0.44. Differential expression analysis was performed in R v3.5.0 using the DESeq2 v1.20.0 and volcano plots were produced with the ggplot2 package.

#### QUANTIFICATION AND STATISTICAL ANALYSIS

Statistical analyses were performed with the GraphPad Prism 6 software. A one-way analysis of variance (ANOVA) followed by a Bonferroni's post hoc test was employed for multiple group comparisons. A Mann-Whitney test of variance and Kruskal-Wallis non-parametric test were performed accordingly with the correspondent experimental design. The statistical details of each experiment can be found in figure legends and the data is presented as mean  $\pm$  SD. Statistically significant values are as follows: \* $p < 0.05$ , \*\* $p < 0.01$ , \*\*\* $p < 0.001$ .

#### DATA AND CODE AVAILABILITY

The accession number for the RNA-seq data generated during this study reported in this paper is Gene Expression Omnibus (GEO): GSE145136.

Cell Reports, Volume 30

## Supplemental Information

### **The Absence of HIF-1 $\alpha$ Increases Susceptibility**

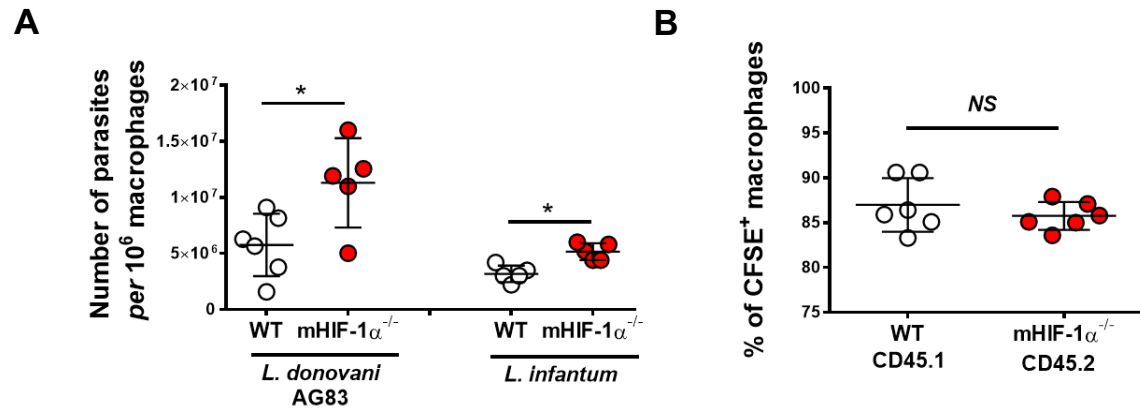
**to *Leishmania donovani* Infection**

**via Activation of BNIP3/mTOR/SREBP-1c Axis**

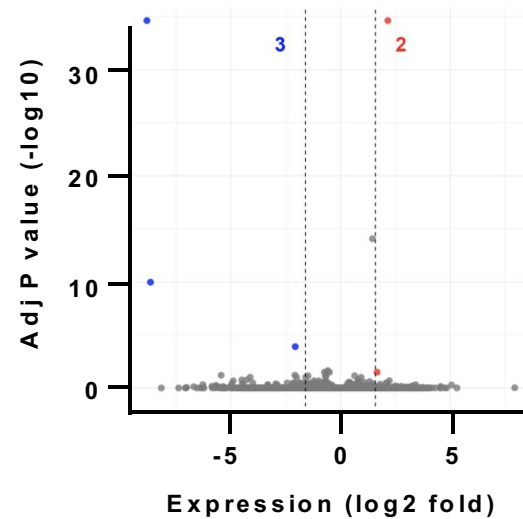
**Inês Mesquita, Carolina Ferreira, Diana Moreira, George Eduardo Gabriel Kluck, Ana Margarida Barbosa, Egídio Torrado, Ricardo Jorge Dinis-Oliveira, Luís Gafeira Gonçalves, Charles-Joly Beauparlant, Arnaud Droit, Luciana Berod, Tim Sparwasser, Neelam Bodhale, Bhaskar Saha, Fernando Rodrigues, Cristina Cunha, Agostinho Carvalho, António Gil Castro, Jérôme Estaquier, and Ricardo Silvestre**



## SUPPLEMENTARY FIGURE 1 (Support of Fig 1)

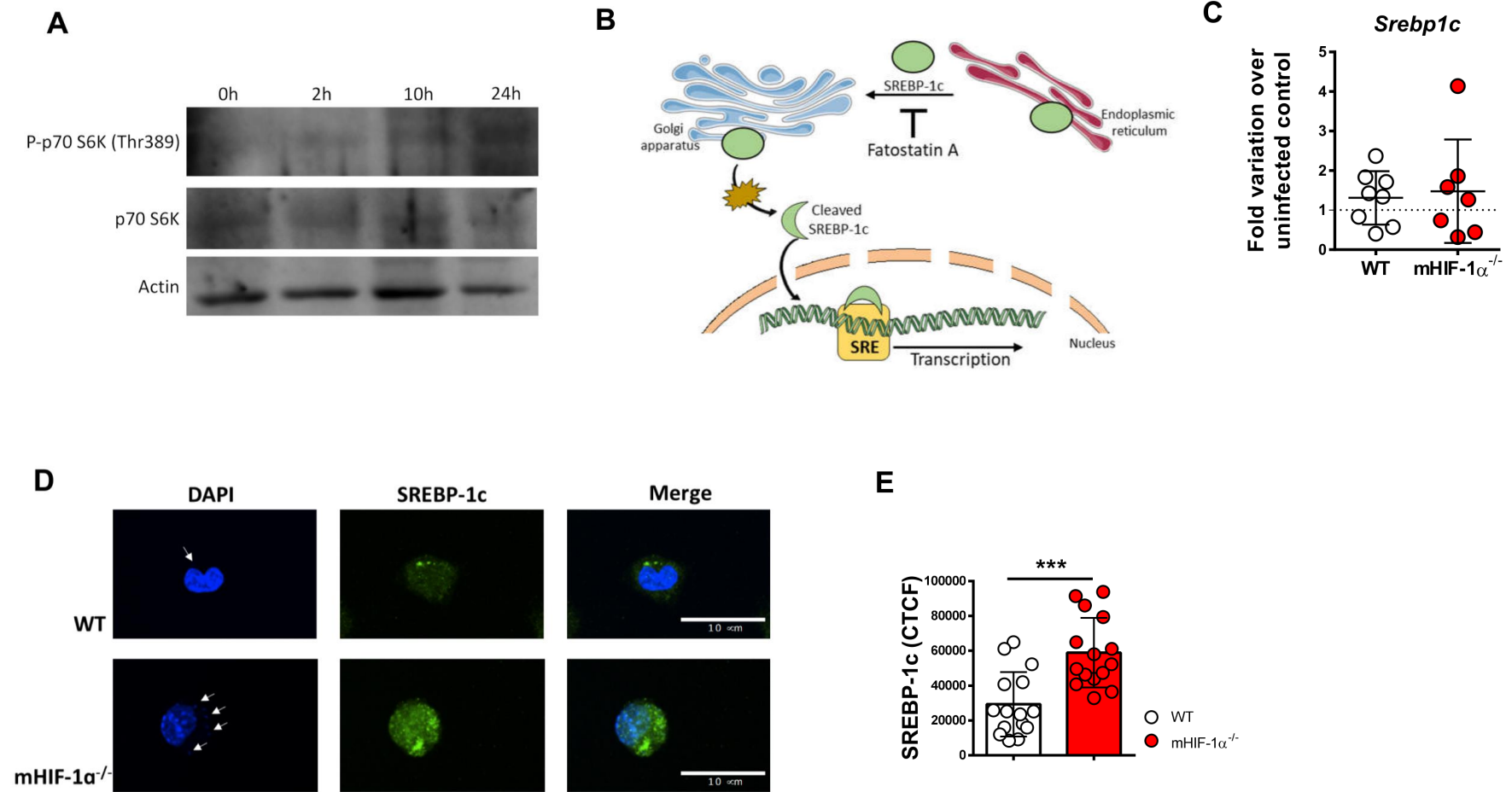


**Supplementary figure 1. HIF-1α<sup>-/-</sup> macrophages display enhanced susceptibility to *L. infantum* and other *L. donovani* strains.** (A) *L. donovani* AG-83 and *L. infantum* viability 5 days post-infection; (B) Co-cultured WT CD45.1 and HIF-1α<sup>-/-</sup> CD45.2 macrophages were infected with CFSE-labelled *L. donovani* promastigotes. Phagocytosis was assessed at 4 hours of infection by flow cytometry. Data is shown as mean ± SD; \*p<0.05.

**SUPPLEMENTARY FIGURE 2 (Support of Fig 2)**

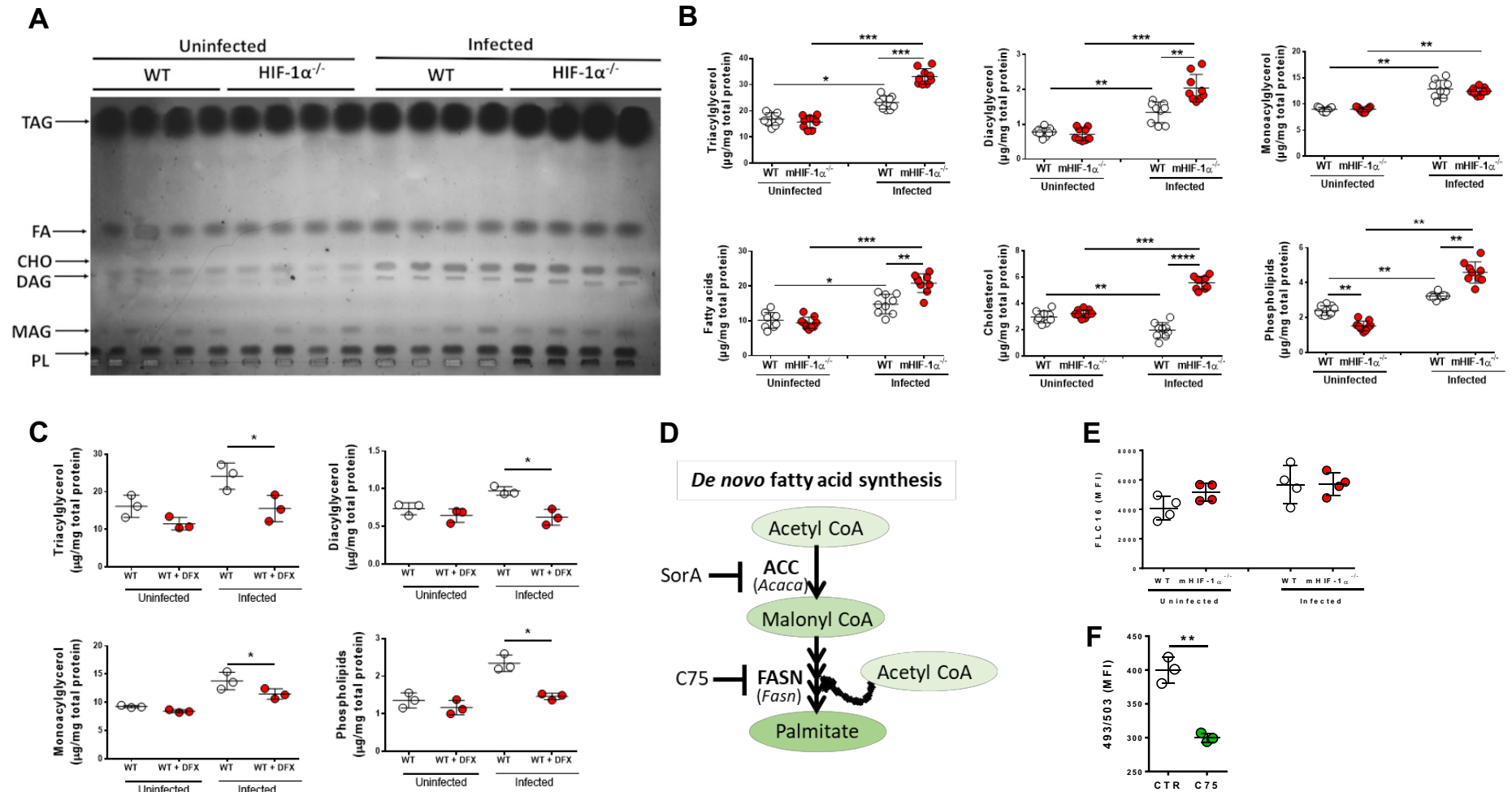
**Supplementary figure 2. Volcano plot analysis of uninfected murine WT and HIF-1 $\alpha$ <sup>-/-</sup> macrophages.** Expression values (log<sub>2</sub> fold) were plotted against the adjusted P value (-log<sub>10</sub>) for the difference in expression. Annotated numbers indicate genes with significant differential expression: upregulated (red=2) or downregulated (blue=3), 1.5 fold or more in HIF-1 $\alpha$ <sup>-/-</sup> macrophages relative to WT cells.

## SUPPLEMENTARY FIGURE 3 (Support of Fig 2 and 3)



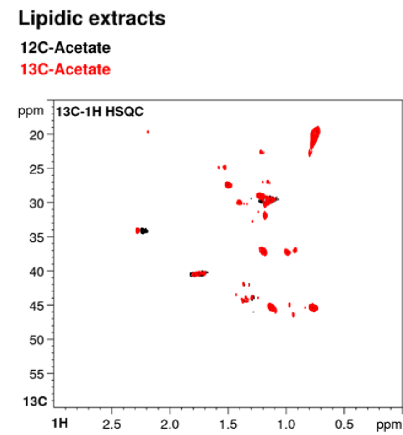
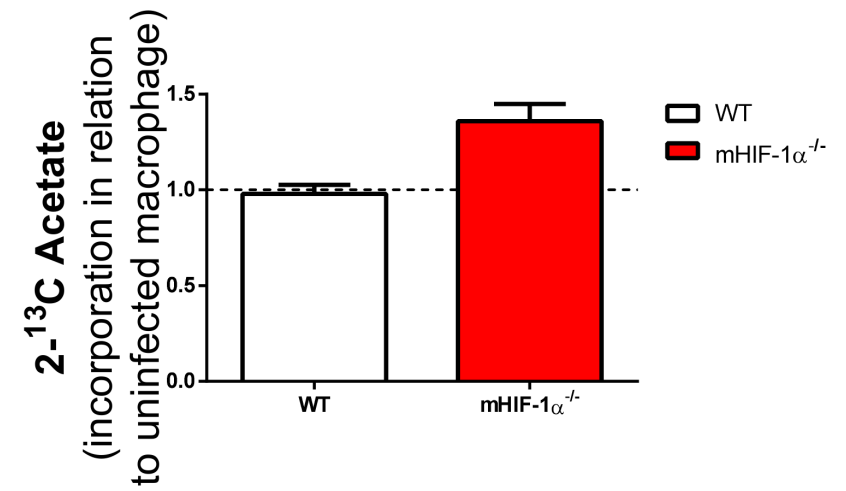
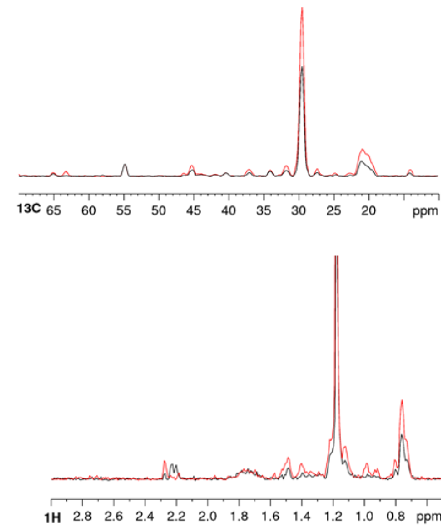
**Supplementary figure 3. SREBP-1c is activated in the absence of HIF-1 $\alpha$  during *L. donovani* infection.** (A) Western blot analysis and densitometry of phospho-p70 S6K, total p70 S6K and beta-actin in uninfected and 2, 10 and 24 hours post-infection HIF-1 $\alpha$ <sup>-/-</sup> macrophages; (B) Schematic representation of the mechanism of action of SREBP. SRE: sterol regulatory element; SREBP: sterol regulatory element binding proteins; (C) qPCR analysis of the transcriptional levels of *Srebp1c* 24 hours post-infection; (D) Immunofluorescence confocal microscopy of *Leishmania*-infected WT and HIF-1 $\alpha$ <sup>-/-</sup> macrophages. At 24 hours post-infection, macrophages were fixed and probed with an anti-SREBP1c antibody; green, SREBP1c; blue, DNA (DAPI). White arrows point to *L. donovani* nucleus; (E) quantification of nuclear SREBP-1c was performed as corrected total cell fluorescence (CTCF) = Integrated Density – (Area of selected cell X Mean fluorescence of background readings).

## SUPPLEMENTARY FIGURE 4 (Support of Fig 4)



**Supplementary figure 4. HPTLC analysis of uninfected and *L. donovani*-infected macrophages.** (A) Schematic representation of high-performance thin layer chromatography (HPTLC) for lipid separation. CHO: cholesterol; DAG: diacylglycerol; FA: fatty acids; MAG: monoacylglycerol; PL: phospholipids; TAG: triacylglycerol; (B) Quantification of intracellular lipids by HPTLC in uninfected and infected WT and HIF-1 $\alpha$ <sup>-/-</sup> macrophages (5 days post-infection); (C) Quantification of intracellular lipids by HPTLC in uninfected and infected WT macrophages, 5 days post-infection. Deferoxamine (DFX) treatment was performed 24 hours post-infection. (D) Schematic representation of fatty acid synthesis. ACC: acetyl-CoA carboxylase; (E) Quantification of palmitate uptake by flow cytometric analysis of Bodipy FL C16 staining in uninfected and infected WT and HIF-1 $\alpha$ <sup>-/-</sup> macrophages (5 days post-infection). (F) Quantification of intracellular neutral lipids by flow cytometry, using the probe Bodipy 493/503, in HIF-1 $\alpha$ <sup>-/-</sup> macrophages treated with C75. . Data is shown as mean  $\pm$  SD; \*p<0.05; \*\*p<0.01; \*\*\*p<0.001.

## SUPPLEMENTARY FIGURE 5 (Support of Fig 4)

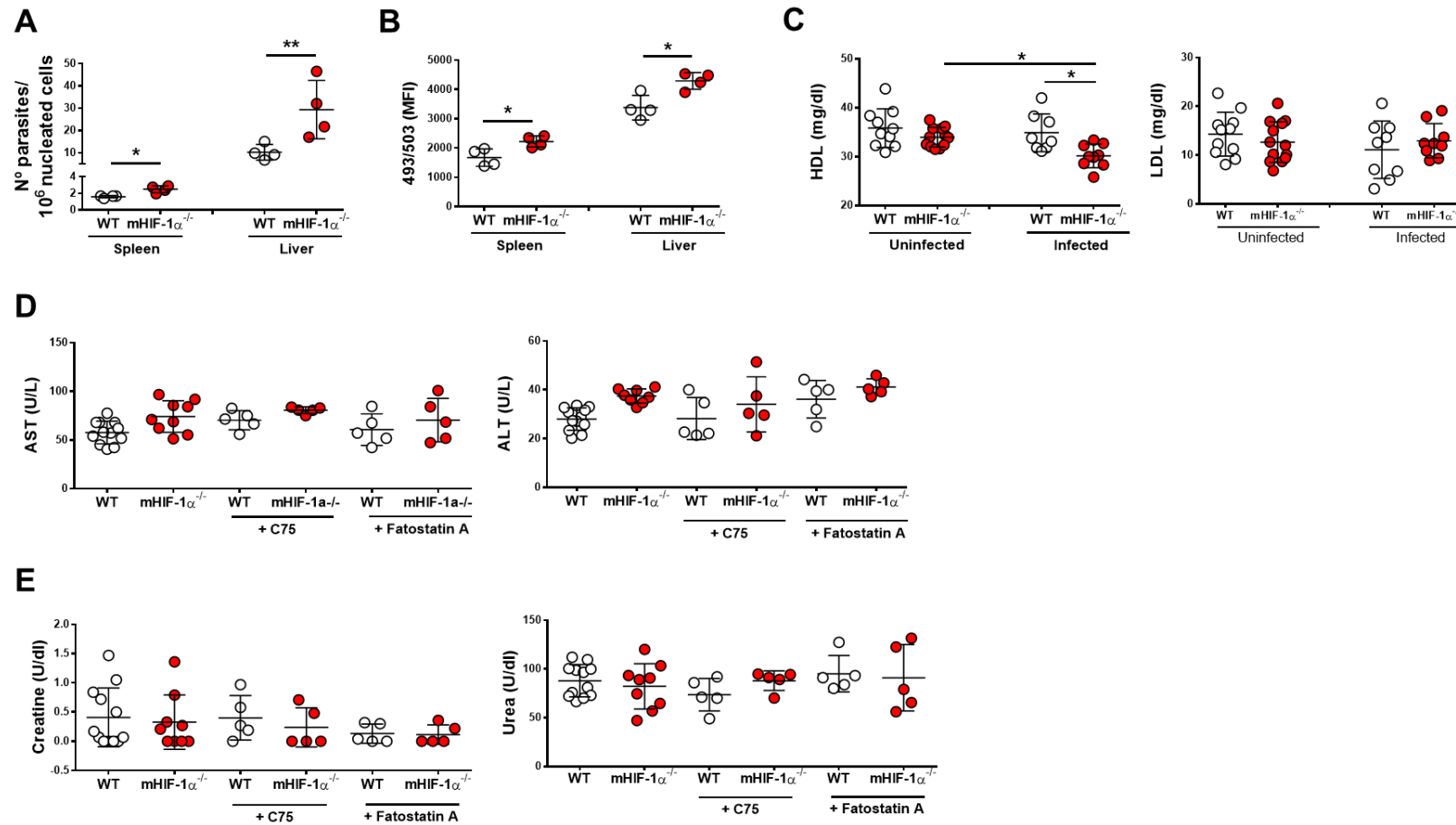
**A****B**

**SUPPLEMENTARY FIGURE 5 (Support of Fig 4)**

**Supplementary figure 5. Increased incorporation of  $^{13}\text{C}$ -acetate on the lipid fraction of *L. donovani* infected HIF-1 $\alpha^{-/-}$ .** (A) Representative  $^{13}\text{C}$ - $^1\text{H}$ -HSQC spectrum of the lipid extracts of *L. donovani* infected HIF-1 $\alpha^{-/-}$  macrophages for three days following a subsequent 24 hours incubation in the presence of  $^{12}\text{C}$ -acetate (black) and U- $^{13}\text{C}$ -acetate (red). HSQC spectrum shows the proton resonances (X-axis) directly linked to  $^{13}\text{C}$  (Y axis) and the spectrum of the incubated with U- $^{13}\text{C}$ -acetate there is an increased in the spectra intensity indicating the incorporation of  $^{13}\text{C}$  from the acetate in the lipids. (B) In the  $^{13}\text{C}$  (upper panel) and  $^1\text{H}$  (lower panel) 1D HSQC projections of the HSQC spectra is possible to observe that the resonances of lipids are more intense in the  $^{13}\text{C}$ -acetate incubation. $^{13}\text{C}$ -labeled acetate incorporation in the lipid fraction. (C) WT and HIF-1 $\alpha^{-/-}$  macrophages were infected with *L. donovani* for three days following a subsequent 24 hours incubation in the presence of  $^{13}\text{C}$ -labeled acetate. After 24 hours incorporation in intracellular lipid fraction was assessed (Mean  $\pm$  SD, n=3).

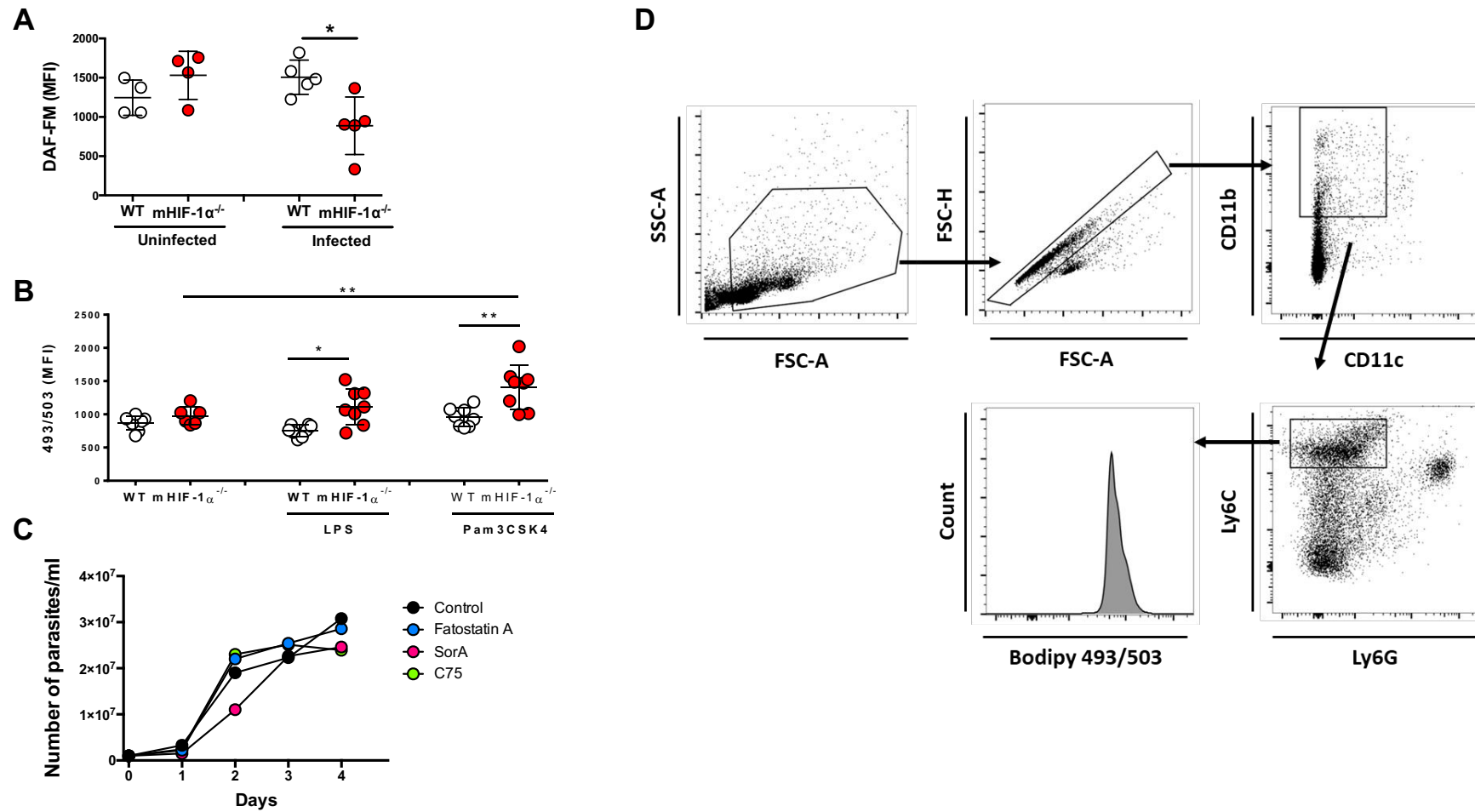


## SUPPLEMENTARY FIGURE 6 (Support of Fig 5 and 6)



**Supplementary figure 6. mHIF-1 $\alpha$ <sup>-/-</sup> mice enhanced susceptibility to *L. donovani* infection is not dose dependent.** (A) Parasite burden in WT and HIF-1 $\alpha$ <sup>-/-</sup> mice 2 weeks after infection with a 10-fold lower inoculum (10 x 10<sup>6</sup> parasites). (B) Quantification of intracellular neutral lipids by flow cytometry, using the probe Bodipy 493/503, in CD11b<sup>+</sup> cells in the spleen and liver of WT and HIF-1 $\alpha$ <sup>-/-</sup>, 2 weeks after infection with a lower inoculum (10 x 10<sup>6</sup> parasites). (C) HDL levels in the serum of WT and HIF-1 $\alpha$ <sup>-/-</sup> mice, 2 weeks post-infection; LDL levels in the serum of WT and HIF-1 $\alpha$ <sup>-/-</sup> mice, 2 weeks post-infection; **C75 and fatostatin A treatment does not induce toxicity.** (D) Alanine transaminase (ALT), aspartate transaminase (AST) and (E) creatine and urea levels on the serum of C75 and fatostatin A-treated and untreated WT and HIF-1 $\alpha$ <sup>-/-</sup>, 10 days post-infection. Data is shown as mean  $\pm$  SD; n=3-10 mice/group. \*p<0.05; \*\*p<0.01.

## SUPPLEMENTARY FIGURE 7 (Support of Discussion and Materials and Methods)



**Supplementary figure 7. Nitric oxide production is impaired on infected HIF-1 $\alpha$ <sup>-/-</sup> macrophages.** (A) Intracellular nitric oxide accumulation was quantified by flow cytometry using the probe DAF-FM, 5 days post-infection. Data is shown as mean  $\pm$  SD; n=4-5 mice/group. \*p<0.05. **The absence of HIF-1 $\alpha$  leads to lipid accumulation upon TLR2 and TLR4 stimulation.** (B) Intracellular neutral lipids were quantified by flow cytometry using the probe Bodipy 493/503, 5 days post-stimulation with LPS (TLR4 ligand) and Pam3CSK4 (TLR2 ligand). Data is shown as mean  $\pm$  SD; n=8 mice/group. \*p<0.05; \*\*p<0.01. **Pharmacological inhibitors do not impact axenic promastigote growth.** Axenic promastigotes (1 x 10<sup>6</sup> parasites/ml) were treated with C75 (green), soraphen A (pink), fatostatin A (blue) or left untreated as control. Parasite growth was measured daily by counting promastigotes with a Neubauer chamber, until cultures reached stationary phase. **Gating strategy for flow cytometry analysis.** The gating strategy is represented: dead cells, debris, platelets and granulocytes were excluded in the first gating step. Subsequently, singlets were selected for posterior analysis. The quantification of Bodipy 493/503 was performed in CD11b<sup>+</sup> Ly6C<sup>+</sup> cells.

**Table S1. Oligonucleotides (related to STAR Methods)**

<b>Name</b>	<b>Forward primer</b>	<b>Reverse primer</b>
<i>M. musculus Fasn</i>	GGAGGTGGTGATAGCCGG TAT	TGGGTAATCATAGAGCCCAG
<i>M. musculus Acaca</i>	AACATCCCCACGCTAAAC AG	CTGACAAGGTGGCGTGAAG
<i>M. musculus Sle2a1</i>	CCAGCTGGGAATCGTCGTT	AAGTCTGCATTGCCCATGAT
<i>M. musculus Pdk1</i>	GGACTTCGGGTCAGTGAA TGC	TCCTGAGAAGATTGTCGGGGA
<i>M. musculus Ldha</i>	TGTCTCCAGCAAAGACTA CTGT	GACTGTACTTGACAATGTTGG GA
<i>M. musculus Sle16a3</i>	GCCACCTCAACGCCTGCTA	TGTCGGGTACACCCATATCCT TA
<i>M. musculus Srebp1c</i>	ATCTCCTAGAGCGAGCGTT G	TATTTAGCAACTGCAGATATC CAAG
<i>M. musculus 18S</i>	GTAACCCGTTGAACCCCAT T	CCATCCAATCGGTAGTAGCG
<i>H. sapiens HIF1A</i>	GCTTTAACTTTGCTG GCCCC	TTTTCGTTGGGTGAGGGGAG
<i>L. donovani</i> kinetoplastid DNA	CTTTTCTGGTCCTCCGGGT AGG	CCACCCGGCCCTATTTTACAC CAA
<i>M. musculus Cxcl9</i>	TGTGGAGTTCGAGGAACC CT	AGTCCGGGATCTA GGCAGGTT
<i>M. musculus Nos2</i>	CTATGGCCGCTTTGATGTG C	TTGGATGCTCCATGGTCAC
<i>M. musculus Fizz1</i>	CCCTGCTGGGATGACTGCT A	CAGTGGTCCAGTCAACGAGT
<i>M. musculus Arg1</i>	TTTTAGGGTTACGGCCGGT G	CCTCGAGGCTGTCTTTTGA
<i>M. musculus Bnip3</i>	TCCTGGGTAGAACTGCACT TC	GCTGGGCATCCAACAGTATTT

**Table S2.** Gender identification for *in vivo* infection (related to Figure 5)

<b>SPLEEN</b>			
<b>Mice</b>	<b>Duration</b>	<b>Number</b>	<b>N° parasites/10<sup>6</sup> nucleated cells (Individual result)</b>
WT Male	2 weeks	5	6,36 - 0,06 - 1,24 - 0,53 - 0,54
WT Female		5	5,46 - 4,58 - 4,85 - 1,73 - 2,61
HIF-1 $\alpha$ <sup>-/-</sup> Male		4	17,72 - 2,89 - 2,46 - 9,16
HIF-1 $\alpha$ <sup>-/-</sup> Female		3	10,5 - 11,23 - 2,64
WT Male	8 weeks	4	27,67 - 19,61 - 60,82 - 23,00
WT Female		4	40,02 - 47,12 - 38,56 - 32,57
HIF-1 $\alpha$ <sup>-/-</sup> Male		4	39,86 - 44,51 - 88,98 - 102,76
HIF-1 $\alpha$ <sup>-/-</sup> Female		4	127,56 - 59,79 - 218,53 - 233,34

<b>LIVER</b>			
<b>Mice</b>	<b>Duration</b>	<b>Number</b>	<b>N° parasites/10<sup>6</sup> nucleated cells (Individual result)</b>
WT Male	2 weeks	4	116,7 - 62,7 - 69,73 - 22,69
WT Female		4	255,58 - 4,38 - 148,90 - 64,47
HIF-1 $\alpha$ <sup>-/-</sup> Male		3	456,90 - 195,2 - 142,82
HIF-1 $\alpha$ <sup>-/-</sup> Female		3	170,93 - 142,93 - 101,48
WT Male	8 weeks	4	5,24 - 7,34 - 6,92 - 4,97
WT Female		4	6,14 - 3,13 - 5,38 - 5,30
HIF-1 $\alpha$ <sup>-/-</sup> Male		4	6,92 - 10,31 - 6,40 - 6,82
HIF-1 $\alpha$ <sup>-/-</sup> Female		4	8,42 - 7,48 - 27,39 - 25,30

**Table S3.** Gender identification for *in vivo* infection (related to Figure 6)

<b>SPLEEN</b>			
<b>Mice</b>	<b>Treatment</b>	<b>Number of mice</b>	<b>N° parasites/10<sup>6</sup> nucleated cells (Individual result)</b>
WT Male	-	6	7,02 - 1,26 - 4,74 - 9,48 - 7,23 - 7,02
WT Female		6	7,25 - 5,42 - 2,13 - 3,24 - 4,25 - 5,22
HIF-1 $\alpha$ <sup>-/-</sup> Male		4	16,85 - 14,04 - 7,94 - 13,54
HIF-1 $\alpha$ <sup>-/-</sup> Female		4	21,2 - 5,68 - 6,01 - 9,89
WT Male	+C75	3	3,14 - 3,65 - 2,94
WT Female		2	7,05 - 6,42
HIF-1 $\alpha$ <sup>-/-</sup> Male		3	3,59 - 1,68 - 3,97
HIF-1 $\alpha$ <sup>-/-</sup> Female		2	4,41 - 4,21
WT Male	+Fatostatin A	3	12,5 - 5 - 3,25
WT Female		2	1,25 - 1,45
HIF-1 $\alpha$ <sup>-/-</sup> Male		3	5,1 - 5,2 - 4,9
HIF-1 $\alpha$ <sup>-/-</sup> Female		2	3,8 - 2,6
<b>LIVER</b>			
<b>Mice</b>	<b>Treatment</b>	<b>Number of mice</b>	<b>N° parasites/10<sup>6</sup> nucleated cells (Individual result)</b>
WT Male	-	5	155,82 - 118,72 - 71,08 - 175,40 - 89,19
WT Female		6	133,25 - 165 - 97 - 97,5 - 99,1 - 14
HIF-1 $\alpha$ <sup>-/-</sup> Male		4	339,90 - 284,10 - 285,02 - 322,15
HIF-1 $\alpha$ <sup>-/-</sup> Female		4	372 - 276 - 185 - 105
WT Male	+C75	3	38,92 - 66,56
WT Female		2	67,09 - 102,2
HIF-1 $\alpha$ <sup>-/-</sup> Male		3	89,09 - 201,5 - 196,6
HIF-1 $\alpha$ <sup>-/-</sup> Female		2	83,69 - 209,9
WT Male	+Fatostatin A	3	170 - 162 - 125
WT Female		2	102 - 95
HIF-1 $\alpha$ <sup>-/-</sup> Male		3	185 - 96 - 90
HIF-1 $\alpha$ <sup>-/-</sup> Female		2	45 - 31

**Defective anti-*Leishmania* T cell effector response in the absence of myeloid HIF-1 $\alpha$**

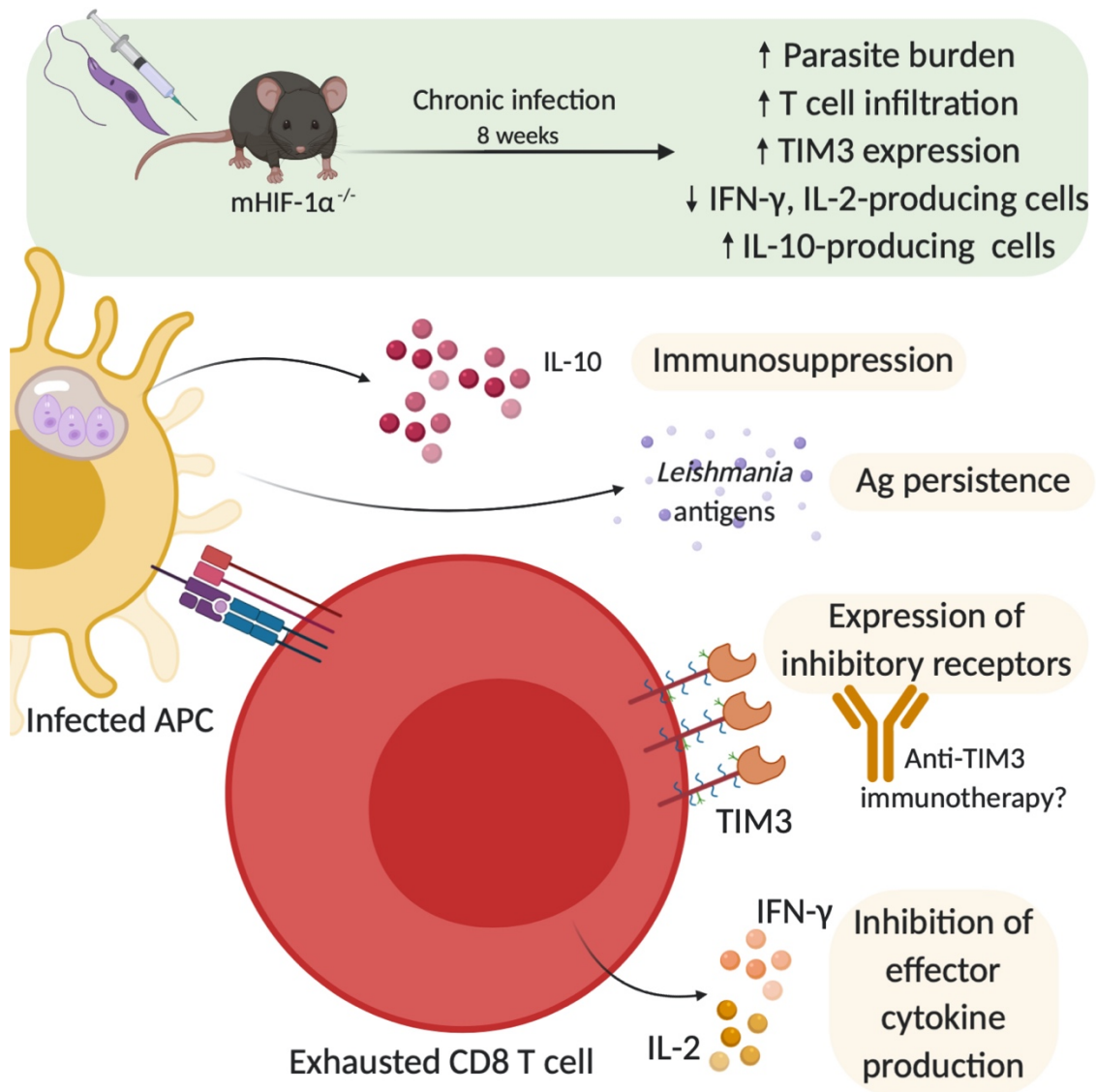
Unpublished data.

**Abstract**

Chronic infections can be associated with T cell exhaustion, which hampers the activity of fully effective T cells, capable of eliminating invading pathogens. As such, the reversion of this state is highly desirable as a way of boosting host microbicidal mechanisms, namely by promoting cytotoxic activity and proliferation of antigen-specific effector T cells. We have previously shown that genetic deficiency of myeloid hypoxia-inducible factor 1 $\alpha$  (HIF-1 $\alpha$ ) associates with susceptibility to acute *Leishmania donovani* infection. In this work, we show that chronically *L. donovani*-infected mHIF-1 $\alpha$ <sup>-/-</sup> mice display exhausted CD4 and CD8 T cells, characterized by enhanced expression of inhibitory receptor T-cell immunoglobulin and mucin domain 3 (TIM-3) and lower production of effector cytokines IL-2 and IFN- $\gamma$ , which ultimately contributes to parasite persistence.



## Graphical abstract



## Introduction

During chronic infections, T cells are constantly subjected to the pressure of pathogenic antigenic and soluble mediators (as IL-10 and TGF- $\beta$ ), which contribute to a phenomenon of cell dysfunction commonly known as T cell exhaustion. This is characterized by a step-wise loss of effector functions, as decreased cytokine production and reduced proliferative capacity, an increased expression of inhibitory receptors, as programmed cell death protein 1 (PD-1) and T-cell immunoglobulin and mucin-domain containing-3 (TIM-3), which associates with specific

transcriptional and metabolic programs (Pauken and Wherry, 2015; Wherry and Kurachi, 2015a). T cell exhaustion was firstly identified in chronic infection with LCMV and associated to immune evasion and viral persistence (Gallimore et al., 1998; Zajac et al., 1998). Currently, it has been described in several chronic infections (Saeidi et al., 2018), despite the need for further mechanistic studies to elucidate the molecular and cellular events responsible for the impairment of the biological functions.

In this work, we show that absence of hypoxia-inducible factor 1 $\alpha$  (HIF-1 $\alpha$ ) in the myeloid compartment induces lymphocyte infiltration in *L. donovani*-parasitized organs. However, infiltrating CD4 and CD8 T cells appear to be dysfunctional, as this does not translate in lower parasite burden. On the contrary, CD4 and CD8 exhausted T cells (Tex) exhibit higher expression of inhibitory receptor TIM-3, as well as lower IFN- $\gamma$  and IL-2 production. Further, an increase of IL-10-producing myeloid cells was found in chronically infected myeloid-restricted HIF-1 $\alpha$  deficient mice (mHIF1 $\alpha$ <sup>-/-</sup>), which may contribute to exhaustion and further parasite persistence. Reinvigoration of T cell response is an attractive response to overcome exhaustion-derived progression of *Leishmania* infection. As such, next steps will include immunotherapy with anti-TIM-3 and blockade of IL-10 signaling, which will be crucial in providing a functional link between T cell exhaustion and susceptibility during chronic *L. donovani* infection in mHIF-1 $\alpha$ <sup>-/-</sup> mice.

## Material and Methods

### Mice

Wild-type (WT) C57BL/6 were purchased from Charles River Laboratories and *Hif1 $\alpha$ <sup>fllox/fllox</sup>* mice crossed with lysozyme M-driven Cre (LysM<sup>Cre</sup>)-transgenic mice on a C57BL/6 background, here identified as myeloid-restricted HIF-1 $\alpha$  deficient mice (mHIF-1 $\alpha$ <sup>-/-</sup>), were kindly provided by Dr. Rui Appelberg (I3S; Porto, Portugal). C57BL/6 WT and mHIF-1 $\alpha$ <sup>-/-</sup> mice were bred and maintained in accredited animal facilities at the Life and Health Sciences Research Institute (ICVS). Mice were housed in groups of 3-6, in HEPA filter-bearing cages, under 12-h light/dark cycles. Autoclaved chow and water was provided *ad libitum* and cages were enriched with nesting materials (paper towels). Males with 8-12 weeks were used. Experimental animal procedures agreed with the European Council Directive (2010/63/EU) guidelines that were transposed into Portuguese law (Decree-Law n.º 113/2013, August 7th). Experiments were conducted with the approval of the UMinho Ethical Committee (process no. SECVS 074/2016) and complied with the

guidelines of the Committee and National Council of Ethics for the Life Sciences (CNECV). RS has an accreditation for animal research given from Portuguese Veterinary Direction (Ministerial Directive 1005/92).

### **Parasite culture**

Cloned lines of virulent *Leishmania donovani* (MHOM/IN/82/Patra1) was maintained with weekly subpassages at 27°C in complete RPMI 1640 medium, supplemented with 10% heat-inactivated fetal bovine serum, 2 mM L-glutamine, 100 U/ml penicillin plus 100 mg/ml streptomycin and 20 mM HEPES buffer. Only parasites under ten passages were used in the experimental work.

### **Experimental *Leishmania* infection**

Mice were randomly allocated into groups and the experimenters were blinded to the different conditions. Mice were infected with  $100 \times 10^6$  (intraperitoneal route) stationary *L. donovani* promastigotes. Weight and general well-being were monitored during the 8-week infection. At the endpoint, mice were anesthetized with volatile isoflurane and blood was withdrawn by cardiac puncture. Euthanasia by cervical dislocation was performed following this procedure. A section of the liver was preserved in 10% formalin during 24 hours, for further hematoxylin and eosin staining. The liver and spleen were mechanically resuspended and cells were recovered for flow cytometry and DNA extraction. DNA was extracted using the phenol-chloroform-isoamyl alcohol method. Briefly, an aqueous suspension with approximately  $1 \times 10^6$  cells was mixed with a mixture of phenol-chloroform-isoamyl alcohol (25:24:1). After centrifugation, the aqueous phase was recovered and incubated overnight with 3M sodium acetate and absolute ethanol. The DNA pellet was washed twice with 70% ethanol and resuspended in RNase/DNase-free water. Parasite burden was assessed, using a TaqMan-based qPCR assay for detection and quantification of *L. donovani* kinetoplastid DNA. Alanine aminotransferase (ALT) and aspartate aminotransferase (AST) levels were quantified in the serum using an AutoAnalyzer, using reagents from the same provider.

### **Flow cytometry**

Surface staining was performed in splenic cell suspensions with the following antibodies: BV605 anti-mouse CD11c, clone N418; APC anti-mouse I-A/I-E, clone M5/114.15.2; BV785 anti-mouse NK1.1, clone PK136; PE/Cy7 anti-mouse CD11b, clone M1/70; BV711 anti-mouse Ly6G,

clone 1A8; PerCP/Cy5.5 anti-mouse Ly6C, clone HK14; APC-Cy7 anti-mouse CD4, clone GK1.5; BV711 anti-mouse CD8, clone 53-6.7; PerCP/Cy5.5 anti-mouse CD44, clone IM7; BV605 anti-mouse CD62L, clone MEL-14; PE/Cy7 anti-mouse PD-1, clone RMP1-30; PE anti-mouse CD366 (TIM-3), clone B8.2C12. For intracellular cytokine staining, splenic cell suspensions were stimulated overnight with soluble *Leishmania* antigen (SLA) and Brefeldin A was added in the final 4 hours. Following this, cells were surface stained, fixated with 2% PFA and permeabilized with 0.5% saponin. Cytokines were stained with FITC anti-mouse IFN- $\gamma$ , clone XMG1.2; APC anti-mouse IL-10, clone JES5-16E3; BV421 anti-mouse IL-2, clone JES6-5H4; PE/Cy7 anti-mouse TNF- $\alpha$ , clone MP6-XT22.

Samples were acquired on a LSRII flow cytometer (BD Biosciences) and data analyzed using FlowJo software. The gating strategy for myeloid cells is depicted on Supplementary Figure 7D.

#### Quantification and statistical analysis

Statistical analyses were performed with the GraphPad Prism 6 software. A one-way analysis of variance (ANOVA) followed by a Bonferroni's post hoc test was employed for multiple group comparisons. A Mann-Whitney test of variance and Kruskal-Wallis non-parametric test were performed accordingly with the correspondent experimental design. The statistical details of each experiment can be found in figure legends and the data is presented as mean  $\pm$  SD. Statistically significant values are as follows: \* $p < 0.05$ , \*\* $p < 0.01$ , \*\*\* $p < 0.001$ .

## Results

### Genetic deficiency of HIF-1 $\alpha$ in the myeloid compartment originates lymphocytic alterations during chronic *L. donovani* infection.

We have previously shown that mHIF-1 $\alpha$ <sup>-/-</sup> mice were more susceptible to acute *L. donovani* infection, when compared to WT counterparts. This was due to a dysregulation of the BNIP3/mTOR/SREBP-1c axis, which culminated in lipid accumulation within target cells and organs (Mesquita et al., 2020). We observe that mHIF-1 $\alpha$ <sup>-/-</sup> remained more susceptible to *L. donovani*, 8 weeks post-infection, as observed by the increased parasite burden in the spleen and liver of infected mHIF-1 $\alpha$ <sup>-/-</sup> mice (figure 1A). Histologically, this finding was accompanied by the

presence of inflammatory infiltrates in liver sections of infected mHIF-1 $\alpha$ <sup>-/-</sup>, which was not present in WT controls (figure S1A). Further, infected mHIF-1 $\alpha$ <sup>-/-</sup> presented increased serum levels of ALT and no alterations on AST levels (figure S1B). The spleens of infected mHIF-1 $\alpha$ <sup>-/-</sup> were greatly enlarged when compared to WT ones, which is shown by the increase in total splenocyte count (figure 1B). By analyzing splenic populations by flow cytometry, we demonstrated that this was driven by accumulation of both CD4 and CD8 T lymphocytes in the spleen of infected mHIF-1 $\alpha$ <sup>-/-</sup> (figure 1C). Although B cells also appear to increase (figure S1C), no major differences were observed in myeloid populations, namely monocytes (gated on Ly6C<sup>+</sup> CD11b<sup>+</sup>), myeloid dendritic cells (gated on Ly6C<sup>+</sup> CD11c<sup>-</sup>) and neutrophils (gated on CD11b<sup>+</sup> Ly6G<sup>hi</sup>) (figure S1D-F).

These findings suggest that genetic deficiency of HIF-1 $\alpha$  in the myeloid compartment dysregulates the adaptive immune response and causes increased lymphocyte infiltration at later stages of *L. donovani* infection.

#### **T cell dysfunction/exhaustion is observed in *L. donovani*-chronically infected mHIF-1 $\alpha$ <sup>-/-</sup>**

Despite the higher accumulation of lymphocytes in parasitized organs, mHIF-1 $\alpha$ <sup>-/-</sup> remain more susceptible to chronic *L. donovani* infection, comparing with WT controls. This could imply a certain degree of dysfunction that prevents T lymphocytes of exerting its antileishmanial functions. As such, we characterized multifunctional T cells by analyzing the production of IL-2, IFN- $\gamma$  and TNF- $\alpha$  in both WT and mHIF-1 $\alpha$ <sup>-/-</sup> mice, as the importance of these cells in immune protection has already been shown (Darrah et al., 2007a). We observed a decreased percentage of both IFN- $\gamma$ <sup>+</sup> and IL-2<sup>+</sup> IFN- $\gamma$ <sup>+</sup>-producing CD4 and CD8 T cells in chronically infected mHIF-1 $\alpha$ <sup>-/-</sup> mice (figure 2A, 2B), while no major differences were found in TNF- $\alpha$  producers (data not shown).

As the loss of cytokine production is a hallmark of T cell exhaustion, we sought to further understand whether CD4 and CD8 T cells from chronically infected mHIF-1 $\alpha$ <sup>-/-</sup> expressed differential levels of exhaustion markers PD-1 and TIM-3. Although no major difference was observed in expression of PD-1 in both CD4 and CD8 T cells (data not shown), an increase of both percentage and number of TIM-3<sup>+</sup> CD4 and CD8 T cells were found in infected mHIF-1 $\alpha$ <sup>-/-</sup> (figure 2C, 2D), which suggests the establishment of a phenotype of exhaustion in both CD4 and CD8 T cells. As high levels of IL-10 can contribute to T cell dysfunction and eventual exhaustion during chronic infections and cancer (Damo and Joshi, 2019; Smith et al., 2018a), we assessed intracellular IL-10 production in splenic myeloid populations and observed increased numbers of

IL-10-producing monocytes (figure S2A), neutrophils (figure S2B) and myeloid dendritic cells (figure S2C). This indicates that the myeloid populations could be contributing for an increased IL-10 pool that could condition T cell function.

## Discussion

During chronicity, as the infection persists, the immunosuppressive environment (rich in cytokines as IL-10 and TGF- $\beta$ ) and the increased antigen load constantly stimulate T cells, leading them to a state of unresponsiveness (Wherry, 2011). The progressive and hierarchical pattern that leads to exhaustion starts typically with loss of IL-2 production, while loss of IFN- $\gamma$  is assumed to occur at more severe stages (Fuller and Zajac, 2003; Wherry et al., 2003). As such, T cell exhaustion may be a potent ally in pathogen's party, allowing it to evade host microbicidal mechanisms.

Some reports started to unveil the role of T cell exhaustion during chronic *Leishmania* infection. Gautam and colleagues showed that CD8 T cells are driven towards an exhaustive phenotype in human VL. CD8 T cells isolated from patients' blood showed increased levels of *IL10* transcripts and exhaustion markers cytotoxic T-lymphocyte antigen 4 (CTLA-4) and PD-1, while transcription levels of *IFNG* were shown to be decreased (Gautam et al., 2014). The increased expression and dysfunctional activation of PD-L1 in blood monocytes has been positively associated with a case of diffuse CL, a rare disease form associated with poor treatment response. Further, PD-L1-positive monocytes presented a decreased capacity of inducing IFN- $\gamma$  and granzyme B production by CD4 and CD8 T cells (Barroso et al., 2018). In addition, T cell exhaustion represents a major clinical challenge, as loss of antigen-specific cells and IFN- $\gamma$  production associates positively with increased VL symptomatology. Interestingly, B7.H1-induced blockage of PD-1 was able to restore both CD4 and CD8 T cell functions, while increasing ROS-derived parasite killing by monocytes (Esch et al., 2013). Anti-PD-1 and anti-PD-L1 have also been suggested as potent therapies for T cell reinvigoration in *L. amazonensis*-infected mice, as smaller lesions and lower parasite burden were observed in treated animals (da Fonseca-Martins et al., 2019). Further, Habib *et al.* showed that expansion of IL-10-producing Foxp3<sup>+</sup> Tregs, as well as PD-1-expressing CD4 and CD8 T cells are likely behind exhaustion-associated pathology. Blockage of PDL-1 led to decreased autophagy, which prevented host nutrient acquisition by *Leishmania* parasites (Habib et al., 2018).

We have shown previously that genetic deficiency in HIF-1 $\alpha$  in the myeloid compartment results in increased parasite burden during acute *Leishmania donovani* infection, when compared to WT counterparts (Mesquita et al., 2020). A similar susceptibility phenotype is observed during chronic infection, as presented in figure 1A. This finding indicates that on the course of the 8-week infection protocol, *L. donovani* parasites persist at higher levels in the spleen and liver of mHIF-1 $\alpha$ <sup>-/-</sup> mice, which might contribute to the increased pool of circulating antigens. This was accompanied by an increased pathology in the liver of chronically infected mHIF-1 $\alpha$ <sup>-/-</sup> mice (figure S1A-B). We also observed an accumulation of both CD4 and CD8 T cells in the spleen of infected mHIF-1 $\alpha$ <sup>-/-</sup> mice (figure 1C-D), while no major differences were observed in the myeloid compartment (figure S1D-F). It is currently accepted that protective immunity against *Leishmania* infection is driven by the development of IL-12-driven Th1 immunity with consequent IFN- $\gamma$  production (Sacks and Noben-Trauth, 2002), while the role of CD8 T cells remains to be fully acknowledged (Novais and Scott, 2015). However, the increased number of splenic CD4 and CD8 T cells in mHIF-1 $\alpha$ <sup>-/-</sup> mice does not correlate with higher protection against infection. Interestingly, a decreased frequency of both IL-2<sup>+</sup> IFN- $\gamma$ <sup>-</sup> and IFN- $\gamma$ <sup>+</sup>-producing CD4 and CD8 T cells was observed in infected mHIF-1 $\alpha$ <sup>-/-</sup> mice (figure 2A-B). This indicates that the increased accumulation of T lymphocytes in the spleen does not translate into a more effective antileishmanial T cell response. Further, an increase in CD4 and CD8 T cells expressing TIM-3 was observed in the spleens of infected mHIF-1 $\alpha$ <sup>-/-</sup> mice (figure 2C-D). The loss of cytokine production and the increased expression of inhibitory markers are hallmarks of T cell exhaustion in distinct disease models (McLane et al., 2019; Wherry and Kurachi, 2015b). As such, we hypothesize that the increased and persistent antigenic load in infected mHIF-1 $\alpha$ <sup>-/-</sup> mice leads to the development of Tex, which retain minimal antileishmanial functions. Soluble mediators, as cytokines, can equally contribute to the sustainment of this phenotype. Recent evidences support a role for IL-10 in promoting the development of exhausted CD8 T cells, which in turn limits their antiviral or antitumor functions (Sawant et al., 2019; Smith et al., 2018a). Further, IL-10 has been shown to synergize with PD-1 to impair T cell function (Brooks et al., 2008; Said et al., 2010). Accordingly, we found a 2-fold increased number of IL-10-producing monocytes, neutrophils and dendritic cells in the spleen of mHIF-1 $\alpha$ <sup>-/-</sup> mice when compared to WT mice (figure S2), which indicates the establishment of an immunosuppressive environment.

### Future perspectives

Next steps will include the assessment of whether blocking the expression of inhibitory receptors or the activity of immunosuppressive molecules (using anti-TIM-3 monoclonal antibodies or anti-IL-10/IL-10R, respectively) is able to reinvigorate T cell function and promote elimination of *Leishmania* parasites. Additionally, the role of other checkpoint molecules (as CTLA-4 and LAG3) and mediators (as TGF- $\beta$ ) during *Leishmania* infection remains to be addressed. Further, it would be interesting to understand how organ-specific metabolic microenvironment contributes to T cell exhaustion, which may open new avenues for combined therapy in VL treatment. Finally, the ultimate goal will include understanding how myeloid-restricted genetic deficiency of HIF-1 $\alpha$  conditions late adaptive immune response towards *L. donovani*.

### Figure legends

**Figure 1. Genetic deficiency of HIF-1 $\alpha$  in the myeloid compartment associates with susceptibility to chronic *L. donovani* infection.** WT and mHIF-1 $\alpha$ <sup>-/-</sup> mice were infected intraperitoneally with 100 x 10<sup>6</sup> stationary *L. donovani* promastigotes for 8 weeks. At the designated endpoint, parasite burden in both the spleen and the liver of WT and mHIF-1 $\alpha$ <sup>-/-</sup> mice was assessed (A). Total number of splenocytes was assessed through cell counting (B), while CD4 (C) and CD8 (D) T cell frequency was analyzed by flow cytometry. Data are shown as mean  $\pm$  SD; n = 4-8 mice/group. \*p < 0.05; \*\*p < 0.01; \*\*\*p < 0.001; \*\*\*\*p < 0.0001.

**Figure 2. CD4 and CD8 T cells from mHIF-1 $\alpha$ <sup>-/-</sup> mice display loss of cytokine production and increased expression of TIM-3.** IL-2<sup>+</sup> IFN- $\gamma$ <sup>+</sup>-producing and IFN- $\gamma$ <sup>+</sup>-producing CD4 (A) and CD8 (B) T cells were assessed by flow cytometry, 8 weeks post-infection in both WT and mHIF-1 $\alpha$ <sup>-/-</sup> mice. Percentage and frequency of TIM-3<sup>+</sup>-expressing CD4 (C) and CD8 (D) T cells was similarly evaluated. Data are shown as mean  $\pm$  SD; n = 4-8 mice/group. \*p < 0.05; \*\*p < 0.01; \*\*\*p < 0.001.

**Figure S1.** Liver sections from 8-week infected mHIF-1 $\alpha$ <sup>-/-</sup> mice were sliced and stained with hematoxylin and eosin staining (A). ALT and AST levels in the serum of both WT and mHIF-1 $\alpha$ <sup>-/-</sup> mice were analyzed 8 weeks post-infection (B). Total numbers of B cells (C), as well as



monocytes (D), dendritic cells (E) and neutrophils (N) were obtained for uninfected and infected WT and mHIF-1 $\alpha$ <sup>-/-</sup> mice. Data are shown as mean  $\pm$  SD; n = 4-6 mice/group. \*p < 0.05.

**Figure S2.** IL-10-producing monocytes (A), dendritic cells (B) and neutrophils (C) were quantified by flow cytometry in the spleen of both WT and mHIF-1 $\alpha$ <sup>-/-</sup> mice. Data are shown as mean  $\pm$  SD; n = 4-5 mice/group. \*p < 0.05.

## FIGURE 1

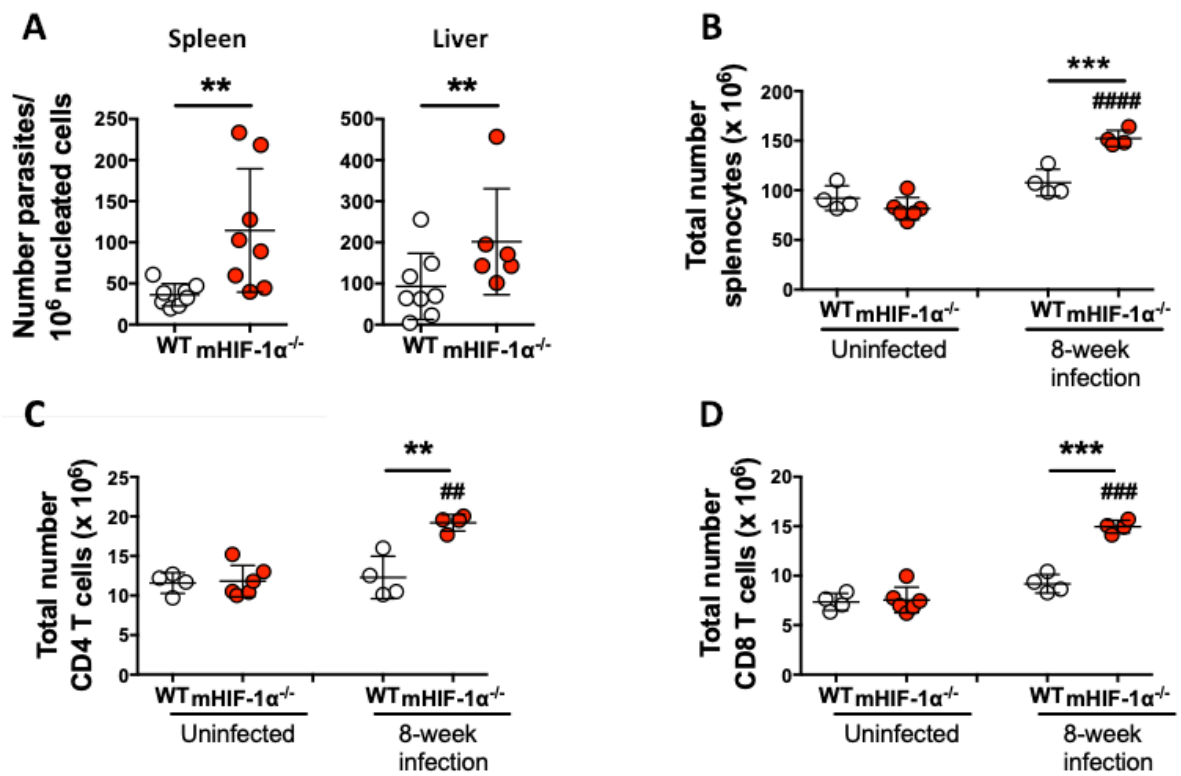


**FIGURE 2**

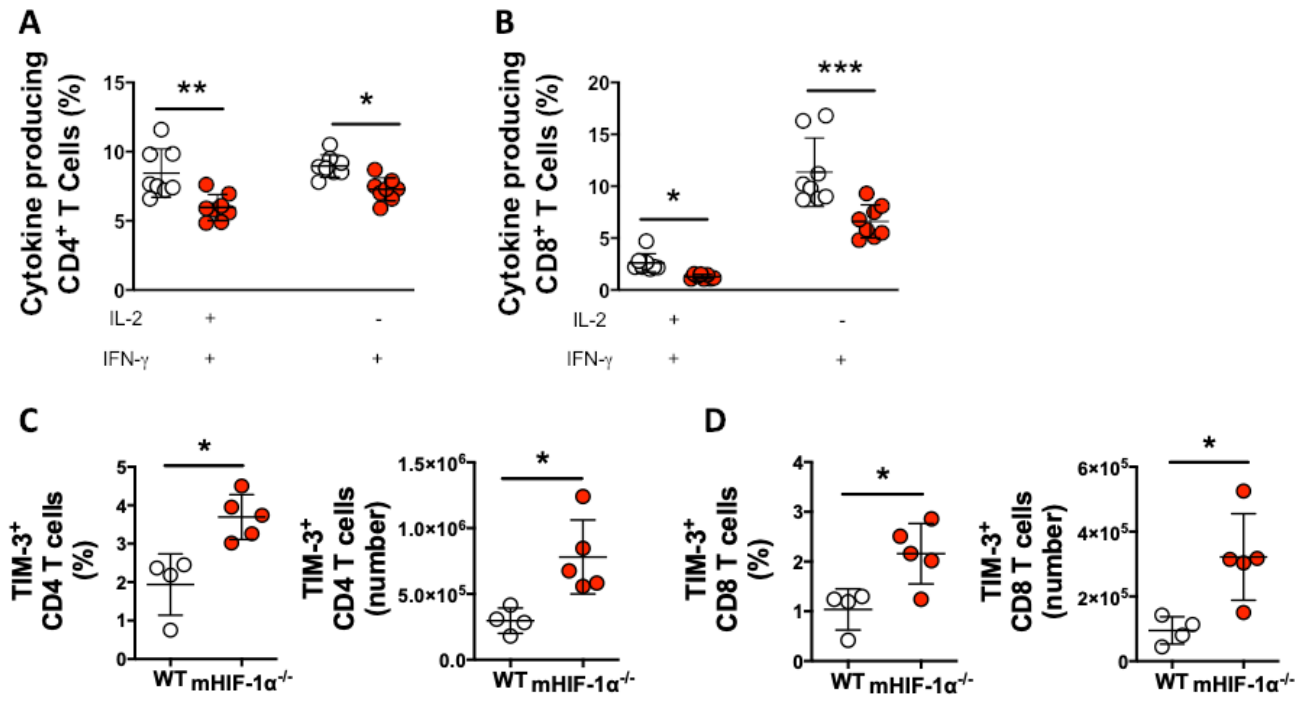


**FIGURE S1 (support of Fig1)**

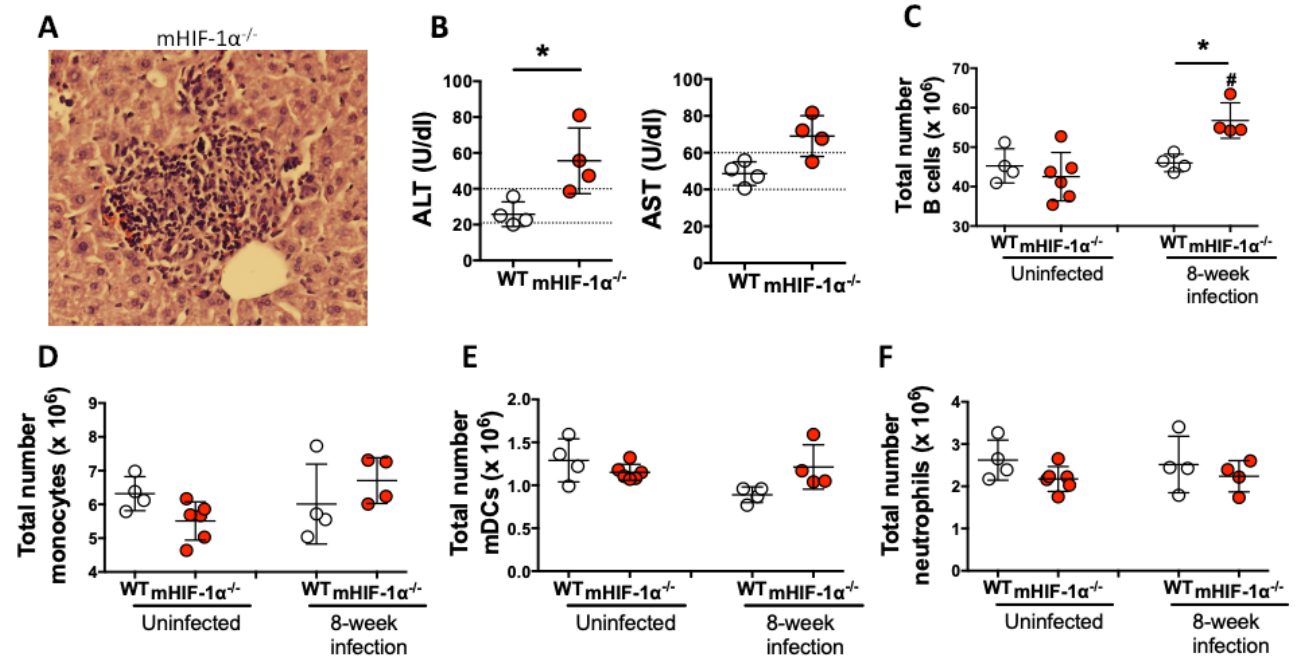
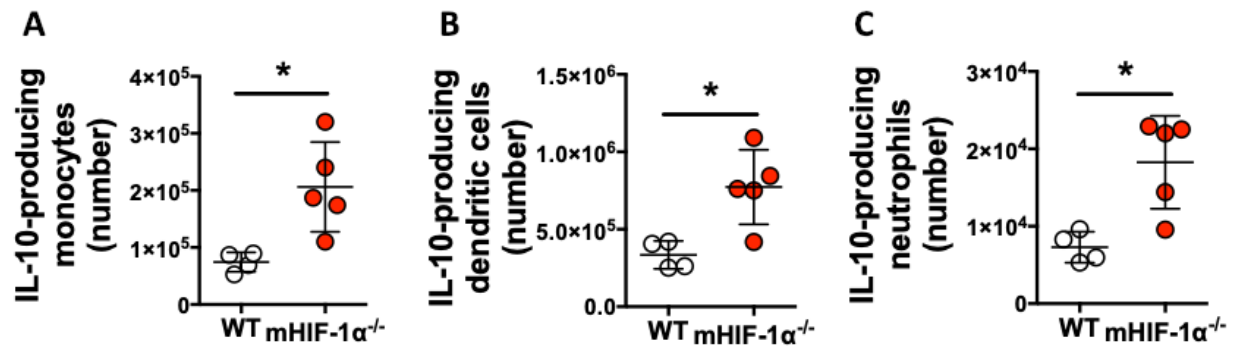


**FIGURE S2 (support of Fig2)**



**The impact of IL-10 dynamic modulation on host immune response against visceral  
leishmaniasis**

Inês Mesquita, Carolina Ferreira, Ana Margarida Barbosa, Catarina Machado Ferreira, Diana  
Moreira, Agostinho Carvalho, Cristina Cunha, Fernando Rodrigues, Ricardo Jorge Dinis-Oliveira,  
Jérôme Estaquier, António Gil Castro, Egídio Torrado, Ricardo Silvestre

Published in *Cytokine*. doi: 10.1016/j.cyto.2018.07.001.



Contents lists available at ScienceDirect

Cytokine

journal homepage: [www.elsevier.com/locate/cytokine](http://www.elsevier.com/locate/cytokine)

## The impact of IL-10 dynamic modulation on host immune response against visceral leishmaniasis



Inês Mesquita<sup>a,b</sup>, Carolina Ferreira<sup>a,b</sup>, Ana Margarida Barbosa<sup>a,b</sup>, Catarina Machado Ferreira<sup>a,b</sup>, Diana Moreira<sup>a,b</sup>, Agostinho Carvalho<sup>a,b</sup>, Cristina Cunha<sup>a,b</sup>, Fernando Rodrigues<sup>a,b</sup>, Ricardo Jorge Dinis-Oliveira<sup>c,d,e</sup>, Jérôme Estaquier<sup>f,g</sup>, António Gil Castro<sup>a,b</sup>, Egídio Torrado<sup>a,b</sup>, Ricardo Silvestre<sup>a,b,\*</sup>

<sup>a</sup> Life and Health Sciences Research Institute (ICVS), School of Health Sciences, University of Minho, Braga, Portugal

<sup>b</sup> ICVS/3B's – PT Government Associate Laboratory, Braga/Guimarães, Portugal

<sup>c</sup> IINFACTS – Institute of Research and Advanced Training in Health Sciences and Technologies, Department of Sciences, University Institute of Health Sciences (IUCS), CESPU, CRL, Gandra, Portugal

<sup>d</sup> UCIBIO, REQUIMTE, Laboratory of Toxicology, Department of Biological Sciences, Faculty of Pharmacy, University of Porto, Porto, Portugal

<sup>e</sup> Department of Public Health and Forensic Sciences, and Medical Education, Faculty of Medicine, University of Porto, Porto, Portugal

<sup>f</sup> CNRS FR 3636, Université Paris Descartes, 75006 Paris, France

<sup>g</sup> Centre de Recherche du CHU de Québec, Université Laval, Québec G1V 4G2, Canada

### ARTICLE INFO

#### Keywords:

Visceral leishmaniasis  
IL-10  
Multifunctional CD4<sup>+</sup> T cells  
IFN- $\gamma$

### ABSTRACT

Leishmaniasis is a vector-borne disease caused by protozoan parasites from the genus *Leishmania*. The most severe form of disease is visceral leishmaniasis (VL), which is fatal if left untreated. It has been demonstrated that interleukin (IL)-10, is associated with disease progression and susceptibility. In this work, we took advantage of a transgenic mouse model that expresses high levels of IL-10 upon zinc sulfate administration (pMT-10). We addressed the role of IL-10 during the initial stages of *L. donovani* infection by analyzing the parasite burden in the spleen and liver of the infected pMT-10 and WT mice as well as the histopathological alterations upon IL-10 induction. Furthermore, the profile of cytokines expressed by T cells was assessed. Our results demonstrate that an increase in IL-10 production has an impact early but not later after infection. This specific temporal role for IL-10-mediated susceptibility to VL is of interest.

### 1. Introduction (1896)

Leishmaniasis is a group of tropical neglected diseases caused by protozoan parasites from the genus *Leishmania*, which range from self-healing cutaneous lesions to fatal visceral disease. *Leishmania donovani* is one of the causative agents of visceral leishmaniasis (VL) responsible for high morbidity and mortality in East Africa and South Asia [13]. Immunity to VL has long been known to depend on the development of type I immune responses characterized by initial production of interleukin-12 (IL-12) by antigen-presenting cells (APCs) that induce interferon- $\gamma$  (IFN- $\gamma$ )-secreting Th1 T cells [11]. These, in turn, will activate and prime host innate cells for the production of microbicidal molecules as reactive nitrogen and oxygen species (RNS and ROS, respectively). However, the presence of a Th1 response does not immediately correlate with protection, whose action is neutralized by immune regulatory

factors [11]. Among those, the role of IL-10 as a major mediator in the suppression of a leishmanicidal immune response has gained a particular attention in the past [1,4,7,8,9]. IL-10 is an anti-inflammatory cytokine induced during experimental and human infections [7], whose levels correlate with disease severity [5,14]. IL-10 has the potential to disable host anti-leishmanial defense and foster visceral infection by compromising Th1 responses and deactivating host phagocytes [4,8]. In contrary, mice deficient in IL-10 or in which IL-10 signaling is blocked are highly resistant to *Leishmania* infection [11]. Yet, the relevance of IL-10 production during the initial innate immune response or upon the establishment of an adaptive immune response is still unknown. Since a coordinated inflammatory response is the hallmark of a protective immune response to infection, we evaluate the early impact of IL-10 expression before or after the onset of a *Leishmania*-specific adaptive immune response. To address this issue, we took advantage of

\* Corresponding author. Life and Health Sciences Research Institute (ICVS), School of Medicine, University of Minho, Braga, Portugal. ICVS/3B's-PT Government Associate Laboratory, Braga/Guimarães, Campus de Gualtar, 4710-057 Braga, Portugal.

E-mail address: [ricardosilvestre@med.uminho.pt](mailto:ricardosilvestre@med.uminho.pt) (R. Silvestre).

<https://doi.org/10.1016/j.cyto.2018.07.001>

Received 5 March 2018; Received in revised form 21 June 2018; Accepted 2 July 2018

Available online 14 July 2018

1043-4666/ © 2018 Elsevier Ltd. All rights reserved.

the pMT-10 mouse model, in which IL-10 was induced by zinc sulfate administration. Herein, we show that overexpression of IL-10 during the initial steps of infection underlies susceptibility to *L. donovani* infection, by modulating the expansion of multifunctional CD4 T cells.

## 2. Material and methods

### 2.1. Animals

pMT-10 on a C57BL/6 background and C57BL/6 mice were maintained under specific pathogen-free at the Life and Health Sciences Research Institute (ICVS, Braga, Portugal) and allowed food and water *ad libitum*. Animals with eight to twelve weeks were used in the experiments. Experimental animal procedures agreed with the European Council Directive (2010/63/EU) guidelines that were transposed into Portuguese law (Decree-Law no. 113/2013, August 7th). Additionally, the experiments were conducted with the approval of the UMinho Ethical Committee (process no. SECVS 074/2016) and complied with the guidelines of the Committee and National Council of Ethics for the Life Sciences (CNECV). RS has an accreditation for animal research given from Portuguese Veterinary Direction (Ministerial Directive 1005/92).

### 2.2. Parasites

A cloned line of virulent *L. donovani* (MHOM/IN/82/Patra1) was maintained by weekly subpassages at 26 °C in RPMI 1640 medium (Lonza, Switzerland) supplemented with 10% heat-inactivated Fetal Bovine Serum (FBS) (Lonza, Switzerland), 2 mM L-glutamine, 100 U/ml penicillin, 100 mg/ml streptomycin and 20 mM HEPES buffer (BioWhittaker, Walkersville, MD). Only *L. donovani* promastigotes under four to ten passages were used in the experiments as previously

defined [6]. To prepare soluble *Leishmania donovani* antigens (SLA),  $50 \times 10^6$  parasites were resuspended in 1 ml of sterile PBS and 10 cycles of freeze/thaw were performed. Total protein content was assessed through BCA method.

### 2.3. In vivo infection

WT and pMT-10 mice were infected intraperitoneally with  $20 \times 10^6$  stationary-phase *L. donovani* promastigotes resuspended in apyrogenic sterile PBS. IL-10 was induced by the administration of 2% sucrose solution containing 50 mM of zinc sulphate (Sigma) in the drinking water as previously described [2]. WT mice received water with 2% of sucrose, as a control. IL-10 induction in pMT-10 mice was performed at early (0–12 days) and late (35–47 days) time points of infection (Fig. 1A). Sixty days post-infection, the animals were euthanized and the spleen, liver and blood were recovered for further biochemical and histopathological analysis.

### 2.4. Parasite burden

DNA was extracted from spleen and liver homogenates using the phenol-chloroform-isoamyl alcohol method. Parasite burden was assessed as previously described [10], using a TaqMan-based qPCR assay for detection and quantification of *L. donovani* kinetoplast DNA.

### 2.5. Flow cytometry analysis

Splenocytes were stimulated with SLA (10 µg/ml) during 18 h to allow the proliferation and functional response of specific T cells. Brefeldin A (10 µg/ml) was added during the last 3 h of SLA stimulation. The anti-mouse monoclonal antibodies used to perform this study were all purchased to BioLegend (CA, USA). Abs used include: FITC

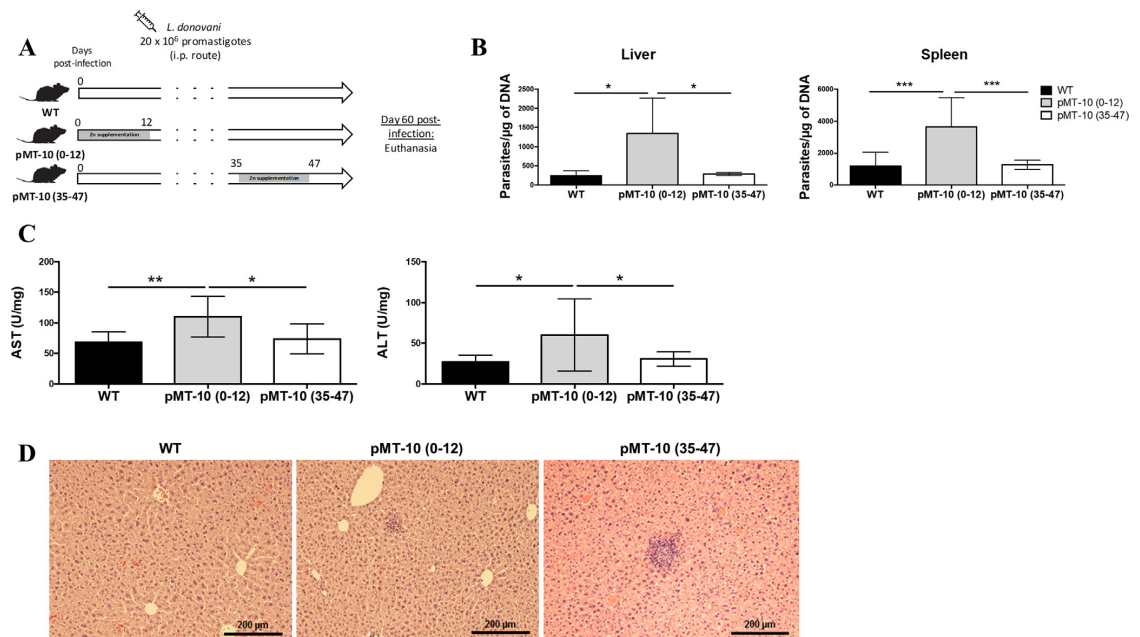


**Fig. 1.** IL-10 overexpression at distinct time points of *Leishmania donovani* infection associates with distinct clinical outcomes. (A) pMT-10 and WT mice were intraperitoneally infected with  $20 \times 10^6$  *L. donovani* promastigotes. The pMT-10 (0–12) group received zinc supplementation from day 0 to 12 post-infection while the pMT-10 (35–47) received from day 35 to 47 post-infection. WT mice were not supplemented with zinc through the course of infection. (B) All animals were sacrificed at day 60 post-infection. Parasite burden in spleen and liver homogenates. (C) ALT and AST levels in the serum of infected animals. (D) H&E staining of liver sections (5 µm). Data is shown as mean  $\pm$  SD; n = 4–6 mice/group. One representative experiment is shown out of two. \*p < 0.05; \*\*p < 0.01; \*\*\*p < 0.001.

anti-mouse TNF Ab, clone MP6-XT22; PerCP/Cy5.5 anti-mouse CD3, clone 145-2C11; PeCy7 anti-mouse IFN- $\gamma$ , clone XMG1.2; APC anti-mouse IL-10; clone JES5-16E3; APC/Cy7 anti-mouse CD4, clone GK1.5; BV421 anti-mouse IL-2, clone JES6-5H4; BV711 anti-mouse CD8, clone 53-6.7. Samples were acquired on a LSRII flow cytometer (BD Biosciences) and data analysed using FlowJo software (TreeStar). Supplementary figure 1 depicts the identification criteria used for selecting the cellular populations of interest.

Supplementary data associated with this article can be found, in the online version, at <https://doi.org/10.1016/j.cyto.2018.07.001>.

2.6. Histology

After mice euthanasia, the liver was perfused with saline solution and fixed with 10% (w/v) formalin. The sections were further dehydrated and embedded in paraffin for further histopathological analysis. Samples were then sectioned for haematoxylin and eosin staining. Bright field images were acquired on a BX6 microscope.

2.7. ALT/AST quantification

ALT and AST levels were quantified in the serum using an AutoAnalyzer (Prestige 24i, PZ Cormay S.A) as previously described [10].

2.8. IL-10 quantification

IL-10 levels were quantified on blood, spleen and liver homogenates by ELISA and the transcriptional levels of *Il10* gene were assessed by real-Time quantitative PCR (qRT-PCR). Briefly, spleen and liver were homogenized and stored for IL-10 quantification using IL-10 mouse uncoated ELISA kit (ThermoScientific) or in TRIreagent (Sigma-Aldrich) for RNA extraction. Total RNA was extracted and the synthesis of cDNA was made with SensiFAST™ cDNA Synthesis Kit (Bioline). qRT-PCR reactions were run for each sample on a Bio-Rad CFX96 Real-Time System C1000 Thermal Cycler (Bio-rad) using SensiFAST SYBR Hi-ROX Kit (Bioline). Primer sequences were obtained from Alfacene (Portugal) and thoroughly tested. The results were normalized to the expression of the housekeeping gene *ubiquitin*. After amplification, cycle threshold-values (Ct-values) were calculated for all samples and gene expression changes were analyzed in the CFX Manager Software (Bio-Rad). The serum, splenic and liver IL-10 transcript and expression levels are shown on Supplementary figure 2A and B respectively.

2.9. Statistical analysis

Statistical analyses were performed with the GraphPad Prism 6 software. A one-way analysis of variance (ANOVA) followed by a Bonferroni's post hoc test was employed for multiple group comparisons. Statistically significant values are as follows: \*p < 0.05, \*\*p < 0.01, \*\*\*p < 0.001.

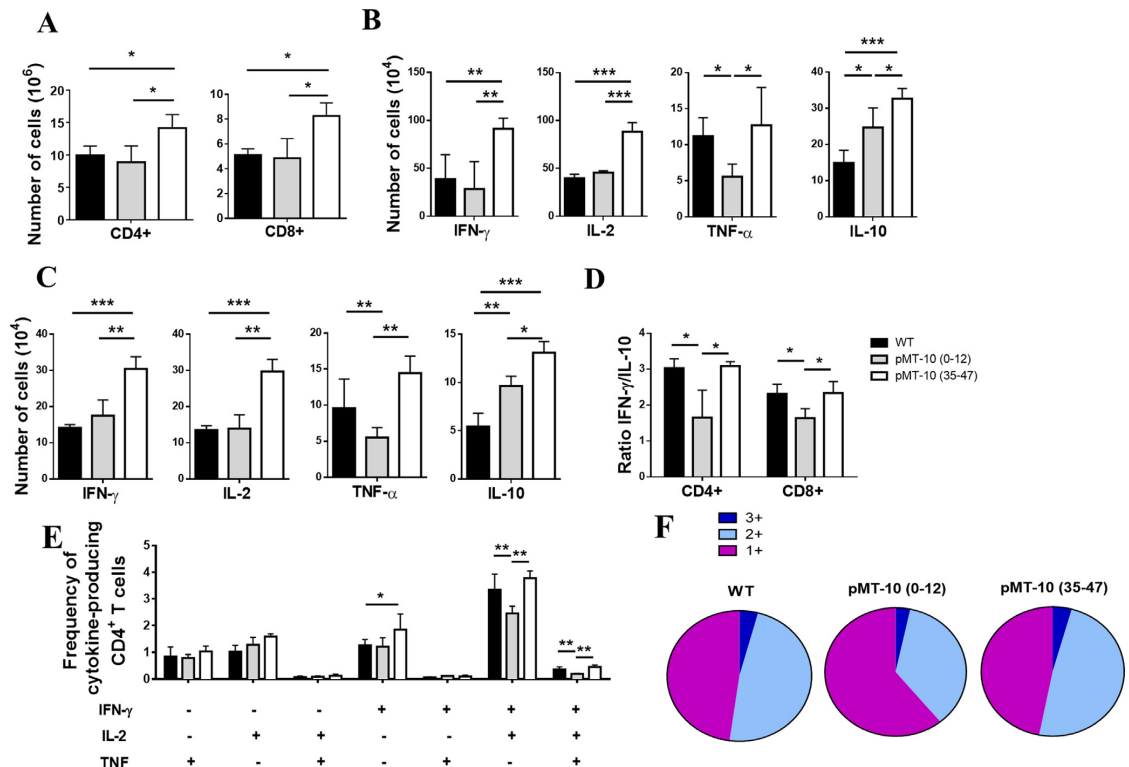


Fig. 2. Early IL-10 overexpression leads to a loss of multifunctional CD4 T cells and lower IFN- $\gamma$ /IL-10 ratios that associates with susceptibility. (A) Total CD4 and CD8 T cells number in the spleen of infected mice. Number of IFN- $\gamma$ , IL-2, TNF- and IL-10-producing CD4 T cells (B) and CD8 T cells (C). (D) IFN- $\gamma$ /IL-10 ratio in CD4 and CD8 T cells. (E) Frequency of cytokine-producing CD4 T cells expressing each of the seven possible combinations of IFN- $\gamma$ , IL-2 and TNF. (F) Fraction of the total response of CD4 T cells comprising cells expressing all three (3+), two (2+) or one cytokine (1+). Data is shown as mean  $\pm$  SD; n = 4–6 mice/group. One representative experiment is shown out of two. \*p < 0.05; \*\*p < 0.01; \*\*\*p < 0.001.

### 3. Results and discussion

To understand the temporal impact of IL-10 during the immune response towards *L. donovani*, we used the pMT-10 mouse model infected with *L. donovani*. IL-10 expression induced by the administration of zinc supplementation in the water was controlled and induced at different time points during the infection. The IL-10 was overexpressed from day 0 to 12 [pMT-10 (0–12)] or from day 35 to 47 [pMT-10 (35–47)] post-infection (Fig. 1A). We demonstrated that overexpression of IL-10 during the initial 12 days of infection led to a significantly increased parasite burden at day 60 post-infection in the major parasitized organs, the spleen and the liver, when compared to WT and pMT-10 (35–47) counterparts (Fig. 1B). In the presence or absence of zinc supplementation in the drinking water, the parasite burdens of C57BL/6 wt were similar disregarding any potential impact of zinc supplementation on the immune response to *Leishmania* infection (data not shown). The increased susceptibility displayed by pMT-10 (0–12) animals was associated with increased serum levels of alanine transaminase (ALT) and aspartate transaminase (AST) (Fig. 1C), which are biomarkers associated with hepatic toxicity [3]. Surprisingly, the overexpression of IL-10 upon the 35th day of infection had no impact on the visceral parasite burden nor on induced liver damage. Nevertheless, a larger number of complex inflammatory infiltrates were found in the liver of infected pMT-10 (35–47) (Fig. 1D). The formation of hepatic granulomas during *Leishmania* infection has been extensively studied. It is currently known that at one week post-infection, T cells are recruited to the granuloma to confine parasitized resident Kupffer cells and prevent parasite dissemination [11]. Overexpression of IL-10 in infected pMT-10 (35–47) displayed larger and more numerous infiltrates than those observed in infected pMT-10 (0–12) mice, suggesting that these might be associated with a lower parasite load when compared to pMT-10 (0–12). Altogether, our results suggest that IL-10 overexpression later after infection, at a moment where the T cell response is established, leads to an increased cellular mobilization to achieve the same control as seen in WT mice. In opposition, overexpression of IL-10 during the initial steps of the infection impacts host ability to control *L. donovani* infection by limiting the development of a protective adaptive immune response. To further address this issue, a qualitative and quantitative analysis of splenic parasite-specific T cells was performed at day 60 post-infection. Our results indicated that the pMT-10 (35–47) group displayed a higher number of both CD4 and CD8 T cells in the spleen when compared to pMT-10 (0–12) and WT mice (Fig. 2A), which is consistent with the inflammatory infiltrates observed in the liver (Fig. 1D). Moreover, the infected pMT-10 (35–47) mice displayed increased *Leishmania*-specific IFN- $\gamma$ - and IL-2-producing CD4 (Fig. 2B) and CD8 T cells (Fig. 2C). Yet, this was accompanied by a significant increase on the number of IL-10-producing CD4 (Fig. 2B) and CD8 T cells (Fig. 2C). In accordance with the observed susceptibility to infection (Fig. 1B), the *L. donovani*-infected pMT-10 (0–12) group displayed lower number of TNF- $\alpha$ -producing CD4 and CD8 T cells and higher number of IL-10-producing CD4 and CD8 T cells (Fig. 2B–C). We and others have previously shown that increased IFN- $\gamma$ /IL-10 ratios are associated with protection against *Leishmania* infection [12,9]. We observed that pMT-10 (0–12) with increased susceptibility to *L. donovani* infection (Fig. 1B) are associated to a lower IFN- $\gamma$ /IL-10 ratio compared to WT and pMT-10 (35–47) mice (Fig. 2D). We next extended the analyses to multifunctional CD4 T cells. Strikingly, we found a loss of CD4 T cells expressing both IFN- $\gamma$  and IL-2 (2+) as well of those expressing the three cytokines (3+ - IFN- $\gamma$ <sup>+</sup> IL-2<sup>+</sup> TNF- $\alpha$ <sup>+</sup>) in infected pMT-10 (0–12) compared to infected WT and pMT-10 (35–47) mice (Fig. 2E). Thus, our results are consistent with the notion that protection against distinct *Leishmania* species is accompanied by the induction of *Leishmania*-specific multifunctional T cell response, shifting qualitatively from single to triple producers Darrah et al. [15], Selvapandiyani et al. (2009). Quantifying the fraction of the total cytokine response comprising three (3+), any two (2+) or any one (1+)

cytokine, we found that over half of the response in the pMT-10 (0–12) was in single-producers, whereas the response in the other groups were dominated by double producer T cells (Fig. 2F). Overall, the early up-regulation of IL-10 seems to be clearly associated with a decrease of IFN- $\gamma$ /IL-10 ratio in T cells dampening multifunctional CD4 T cells. Such immunologic landscape contributes therefore for the establishment of a successful infection.

### 4. Conclusions

In this work, we disclose a temporally-regulated role for IL-10 during the initial steps on infection, which impacts the pathogenesis of VL. We demonstrate that the presence of high levels of IL-10 in the initial phase of infection culminates in higher susceptibility, which is mainly associated to the development of a permissive environment characterized by a decreased frequency of multifunctional CD4 T cells. Interestingly, our results highlight the role of IL-10 in the very early phase of infection. Indeed, despite higher levels of IL-10 at the steady state (days 35) and of IL-10 expressing CD4 and CD8 T cells, IFN- $\gamma$  remains elevated. As such, the overexpression of IL-10 upon the establishment of the adaptive immune response do not impact parasite burden. Overall, this work shed some light on the temporal impact of IL-10 on host immune responses against visceral leishmaniasis.

### Acknowledgement and funding

This work was supported by the Northern Portugal Regional Operational Programme (NORTE 2020), under the Portugal 2020 Partnership Agreement, through the European Regional Development Fund (FEDER) (NORTE-01-0145-FEDER-000013) and the Fundação para a Ciência e Tecnologia (FCT) (contracts SFRH/BD/120371/2016 to IM, PD/BDE/127830/2016 to CF, SFRH/BD/120371/2016 to AMB, IF/01147/2013 to RDO, IF/01390/2014 to ET, IF/00735/2014 to AC, SFRH/BPD/96176/2013 to CC and IF/00021/2014 to RS), and Infect-Era (project INLEISH). JE also thanks the Canada Research Chair program for financial assistance.

### References

- [1] Y. Belkaid, et al., The role of interleukin (IL)-10 in the persistence of *Leishmania major* in the skin after healing and the therapeutic potential of anti-IL-10 receptor antibody for sterile cure, *J. Exp. Med.* 194 (10) (2001) 1497–1506, <https://doi.org/10.1084/jem.194.10.1497>.
- [2] A. Cardoso, et al., The dynamics of interleukin-10-afforded protection during dextran sulfate sodium-induced colitis, *Front. Immunol.* 9 (MAR) (2018), <https://doi.org/10.3389/fimmu.2018.00400>.
- [3] S. Gowda, et al., A review on laboratory liver function tests, *Pan African Med. J.* 3 (November) (2009) 17, <https://doi.org/10.11604/pamj.2009.3.17.125>.
- [4] M.M. Kane, D.M. Mosser, The role of IL-10 in promoting disease progression in leishmaniasis, *J. Immunol.* 166 (2) (2001) 1141–1147, <https://doi.org/10.4049/jimmunol.166.2.1141>.
- [5] C.L. Karp, et al., In vivo cytokine profiles in patients with kala-azar. Marked elevation of both interleukin-10 and interferon-gamma, *J. Clin. Investigat.* 91 (4) (1993) 1644–1648, <https://doi.org/10.1172/JCI116372>.
- [6] D. Moreira, et al., Impact of continuous axenic cultivation in *Leishmania infantum* virulence, *PLoS Neglected Trop. Dis.* 6 (1) (2012), <https://doi.org/10.1371/journal.pntd.0001469>.
- [7] H.W. Murray, et al., Interleukin-10 (IL-10) in experimental visceral leishmaniasis and IL-10 receptor blockade as immunotherapy, *Infect. Immunol.* 70 (11) (2002) 6284–6293, <https://doi.org/10.1128/IAI.70.11.6284-6293.2002>.
- [8] S. Nylén, D. Sacks, Interleukin-10 and the pathogenesis of human visceral leishmaniasis, *Trends Immunol.* (2007) 378–384, <https://doi.org/10.1016/j.it.2007.07.004>.
- [9] J. Paul, S. Karmakar, T. De, TLR-mediated distinct IFN- $\gamma$ /IL-10 pattern induces protective immunity against murine visceral leishmaniasis, *Eur. J. Immunol.* 42 (8) (2012) 2087–2099, <https://doi.org/10.1002/eji.201242428>.
- [10] V. Rodrigues, et al., Abortive T follicular helper development is associated with a defective humoral response in *Leishmania infantum*-infected macaques, *PLoS Pathogens* 10 (4) (2014), <https://doi.org/10.1371/journal.ppat.1004096>.
- [11] V. Rodrigues, et al., Regulation of immunity during visceral *Leishmania* infection, *Parasites Vectors* (2016), <https://doi.org/10.1186/s13071-016-1412-x>.
- [12] R. Silvestre, et al., SIR2-deficient *Leishmania infantum* induces a defined IFN- $\gamma$ /IL-10 pattern that correlates with protection, *J. Immunol.* (Baltimore, Md.: 1950) 179 (5) (2007) 3161–3170 (doi: 179/5/3161 [pii]).

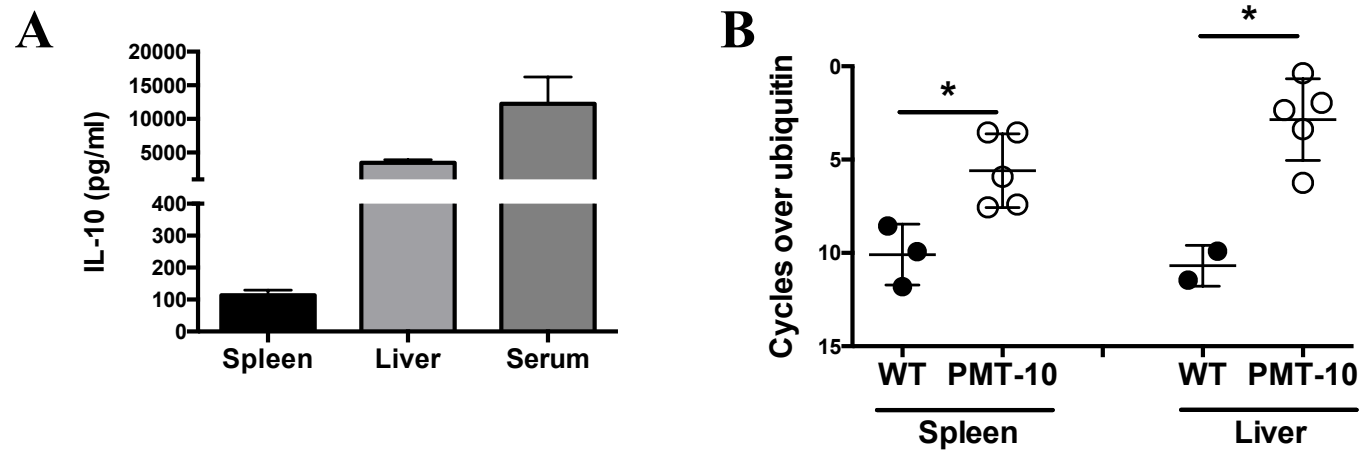


*I. Mesquita et al.*

*Cytokine 112 (2018) 16–20*

- [13] WHO, Control of the Leishmaniases. World Health Organization, Geneva, Tech. Rep. Ser. 949 (March) (2010) 22–26.
- [14] S. Saha, et al., IL-10- and TGF-beta-mediated susceptibility in kala-azar and post-kala-azar dermal leishmaniasis: the significance of amphotericin B in the control of *Leishmania donovani* infection in India, *J. Immunol.* 179 (8) (2007) 5592–5603, <https://doi.org/10.4049/jimmunol.179.8.5592>.
- [15] P.A. Darrah, et al., Multifunctional TH1 cells define a correlate of vaccine-mediated protection against *Leishmania major*, *Nat. Med.* 13 (7) (2007) 843–850, <https://doi.org/10.1038/nm1592>.

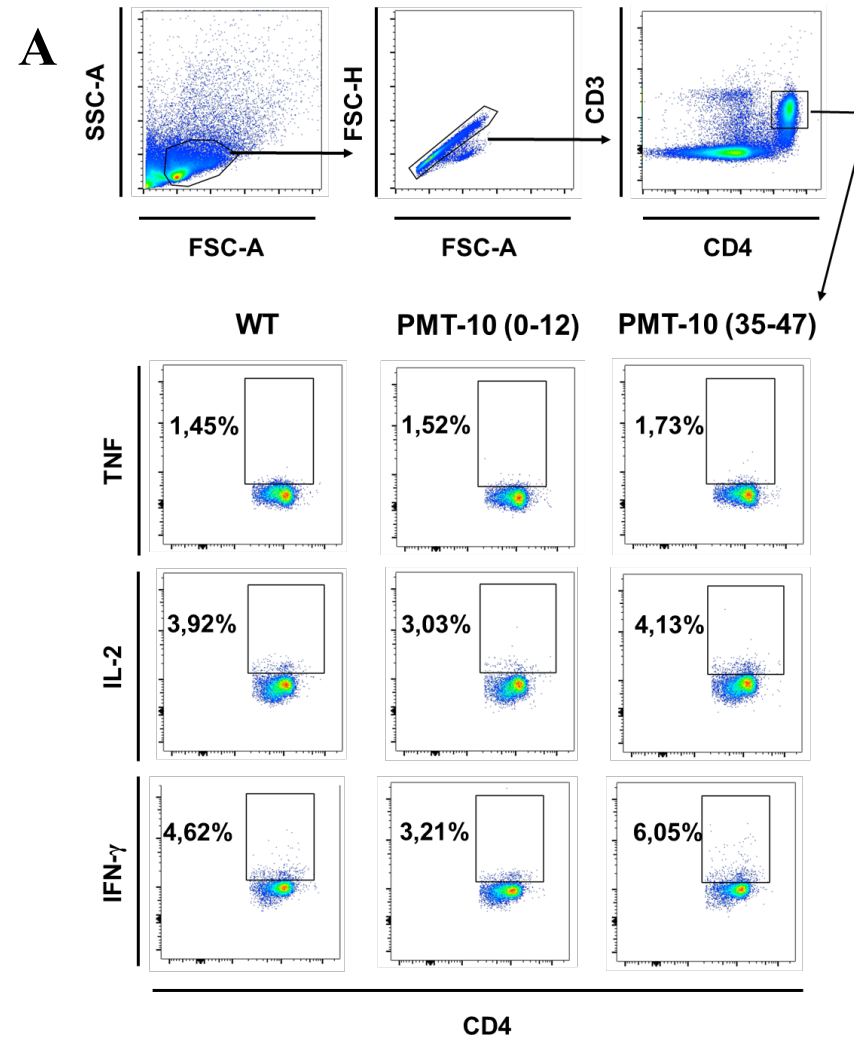
## Supplementary figure 1



### Supplementary figure 1: Zinc administration to pMT-10 mice results in increased levels of IL-10 in the spleen, liver and serum.

Zinc was administered in the drinking water to pMT-10 mice during 12 days. Mice were euthanized and the serum, spleen and liver were recovered. IL-10 levels in the spleen and liver homogenates, as well as the serum, were analyzed by ELISA (A). The transcription levels of the *I110* gene were analyzed in spleen and liver extracts by RT-PCR and normalized to the levels of housekeeping gene Ubiquitin (B).

## Supplementary figure 2



**Supplementary figure 2: Gating strategy for flow cytometry analysis.** Lymphocytes were initially gated on SSC-A and FSC-A and doublets were then excluded. The CD3<sup>+</sup> CD4<sup>+</sup> population was chosen and the frequency of TNF, IL-2 and IFN- $\gamma$  positive CD4 T cells was extracted.

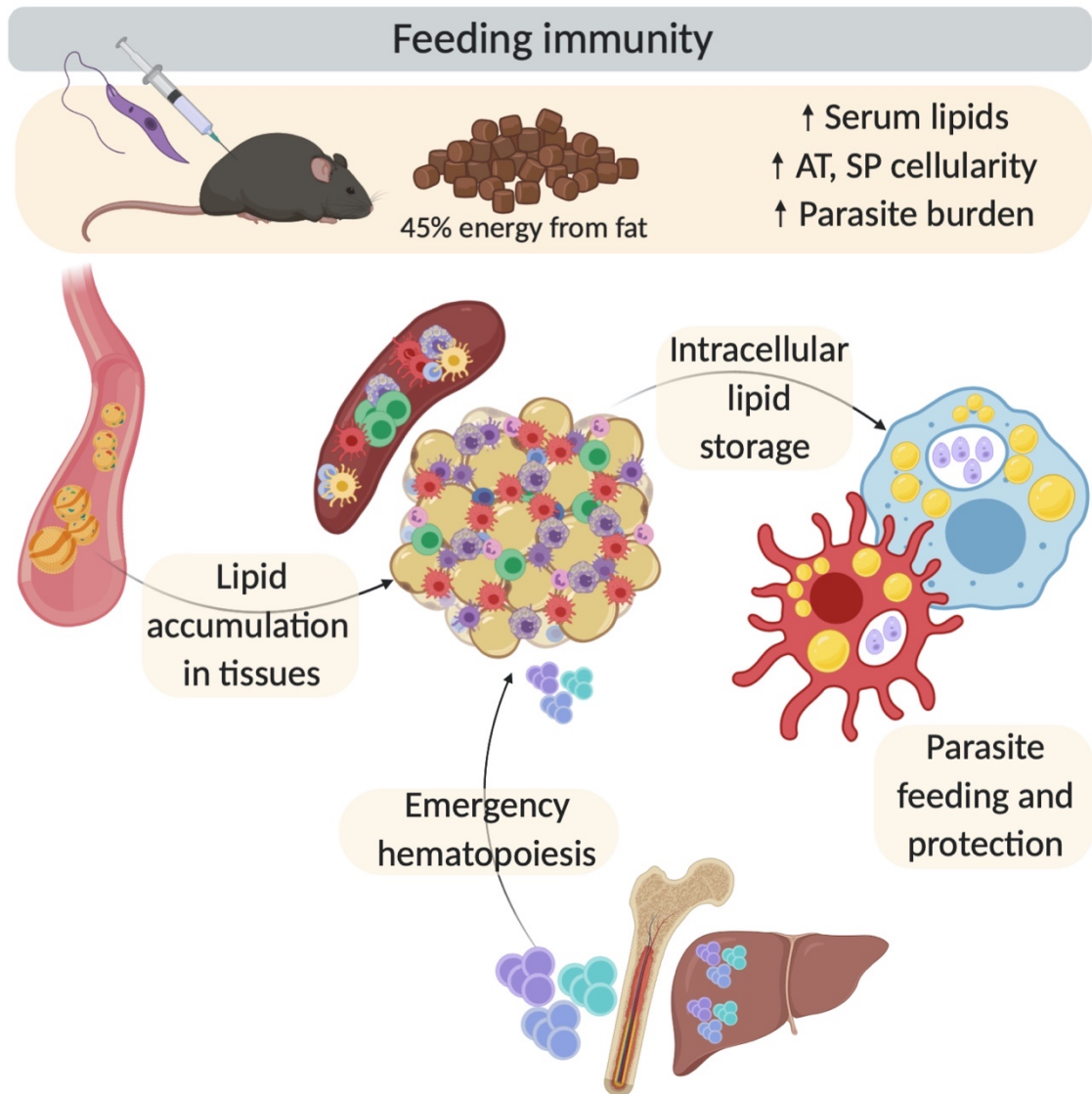
**Feeding immunity: development of new nutraceuticals for visceral leishmaniasis**

Unpublished data.

**Abstract**

A balanced and adequate nutrition is responsible for the development of an effective immune response. Alterations on nutritional states have been associated to the emerging worldwide epidemic of obesity and overweight, which has contributed to an increased prevalence of inflammatory and chronic diseases. It has become clear that nutrition has a vital role in immune response, which goes in line with a marked reduction in immunity that is observed during alterations of nutritional states. Further, it has been shown that this is correlated with an increased susceptibility to pathogens that take advantage of poor host fitness to thrive. As such, understanding the link between the metabolic environment and its importance for microbicidal immune responses is warranted. In this work, we aim at unveiling the mechanisms behind diet-induced systemic alterations in tissue-specific immune responses to *Leishmania* infection, which have been shown to succeed in lipid-rich environments. Upon high-fat diet feeding (45% energy from fat), we observe *L. donovani* accumulation in visceral organs that display increased cellularity in overweighted mice. This raises the hypothesis that overweight and obesity may condition cellular recruitment and tissue immunity, thus contributing to parasite persistence.

Graphical abstract



Introduction

Overweight and obesity are estimated to result in approximately 2.8 million of deaths per year (WHO, 2018). However, overall disease burden goes beyond this number, when acknowledging the co-morbidities associated, as cardiovascular diseases, metabolic and immune dysfunction. Although the crosstalk between nutritional diseases, immune system and inflammation has been shown to greatly impact immune cell behavior (Federico et al., 2010; Ferrante, 2013b, 2013a; Kumari et al., 2018), how this correlates with alteration in microbicidal

response towards pathogens remains to be elucidated. It is estimated that obesity caused a 4.7-fold increased risk for infection (Serrano et al., 2010). This suggests that nutritional diseases create a favorable niche for pathogens to successfully persist (Karlsson et al., 2010; Smith et al., 2007; Wieland et al., 2005), as diet-induced reshaping of the immune system may tilt the balance towards harboring the pathogens, instead of clearing it. Interestingly, the white adipose tissue, a *bona fide* endocrine organ, whose size and cellularity greatly depends on the overall nutritional status, docks immune cells with distinct effector functions, which are essential in the balance of susceptibility and resistance to infections (Ferrante, 2013a; Grant and Dixit, 2015; Han et al., 2017).

*Leishmania donovani* is a protozoan parasite that causes an aggressive form of visceral leishmaniasis (VL), which is fatal if left untreated. Despite the complex metabolic regulation that governs the interaction between host and pathogen, we and other have shown that fat accumulation ultimately favors parasite proliferation (Mesquita et al., 2020; Rabhi et al., 2016). Consistently, it has been reported that murine models of obesity display a higher susceptibility to *Leishmania* parasites (Sarnáglia et al., 2016; Silva et al., 2018). Interestingly, the efficacy of leishmanicidal drugs is greatly reduced in the context of nutritional diseases (Moreira et al., in preparation), which adds a layer of complexity to VL therapy management.

A deeper understanding of the cellular and molecular events that govern resistance and susceptibility to *Leishmania* infection is needed, in order to develop new approaches to circumvent current challenges. As such, in this work, we propose that the metabolic dysregulation originated by nutritional alterations contributes for an impairment of host immunity against *L. donovani*. We aim at understanding the impact of dietary alterations in the immune landscape during *L. donovani* infection, as well as identifying circulating and organ-specific metabolites associated to the development of a protective response. This will ultimately allow the development of nutraceuticals as therapy adjuvants for visceral leishmaniasis.

## **Material and Methods**

### **Mice**

C57BL/6 were purchased from Charles River Laboratories and C57BL/6 WT and were bred and maintained in accredited animal facilities at the Life and Health Sciences Research Institute (ICVS). Mice were housed in groups of 3-6, in HEPA filter-bearing cages, under 12-h light/dark cycles. From 4 weeks on, control mice were fed with autoclaved, standard fat diet (SFD;

PF1915; 10% energy from fats; Gross Energy: 3800 kCal/kg), while high fat diet (HFD) fed mice received irradiated diet (PF1916; 45% energy from fats; Gross Energy: 5000 kCal/kg). All animals received food and water *ad libitum* and the cages were enriched with nesting materials (paper towels). Weight was monitored throughout the duration of the experiment. Experimental animal procedures agreed with the European Council Directive (2010/63/EU) guidelines that were transposed into Portuguese law (Decree-Law n.º113/2013, August 7th). Experiments were conducted with the approval of the UMinho Ethical Committee (process no. SECVS 074/2016) and complied with the guidelines of the Committee and National Council of Ethics for the Life Sciences (CNECV). RS has an accreditation for animal research given from Portuguese Veterinary Direction (Ministerial Directive 1005/92).

### **Parasite culture**

Cloned lines of virulent *Leishmania donovani* (MHOM/IN/82/Patra1) was maintained with weekly subpassages at 27°C in complete RPMI 1640 medium, supplemented with 10% heat-inactivated fetal bovine serum, 2 mM L-glutamine, 100 U/ml penicillin plus 100 mg/ml streptomycin and 20 mM HEPES buffer. Only parasites under ten passages were used in the experimental work.

### **Experimental *Leishmania* infection**

Mice were randomly allocated into groups and the experimenters were blinded to the different conditions. Mice were infected with  $100 \times 10^6$  (intraperitoneal route) stationary *L. donovani* promastigotes. Weight and general well-being were monitored during the 4-week infection. At the endpoint, mice were anesthetized with volatile isoflurane and blood was withdrawn by cardiac puncture. Euthanasia by cervical dislocation was performed following this procedure. The bone marrow, liver and spleen were mechanically resuspended and cells were recovered for flow cytometry and DNA extraction. The epididymal white adipose tissue was incubated with 100 µg/ml Liberase TM Research Grade medium for 2 hours, at 37°C with agitation (200 rpm). The tissue was then mechanically destroyed and the obtained cell suspension was stromal vascular fraction (SVF). DNA was extracted using the phenol-chloroform-isoamyl alcohol method. Briefly, an aqueous suspension with approximately  $1 \times 10^6$  cells was mixed with a mixture of phenol-chloroform-isoamyl alcohol (25:24:1). After centrifugation, the aqueous phase was recovered and incubated overnight with 3M sodium acetate and absolute ethanol. The DNA pellet was washed twice with 70% ethanol

and resuspended in RNase/DNase-free water. Parasite burden was assessed, using a TaqMan-based qPCR assay for detection and quantification of *L. donovani* kinetoplastid DNA. Triglyceride, glucose and cholesterol levels were quantified in the serum using an AutoAnalyzer, using reagents from the same provider.

#### **Tissue preservation for metabolomics**

Following portal vein perfusion with ice-cold saline, 50 mg of liver was recovered and immediately snap-frozen, for further metabolomics analysis.

#### **Quantification and statistical analysis**

Statistical analyses were performed with the GraphPad Prism 6 software. A one-way analysis of variance (ANOVA) followed by a Bonferroni's post hoc test was employed for multiple group comparisons. A Mann-Whitney test of variance and Kruskal-Wallis non-parametric test were performed accordingly with the correspondent experimental design. The statistical details of each experiment can be found in figure legends and the data is presented as mean  $\pm$  SD. Statistically significant values are as follows: \* $p < 0.05$ , \*\* $p < 0.01$ , \*\*\* $p < 0.001$ .

### **Results**

In this initial pilot study, we sought to establish the model of *Leishmania donovani* infection in diet-induced overweighted/obese mice, as a proxy for studying the relation between nutritional diseases and susceptibility to infectious diseases. For this, we fed mice (starting at 4 weeks after birth) with HFD, in which 45% of the energy is obtained from fat and yields approximately 5000 kCal/kg. In opposition, SFD chow (with 10% of fats and 3800 kCal/kg) was also given to control mice. Currently, there are several 60% HFD available, which in turn produce faster results in terms of fattening. However, some concerns regarding the utilization of such a high percentage of fat have arisen, mainly because it represents an enormous distortion when compared to control diets, which possess only 10% of fats. Furthermore, the typical American and European diet styles contain between 30-40% of fats, which suggest that 45% fat diets are more relevant and mimic human physiology and obesity development (Speakman, 2019).



Mice were fed with SFD or HFD for 14 weeks and animal welfare and weight variations were weekly monitored (figure 1A). The average weight of HFD-fed mice ( $34.84 \pm 4.205$ ) was significantly higher, when compared to mice fed with SFD ( $29.60 \pm 1.584$ ) (figure 1B). Accordingly, serum analysis revealed increased levels of both cholesterol and triglycerides (figure 1C) in HFD mice, while no differences were found on glucose concentration (figure 1D). The increased weight and levels of lipids in the serum of HFD mice were in accordance with previously published data (Eisinger et al., 2014). Upon confirmation of the expected phenotype, mice from both groups were split in groups and infected during 4 weeks with *L. donovani* promastigotes or left uninfected as controls. During the course of the 4 weeks of infection, diets were maintained. To understand the impact of HFD in parasitized organs, we weighted the liver and quantified total cell number in the spleen and white adipose tissue (WAT) in the distinct groups. We found no differences in the liver of SFD and HFD mice, regardless of whether they were infected or left uninfected (figure 2A). We observed an increased in the total splenocyte count in infected HFD-fed mice, when compared to uninfected controls (figure 2B), as well as a tendency for an increase in the number of adipose tissue-derived stromal vascular fraction cells in HFD-fed mice (figure 2C). Previous reports have shown that WAT expansion may associate with increased infiltration of immune cells (Cox et al., 2019; de Heredia et al., 2012; Misumi et al., 2019), which could be of vital importance during *Leishmania* infection, as these parasites infect mainly phagocytes. We found that HFD-fed mice were more susceptible to *L. donovani* infection, as observed by the increased parasite burden in the spleen (figure 3A). No major differences were observed in the liver and the bone marrow between SFD and HFD mice. Interestingly, the parasite burden was found to be higher in the WAT of HFD-fed mice (figure 3A), which could be attributed to a higher recruitment of immune cells to the inflamed adipose tissue. In addition to this, fractions of liver from the distinct groups was snap-frozen for further metabolomics analysis, in order to identify which metabolites are significantly altered between uninfected and infected groups, as well as between SFD-fed and HFD-fed mice.

### **On-going work**

We will proceed to a metabolomic analysis and the construction of an interactive map with completed host metabolomic profile by analyzing qualitative and quantitative perturbations of the pathways induced in overweight vis-à-vis lean mice. Upon identification of key players, we intend to administer in vivo  $^{13}\text{C}$ -labelled metabolites to elucidate organ-specific metabolic fluxes. With this,

we aim at understanding how the tissue-specific metabolic environment modulates immune cell function and, consequently, parasite burden. Alongside, a thorough characterization of immune populations in parasitized organs will be performed to assess the impact of nutrition in the adequate development of anti-*Leishmania* effector functions during acute and chronic infection. This will also include a study of resident versus recruited populations, which will contribute to a deeper understanding on how nutrition conditions local immunity towards infection. The integration of the metabolomic information regarding the parasite burden and the impact on immune anti-*Leishmania* response will reveal the key nodes in the metabolomic network that can be targeted to reverse susceptibility to the infection

### Future perspectives

As outlined on the introduction, the main tasks of this work include:

- Understand how dietary alterations (in here prototyped by the development of a state of overweight/obesity using modified diets) will impact the immune landscape during *L. donovani* infection;
- Understand how tissue-specific metabolic dysregulation will condition resistance against visceral leishmaniasis;
- Identify circulating and organ-specific metabolites that could associate to a protective response against *L. donovani* infection.

Upon successful completion of the abovementioned tasks, we intend to obtain a small number of altered metabolites, which will be administered in combination with conventional therapy (amphotericin B) during chronic *L. donovani* infection. This will serve as basis for the development of nutraceuticals as therapy adjuvants for visceral leishmaniasis.

### Figure legends

**Figure 1. Establishment of diet-induced obesity/overweight in C57BL/6 mice.** Schematic representation of feeding and infection protocol (A). Mice weight, 14 weeks after initiation of diets (B). Quantification of serum levels of lipids (triglycerides and cholesterol) (C) and glucose (D). HFD:

high fat diet; INF: infected; UNINF: uninfected; SFD: standard fat diet. Data are shown as mean  $\pm$  SD; n = 28-30 mice/group. \*\*p < 0.01; \*\*\*\*p < 0.0001.

**Figure 2. *L. donovani* infection of normal weighted and overweighted mice.** Liver weight at the experimental endpoint (A). Total quantification of splenocytes (B) and WAT stromal vascular fraction (C). HFD: high fat diet; INF: infected; UNINF: uninfected; SFD: standard fat diet; WAT: white adipose tissue. Data are shown as mean  $\pm$  SD; n = 6-7 mice/group. \*\*p < 0.01.

**Figure 3. Parasite burden in normal weighted and overweighted mice.** Parasite burden in the spleen, liver, BN and WAT in SFD- and HFD-fed mice. BN: bone marrow; HFD: high fat diet; SFD: standard fat diet; WAT: white adipose tissue. Data are shown as mean  $\pm$  SD; n = 4-6 mice/group. \*p < 0.05; \*\*p < 0.01.

**FIGURE 1**

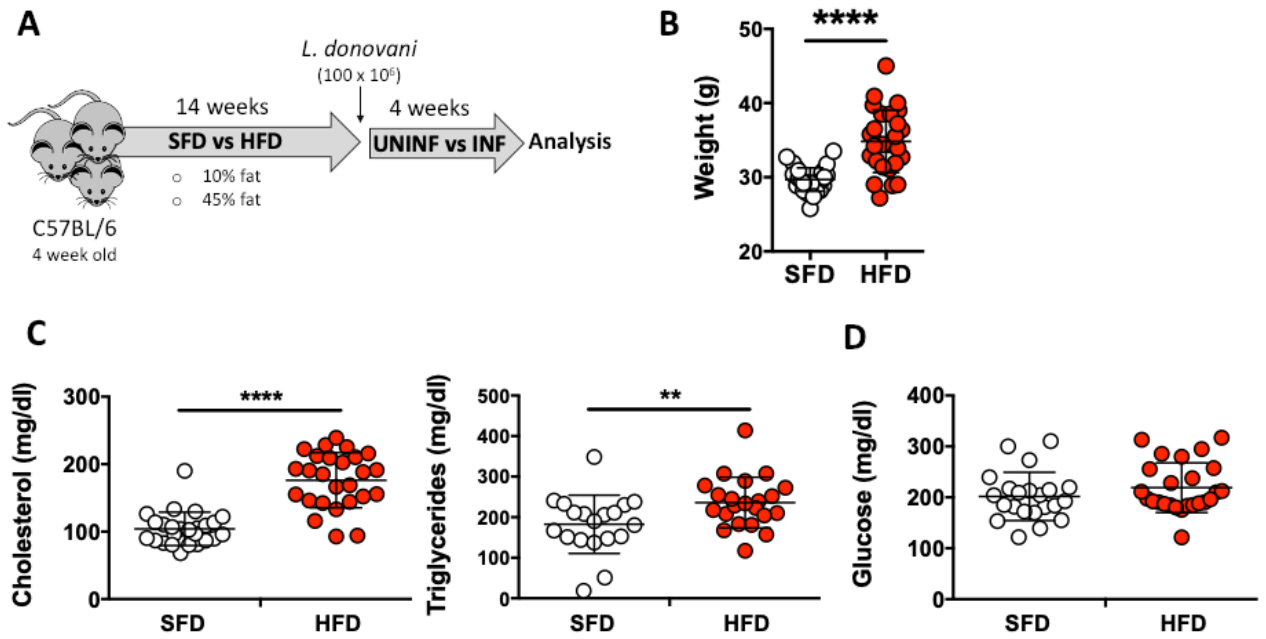


**FIGURE 2**

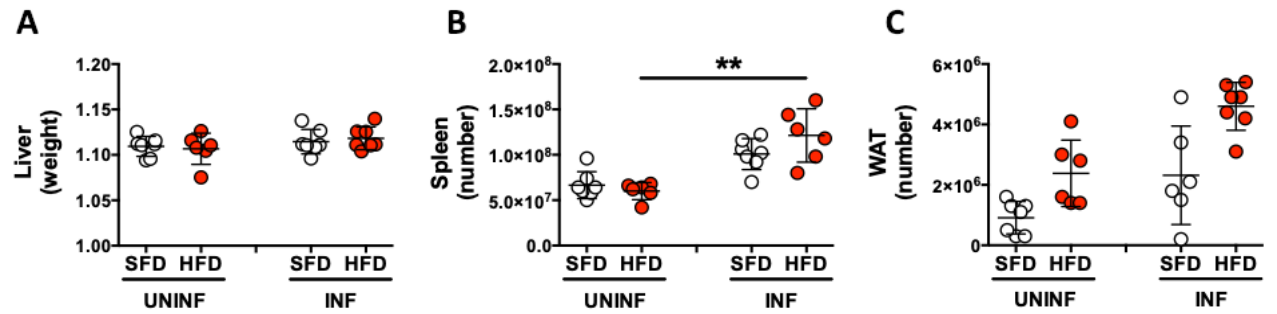
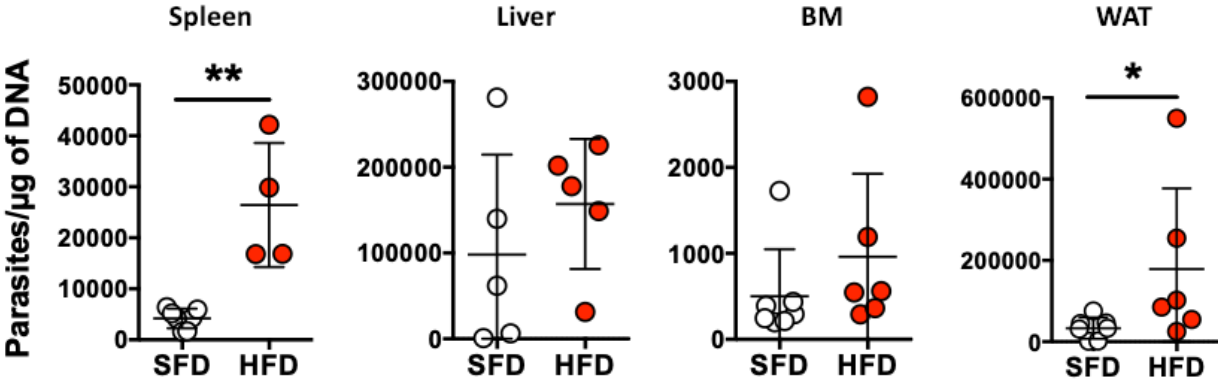


FIGURE 3



## CHAPTER IV DISCUSSION

## 1. Parasite-host immunometabolic crosstalk: how lipids condition the biology of *Leishmania* infection

### 1.1 HIF-1 $\alpha$ mediates cellular reprogramming of lipid metabolism

Reprogramming of host cell metabolism is a valuable strategy employed by *Leishmania* parasites to successfully thrive, as it allows for the establishment of a permissive niche within host cells. Our group was a pioneer in the elucidation on how *Leishmania* parasites modulate macrophage metabolism. It was shown that host metabolic pathways are hijacked by *L. infantum* parasites, which culminates in a shift of macrophage metabolism from glycolytic (6 hours post-infection) to a permissive mitochondrial metabolism (18 hours post-infection) (Moreira et al., 2015). This was mediated by LBK1/SIRT1-mediated activation of key energetic sensor AMPK, which is responsible for establishing an anti-inflammatory microenvironment, prone to harbor invading pathogens. This study uncovered a subversion mechanism employed by *Leishmania* parasites that aims at rewiring host cell metabolism in their own advantage. This prompt us to unveil the contribution of other energetic sensors, as HIF-1 $\alpha$ , which is known to regulate the inflammatory response of immune cells, through a switch towards glucose fermentation. However, despite the known role of this factor in glycolysis, some growing controversy regarding the role of HIF-1 $\alpha$  in lipid metabolism has arisen, with some authors stating a role for this factor in preventing lipid accumulation, while other observed increased lipid storage driven by HIF-1 $\alpha$ . Nishiyama and colleagues showed that HIF-1 $\alpha$  has a protective role in the development of ethanol-induced fatty liver via activation of the HIF-1-regulated transcriptional repressor DEC1. Genetic deficiency of HIF-1 $\alpha$  in the hepatocytes led to downstream activation of SREBP-1c and ACC, contributing to the observed hepatic steatosis (Nishiyama et al., 2012). Interestingly, Arai *et al.* showed that loss of *Hif1a* gene suppresses peroxisomal FAO and induction of peroxisome proliferator-activated receptor (PPAR) $\alpha$  coactivator, lipin1, responsible for the last step of triglycerides synthesis. This culminated in hepatic lipid accumulation during nonalcoholic fatty liver disease (Arai et al., 2018). Our data shows that during infection genetic deficiency of HIF-1 $\alpha$  resulted in the upregulation of host lipogenic machinery via BNIP3 downregulation and consequent mTOR/SREBP-1c activation. This increased lipid accumulation was responsible for driving higher susceptibility to *L. donovani*, both *in vitro* and *in vivo*, which was reverted upon pharmacological inhibition of key lipogenic enzymes ACC and FASN (Mesquita et al., 2020). Although we found a negligible role for HIF-2 in

the modulation of lipid metabolism (data not shown), it has been shown that this factor has a crucial role in regulating this pathway (Mylonis et al., 2019). Other studies have suggested that HIF-1 $\alpha$  induction contributes to lipid accumulation. Mylonis and colleagues showed that hypoxia-driven activation of HIF-1 directly binds to *Lpin1* promoter and activates lipin 1 transcription, thus contributing to triglyceride synthesis and accumulation (Mylonis et al., 2012). Similarly, it was shown that LDs accumulate during hypoxia in a HIF-1 $\alpha$ -dependent fashion, which is crucial to protect cells against ROS toxicity and to impair tumorigenesis (Bensaad et al., 2014). Du and colleagues demonstrated that lipid deposition in clear cell renal carcinoma is orchestrated by HIF-induced *CPT1A* gene inhibition, which forces lipid droplet accumulation for storage (Du et al., 2017).

Altogether, these evidences point to an universal role of HIF-1 $\alpha$  in the modulation of lipid metabolism, highlighting a cell- and context-specific impact that could operate differently in distinct models of inflammation.

## 1.2 Intracellular lipids as major hubs in *Leishmania*-host interaction

The complex interaction between host and *Leishmania* is regulated by an immense panoply of factors, which include parasite-associated factors, host genetics and, importantly, metabolic regulation at a cellular and organismal level. Interestingly, several reports have addressed the impact of lipids during *Leishmania* infection, which emphasizes a crucial role for these macromolecules in several aspects of host-pathogen crosstalk. By taking advantage of host lipids, *Leishmania* parasites impose a nutritional strategy to increase survival odds and proliferation rate, as we will address.

It has been demonstrated that host LDs accumulate in the vicinity and within the parasitophorous vacuole (Rabhi et al., 2016; Rodríguez et al., 2017). Further, we showed that lipid accumulation in parasitized cells associates with higher parasite burden (Mesquita et al., 2020). This suggests that *Leishmania* parasites are proficient at exploiting host lipid machinery in their own advantage. However, the question remains about which mechanisms justify the importance of lipids for *Leishmania* parasites. Similarly to what happens with other eukaryotic cells, lipids are important for the building and remodeling of newly formed membranes, which may be important during promastigote-amastigote transition and parasite proliferation. Accordingly, lipid composition and distribution between the promastigote and amastigote forms change dramatically, which



results in major changes in surface membrane and parasitophorous vacuole composition (Bouazizi-Ben Messaoud et al., 2017). Additionally, while fatty acids are mainly used for the formation of new membranes in the promastigote stage, amastigotes actively catabolize fatty acids for the TCA cycle, to circumvent reduced glucose uptake (McConville et al., 2015). Further, although *Leishmania* parasites are capable of synthesizing some lipids as C18 fatty acids (Kloehn et al., 2015), other lipids are acquired via salvage pathways due to the lack of complex biosynthetic machinery. This means that *Leishmania* parasites can scavenge lipids from the host cell, which justifies partially the recruitment of LDs to the PV as well as the positive correlation between lipid accumulation and success of infection. Besides the role of host lipids in feeding both energetic and biosynthetic needs of *Leishmania* parasites, the accumulation of LDs in infected cells may prevent the action of host microbicidal molecules that aim for parasite killing. The role of lipids as antioxidant was described by Bailey and colleagues that demonstrated that LDs protect glial cells against toxic peroxidation reactions (Bailey et al., 2015a). As such, we hypothesize that the colocalization of parasites and LDs is not casual, but instead may represent a strategy of parasite protection from host ROS. Consistently, upon analyzing spleen and liver extracts of *Leishmania*-infected mHIF-1 $\alpha$ <sup>-/-</sup> we found higher levels of lipid peroxidation marker malondialdehyde, when compared to WT controls. This suggests lipids as protective agents against host microbicidal mechanisms by shielding *Leishmania* parasite from the direct ROS-mediated killing. However, whether this mechanism is essential for *Leishmania* survival remains to be addressed.

### 1.3 Targeting lipids: new avenues in antileishmanial therapy?

Cholesterol has been shown to be of crucial importance for *Leishmania* infection, impacting its biological phenomenon from phagocytosis to the development of an adequate immune response (Pucadyil and Chattopadhyay, 2007). Scavenge of host cholesterol has shown to be essential during *Leishmania* infection, as treatment of macrophages with cholesterol-depleting agent cyclodextrin or sterol-binding antibiotic nystatin negatively impact *Leishmania* entry and the extent of infection (Pucadyil et al., 2004; Tewary et al., 2006). This suggests that *Leishmania* parasites are actively hijacking host cholesterol, in opposition to synthesizing it, as these parasites do not possess biosynthetic machinery necessary for cholesterol synthesis (Yao and Wilson, 2016). However, there is some controversy regarding the predictive impact of serum cholesterol on resistance/susceptibility towards leishmaniasis. Ghosh *et al.* demonstrated that

GP63 cleaves Dicer1 to prevent miR-122 formation, which culminates in the lowering of serum cholesterol and triglycerides (Ghosh et al., 2013). However, the impact of serum cholesterol and triglycerides in chronic infections remains to be addressed. This is further supported by the fact that GP63 is predominantly expressed in promastigote membrane (Medina-Acosta et al., 1989), while its role during the amastigote phase remains debatable. As such, promastigote-driven GP63 could have an initial impact on early stages of infection, being lost in chronicity. In opposition, we have shown that increased lipid accumulation in parasitized cells, as well as higher levels of serum cholesterol and triglycerides associate positively with higher susceptibility towards VL (Mesquita et al., 2020). Importantly, reversion of susceptibility and altered serum parameters was achieved through blockage of lipogenesis. Furthermore, the utilization of cholesterol-lowering drugs statins has been shown to inhibit *Leishmania* infection due to an overall depletion of host cholesterol (Kumar et al., 2016; Parihar et al., 2016). This suggests that both triglyceridemia and cholesterolemia may associate as poor prognosis factors for leishmaniasis, while normalization of serum lipid levels results in control of infection.

Statins are commercially available cholesterol-lowering drugs that target cholesterol biosynthesis through inhibition of HMG-CoA Reductase. Considering its mechanism of action, low toxicity and easy administration (*per os*), statins have been suggested as adjuvant treatment for distinct infections, including *Staphylococcus aureus*, *Escherichia coli*, *Pseudomonas aeruginosa*, *Serratia marcescens* and *Mycobacterium tuberculosis* (Ko et al., 2018; Parihar et al., 2014). Interestingly, statins are also attractive approaches for treatment of diseases caused by *Toxoplasma gondii* and *Leishmania* parasites (Li et al., 2013; Parihar et al., 2016). Simvastatin is effective in reducing *L. major* burden in the footpad and popliteal lymph nodes via both topical and systemic administration, as assessed by decreased footpad swelling. However, this may be independent of immune-mediated effects, as no differences were observed in immune populations nor cytokine production after simvastatin treatment. However, simvastatin enhanced both hydrogen peroxide production and phagosome maturation in infected macrophages, which contributed to *L. major* elimination (Parihar et al., 2016). We have also observed that simvastatin administration through oral gavage decreased the parasite burden in the spleen, liver and bone marrow of infected mHIF-1 $\alpha$ <sup>-/-</sup>, although no major differences were observed in treated and untreated WT counterparts. Further, serum levels of cholesterol and triglycerides were also normalized to WT levels (unpublished data). We hypothesize that statin treatment originated both

systemic and local antileishmanial mechanisms, similar to what has been described. However, the exact mechanisms behind this effect remain to be fully addressed.

#### 1.4 Immunometabolic-related gene polymorphisms in *Leishmania* infection

Host genetics play a crucial role in the clinical manifestations of *Leishmania* infection, as it will determine the effectiveness of the elicited immune response. Several polymorphisms related to immune function players have been associated with altered response towards *Leishmania* infection. Interestingly, polymorphisms in the promoter region of *TNFA* (-308G/A) that originated increased cytokine production have been associated with susceptibility to MCL caused by *L. V. braziliensis* (Cabrera et al., 1995). Similarly, increased levels of IL-10, linked to polymorphisms in the promoter of the *IL10* gene (-819C/T) have also correlated with cutaneous lesion development (Salhi et al., 2008). A recent study has also evaluated the conjoined contribution these two SNPs for the clinical outcome of CL (Mera-Ramírez et al., 2017). A functional *IL6* (-174G/C) promoter polymorphism has also been shown to lead to lower IL-6 production by infected macrophages, which associated positively with increased susceptibility to MCL (Castellucci et al., 2006). These evidences suggest that an imbalance in cytokine production driven by polymorphisms in host genetic factors are important determinants for the success of *Leishmania* infection. Further, the -2518bp promoter polymorphism at *CCL2/MCP1* correlated with elevated plasma levels of MCP-1, which associated the G allele of the *CCL2* -2518bp promoter SNP and susceptibility to *L. braziliensis*-induced ML caused (Ramasawmy et al., 2010). Interestingly, *in vitro* studies showed that MCP-1 and IFN- $\gamma$  are crucial for eliciting recruitment of CCR2<sup>+</sup> macrophages to effectively kill *Leishmania* parasites (Conrad et al., 2007). This goes in line with the putative utilization of MCP-1 as a biomarker of immunity, as MCP-1 was found to be significantly increased in patients with cured VL (Ibarra-Meneses et al., 2017). Genome-wide association studies have also shown that HLA-DRB1-HLA-DQA1 HLA class II region associates with susceptibility to visceral leishmaniasis in both India and Brazil (Fakiola et al., 2013).

As such, identifying genetic polymorphisms associated with susceptibility to *Leishmania* infection is a valuable strategy that may aid the development of specific and individualized therapies. It has been shown that the transcriptional levels of *HIF1A* is lower in individuals carrying CT/TT genotypes at rs2057482 compared to CC carriers. This SNP is localized in the 3'-UTR region of *HIF1A* and close to two predicted microRNA binding sites (hsa-miR-199a/b-5p and hsa-

miR-340), which repress HIF-1 $\alpha$  transcription and expression. In our work, we demonstrated that genetic variation on *HIF1A* gene (rs2057482) associates with lower levels of HIF-1 $\alpha$ , increased lipogenesis and higher *L. donovani* viability (Mesquita et al., 2020). Importantly, given that rs2057482 allele frequency is 15.9% when considering worldwide population, it is expected to have a major impact in individual response to different diseases. This suggests the utilization of *HIF1A* genetic polymorphisms as a prognosis factor for VL, as increased frequencies of rs2057482 are found in regions with higher number of VL cases (Asia – 39.88%; Sub-Saharan Africa – 46.02%).

In line with this, the rs2057482 polymorphism has also been associated to different diseases, highlighting the importance of HIF-1 $\alpha$  in several biological processes. Several studies have shown that rs2057482 associates with decreased overall cancer risk (Wu et al., 2019), which may indicate a biological advantage of expressing HIF-1 $\alpha$ , as it promotes hypoxia adaptation. Interestingly, hepatocellular carcinoma patients with variant alleles (CT/TT) of rs2057482 had a significant decreased risk, in comparison with patients with the CC genotype. This suggests that the SNP rs2057482 can be used to predict the clinical outcome of hepatocellular carcinoma patients after surgery (Guo et al., 2015). Similarly, rs2057482-CC genotype associated with pancreatic ductal adenocarcinoma risk and worse clinical outcomes (Wang et al., 2016). However, despite the high frequencies of rs2057482, its role in infections has been scarcely addressed. A study from Peckham-Gregory and colleagues showed that rs2057482-CT associates with AIDS-associated non-Hodgkin lymphoma risk (Peckham-Gregory et al., 2016).

This cluster of evidences suggest that a deeper understanding of individual variations, mainly the existence of genetic polymorphisms that condition disease severity and progression, are required to further orientate personalized therapy.

## 2. Adaptive immunity during *Leishmania* infection: Prospects for immunotherapy

### 2.1 Immune cells and associated mediators during antileishmanial T cell responses

The immune response and the immune-related microenvironment are a crucial characteristic of both organ-specific and systemic protection against *Leishmania* infection. Given the protective role of T cells in *Leishmania* infection, T cell exhaustion is a phenomenon that merits further studies, as it may unveil novel therapeutic avenues against leishmaniasis. Previous studies have shown that exhaustion has a crucial impact in antileishmanial immune response, as it may hinder T cells dysfunctional and unable to elicit proper killing mechanisms (Barroso et al., 2018; Esch et al., 2013; Gautam et al., 2014). We showed that increased susceptibility in the absence of myeloid HIF-1 $\alpha$  is likely associated with progressive T cell exhaustion, as a decrease in IL-2- and IFN- $\gamma$ -producing, as well as an increase in TIM-3-expressing T cells were found in chronically infected mHIF-1 $\alpha$ <sup>-/-</sup> mice (Chapter IV, Section 2). However, further studies using anti-TIM-3 monoclonal antibodies are required to understand if T cell reinvigoration is able to revert mHIF-1 $\alpha$ <sup>-/-</sup>-associated susceptibility. Furthermore, the underlying causes that may contribute to T cell exhaustion in the context of myeloid HIF-1 $\alpha$  deficiency remains to be addressed.

Considering the higher parasite burden found in infected mHIF-1 $\alpha$ <sup>-/-</sup> mice, it is possible that an increase in the levels of circulating antigens can contribute to T cell exhaustion. It has already been shown for distinct infection models that T cell exhaustion is associated with pathogen burden and persistence of infection. The severity of T cell dysfunction and further loss is positively associated to the high replicative capacity of the infectious agents (Zuniga and Harker, 2012). Although mHIF-1 $\alpha$ <sup>-/-</sup> mice display approximately a 2-fold increase in splenic and hepatic parasite burden, when compared to WT, whether or not this is sufficient to contribute or even cause the observed T cell exhaustion remains to be addressed.

Following our previously published work, we observed that splenic and hepatic CD11b<sup>+</sup> cells from infected mHIF-1 $\alpha$ <sup>-/-</sup> mice accumulate intracellular neutral lipids. Additionally, due to a systemic lipid accumulation, parasitized organs, as the liver, display a generalized lipid distribution, which is not restricted to HIF-1 $\alpha$ -deficient myeloid cells (Mesquita et al., 2020). This suggests that the observed metabolic dysregulation may transversally affect all immune cells. As previously described, an optimal nutrient microenvironment is necessary for the development of adequate immunity: an unbalanced proportion of nutrients (in here prototyped by an excessive lipid

concentration) may condition antileishmanial host response. As such, immune cells in parasitized organs from mHIF-1 $\alpha$ <sup>-/-</sup> mice display impaired functions, namely in terms of cytokine and ROS production and initiation of adaptive immune response. This is particularly important when acknowledging that lipid accumulation may impair proper T cell priming and function due to alterations of MHC presentation. It has already been shown that lipid accumulation and further peroxidation in DCs culminates in reduced capacity for antigen cross-presentation (Cao et al., 2014; Herber et al., 2010; Veglia et al., 2017) and consequent inhibition of antitumoral T cell responses (Cubillos-Ruiz et al., 2015). Interestingly, Ibrahim and colleagues identified two hepatic populations of CD11c<sup>+</sup> DCs, with higher (high-DC) and lower (low-DC) lipid accumulation. In the context of a lipid-rich and inflammatory environment, high-DCs produce pro-inflammatory cytokines and display increased antigen presentation. However, low-DCs are highly tolerogenic and induce high-DCs apoptosis, which contributes to impaired hepatic immunity (Ibrahim et al., 2012). As macrophages represent the main reservoirs for *Leishmania* parasites, the observed rewiring of cellular metabolism towards lipid accumulation is dramatically impairing its microbicidal properties (Mesquita et al., 2020). Accumulation of peroxidized lipids greatly influence macrophage polarization (Seo et al., 2015) and consequently its effector functions.

The establishment of an immunosuppressive environment has been associated with the establishment of T cell dysfunction. IL-10 is a potent immunoregulatory cytokine that has been identified as a potential target in T cell exhaustion due to its critical role in dampening inflammation (Moore et al., 2001). Recent evidences showed that IL-10 directly reduces antigen sensitivity in CD8 T cells, while impairing its TCR signal transduction capacity during chronic LCMV infection (Smith et al., 2018b). Our results showed an increase in the number of splenic IL-10-producing neutrophils, monocytes and dendritic cells in chronically *L. donovani*-infected mHIF-1 $\alpha$ <sup>-/-</sup> mice, which suggests the buildup of an immunosuppressive environment (Chapter IV, Section 2). This goes in line with our previous work showing that early IL-10 overexpression results in higher parasite burden, as well as loss of multifunctional CD4 T cells and lower IFN- $\gamma$ /IL-10 ratio (Mesquita et al., 2018b). Early induction of IL-10 (from 0-12 days post-infection) using the transgenic mouse model pMT-10 resulted in a decreased frequency of IFN- $\gamma$ <sup>+</sup>, IFN- $\gamma$ <sup>+</sup>IL-2<sup>+</sup> and IFN- $\gamma$ IL-2<sup>+</sup>TNF- $\alpha$ <sup>+</sup>-producing CD4 T cells. The establishment of an immunosuppressive environment is not solely restricted to local microenvironments, as observed in parasitized organs, but also spread systemically, as high levels of IL-10 are also found in the serum. Although the reasons behind the increased parasite burden remains to be fully addressed, it is likely that the elevated IL-10

production contributes to T cell dysfunction and impaired antileishmanial activity. Interestingly, multifunctional T cells have been associated with vaccine-mediated protection and effective control of disease during influenza virus (Brown et al., 2012; Talker et al., 2015), *Mycobacterium tuberculosis* (Caccamo et al., 2010; Kaveh et al., 2012; Lewinsohn et al., 2017) and also cutaneous *Leishmania* infection (Darrah et al., 2007b; Macedo et al., 2012). Darrah and colleagues showed that increased IL-10 production upon vaccination of *L. major*-infected mice limited production of IL-12 by dendritic cells, thus hampering the generation of multifunctional Th1 cells. Inhibition of IL-10-mediated effects, either by using genetically deficient IL-10<sup>-/-</sup> mice or by blocking IL-10 signaling through administration of  $\alpha$ -IL-10R, offered complete protection, as lesion sites were found to be decreased, similarly to parasite burden (Darrah et al., 2010). This cluster of data suggests that IL-10 production is causally linked to the loss of multifunctional T cells during *Leishmania* infection, which eventually culminates in increased parasite load and pathology.

## 2.2 Immunotherapy in the treatment of leishmaniasis

The success of checkpoint blockage (using anti-PD-1 and anti-PD-L1 monoclonal antibodies) for cancer immunotherapy has highlighted that these therapies could also be useful in the treatment of chronic infectious diseases. In these cases, reinvigoration of exhausted T cells is a desired outcome, as T cells may sustain potent antiviral and antiparasitic functions. It was reported that during untreated HIV infection, PD-1 and TIM-3 levels are increased in cytotoxic and antigen-specific CD8 T cells. Interestingly, blockage of both PD-1 and PD-L1 resulted in increased HIV-specific CD8 T cells, with higher killing capacity (Day et al., 2006; Trautmann et al., 2006). A recent study has shown that treatment with anti-PD-1 and anti-PD-L1 results in increased IFN- $\gamma$ <sup>+</sup> CD4 and CD8 T cells, which culminates in decreased *L. amazonensis* burden and reduced lesion sizes. No major differences were observed in IL-10 production in infected paws after immunotherapy, although both IL-4 and TGF- $\beta$  were found to be decreased during anti-PD-1 treatment (da Fonseca-Martins et al., 2019). Jayaraman and colleagues demonstrated that during *M. tuberculosis* infection TIM-3<sup>+</sup>PD-1<sup>+</sup> T cells were poor producers of IL-2, IFN- $\gamma$  and TNF, while alternatively producing IL-10. Consistently, anti-TIM-3 treatment was shown to decrease bacterial loads, suggesting immunotherapy as an effective therapeutic strategy (Jayaraman et al., 2016). Similar efficacy for anti-TIM-3 therapy was observed for hepatitis C and hepatitis B virus infections (Golden-Mason et al., 2009; Ju et al., 2009). The efficacy of anti-IL-10R antibodies in the

persistence of *L. major* skin infection has been elucidated in a seminal work by Belkaid and colleagues. In this work, IL-10-deficient Balb/c mice were able to clear the infection from the primary site, as well as draining lymph nodes. Further, treatment of resistant C57BL/6 mice with anti-IL-10R antibody achieved sterile cure, as *Leishmania* parasites were not detected in the ears and lymph nodes of previously infected mice (Belkaid et al., 2001). IL-10 production during *L. major* infection was ascribed to T cells, as T cell-specific IL-10-deficient mice display a healing phenotype. Further, BALB/c mice showed a two-fold reduction of IL-10-secreting CD4 T cells, following a protocol of DC immunization based on fragmented BMDC treated with *Leishmania* antigen and CpG oligodeoxynucleotides (Schwarz et al., 2013).

This cluster of data suggest that reinvigoration of T cells, which aims for a shift towards an increase in IFN- $\gamma$  and a decrease in IL-10 production, is a valuable strategy to fight leishmaniasis. This may be achieved by blocking either immune checkpoints as PD-1, PD-L1 and TIM-3 with monoclonal antibodies or by reducing the signaling of immunosuppressive cytokines, as IL-10. However, these therapeutic strategies are often not innocuous: while reducing the activity of cytokines as IL-10 is advantageous to hamper T cell dysfunction, it may also increase inflammation and culminate in tissue damage and pathology. Further, reversing T cell exhaustion with checkpoint blockade is important to reinvigorate T cells, but it may also increase the spawn of pathological T cells, which can contribute to immunopathology. Further studies are required to identify the benefits of using immunotherapy during leishmaniasis treatment.



### 3. The adipose tissue as a reservoir for *Leishmania* parasites

Several studies, including ours, have highlighted the importance of lipids during *Leishmania* infection, which suggests the adipose tissue as a privileged site for parasite protection. We have showed that *Leishmania* parasites are able to infect adipose tissue SVF (Chapter IV, Section 4), which includes a panoply of cells as preadipocytes, fibroblasts and immune cells. Although *Leishmania* parasites are known to primarily infect phagocytes, they can virtually infect any cell that possesses phagocytosis receptors. As such, although we expect adipose tissue macrophages to be the primary targets of *Leishmania*, whether other cells are infected remains to be addressed.

Another feature that may impact the capacity of the adipose tissue to harbor *Leishmania* parasites is the increased adiposity observed during malnutrition states, as overweight and obesity. This is particularly relevant when acknowledging that obesity is a worldwide problem and that the overall disease burden and associated co-morbidities are increasing exponentially. These malnutrition states are associated with reductions in immunity and increased susceptibility to infectious agents that take advantage of poor host fitness to thrive and provoke pathogenesis (Marcos et al., 2003; Morse and High, 2014). The limited available data estimates that obesity originates a 4.7-fold increased risk for infection (Serrano et al., 2010). Recent evidences have also highlighted that circulating nutrients acquired in the diet have a crucial role in determining immune cell function and behavior (Alwarawrah et al., 2018; Cohen et al., 2017; Smith, 2007), which suggests that changes in the host nutritional status greatly impact in the outcome of infections.

Adipose tissue expansion is generally accompanied by infiltration of immune cells, which changes the local and systemic inflammatory status of the host (Ferrante, 2013a). While macrophages generally represent around 5% of the cells in the adipose tissue, obesity may increase this number up to ~50% (Weisberg et al., 2003). Interestingly, it has been shown that ATMs accumulate around adipocytes in crown-like structures that ingest dying adipocytes and contribute to overall inflammation (Murano et al., 2008). Although several studies have highlighted the contribution of ATMs to insulin resistance and low-grade inflammation (Russo and Lumeng, 2018), a seminal study by Lumeng and colleagues showed the exclusive presence of a F4/80<sup>+</sup>CD11b<sup>+</sup>CD11c<sup>-</sup> population of ATMs in the adipose tissue of obese mice, which has been characterized as proinflammatory (Lumeng et al., 2007). These cells appear to be highly plastic and responsive to nutritional or local tissue cues (Li et al., 2010). Additionally,

F4/80<sup>+</sup>CD11b<sup>+</sup>CD11c<sup>+</sup> ATMs display higher accumulation of LDs, which are associated with lysosome biogenesis. On the contrary, F4/80<sup>+</sup>CD11b<sup>+</sup>CD11c<sup>-</sup> macrophages are thought to be resident cells, polarized into a M2-like phenotype (Xu et al., 2013). Considering the close contact with adipocytes and the privileged accessibility to lipids, it is possible to hypothesize that these macrophages may harbor and protect *Leishmania* parasites, while feeding them with lipids that are scavenged from dying adipocytes. In addition, it is expectable that these two populations will have distinct infection rates, as each subset displays different inflammatory and metabolic characteristics. This will greatly condition local tissue immunity, as more permissive cells may prevent *Leishmania* elimination by host microbicidal mechanisms. We may hypothesize that F4/80<sup>+</sup>CD11b<sup>+</sup>CD11c<sup>+</sup> ATMs are likely to display a higher infection burden, as they accumulate far more intracellular lipids, possibly due to increased adipocyte lipolysis. A recent work from Hill and colleagues identified a population of ATMs, characterized by CD9 expression that accumulated around dead adipocytes, in the designated crown-like structures. This population displayed high levels of intracellular lipids within vacuolar structures and expressed a highly proinflammatory transcriptome, thus indicating a strong contribution to obesity-related inflammation. Further, lipid-laden CD9<sup>+</sup> ATMs were equally found in visceral adipose tissue from human patients, with its presence correlating with body mass, which likely associates with the inflammatory signature from the obese adipose tissue (Hill et al., 2018).

We showed that HFD-fed mice displayed increased accumulation of cells in the spleen and white adipose tissue, as well as increased *L. donovani* burden in such organs, when compared to SFD-fed mice. Hypothetically, the increased cellularity in these organs may contribute directly to the increased burden, if considering that the number of myeloid cells (and therefore host cells) is increased in states of overweight/obesity. Also, a possible increase in T lymphocytes within these tissues does not necessarily translate into a more protective response, as their functions may be hindered by tissue-specific metabolic dysregulation. Consistently, previous studies have shown that diet-induced obesity induces myelopoiesis and lymphopoiesis (Singer et al., 2014; Trottier et al., 2012), which indicates that nutrition greatly influences hematopoietic output, replenishment of hematopoietic cells and, ultimately, tissue immunity. Indeed, alterations in the bone marrow niche and hematopoiesis are likely involved in parasite persistence, as several works demonstrated the impact of these pathways in *Leishmania* proliferation and survival (Abidin et al., 2017; Carvalho-Gontijo et al., 2018; Cotterell et al., 2000). Consequently, diet-induced overweight/obesity may actively impair the recruitment of immune cells to sites of inflammation and contribute to the

observed infection outcome. Additionally, the increased circulation of lipids in the serum and deposition in target tissues may contribute to susceptibility, as the parasites may easily access and scavenge host lipids.

Previous results from our group showed that amphotericin B, a first-line drug for VL, displays low efficacy in eliminating *L. infantum* from fat-laden macrophages as well as from the adipose tissue of overweight mice (Moreira *et al.*, in preparation). This may be attributed to a low penetration of this drug in lipid-rich tissues due to its pharmacokinetics properties, which suggests that the adipose tissue may serve as a reservoir for *Leishmania* parasites. As such, while lipids are thought to directly feed the parasites and further protect them from microbicidal mechanisms, another layer of complexity is added when understanding that fat accumulation may impact antileishmanial therapies. This is of great importance when acknowledging that the epidemics of obesity is quickly spreading around the world, as it will likely further complicate VL treatment in both developed and developing countries.

#### 4. Concluding remarks

In this work, we demonstrated the intricate relationship between metabolism and immunity during *Leishmania donovani* infection, as we approached different perspectives of host-pathogen interaction. We highlighted how basic science, which includes the study of cellular and metabolic processes that are altered upon infection, dynamically fuses with translational science, thus contributing to the further development of a rational and more directed therapy. By studying the metabolic network that is altered upon infection, we identified HIF-1 $\alpha$  as a resistance factor towards *L. donovani* infection. This underlines the importance of assessing genetic polymorphisms that may condition inter-individual response to therapy. Further, we also demonstrated that the absence of this factor in the myeloid compartment conditions adaptive immunity by contributing to T cell exhaustion. However, other factors may interfere with host response to the parasites, as IL-10 induction early after infection was shown to be detrimental and culminate in loss of multifunctional T cells and increased susceptibility to infection. Finally, we identified the adipose tissue as a central reservoir for *Leishmania* parasites, which poses a new challenge to therapeutics and VL cure.

## CHAPTER V FUTURE PERSPECTIVES

The fast-growing pace of scientific research and development in health sciences, particularly, in the emerging field of immunometabolism has contributed with new strategies to tackle and defeat infectious diseases. The knowledge on how metabolic pathways ignite cellular functions have merged with the understanding of what do immune cells require to perform optimal functions, giving rise to new therapeutic avenues. Nowadays, it is easier than ever to go from bench to bedside, which would not be possible without acknowledging and crosslinking basic and translational science. However, as this knowledge translates into the rise of new and innovative approaches, the need for personalized medicine also becomes clearer, thus bringing further challenges into therapeutics.

In this work, we showed that genetic deficiency of myeloid HIF-1 $\alpha$  originates systemic lipid dysregulation and consequent susceptibility to *L. donovani* infection, highlighting the role of this factor as a resistance hub towards leishmaniasis. Alongside, we have identified a loss-of-function SNP in the human *HIF1A* gene that similarly associates with higher susceptibility to *Leishmania donovani* infection. Considering the high prevalence of this polymorphism in regions that are endemic for VL, it is crucial to recognize the potential impact of such variations in individualized response to therapy. Additionally, cholesterol- and triglyceride-lowering therapies that aim at normalizing serum lipid parameters have the potential to be integrated in current VL treatment, as they retain low toxicity and may contribute to enhanced resistance towards infection. Indeed, cholesterol-lowering drugs as statins have been suggested as effective treatment options for different diseases, including leishmaniasis, and currently statins are the most prescribed drugs worldwide, mainly due to the absence of severe side effects and low toxicity. However, further studies that aim at elucidating the potential synergic or additive effect of such drugs in combination with currently available VL therapy are required.

The dawn of modern immunotherapy started with the appreciation that blocking immune checkpoint molecules would be useful in some cancers, as T cell reinvigoration appeared to be essential to promote tumor killing and rejection. Immunotherapy has recently been extended to other diseases, as checkpoint inhibitors proved to be of therapeutic value for inflammatory and infectious diseases. Herein, we showed that chronic *L. donovani* infection leads to T cell exhaustion in mHIF-1 $\alpha$ <sup>-/-</sup> mice, which is characterized by upregulation of inhibitory receptor TIM-3. Considering existing reports, it is expectable that TIM-3 blockade may pose an attractive immunotherapeutic approach, which aims at the reinvigoration of antileishmanial T cell responses. However, whether this is sufficient to promote sterile cure in the context of leishmaniasis, remains to be addressed.

Also, the influence of other checkpoint inhibitors as well as modulators of the immunosuppressive environment in parasitized tissues has not been studied in this context.

The global and continuously growing emergence of obesity, which is no longer restricted to developed countries, came to further complicate therapeutic options for infectious diseases. The adipose tissue is now considered as a *bona fide* immune organ, capable of harboring and protecting parasitic agents within its intricate network, as we have demonstrated. Our group has also observed therapeutic failure in *Leishmania*-infected overweighted mice treated with first-line agent amphotericin B, as parasites were eliminated at a lesser extent, when compared to normal weighted mice. Although the mechanistic explanations behind this remain elusive, a role for the adipose tissue as energy reservoir and protective hub against host microbiodical mechanisms has been suggested. This cluster of data shows that the therapeutic regimen for leishmaniasis treatment should be adjusted to individual body parameters, as increased adiposity and metabolic syndrome may condition response to therapy.

Overall, several questions remain as to how we may improve therapy response and efficacy for leishmaniasis treatment. Nonetheless, we have contributed to deepen the knowledge on how metabolism conditions immunity during infection and how we can (and should) take advantage of this to pave new lanes for leishmaniasis treatment.



## REFERENCES

- Abidin, B.M., Hammami, A., Stäger, S., and Heinonen, K.M. (2017). Infection-adapted emergency hematopoiesis promotes visceral leishmaniasis. *PLoS Pathog.*
- Aga, E., Katschinski, D.M., van Zandbergen, G., Laufs, H., Hansen, B., Müller, K., Solbach, W., and Laskay, T. (2002). Inhibition of the Spontaneous Apoptosis of Neutrophil Granulocytes by the Intracellular Parasite *Leishmania major*. *J. Immunol.*
- Akram, M. (2014). Citric Acid Cycle and Role of its Intermediates in Metabolism. *Cell Biochem. Biophys.* 68, 475–478.
- Alves-Ferreira, E.V.C., Ferreira, T.R., Walrad, P., Kaye, P.M., and Cruz, A.K. (2020). *Leishmania braziliensis* prostaglandin F2 $\alpha$  synthase impacts host infection. *Parasites and Vectors.*
- Alwarawrah, Y., Kiernan, K., and MacIver, N.J. (2018). Changes in nutritional status impact immune cell metabolism and function. *Front. Immunol.* 9.
- Arai, T., Tanaka, M., and Goda, N. (2018). HIF-1-dependent lipin1 induction prevents excessive lipid accumulation in choline-deficient diet-induced fatty liver. *Sci. Rep.*
- Araújo-Santos, T., Rodríguez, N.E., Moura-Pontes, S., Dixt, U.G., Abánades, D.R., Bozza, P.T., Wilson, M.E., and Borges, V.M. (2014). Role of prostaglandin F2 $\alpha$  production in lipid bodies from *Leishmania infantum chagasi*: Insights on virulence. *J. Infect. Dis.*
- Arenas, R., Torres-Guerrero, E., Quintanilla-Cedillo, M.R., and Ruiz-Esmenjaud, J. (2017). *Leishmaniasis: A review.* F1000Research.
- Ato, M., Stäger, S., Engwerda, C.R., and Kaye, P.M. (2002). Defective CCR7 expression on dendritic cells contributes to the development of visceral leishmaniasis. *Nat. Immunol.*
- Ato, M., Maroof, A., Zubairi, S., Nakano, H., Kakiuchi, T., and Kaye, P.M. (2006). Loss of Dendritic Cell Migration and Impaired Resistance to *Leishmania donovani* Infection in Mice Deficient in CCL19 and CCL21. *J. Immunol.*
- Azevedo, E.P., Rochaël, N.C., Guimarães-Costa, A.B., De Souza-Vieira, T.S., Ganilho, J., Saraiva, E.M., Palhano, F.L., and Foguel, D. (2015). A metabolic shift toward pentose phosphate pathway is necessary for amyloid fibril- and phorbol 12-myristate 13-Acetate-induced neutrophil extracellular trap (NET) formation. *J. Biol. Chem.*
- Bailey, A.P., Koster, G., Guillermier, C., Lechene, C.P., Postle, A.D., Gould Correspondence, A.P., Hirst, E.M.A., Macrae, J.I., and Gould, A.P. (2015a). Antioxidant Role for Lipid Droplets in a Stem



Cell Niche of *Drosophila*. *Cell* 163, 340–353.

Bailey, A.P., Koster, G., Guillermier, C., Hirst, E.M.A., MacRae, J.I., Lechene, C.P., Postle, A.D., and Gould, A.P. (2015b). Antioxidant Role for Lipid Droplets in a Stem Cell Niche of *Drosophila*. *Cell*.

Bakan, I., and Laplante, M. (2012). Connecting mTORC1 signaling to SREBP-1 activation. *Curr. Opin. Lipidol.*

Barroso, D.H., Falcão, S.D.A.C., da Motta, J. de O.C., dos Santos, L.S., Takano, G.H.S., Gomes, C.M., Fiuza Favali, C.B., Lima, B.D. de, and Ribeiro Sampaio, R.N. (2018). PD-L1 May Mediate T-Cell Exhaustion in a Case of Early Diffuse Leishmaniasis Caused by *Leishmania* (*L.*) *amazonensis*. *Front. Immunol.*

Belkaid, Y., Mendez, S., Lira, R., Kadambi, N., Milon, G., and Sacks, D. (2000). A Natural Model of *Leishmania major* Infection Reveals a Prolonged “Silent” Phase of Parasite Amplification in the Skin Before the Onset of Lesion Formation and Immunity. *J. Immunol.*

Belkaid, Y., Hoffmann, K.F., Mendez, S., Kamhawi, S., Udey, M.C., Wynn, T.A., and Sacks, D.L. (2001). The Role of Interleukin (IL)-10 in the Persistence of *Leishmania major* in the Skin after Healing and the Therapeutic Potential of Anti-IL-10 Receptor Antibody for Sterile Cure. *J. Exp. Med.* 194, 1497–1506.

Belkaid, Y., Piccirillo, C.A., Mendez, S., Shevach, E.M., and Sacks, D.L. (2002). CD4+CD25+ regulatory T cells control *Leishmania major* persistence and immunity. *Nature*.

Bensch, B., Johnson, A.L., Kurachi, M., Odorizzi, P.M., Pauken, K.E., Attanasio, J., Stelekati, E., McLane, L.M., Paley, M.A., Delgoffe, G.M., et al. (2016). Bioenergetic Insufficiencies Due to Metabolic Alterations Regulated by the Inhibitory Receptor PD-1 Are an Early Driver of CD8+ T Cell Exhaustion. *Immunity*.

Bensaad, K., Favaro, E., Lewis, C.A., Peck, B., Lord, S., Collins, J.M., Pinnick, K.E., Wigfield, S., Buffa, F.M., Li, J.L., et al. (2014). Fatty acid uptake and lipid storage induced by HIF-1 $\alpha$  contribute to cell growth and survival after hypoxia-reoxygenation. *Cell Rep.*

Berg, J.M., Tymoczko, J.L., and Stryer, L. (2002). The Metabolism of Glucose 6-Phosphate by the Pentose Phosphate Pathway Is Coordinated with Glycolysis. In *Biochemistry*, p.

Bhattacharjee, A., Majumder, S., Das, S., Ghosh, S., Biswas, S., and Majumdar, S. (2016).

*Leishmania donovani*-induced prostaglandin E2 generation is critically dependent on host Toll-like receptor 2-cytosolic phospholipase A2 signaling. *Infect. Immun.*

Borregaard, N., and Herlin, T. (1982). Energy metabolism of human neutrophils during

phagocytosis. *J. Clin. Invest.*

Van den Bossche, J., Baardman, J., Otto, N.A., van der Velden, S., Neele, A.E., van den Berg, S.M., Luque-Martin, R., Chen, H.J., Boshuizen, M.C.S., Ahmed, M., et al. (2016). Mitochondrial Dysfunction Prevents Repolarization of Inflammatory Macrophages. *Cell Rep.*

Bouazizi-Ben Messaoud, H., Guichard, M., Lawton, P., Delton, I., and Azzouz-Maache, S. (2017). Changes in Lipid and Fatty Acid Composition During Intramacrophagic Transformation of *Leishmania donovani* Complex Promastigotes into Amastigotes. *Lipids.*

Bozza, P.T., Bakker-Abreu, I., Navarro-Xavier, R.A., and Bandeira-Melo, C. (2011). Lipid body function in eicosanoid synthesis: An update. *Prostaglandins Leukot. Essent. Fat. Acids.*

Bronte, V., and Zanovello, P. (2005). Regulation of immune responses by L-arginine metabolism. *Nat. Rev. Immunol.* 5, 641–654.

Brooks, D.G., Ha, S.J., Elsaesser, H., Sharpe, A.H., Freeman, G.J., and Oldstone, M.B.A. (2008). IL-10 and PD-L1 operate through distinct pathways to suppress T-cell activity during persistent viral infection. *Proc. Natl. Acad. Sci. U. S. A.*

Brown, D.M., Lee, S., Garcia-Hernandez, M. d. I. L., and Swain, S.L. (2012). Multifunctional CD4 Cells Expressing Gamma Interferon and Perforin Mediate Protection against Lethal Influenza Virus Infection. *J. Virol.*

Brugarolas, J., Lei, K., Hurley, R.L., Manning, B.D., Reiling, J.H., Hafen, E., Witters, L.A., Ellisen, L.W., and Kaelin, W.G. (2004). Regulation of mTOR function in response to hypoxia by REDD1 and the TSC1/TSC2 tumor suppressor complex. *Genes Dev.*

Brunton, J., Steele, S., Ziehr, B., Moorman, N., and Kawula, T. (2013). Feeding Uninvited Guests: MTOR and AMPK Set the Table for Intracellular Pathogens. *PLoS Pathog.*

Burza, S., Croft, S.L., and Boelaert, M. (2018). Leishmaniasis. *Lancet* 392, 951–970.

Cabrera, M., Shaw, M.A., Sharpies, C., Williams, H., Castes, M., Convit, J., and Blackwell, J.M. (1995). Polymorphism in tumor necrosis factor genes associated with mucocutaneous leishmaniasis. *J. Exp. Med.*

Caccamo, N., Guggino, G., Joosten, S.A., Gelsomino, G., Di Carlo, P., Titone, L., Galati, D., Bocchino, M., Matarese, A., Salerno, A., et al. (2010). Multifunctional CD4+ T cells correlate with active *Mycobacterium tuberculosis* infection. *Eur. J. Immunol.*

Cao, W., Ramakrishnan, R., Tuyrin, V.A., Veglia, F., Condamine, T., Amoscato, A., Mohammadyani, D., Johnson, J.J., Min Zhang, L., Klein-Seetharaman, J., et al. (2014). Oxidized Lipids Block Antigen Cross-Presentation by Dendritic Cells in Cancer. *J. Immunol.* 192, 2920–

2931.

Caradonna, K.L., Engel, J.C., Jacobi, D., Lee, C.H., and Burleigh, B.A. (2013). Host metabolism regulates intracellular growth of *trypanosoma cruzi*. *Cell Host Microbe* *13*, 108–117.

Carling, D., Zammit, V.A., and Hardie, D.G. (1987). A common bicyclic protein kinase cascade inactivates the regulatory enzymes of fatty acid and cholesterol biosynthesis. *FEBS Lett.*

Carrera, L., Gazzinelli, R.T., Badolato, R., Hieny, S., Müller, W., Kühn, R., and Sacks, D.L. (1996). *Leishmania promastigotes* selectively inhibit interleukin 12 induction in bone marrow-derived macrophages from susceptible and resistant mice. *J. Exp. Med.*

Carvalho-Gontijo, R., Moreira, D.R., Resende, M., Costa-Silva, M.F., Peruhype-Magalhães, V., Ribeiro, C.M.F., Ribeiro, D.D., Silvestre, R., Cordeiro-da-Silva, A., Martins-Filho, O.A., et al. (2018). Infection of hematopoietic stem cells by *Leishmania infantum* increases erythropoiesis and alters the phenotypic and functional profiles of progeny. *Cell. Immunol.*

Castellano, L.R., Filho, D.C., Argiro, L., Dessen, H., Prata, A., Dessen, A., and Rodrigues, V. (2009). Th1/Th2 immune responses are associated with active cutaneous leishmaniasis and clinical cure is associated with strong interferon- $\gamma$  production. *Hum. Immunol.* *70*, 383–390.

Castellucci, L., Menezes, E., Oliveira, J., Magalhães, A., Guimarães, L.H., Lessa, M., Ribeiro, S., Reale, J., Noronha, E.F., Wilson, M.E., et al. (2006). IL6 -174 G/C Promoter Polymorphism Influences Susceptibility to Mucosal but Not Localized Cutaneous Leishmaniasis in Brazil. *J. Infect. Dis.*

Chakraborty, D., Banerjee, S., Sen, A., Banerjee, K.K., Das, P., and Roy, S. (2005). *Leishmania donovani* Affects Antigen Presentation of Macrophage by Disrupting Lipid Rafts. *J. Immunol.*

Chaparro, V., Leroux, L.P., Zimmermann, A., Jardim, A., Johnston, B., Descoteaux, A., and Jaramillo, M. (2019). *Leishmania donovani* lipophosphoglycan increases Macrophage-Dependent chemotaxis of CXCR6-Expressing cells via CXCL16 induction. *Infect. Immun.*

Cheng, S.C., Quintin, J., Cramer, R.A., Shephardson, K.M., Saeed, S., Kumar, V., Giamarellos-Bourboulis, E.J., Martens, J.H.A., Rao, N.A., Aghajani-Refah, A., et al. (2014). mTOR- and HIF-1 $\alpha$ -mediated aerobic glycolysis as metabolic basis for trained immunity. *Science* (80- ).

Cohen, S., Danzaki, K., and MacIver, N.J. (2017). Nutritional effects on T-cell immunometabolism. *Eur. J. Immunol.* *47*, 225–235.

Conrad, S.M., Strauss-Ayali, D., Field, A.E., Mack, M., and Mosser, D.M. (2007). *Leishmania*-derived murine monocyte chemoattractant protein 1 enhances the recruitment of a restrictive population of CC chemokine receptor 2-positive macrophages. *Infect. Immun.*

Contreras, I., Estrada, J.A., Guak, H., Martel, C., Borjian, A., Ralph, B., Shio, M.T., Fournier, S., Krawczyk, C.M., and Olivier, M. (2014). Impact of *Leishmania mexicana* Infection on Dendritic Cell Signaling and Functions. *PLoS Negl. Trop. Dis.*

Cotterell, S.E.J., Engwerda, C.R., and Kaye, P.M. (2000). Enhanced hematopoietic activity accompanies parasite expansion in the spleen and bone marrow of mice infected with *Leishmania donovani*. *Infect. Immun.* *68*, 1840–1848.

Cox, A.R., Chernis, N., Masschelin, P.M., and Hartig, S.M. (2019). Immune Cells Gate White Adipose Tissue Expansion. *Endocrinology*.

Cramer, T., Yamanishi, Y., Clausen, B.E., Förster, I., Pawlinski, R., Mackman, N., Haase, V.H., Jaenisch, R., Corr, M., Nizet, V., et al. (2003). HIF-1 $\alpha$  is essential for myeloid cell-mediated inflammation. *Cell* *112*, 645–657.

Cubillos-Ruiz, J.R., Silberman, P.C., Rutkowski, M.R., Chopra, S., Perales-Puchalt, A., Song, M., Zhang, S., Bettigole, S.E., Gupta, D., Holcomb, K., et al. (2015). ER Stress Sensor XBP1 Controls Anti-tumor Immunity by Disrupting Dendritic Cell Homeostasis. *Cell*.

Cunningham, A.C. (2002). Parasitic adaptive mechanisms in infection by *Leishmania*. *Exp. Mol. Pathol.*

Damo, M., and Joshi, N.S. (2019). Treg cell IL-10 and IL-35 exhaust CD8<sup>+</sup> T cells in tumors. *Nat. Immunol.* *20*, 674–675.

Dantas-Torres, F., Lainson, R., and Rangel, E.F. (2006). *Leishmania infantum* versus *Leishmania chagasi*: Do not forget the law of priority. *Mem. Inst. Oswaldo Cruz*.

Darrah, P.A., Patel, D.T., De Luca, P.M., Lindsay, R.W.B., Davey, D.F., Flynn, B.J., Hoff, S.T., Andersen, P., Reed, S.G., Morris, S.L., et al. (2007a). Multifunctional TH1 cells define a correlate of vaccine-mediated protection against *Leishmania major*. *Nat. Med.* *13*, 843–850.

Darrah, P.A., Patel, D.T., De Luca, P.M., Lindsay, R.W.B., Davey, D.F., Flynn, B.J., Hoff, S.T., Andersen, P., Reed, S.G., Morris, S.L., et al. (2007b). Multifunctional TH1 cells define a correlate of vaccine-mediated protection against *Leishmania major*. *Nat. Med.*

Darrah, P.A., Hegde, S.T., Patel, D.T., Lindsay, R.W.B., Chen, L., Roederer, M., and Seder, R.A. (2010). IL-10 production differentially influences the magnitude, quality, and protective capacity of Th1 responses depending on the vaccine platform. *J. Exp. Med.*

Day, C.L., Kaufmann, D.E., Kiepiela, P., Brown, J.A., Moodley, E.S., Reddy, S., Mackey, E.W., Miller, J.D., Leslie, A.J., DePierres, C., et al. (2006). PD-1 expression on HIV-specific T cells is associated with T-cell exhaustion and disease progression. *Nature*.

Dodd, K.M., Yang, J., Shen, M.H., Sampson, J.R., and Tee, A.R. (2015). mTORC1 drives HIF-1 $\alpha$  and VEGF-A signalling via multiple mechanisms involving 4E-BP1, S6K1 and STAT3. *Oncogene*.

Du, W., Zhang, L., Brett-Morris, A., Aguila, B., Kerner, J., Hoppel, C.L., Puchowicz, M., Serra, D., Herrero, L., Rini, B.I., et al. (2017). HIF drives lipid deposition and cancer in ccRCC via repression of fatty acid metabolism. *Nat. Commun.* 8.

Eisinger, K., Liebisch, G., Schmitz, G., Aslanidis, C., Krautbauer, S., and Buechler, C. (2014). Lipidomic analysis of serum from high fat diet induced obese mice. *Int. J. Mol. Sci.*

Esch, K.J., Juelsgaard, R., Martinez, P.A., Jones, D.E., and Petersen, C.A. (2013). Programmed Death 1–Mediated T Cell Exhaustion during Visceral Leishmaniasis Impairs Phagocyte Function. *J. Immunol.*

Fakiola, M., Strange, A., Cordell, H.J., Miller, E.N., Pirinen, M., Su, Z., Mishra, A., Mehrotra, S., Monteiro, G.R., Band, G., et al. (2013). Common variants in the HLA-DRB1-HLA-DQA1 HLA class II region are associated with susceptibility to visceral leishmaniasis. *Nat. Genet.*

Federico, A., D’Aiuto, E., Borriello, F., Barra, G., Gravina, A.G., Romano, M., and de Palma, R. (2010). Fat: A matter of disturbance for the immune system. *World J. Gastroenterol.* 16, 4762–4772.

Ferrante, A.W. (2013a). The immune cells in adipose tissue. *Diabetes, Obes. Metab.* 15, 34–38.

Ferrante, A.W. (2013b). Macrophages, fat, and the emergence of immunometabolism. *J. Clin. Invest.* 123, 4992–4993.

da Fonseca-Martins, A.M., Ramos, T.D., Pratti, J.E.S., Firmino-Cruz, L., Gomes, D.C.O., Soong, L., Saraiva, E.M., and de Matos Guedes, H.L. (2019). Immunotherapy using anti-PD-1 and anti-PD-L1 in *Leishmania amazonensis*-infected BALB/c mice reduce parasite load. *Sci. Rep.* 9, 20275.

Fuller, M.J., and Zajac, A.J. (2003). Ablation of CD8 and CD4 T Cell Responses by High Viral Loads. *J. Immunol.*

Furuta, E., Pai, S.K., Zhan, R., Bandyopadhyay, S., Watabe, M., Mo, Y.Y., Hirota, S., Hosobe, S., Tsukada, T., Miura, K., et al. (2008). Fatty acid synthase gene is up-regulated by hypoxia via activation of Akt and sterol regulatory element binding protein-1. *Cancer Res.*

Galanis, A., Pappa, A., Giannakakis, A., Lanitis, E., Dangaj, D., and Sandaltzopoulos, R. (2008). Reactive oxygen species and HIF-1 signalling in cancer. *Cancer Lett.*

Gallimore, A., Glithero, A., Godkin, A., Tissot, A.C., Plückthun, A., Elliott, T., Hengartner, H., and Zinkernagel, R. (1998). Induction and exhaustion of lymphocytic choriomeningitis virus-specific

cytotoxic T lymphocytes visualized using soluble tetrameric major histocompatibility complex class I-peptide complexes. *J. Exp. Med.*

Garcia, D., and Shaw, R.J. (2017). AMPK: Mechanisms of Cellular Energy Sensing and Restoration of Metabolic Balance. *Mol. Cell.*

Gautam, S., Kumar, R., Singh, N., Singh, A.K., Rai, M., Sacks, D., Sundar, S., and Nylén, S. (2014). CD8 T cell exhaustion in human visceral leishmaniasis. *J. Infect. Dis.*

Geiger, R., Rieckmann, J.C., Wolf, T., Basso, C., Feng, Y., Fuhrer, T., Kogadeeva, M., Picotti, P., Meissner, F., Mann, M., et al. (2016). L-Arginine Modulates T Cell Metabolism and Enhances Survival and Anti-tumor Activity. *Cell.*

Ghalib, H.W., Piuvezam, M.R., Skeiky, Y.A.W., Siddig, M., Hashim, F.A., El-Hassan, A.M., Russo, D.M., and Reed, S.G. (1993). Interleukin 10 production correlates with pathology in human *Leishmania donovani* infections. *J. Clin. Invest.* 92, 324–329.

Ghosh, J., Das, S., Guha, R., Ghosh, D., Naskar, K., Das, A., and Roy, S. (2012). Hyperlipidemia offers protection against *Leishmania donovani* infection: Role of membrane cholesterol. *J. Lipid Res.*

Ghosh, J., Bose, M., Roy, S., and Bhattacharyya, S.N. (2013). *Leishmania donovani* targets *dicer1* to downregulate miR-122, lower serum cholesterol, and facilitate murine liver infection. *Cell Host Microbe.*

Ghosh, M., Roy, K., Das Mukherjee, D., Chakrabarti, G., Roy Choudhury, K., and Roy, S. (2014). *Leishmania donovani* Infection Enhances Lateral Mobility of Macrophage Membrane Protein Which Is Reversed by Liposomal Cholesterol. *PLoS Negl. Trop. Dis.*

Gimm, T., Wiese, M., Teschemacher, B., Deggerich, A., Schödel, J., Knaup, K.X., Hackenbeck, T., Hellerbrand, C., Amann, K., Wiesener, M.S., et al. (2010). Hypoxia-inducible protein 2 is a novel lipid droplet protein and a specific target gene of hypoxia-inducible factor-1. *FASEB J.*

Ginger, M.L. (2006). Niche metabolism in parasitic protozoa. *Philos. Trans. R. Soc. B Biol. Sci.*

Golden-Mason, L., Palmer, B.E., Kassam, N., Townshend-Bulson, L., Livingston, S., McMahon, B.J., Castelblanco, N., Kuchroo, V., Gretch, D.R., and Rosen, H.R. (2009). Negative Immune Regulator Tim-3 Is Overexpressed on T Cells in Hepatitis C Virus Infection and Its Blockade Rescues Dysfunctional CD4+ and CD8+ T Cells. *J. Virol.*

Grant, R.W., and Dixit, V.D. (2015). Adipose tissue as an immunological organ. *Obesity* 23, 512–518.

Griess, B., Mir, S., Datta, K., and Teoh-Fitzgerald, M. (2020). Scavenging reactive oxygen species

selectively inhibits M2 macrophage polarization and their pro-tumorigenic function in part, via Stat3 suppression. *Free Radic. Biol. Med.*

Guak, H., Al Habyan, S., Ma, E.H., Aldossary, H., Al-Masri, M., Won, S.Y., Ying, T., Fixman, E.D., Jones, R.G., McCaffrey, L.M., et al. (2018). Glycolytic metabolism is essential for CCR7 oligomerization and dendritic cell migration. *Nat. Commun.*

Guo, X., Li, D., Chen, Y., An, J., Wang, K., Xu, Z., Chen, Z., and Xing, J. (2015). SNP rs2057482 in HIF1A gene predicts clinical outcome of aggressive hepatocellular carcinoma patients after surgery. *Sci. Rep.* 5.

Gwinn, D.M., Shackelford, D.B., Egan, D.F., Mihaylova, M.M., Mery, A., Vasquez, D.S., Turk, B.E., and Shaw, R.J. (2008). AMPK Phosphorylation of Raptor Mediates a Metabolic Checkpoint. *Mol. Cell.*

Habib, S., El Andaloussi, A., Elmasry, K., Handoussa, A., Azab, M., Elsayey, A., Al-Hendy, A., and Ismail, N. (2018). PDL-1 blockade prevents T cell exhaustion, inhibits autophagy, and promotes clearance of *Leishmania donovani*. *Infect. Immun.*

Hall, L.R., and Titus, R.G. (1995). Sand fly vector saliva selectively modulates macrophage functions that inhibit killing of *Leishmania major* and nitric oxide production. *J. Immunol.*

Hamers, A.A.J., and Pillai, A.B. (2018). A sweet alternative: maintaining M2 macrophage polarization. *Sci. Immunol.*

Han, S.-J., Zaretsky, A., Andrade-Oliveira, V., Brenchley, J., Brodsky, I., and Belkaid, Y. (2017). White Adipose Tissue Is a Reservoir for Memory T Cells and Promotes Protective Memory Responses to Infection. *Immunity* 47, 1154–1168.

Harada, H., Itasaka, S., Kizaka-Kondoh, S., Shibuya, K., Morinibu, A., Shinomiya, K., and Hiraoka, M. (2009). The Akt/mTOR Pathway Assures the Synthesis of HIF-1 $\alpha$  Protein in a Glucose- and Reoxygenation-dependent Manner in Irradiated Tumors. *J. Biol. Chem.* 284, 5332–5342.

Hardie, D.G., and Pan, D. a (2002). Regulation of fatty acid synthesis and oxidation by the AMP-activated protein kinase. *Biochem. Soc. Trans.* 30, 1064–1070.

Hawley, S.A., Pan, D.A., Mustard, K.J., Ross, L., Bain, J., Edelman, A.M., Frenguelli, B.G., and Hardie, D.G. (2005). Calmodulin-dependent protein kinase kinase- $\beta$  is an alternative upstream kinase for AMP-activated protein kinase. *Cell Metab.*

He, L., Gomes, A.P., Wang, X., Yoon, S.O., Lee, G., Nagiec, M.J., Cho, S., Chavez, A., Islam, T., Yu, Y., et al. (2018). mTORC1 Promotes Metabolic Reprogramming by the Suppression of GSK3-

Dependent Foxk1 Phosphorylation. *Mol. Cell*.

Hefnawy, A., Berg, M., Dujardin, J.C., and De Muylder, G. (2017). Exploiting Knowledge on Leishmania Drug Resistance to Support the Quest for New Drugs. *Trends Parasitol.*

Heinzel, F.P., Sadick, M.D., Holaday, B.J., Coffman, R.L., and Locksley, R.M. (1989). Reciprocal expression of interferon  $\gamma$  or interleukin 4 during the resolution or progression of murine leishmaniasis. Evidence for expansion of distinct helper T cell subsets. *J. Exp. Med.*

Helft, J., Böttcher, J., Chakravarty, P., Zelenay, S., Huotari, J., Schraml, B.U., Goubau, D., and Reis e Sousa, C. (2015). GM-CSF Mouse Bone Marrow Cultures Comprise a Heterogeneous Population of CD11c+MHCII+ Macrophages and Dendritic Cells. *Immunity*.

Herber, D.L., Cao, W., Nefedova, Y., Novitskiy, S. V., Nagaraj, S., Tyurin, V.A., Corzo, A., Cho, H.I., Celis, E., Lennox, B., et al. (2010). Lipid accumulation and dendritic cell dysfunction in cancer. *Nat. Med.*

de Heredia, F.P., Gómez-Martínez, S., and Marcos, A. (2012). Obesity, inflammation and the immune system. *Proc. Nutr. Soc.* *71*, 332–338.

Hill, D.A., Lim, H.W., Kim, Y.H., Ho, W.Y., Foong, Y.H., Nelson, V.L., Nguyen, H.C.B., Chegireddy, K., Kim, J., Habbertheuer, A., et al. (2018). Distinct macrophage populations direct inflammatory versus physiological changes in adipose tissue. *Proc. Natl. Acad. Sci. U. S. A.*

Houten, S.M., and Wanders, R.J.A. (2010). A general introduction to the biochemistry of mitochondrial fatty acid  $\beta$ -oxidation. *J. Inherited Metab. Dis.* *33*, 469–477.

Ibarra-Meneses, A. V., Sanchez, C., Alvar, J., Moreno, J., and Carrillo, E. (2017). Monocyte chemotactic protein 1 in plasma from soluble Leishmania antigen-stimulated whole blood as a potential biomarker of the cellular immune response to Leishmania infantum. *Front. Immunol.*

Ibrahim, J., Nguyen, A.H., Rehman, A., Ochi, A., Jamal, M., Graffeo, C.S., Henning, J.R., Zambirinis, C.P., Fallon, N.C., Barilla, R., et al. (2012). Dendritic cell populations with different concentrations of lipid regulate tolerance and immunity in mouse and human liver. *Gastroenterology*.

Inoki, K., Zhu, T., and Guan, K.L. (2003). TSC2 Mediates Cellular Energy Response to Control Cell Growth and Survival. *Cell*.

Jantsch, J., Chakravorty, D., Turza, N., Prechtel, A.T., Buchholz, B., Gerlach, R.G., Volke, M., Gläsner, J., Warnecke, C., Wiesener, M.S., et al. (2008). Hypoxia and Hypoxia-Inducible Factor-1 $\alpha$  Modulate Lipopolysaccharide-Induced Dendritic Cell Activation and Function. *J. Immunol.*

Jaramillo, M., Gomez, M.A., Larsson, O., Shio, M.T., Topisirovic, I., Contreras, I., Luxenburg, R.,



Rosenfeld, A., Colina, R., McMaster, R.W., et al. (2011). Leishmania repression of host translation through mTOR cleavage is required for parasite survival and infection. *Cell Host Microbe*.

Jayaraman, P., Jacques, M.K., Zhu, C., Steblenko, K.M., Stowell, B.L., Madi, A., Anderson, A.C., Kuchroo, V.K., and Behar, S.M. (2016). TIM3 Mediates T Cell Exhaustion during Mycobacterium tuberculosis Infection. *PLoS Pathog*.

Ju, Y., Hou, N., Zhang, X., Zhao, D., Liu, Y., Wang, J., Luan, F., Shi, W., Zhu, F., Sun, W., et al. (2009). Blockade of tim-3 pathway ameliorates interferon- $\gamma$  production from hepatic cd8<sup>+</sup> T cells in a mouse model of hepatitis B virus infection. *Cell. Mol. Immunol*.

Jung, S.N., Yang, W.K., Kim, J., Kim, H.S., Kim, E.J., Yun, H., Park, H., Kim, S.S., Choe, W., Kang, I., et al. (2008). Reactive oxygen species stabilize hypoxia-inducible factor-1 alpha protein and stimulate transcriptional activity via AMP-activated protein kinase in DU145 human prostate cancer cells. *Carcinogenesis*.

Karlsson, E.A., Sheridan, P.A., and Beck, M.A. (2010). Diet-Induced Obesity Impairs the T Cell Memory Response to Influenza Virus Infection. *J. Immunol.* *184*, 3127–3133.

Karp, C.L., El-Safi, S.H., Wynn, T.A., Satti, M.M.H., Kordofani, A.M., Hashim, F.A., Hag-Ali, M., Neva, F.A., Nutman, T.B., and Sacks, D.L. (1993). In vivo cytokine profiles in patients with kala-azar. Marked elevation of both interleukin-10 and interferon-gamma. *J. Clin. Invest.*

Kaveh, D.A., Whelan, A.O., and Hogarth, P.J. (2012). The duration of antigen-stimulation significantly alters the diversity of multifunctional CD4 T cells measured by intracellular cytokine staining. *PLoS One*.

KEMP, M., HEY, A.S., KURTZHALS, J.A.L., RISTENSEN, C.B.V.C., GAAFAR, A., MUSTAFA, M.D., KORDOFANI, A.A.Y., ISMAIL, A., KHARAZMI, A., and THEANDER, T.G. (2008). Dichotomy of the human T cell response to Leishmania antigens. I. Th1-like response to Leishmania major promastigote antigens in individuals recovered from cutaneous leishmaniasis. *Clin. Exp. Immunol*.

Khadir, F., Shaler, C.R., Oryan, A., Rudak, P.T., Mazzuca, D.M., Taheri, T., Dikeakos, J.D., Haeryfar, S.M.M., and Rafati, S. (2018). Therapeutic control of leishmaniasis by inhibitors of the mammalian target of rapamycin. *PLoS Negl. Trop. Dis.*

Kim, J.W., Tchernyshyov, I., Semenza, G.L., and Dang, C. V. (2006). HIF-1-mediated expression of pyruvate dehydrogenase kinase: A metabolic switch required for cellular adaptation to hypoxia. *Cell Metab.*

Kim, S.-J., Tang, T., Abbott, M., Viscarra, J.A., Wang, Y., and Sul, H.S. (2016). AMPK Phosphorylates Desnutrin/ATGL and Hormone-Sensitive Lipase To Regulate Lipolysis and Fatty Acid Oxidation within Adipose Tissue. *Mol. Cell. Biol.*

Kloehn, J., Saunders, E.C., O'Callaghan, S., Dagley, M.J., and McConville, M.J. (2015). Characterization of Metabolically Quiescent Leishmania Parasites in Murine Lesions Using Heavy Water Labeling. *PLoS Pathog.*

Knobloch, M., Pilz, G.A., Ghesquière, B., Kovacs, W.J., Wegleiter, T., Moore, D.L., Hruzova, M., Zamboni, N., Carmeliet, P., and Jessberger, S. (2017). A Fatty Acid Oxidation-Dependent Metabolic Shift Regulates Adult Neural Stem Cell Activity. *Cell Rep.* 20, 2144–2155.

Ko, H.H.T., Lareu, R.R., Dix, B.R., and Hughes, J.D. (2018). In vitro antibacterial effects of statins against bacterial pathogens causing skin infections. *Eur. J. Clin. Microbiol. Infect. Dis.*

Kone, A.K., Niaré, D.S., Piarroux, M., Izri, A., Marty, P., Laurens, M.B., Piarroux, R., Thera, M.A., and Doumbo, O.K. (2019). Visceral Leishmaniasis in West Africa: Clinical Characteristics, Vectors, and Reservoirs. *J. Parasitol. Res.*

Kornberg, H. (2000). Krebs and his trinity of cycles. *Nat. Rev. Mol. Cell Biol.* 1, 225–228.

Krawczyk, C.M., Holowka, T., Sun, J., Blagih, J., Amiel, E., DeBerardinis, R.J., Cross, J.R., Jung, E., Thompson, C.B., Jones, R.G., et al. (2010). Toll-like receptor-induced changes in glycolytic metabolism regulate dendritic cell activation. *Blood.*

Kumar, A., Das, S., Mandal, A., Verma, S., Abhishek, K., Kumar, A., Kumar, V., Ghosh, A.K., and Das, P. (2018). Leishmania infection activates host mTOR for its survival by M2 macrophage polarization. *Parasite Immunol.*

Kumar, G.A., Roy, S., Jafurulla, M., Mandal, C., and Chattopadhyay, A. (2016). Statin-induced chronic cholesterol depletion inhibits Leishmania donovani infection: Relevance of optimum host membrane cholesterol. *Biochim. Biophys. Acta - Biomembr.*

Kumari, M., Heeren, J., and Scheja, L. (2018). Regulation of immunometabolism in adipose tissue. *Semin. Immunopathol.* 40, 189–202.

Lacey, D.C., Achuthan, A., Fleetwood, A.J., Dinh, H., Roiniotis, J., Scholz, G.M., Chang, M.W., Beckman, S.K., Cook, A.D., and Hamilton, J.A. (2012). Defining GM-CSF- and Macrophage-CSF-Dependent Macrophage Responses by In Vitro Models. *J. Immunol.*

Lal, C.S., Verma, N., Rabidas, V.N., Ranjan, A., Pandey, K., Verma, R.B., Singh, D., Kumar, S., and Das, P. (2010). Total serum cholesterol determination can provide understanding of parasite burden in patients with visceral leishmaniasis infection. *Clin. Chim. Acta.*

Land, S.C., and Tee, A.R. (2007). Hypoxia-inducible factor 1 $\alpha$  is regulated by the mammalian target of rapamycin (mTOR) via an mTOR signaling motif. *J. Biol. Chem.*

Lane, A.N., and Fan, T.W.M. (2015). Regulation of mammalian nucleotide metabolism and biosynthesis. *Nucleic Acids Res.* *43*, 2466–2485.

Laplante, M., and Sabatini, D.M. (2009). mTOR signaling at a glance. *J. Cell Sci.*

Laskay, T., Van Zandbergen, G., and Solbach, W. (2003). Neutrophil granulocytes - Trojan horses for *Leishmania major* and other intracellular microbes? *Trends Microbiol.*

Lee, J., Ellis, J.M., and Wolfgang, M.J. (2015). Adipose fatty acid oxidation is required for thermogenesis and potentiates oxidative stress-induced inflammation. *Cell Rep.* *10*, 266–279.

Lestinova, T., Rohousova, I., Sima, M., de Oliveira, C.I., and Volf, P. (2017). Insights into the sand fly saliva: Blood-feeding and immune interactions between sand flies, hosts, and *Leishmania*. *PLoS Negl. Trop. Dis.*

Lewinsohn, D.A., Lewinsohn, D.M., and Scriba, T.J. (2017). Polyfunctional CD4<sup>+</sup> T cells as targets for tuberculosis vaccination. *Front. Immunol.*

Li, P., Yin, Y.-L., Li, D., Woo Kim, S., and Wu, G. (2007). Amino acids and immune function. *Br. J. Nutr.* *98*, 237–252.

Li, P., Lu, M., Nguyen, M.T.A., Bae, E.J., Chapman, J., Feng, D., Hawkins, M., Pessin, J.E., Sears, D.D., Nguyen, A.K., et al. (2010). Functional heterogeneity of CD11c-positive adipose tissue macrophages in diet-induced obese mice. *J. Biol. Chem.*

Li, Z.H., Ramakrishnan, S., Striepen, B., and Moreno, S.N.J. (2013). *Toxoplasma gondii* Relies on Both Host and Parasite Isoprenoids and Can Be Rendered Sensitive to Atorvastatin. *PLoS Pathog.*

Liberopoulos, E., Alexandridis, G., Bairaktari, E., and Elisaf, M. (2002). Severe hypocholesterolemia with reduced serum Lipoprotein(a) in a patient with visceral leishmaniasis. *Ann. Clin. Lab. Sci.*

Libisch, M.G., Faral-Tello, P., Garg, N.J., Radi, R., Piacenza, L., and Robello, C. (2018). Early *Trypanosoma cruzi* infection triggers mTORC1-mediated respiration increase and mitochondrial biogenesis in human primary cardiomyocytes. *Front. Microbiol.*

Lim, A.R., Rathmell, W.K., and Rathmell, J.C. (2020). The tumor microenvironment as a metabolic barrier to effector T cells and immunotherapy. *Elife* *9*.

Liu, Y., Ma, Z., Zhao, C., Wang, Y., Wu, G., Xiao, J., McClain, C.J., Li, X., and Feng, W. (2014). HIF-1 $\alpha$  and HIF-2 $\alpha$  are critically involved in hypoxia-induced lipid accumulation in hepatocytes

through reducing PGC-1 $\alpha$ -mediated fatty acid  $\beta$ -oxidation. *Toxicol. Lett.* *226*, 117–123.

Lodge, R., Diallo, T.O., and Descoteaux, A. (2006). *Leishmania donovani* lipophosphoglycan blocks NADPH oxidase assembly at the phagosome membrane. *Cell. Microbiol.*

Louzir, H., Melby, P.C., Salah, A.B., Marrakchi, H., Aoun, K., Ismail, R.B., and Dellagi, K. (1998). Immunologic Determinants of Disease Evolution in Localized Cutaneous Leishmaniasis due to *Leishmania major*. *J. Infect. Dis.*

Lumeng, C.N., Bodzin, J.L., and Saltiel, A.R. (2007). Obesity induces a phenotypic switch in adipose tissue macrophage polarization. *J. Clin. Invest.*

Macedo, A.B.B., Sánchez-Arcila, J.C., Schubach, A.O., Mendonça, S.C.F., Marins-Dos-Santos, A., De Fatima Madeira, M., Gagini, T., Pimentel, M.I.F., and De Luca, P.M. (2012). Multifunctional CD4 +T cells in patients with American cutaneous leishmaniasis. *Clin. Exp. Immunol.*

Magnuson, B., Ekim, B., and Fingar, D.C. (2012). Regulation and function of ribosomal protein S6 kinase (S6K) within mTOR signalling networks. *Biochem. J.*

Marcos, A., Nova, E., and Montero, A. (2003). Changes in the immune system are conditioned by nutrition. *Eur. J. Clin. Nutr.* *57*, S66–S69.

Marhold, M., Tomasich, E., El-Gazzar, A., Heller, G., Spittler, A., Horvat, R., Krainer, M., and Horak, P. (2015). HIF1 $\alpha$  Regulates mTOR Signaling and Viability of Prostate Cancer Stem Cells. *Mol. Cancer Res.*

Márquez, J.D.R., Ana, Y., Baigorri, R.E., Stempi, C.C., and Cerban, F.M. (2018). Mammalian target of rapamycin inhibition in *Trypanosoma cruzi*-infected macrophages leads to an intracellular profile that is detrimental for infection. *Front. Immunol.*

Martinez, F.O., and Gordon, S. (2014). The M1 and M2 paradigm of macrophage activation: Time for reassessment. *F1000Prime Rep.*

Matte, C., Maion, G., Mourad, W., and Olivier, M. (2001). *Leishmania donovani*-induced macrophages cyclooxygenase-2 and prostaglandin E2 synthesis. *Parasite Immunol.*

Mayer, C.T., Ghorbani, P., Nandan, A., Dudek, M., Arnold-Schrauf, C., Hesse, C., Berod, L., Stüve, P., Puttur, F., Merad, M., et al. (2014). Selective and efficient generation of functional Batf3-dependent CD1031 dendritic cells from mouse bone marrow. *Blood.*

McConville, M.J., and Naderer, T. (2011). Metabolic pathways required for the intracellular survival of *Leishmania*. *Annu. Rev. Microbiol.* *65*, 543–561.

McConville, M.J., de Souza, D., Saunders, E., Likic, V.A., and Naderer, T. (2007). Living in a phagolysosome; metabolism of *Leishmania amastigotes*. *Trends Parasitol.* *23*, 368–375.

McConville, M.J., Saunders, E.C., Kloehn, J., and Dagley, M.J. (2015). Leishmania carbon metabolism in the macrophage phagolysosome- feast or famine? *F1000Research*.

McFarlane, E., Mokgethi, T., Kaye, P.M., Hurdal, R., Brombacher, F., Alexander, J., and Carter, K.C. (2019). IL-4 Mediated Resistance of BALB/c Mice to Visceral Leishmaniasis Is Independent of IL-4R $\alpha$  Signaling via T Cells. *Front. Immunol.* *10*.

McLane, L.M., Abdel-Hakeem, M.S., and Wherry, E.J. (2019). CD8 T Cell Exhaustion During Chronic Viral Infection and Cancer. *Annu. Rev. Immunol.*

Medina-Acosta, E., Karess, R.E., Schwartz, H., and Russell, D.G. (1989). The promastigote surface protease (gp63) of Leishmania is expressed but differentially processed and localized in the amastigote stage. *Mol. Biochem. Parasitol.*

Meier, C.L., Svensson, M., and Kaye, P.M. (2003). Leishmania -Induced Inhibition of Macrophage Antigen Presentation Analyzed at the Single-Cell Level . *J. Immunol.*

Mera-Ramírez, A., Castillo, A., Orobio, Y., Gómez, M.A., and Gallego-Marin, C. (2017). Screening of TNF $\alpha$ , IL-10 and TLR4 single nucleotide polymorphisms in individuals with asymptomatic and chronic cutaneous leishmaniasis in Colombia: a pilot study. *BMC Infect. Dis.*

Mesquita, I., and Rodrigues, F. (2018). Cellular Metabolism at a Glance. *Exp. Suppl.*

Mesquita, I., Varela, P., Belinha, A., Gaifem, J., Laforge, M., Vergnes, B., Estaquier, J., and Silvestre, R. (2016a). Exploring NAD<sup>+</sup> metabolism in host-pathogen interactions. *Cell. Mol. Life Sci.* *73*, 1225–1236.

Mesquita, I., Moreira, D., Sampaio-Marques, B., Laforge, M., Cordeiro-da-Silva, A., Ludovico, P., Estaquier, J., and Silvestre, R. (2016b). AMPK in Pathogens. *EXS* *107*.

Mesquita, I., Vergnes, B., and Silvestre, R. (2018a). Alterations on Cellular Redox States upon Infection and Implications for Host Cell Homeostasis. *Exp. Suppl.*

Mesquita, I., Ferreira, C., Barbosa, A.M., Ferreira, C.M., Moreira, D., Carvalho, A., Cunha, C., Rodrigues, F., Dinis-Oliveira, R.J., Estaquier, J., et al. (2018b). The impact of IL-10 dynamic modulation on host immune response against visceral leishmaniasis. *Cytokine*.

Mesquita, I., Ferreira, C., Moreira, D., Kluck, G.E.G., Barbosa, A.M., Torrado, E., Dinis-Oliveira, R.J., Gonçalves, L.G., Beauparlant, C.-J., Droit, A., et al. (2020). The Absence of HIF-1 $\alpha$  Increases Susceptibility to Leishmania donovani Infection via Activation of BNIP3/mTOR/SREBP-1c Axis. *Cell Rep.* *30*, 4052-4064.e7.

Mildner, A., and Jung, S. (2014). Development and function of dendritic cell subsets. *Immunity*.

Mills, C.D., Kincaid, K., Alt, J.M., Heilman, M.J., and Hill, A.M. (2000). M-1/M-2 Macrophages

and the Th1/Th2 Paradigm. *J. Immunol.*

Misumi, I., Starmer, J., Uchimura, T., Beck, M.A., Magnuson, T., and Whitmire, J.K. (2019). Obesity Expands a Distinct Population of T Cells in Adipose Tissue and Increases Vulnerability to Infection. *Cell Rep.*

Mohapatra, S., Ramakrishan, L., Samantaray, J., and Dash, S. (2014). Lipid derangement as diagnostic and prognostic indicator for visceral leishmaniasis patients. *Trop. Parasitol.*

Moore, K.W., Malefyt, R.D.W., Robert, L., and Garra, A.O. (2001). Interleukin -10 and the Interleukin -10 Receptor. *Mol. Cell. Biol.*

Moradin, N., and Descoteaux, A. (2012). *Leishmania* promastigotes: building a safe niche within macrophages. *Front. Cell. Infect. Microbiol.* 2.

Moreira, D., Rodrigues, V., Abengozar, M., Rivas, L., Rial, E., Laforge, M., Li, X., Foretz, M., Violet, B., Estaquier, J., et al. (2015). *Leishmania infantum* Modulates Host Macrophage Mitochondrial Metabolism by Hijacking the SIRT1-AMPK Axis. *PLoS Pathog.* 11, 1–24.

Moreira, D., Estaquier, J., Cordeiro-da-Silva, A., and Silvestre, R. (2018). Metabolic Crosstalk Between Host and Parasitic Pathogens. *Exp. Suppl.*

Morse, C.G., and High, K.P. (2014). Nutrition, Immunity, and Infection. In Mandell, Douglas, and Bennett's Principles and Practice of Infectious Diseases, pp. 125–133.

Mukherjee, M., Basu Ball, W., and Das, P.K. (2014). *Leishmania donovani* activates SREBP2 to modulate macrophage membrane cholesterol and mitochondrial oxidants for establishment of infection. *Int. J. Biochem. Cell Biol.*

Munder, M., Eichmann, K., and Modolell, M. (1998). Alternative metabolic states in murine macrophages reflected by the nitric oxide synthase/arginase balance: competitive regulation by CD4+ T cells correlates with Th1/Th2 phenotype. *J. Immunol.*

Munn, D.H., Shafizadeh, E., Attwood, J.T., Bondarev, I., Pashine, A., and Mellor, A.L. (1999). Inhibition of T cell proliferation by macrophage tryptophan catabolism. *J. Exp. Med.*

Murano, I., Barbatelli, G., Parisani, V., Latini, C., Muzzonigro, G., Castellucci, M., and Cinti, S. (2008). Dead adipocytes, detected as crown-like structures, are prevalent in visceral fat depots of genetically obese mice. *J. Lipid Res.*

Murray, P.J., Allen, J.E., Biswas, S.K., Fisher, E.A., Gilroy, D.W., Goerdt, S., Gordon, S., Hamilton, J.A., Ivashkiv, L.B., Lawrence, T., et al. (2014). Macrophage Activation and Polarization: Nomenclature and Experimental Guidelines. *Immunity* 41, 14–20.

Mylonis, I., Sembongi, H., Befani, C., Liakos, P., Siniossoglou, S., and Simos, G. (2012). Hypoxia

causes triglyceride accumulation by HIF-1-mediated stimulation of lipin 1 expression. *J. Cell Sci.*

Mylonis, I., Simos, G., and Paraskeva, E. (2019). Hypoxia-Inducible Factors and the Regulation of Lipid Metabolism. *Cells*.

Naderer, T., and McConville, M.J. (2008). The Leishmania-macrophage interaction: A metabolic perspective. *Cell. Microbiol.* *10*, 301–308.

Nagajyothi, F., Desruisseaux, M.S., Thiruvur, N., Weiss, L.M., Braunstein, V.L., Albanese, C., Teixeira, M.M., De Almeida, C.J., Lisanti, M.P., Scherer, P.E., et al. (2008). Trypanosoma cruzi Infection of cultured adipocytes results in an inflammatory phenotype. *Obesity*.

Nagy, C., and Haschemi, A. (2015). Time and demand are two critical dimensions of immunometabolism: The process of macrophage activation and the pentose phosphate pathway. *Front. Immunol.*

Nathan, C.F., and Hibbs, J.B. (1991). Role of nitric oxide synthesis in macrophage antimicrobial activity. *Curr. Opin. Immunol.*

Netea, M.G., Joosten, L.A.B., Latz, E., Mills, K.H.G., Natoli, G., Stunnenberg, H.G., O'Neill, L.A.J., and Xavier, R.J. (2016). Trained immunity: A program of innate immune memory in health and disease. *Science* (80- ).

Newsholme, P., Procopio, J., Ramos Lima, M.M., Pithon-Curi, T.C., and Curi, R. (2003). Glutamine and glutamate - Their central role in cell metabolism and function. *Cell Biochem. Funct.*

Nguyen, T.P., Frank, A.R., and Jewell, J.L. (2017). Amino acid and small GTPase regulation of mTORC1. *Cell. Logist.*

Nishi, K., Oda, T., Takabuchi, S., Oda, S., Fukuda, K., Adachi, T., Semenza, G.L., Shingu, K., and Hirota, K. (2008). LPS induces hypoxia-inducible factor 1 activation in macrophage- differentiated cells in a reactive oxygen species-dependent manner. *Antioxidants Redox Signal.*

Nishiyama, Y., Goda, N., Kanai, M., Niwa, D., Osanai, K., Yamamoto, Y., Senoo-Matsuda, N., Johnson, R.S., Miura, S., Kabe, Y., et al. (2012). HIF-1 $\alpha$  induction suppresses excessive lipid accumulation in alcoholic fatty liver in mice. *J. Hepatol.* *56*, 441–447.

Novais, F.O., and Scott, P. (2015). CD8+ T cells in cutaneous leishmaniasis: the good, the bad, and the ugly. *Semin. Immunopathol.*

O'Neill, H.M., Holloway, G.P., and Steinberg, G.R. (2013). AMPK regulation of fatty acid metabolism and mitochondrial biogenesis: Implications for obesity. *Mol. Cell. Endocrinol.* *366*, 135–151.

Owens, B.M.J., Beattie, L., Moore, J.W.J., Brown, N., Mann, J.L., Dalton, J.E., Maroof, A., and Kaye, P.M. (2012). IL-10-producing Th1 cells and disease progression are regulated by distinct CD11c<sup>+</sup> cell populations during visceral leishmaniasis. *PLoS Pathog.*

Papandreou, I., Cairns, R.A., Fontana, L., Lim, A.L., and Denko, N.C. (2006). HIF-1 mediates adaptation to hypoxia by actively downregulating mitochondrial oxygen consumption. *Cell Metab.*

Parihar, S.P., Guler, R., Khutlang, R., Lang, D.M., Hurdayal, R., Mhlanga, M.M., Suzuki, H., Marais, A.D., and Brombacher, F. (2014). Statin therapy reduces the mycobacterium tuberculosis burden in human macrophages and in mice by enhancing autophagy and phagosome maturation. *J. Infect. Dis.*

Parihar, S.P., Hartley, M.A., Hurdayal, R., Guler, R., and Brombacher, F. (2016). Topical Simvastatin as Host-Directed Therapy against Severity of Cutaneous Leishmaniasis in Mice. *Sci. Rep.*

Pauken, K.E., and Wherry, E.J. (2015). SnapShot: T Cell Exhaustion. *Cell* 163, 1038-1038e1.

Peckham-Gregory, E.C., Thapa, D.R., Martinson, J., Duggal, P., Penugonda, S., Bream, J.H., Chang, P.Y., Dandekar, S., Chang, S.C., Detels, R., et al. (2016). MicroRNA-related polymorphisms and non-Hodgkin lymphoma susceptibility in the Multicenter AIDS Cohort Study. *Cancer Epidemiol.*

Ponte-Sucre, A., Gamarro, F., Dujardin, J.C., Barrett, M.P., López-Vélez, R., García-Hernández, R., Pountain, A.W., Mwenechanya, R., and Papadopoulou, B. (2017). Drug resistance and treatment failure in leishmaniasis: A 21st century challenge. *PLoS Negl. Trop. Dis.*

Porstmann, T., Santos, C.R., Griffiths, B., Cully, M., Wu, M., Leever, S., Griffiths, J.R., Chung, Y.L., and Schulze, A. (2008). SREBP Activity Is Regulated by mTORC1 and Contributes to Akt-Dependent Cell Growth. *Cell Metab.*

Potter, M., Newport, E., and Morten, K.J. (2016). The Warburg effect: 80 years on. *Biochem. Soc. Trans.*

Pucadyil, T.J., and Chattopadhyay, A. (2007). Cholesterol: a potential therapeutic target in *Leishmania* infection? *Trends Parasitol.* 23, 49–53.

Pucadyil, T.J., Tewary, P., Madhubala, R., and Chattopadhyay, A. (2004). Cholesterol is required for *Leishmania donovani* infection: Implications in leishmaniasis. *Mol. Biochem. Parasitol.*

Qiu, B., Ackerman, D., Sanchez, D.J., Li, B., Ochocki, J.D., Grazioli, A., Bobrovnikova-Marjon, E., Alan Diehl, J., Keith, B., and Celeste Simon, M. (2016). HIF2 $\alpha$ -dependent lipid storage promotes endoplasmic reticulum homeostasis in clear-cell renal cell carcinoma. *Cancer Discov.*



Rabhi, S., Rabhi, I., Trentin, B., Piquemal, D., Regnault, B., Goyard, S., Lang, T., Descoteaux, A., Enninga, J., and Guizani-Tabbane, L. (2016). Lipid droplet formation, their localization and dynamics during leishmania major macrophage infection. *PLoS One* *11*.

Ramasawmy, R., Menezes, E., Magalhães, A., Oliveira, J., Castellucci, L., Almeida, R., Rosa, M.E.A., Guimarães, L.H., Lessa, M., Noronha, E., et al. (2010). The -2518bp promoter polymorphism at CCL2/MCP1 influences susceptibility to mucosal but not localized cutaneous leishmaniasis in Brazil. *Infect. Genet. Evol.* *10*, 607–613.

Rankin, E.B., Rha, J., Selak, M.A., Unger, T.L., Keith, B., Liu, Q., and Haase, V.H. (2009). Hypoxia-Inducible Factor 2 Regulates Hepatic Lipid Metabolism. *Mol. Cell. Biol.* *29*, 4527–4538.

Rath, M., Müller, I., Kropf, P., Closs, E.I., and Munder, M. (2014). Metabolism via arginase or nitric oxide synthase: Two competing arginine pathways in macrophages. *Front. Immunol.*

Reiner, S.L., Zheng, S., Wang, Z.E., Stowring, L., and Locksley, R.M. (1994). Leishmania promastigotes evade interleukin 12 (IL-12) induction by macrophages and stimulate a broad range of cytokines from CD4 + T Cells during Initiation of Infection. *J. Exp. Med.*

Resende, M., Moreira, D., Augusto, J., Cunha, J., Neves, B., Cruz, M.T., Estaquier, J., Cordeiro-da-Silva, A., and Silvestre, R. (2013). Leishmania-Infected MHC Class IIhigh Dendritic Cells Polarize CD4+ T Cells toward a Nonprotective T-bet+ IFN- + IL-10+ Phenotype. *J. Immunol.* *191*, 262–273.

Rey, S., Luo, W., Shimoda, L.A., and Semenza, G.L. (2011). Metabolic reprogramming by HIF-1 promotes the survival of bone marrow-derived angiogenic cells in ischemic tissue. *Blood*.

Del Rey, M.J., Valín, Á., Usategui, A., García-Herrero, C.M., Sánchez-Aragó, M., Cuezva, J.M., Galindo, M., Bravo, B., Cañete, J.D., Blanco, F.J., et al. (2017). Hif-1 $\alpha$  Knockdown Reduces Glycolytic Metabolism and Induces Cell Death of Human Synovial Fibroblasts under Normoxic Conditions. *Sci. Rep.*

Rhodes, J.W., Tong, O., Harman, A.N., and Turville, S.G. (2019). Human dendritic cell subsets, ontogeny, and impact on HIV infection. *Front. Immunol.*

Riffelmacher, T., Clarke, A., Richter, F.C., Stranks, A., Pandey, S., Danielli, S., Hublitz, P., Yu, Z., Johnson, E., Schwerd, T., et al. (2017). Autophagy-Dependent Generation of Free Fatty Acids Is Critical for Normal Neutrophil Differentiation. *Immunity*.

Rittig, M.G., and Bogdan, C. (2000). Leishmania-host-cell interaction: Complexities and alternative views. *Parasitol. Today*.

Roberts, M.T.M. (2005). Current understandings on the immunology of leishmaniasis and recent

developments in prevention and treatment. *Br. Med. Bull.*

Rodríguez-Espinosa, O., Rojas-Espinosa, O., Moreno-Altamirano, M.M.B., López-Villegas, E.O., and Sánchez-García, F.J. (2015). Metabolic requirements for neutrophil extracellular traps formation. *Immunology*.

Rodriguez, P.C., Zea, A.H., DeSalvo, J., Culotta, K.S., Zabaleta, J., Quiceno, D.G., Ochoa, J.B., and Ochoa, A.C. (2003). L-Arginine Consumption by Macrophages Modulates the Expression of CD3 $\zeta$  Chain in T Lymphocytes. *J. Immunol.*

Rodríguez, N.E., Lockard, R.D., Turcotte, E.A., Araújo-Santos, T., Bozza, P.T., Borges, V.M., and Wilson, M.E. (2017). Lipid bodies accumulation in *Leishmania infantum*-infected C57BL/6 macrophages. *Parasite Immunol.* 39.

Rogers, M., Kropf, P., Choi, B.S., Dillon, R., Podinovskaia, M., Bates, P., and Müller, I. (2009). Proteophosphoglycans regurgitated by *Leishmania*-infected sand flies target the L-arginine metabolism of host macrophages to promote parasite survival. *PLoS Pathog.*

Roy, K., Mandloi, S., Chakrabarti, S., and Roy, S. (2016). Cholesterol Corrects Altered Conformation of MHC-II Protein in *Leishmania donovani* Infected Macrophages: Implication in Therapy. *PLoS Negl. Trop. Dis.*

Russo, L., and Lumeng, C.N. (2018). Properties and functions of adipose tissue macrophages in obesity. *Immunology*.

Sacks, D., and Noben-Trauth, N. (2002). The immunology of susceptibility and resistance to *Leishmania major* in mice. *Nat. Rev. Immunol.*

Saeidi, A., Zandi, K., Cheok, Y.Y., Saeidi, H., Wong, W.F., Lee, C.Y.Q., Cheong, H.C., Yong, Y.K., Larsson, M., and Shankar, E.M. (2018). T-cell exhaustion in chronic infections: Reversing the state of exhaustion and reinvigorating optimal protective immune responses. *Front. Immunol.*

Sag, D., Carling, D., Stout, R.D., and Suttles, J. (2008). Adenosine 5'-Monophosphate-Activated Protein Kinase Promotes Macrophage Polarization to an Anti-Inflammatory Functional Phenotype. *J. Immunol.*

Saha, A., Biswas, A., Srivastav, S., Mukherjee, M., Das, P.K., and Ukil, A. (2014). Prostaglandin E<sub>2</sub> Negatively Regulates the Production of Inflammatory Cytokines/Chemokines and IL-17 in Visceral Leishmaniasis. *J. Immunol.*

Said, E.A., Dupuy, F.P., Trautmann, L., Zhang, Y., Shi, Y., El-Far, M., Hill, B.J., Noto, A., Ancuta, P., Peretz, Y., et al. (2010). Programmed death-1-induced interleukin-10 production by monocytes impairs CD4 + T cell activation during HIV infection. *Nat. Med.*

Saini, S., Singh, B., Prakash, S., Kumari, S., Kureel, A.K., Dube, A., Sahasrabudde, A.A., and Rai, A.K. (2020). Parasitic load determination by differential expressions of 5-lipoxygenase and PGE2 synthases in visceral leishmaniasis. *Prostaglandins Other Lipid Mediat.*

Salceda, S., and Caro, J. (1997). Hypoxia-inducible factor 1 $\alpha$  (HIF-1 $\alpha$ ) protein is rapidly degraded by the ubiquitin-proteasome system under normoxic conditions. Its stabilization by hypoxia depends on redox-induced changes. *J. Biol. Chem.*

Salhi, A., Rodrigues, V., Santoro, F., Dessein, H., Romano, A., Castellano, L.R., Sertorio, M., Rafati, S., Chevillard, C., Prata, A., et al. (2008). Immunological and Genetic Evidence for a Crucial Role of IL-10 in Cutaneous Lesions in Humans Infected with *Leishmania braziliensis*. *J. Immunol.*

Sancak, Y., Peterson, T.R., Shaul, Y.D., Lindquist, R.A., Thoreen, C.C., Bar-Peled, L., and Sabatini, D.M. (2008). The rag GTPases bind raptor and mediate amino acid signaling to mTORC1. *Science* (80- ).

Sarnáglia, G.D., Covre, L.P., Pereira, F.E.L., De Matos Guedes, H.L., Faria, A.M.C., Dietze, R., Rodrigues, R.R., Maioli, T.U., and Gomes, D.C.O. (2016). Diet-induced obesity promotes systemic inflammation and increased susceptibility to murine visceral leishmaniasis. *Parasitology* *143*, 1647–1655.

Satoskar, A., Bluethmann, H., and Alexander, J. (1995). Disruption of the murine interleukin-4 gene inhibits disease progression during *Leishmania mexicana* infection but does not increase control of *Leishmania donovani* infection. *Infect. Immun.*

Sawant, D. V., Yano, H., Chikina, M., Zhang, Q., Liao, M., Liu, C., Callahan, D.J., Sun, Z., Sun, T., Tabib, T., et al. (2019). Adaptive plasticity of IL-10<sup>+</sup> and IL-35<sup>+</sup> Treg cells cooperatively promotes tumor T cell exhaustion. *Nat. Immunol.*

Saxton, R.A., Chantranupong, L., Knockenhauer, K.E., Schwartz, T.U., and Sabatini, D.M. (2016). Mechanism of arginine sensing by CASTOR1 upstream of mTORC1. *Nature.*

Scharton-Kersten, T., Afonso, L.C., Wysocka, M., Trinchieri, G., and Scott, P. (1995). IL-12 is required for natural killer cell activation and subsequent T helper 1 cell development in experimental leishmaniasis. *J. Immunol.*

Schurich, A., Pallett, L.J., Jajbhay, D., Wijngaarden, J., Otano, I., Gill, U.S., Hansi, N., Kennedy, P.T., Nastouli, E., Gilson, R., et al. (2016). Distinct Metabolic Requirements of Exhausted and Functional Virus-Specific CD8 T Cells in the Same Host. *Cell Rep.*

Schwarz, T., Remer, K.A., Nahrendorf, W., Masic, A., Siewe, L., Müller, W., Roers, A., and Moll,

H. (2013). T Cell-Derived IL-10 Determines Leishmaniasis Disease Outcome and Is Suppressed by a Dendritic Cell Based Vaccine. *PLoS Pathog.*

Seçmeer, G., Cengiz, A.B., Gürgey, A., Kara, A., Cultu, O., Tavit, B., and Devrim, I. (2006). Hypertriglyceridemia and decreased high-density lipoprotein could be a clue for visceral leishmaniasis. *Infect. Dis. Clin. Pract.*

Semini, G., Paape, D., Paterou, A., Schroeder, J., Barrios-Llerena, M., and Aebischer, T. (2017). Changes to cholesterol trafficking in macrophages by Leishmania parasites infection. *Microbiologyopen* 6.

Seo, J.W., Yang, E.J., Yoo, K.H., and Choi, I.H. (2015). Macrophage differentiation from monocytes is influenced by the lipid oxidation degree of low density lipoprotein. *Mediators Inflamm.*

Serrano, P.E., Khuder, S.A., and Fath, J.J. (2010). Obesity as a Risk Factor for Nosocomial Infections in Trauma Patients. *J. Am. Coll. Surg.* 211, 61–67.

Shahi, M., Mohajery, M., Shamsian, S.A.A., Nahrevanian, H., and Yazdanpanah, S.M.J. (2013). Comparison of Th1 and Th2 responses in non-healing and healing patients with cutaneous leishmaniasis. *Reports Biochem. Mol. Biol.*

Shaw, R.J., Kosmatka, M., Bardeesy, N., Hurley, R.L., Witters, L.A., DePinho, R.A., and Cantley, L.C. (2004). The tumor suppressor LKB1 kinase directly activates AMP-activated kinase and regulates apoptosis in response to energy stress. *Proc. Natl. Acad. Sci. U. S. A.*

Sher, A., Pearce, E., and Kaye, P. (2003). Shaping the immune response to parasites: Role of dendritic cells. *Curr. Opin. Immunol.*

Shirzadi, M.R. (2019). <p>Lipsosomal amphotericin B: a review of its properties, function, and use for treatment of cutaneous leishmaniasis</p>. *Res. Rep. Trop. Med.*

Silva, F.C., Martins, V.D., Caixeta, F., Baptista Carneiro, M., Ribeiro Goes, G., Paiva, N.C., Carneiro, C.M., Vieira, L.Q., Faria, A.M.C., and Maioli, T.U. (2018). Obesity impairs resistance to *Leishmania major* infection in C57BL/6 mice. *BioRxiv.*

Singer, K., DelProposto, J., Lee Morris, D., Zamarron, B., Mergian, T., Maley, N., Cho, K.W., Geletka, L., Subbaiah, P., Muir, L., et al. (2014). Diet-induced obesity promotes myelopoiesis in hematopoietic stem cells. *Mol. Metab.* 3, 664–675.

Smith, C.W. (2007). Diet and leukocytes. *Am. J. Clin. Nutr.* 86, 1257–1258.

Smith, A.G., Sheridan, P.A., Harp, J.B., and Beck, M.A. (2007). Diet-induced obese mice have increased mortality and altered immune responses when infected with influenza virus. *J. Nutr.*

137, 1236–1243.

Smith, L.K., Boukhaled, G.M., Condotta, S.A., Mazouz, S., Guthmiller, J.J., Vijay, R., Butler, N.S., Bruneau, J., Shoukry, N.H., Krawczyk, C.M., et al. (2018a). Interleukin-10 Directly Inhibits CD8+ T Cell Function by Enhancing N-Glycan Branching to Decrease Antigen Sensitivity. *Immunity*.

Smith, L.K., Boukhaled, G.M., Condotta, S.A., Mazouz, S., Guthmiller, J.J., Vijay, R., Butler, N.S., Bruneau, J., Shoukry, N.H., Krawczyk, C.M., et al. (2018b). Interleukin-10 Directly Inhibits CD8+ T Cell Function by Enhancing N-Glycan Branching to Decrease Antigen Sensitivity. *Immunity* 48, 299-312.e5.

Speakman, J.R. (2019). Use of high-fat diets to study rodent obesity as a model of human obesity. *Int. J. Obes.*

Spirig, R., Djafarzadeh, S., Regueira, T., Shaw, S.G., von Garnier, C., Takala, J., Jakob, S.M., Rieben, R., and Lepper, P.M. (2010). Effects of TLR Agonists on the Hypoxia-Regulated Transcription Factor HIF-1 $\alpha$  and Dendritic Cell Maturation under Normoxic Conditions. *PLoS One* 5, e10983.

Stäger, S., Alexander, J., Carter, K.C., Brombacher, F., and Kaye, P.M. (2003). Both interleukin-4 (IL-4) and IL-4 receptor  $\alpha$  signaling contribute to the development of hepatic granulomas with optimal antileishmanial activity. *Infect. Immun.*

Staron, M.M., Gray, S.M., Marshall, H.D., Parish, I.A., Chen, J.H., Perry, C.J., Cui, G., Li, M.O., and Kaech, S.M. (2014). The Transcription Factor FoxO1 Sustains Expression of the Inhibitory Receptor PD-1 and Survival of Antiviral CD8+ T Cells during Chronic Infection. *Immunity*.

Stein, M., Keshav, S., Harris, N., and Gordon, S. (1992). Interleukin 4 potently enhances murine macrophage mannose receptor activity: A marker of alternative immunologic macrophage activation. *J. Exp. Med.*

Stern, J.J., Oca, M.J., Rubin, B.Y., Anderson, S.L., and Murray, H.W. (1988). Role of L3T4+ and Lyt-2+ cells in experimental visceral leishmaniasis. *J. Immunol.*

Steverding, D. (2017). The history of leishmaniasis. *Parasites and Vectors*.

Sundar, S., and Jaya, J. (2010). Liposomal amphotericin B and leishmaniasis: Dose and response. *J. Glob. Infect. Dis.*

Talker, S.C., Koinig, H.C., Stadler, M., Graage, R., Klingler, E., Ladinig, A., Mair, K.H., Hammer, S.E., Weissenböck, H., Dürrwald, R., et al. (2015). Magnitude and kinetics of multifunctional CD4+ and CD8 $\beta$ + T cells in pigs infected with swine influenza A virus. *Vet. Res.*

Tanowitz, H.B., Scherer, P.E., Mota, M.M., and Figueiredo, L.M. (2017). Adipose Tissue: A Safe

Haven for Parasites? *Trends Parasitol.* *33*, 276–284.

Teixeira, C., Gomes, R., Oliveira, F., Meneses, C., Gilmore, D.C., Elnaiem, D.E.A., Valenzuela, J.G., and Kamhawi, S. (2014). Characterization of the Early Inflammatory Infiltrate at the Feeding Site of Infected Sand Flies in Mice Protected from Vector-Transmitted *Leishmania major* by Exposure to Uninfected Bites. *PLoS Negl. Trop. Dis.*

Teixeira, L., Moreira, J., Melo, J., Bezerra, F., Marques, R.M., Ferreirinha, P., Correia, A., Monteiro, M.P., Ferreira, P.G., and Vilanova, M. (2015). Immune response in the adipose tissue of lean mice infected with the protozoan parasite *Neospora caninum*. *Immunology* *145*, 242–257.

Tewary, P., Veena, K., Pucadyil, T.J., Chattopadhyay, A., and Madhubala, R. (2006). The sterol-binding antibiotic nystatin inhibits entry of non-opsonized *Leishmania donovani* into macrophages. *Biochem. Biophys. Res. Commun.*

Thwe, P.M., Pelgrom, L., Cooper, R., Beauchamp, S., Reisz, J.A., D'Alessandro, A., Everts, B., and Amiel, E. (2017). Cell-Intrinsic Glycogen Metabolism Supports Early Glycolytic Reprogramming Required for Dendritic Cell Immune Responses. *Cell Metab.*

Trautmann, L., Janbazian, L., Chomont, N., Said, E.A., Gimmig, S., Bessette, B., Boulassel, M.R., Delwart, E., Sepulveda, H., Balderas, R.S., et al. (2006). Upregulation of PD-1 expression on HIV-specific CD8<sup>+</sup> T cells leads to reversible immune dysfunction. *Nat. Med.*

Trottier, M.D., Naaz, A., Li, Y., and Fraker, P.J. (2012). Enhancement of hematopoiesis and lymphopoiesis in diet-induced obese mice. *Proc. Natl. Acad. Sci.* *109*, 7622–7629.

Tsagozis, P., Karagouni, E., and Dotsika, E. (2003). CD8<sup>+</sup> T cells with parasite-specific cytotoxic activity and a Tc1 profile of cytokine and chemokine secretion develop in experimental visceral leishmaniasis. *Parasite Immunol.*

Tsagozis, P., Karagouni, E., and Dotsika, E. (2005). Function of CD8<sup>+</sup> T lymphocytes in a self-curing mouse model of visceral leishmaniasis. *Parasitol. Int.*

Veglia, F., Tyurin, V.A., Mohammadyani, D., Blasi, M., Duperret, E.K., Donthireddy, L., Hashimoto, A., Kapralov, A., Amoscato, A., Angelini, R., et al. (2017). Lipid bodies containing oxidatively truncated lipids block antigen cross-presentation by dendritic cells in cancer. *Nat. Commun.* *8*.

Viola, A., Munari, F., Sánchez-Rodríguez, R., Scolaro, T., and Castegna, A. (2019). The Metabolic Signature of Macrophage Responses. *Front. Immunol.*

Wang, F., Zhang, S., Vuckovic, I., Jeon, R., Lerman, A., Folmes, C.D., Dzeja, P.P., and Herrmann,

J. (2018). Glycolytic Stimulation Is Not a Requirement for M2 Macrophage Differentiation. *Cell Metab.*

Wang, S., Tsun, Z.Y., Wolfson, R.L., Shen, K., Wyant, G.A., Plovanich, M.E., Yuan, E.D., Jones, T.D., Chantranupong, L., Comb, W., et al. (2015). Lysosomal amino acid transporter SLC38A9 signals arginine sufficiency to mTORC1. *Science* (80-. ).

Wang, T., Liu, H., Lian, G., Zhang, S.Y., Wang, X., and Jiang, C. (2017). HIF1  $\alpha$ -Induced Glycolysis Metabolism Is Essential to the Activation of Inflammatory Macrophages. *Mediators Inflamm.*

Wang, X., Ren, H., Zhao, T., Ma, W., Dong, J., Zhang, S., Xin, W., Yang, S., Jia, L., and Hao, J. (2016). Single nucleotide polymorphism in the microRNA-199a binding site of HIF1A gene is associated with pancreatic ductal adenocarcinoma risk and worse clinical outcomes. *Oncotarget* 7.

Wculek, S.K., Khouili, S.C., Priego, E., Heras-Murillo, I., and Sancho, D. (2019). Metabolic Control of Dendritic Cell Functions: Digesting Information. *Front. Immunol.*

Weisberg, S.P., McCann, D., Desai, M., Rosenbaum, M., Leibel, R.L., and Ferrante, A.W. (2003). Obesity is associated with macrophage accumulation in adipose tissue. *J. Clin. Invest.* 112, 1796–1808.

Welte, M.A., and Gould, A.P. (2017). Lipid droplet functions beyond energy storage. *Biochim. Biophys. Acta - Mol. Cell Biol. Lipids.*

Werth, N., Beerlage, C., Rosenberger, C., Yazdi, A.S., Edelmann, M., Amr, A., Bernhardt, W., von Eiff, C., Becker, K., Schäfer, A., et al. (2010). Activation of hypoxia inducible factor 1 is a general phenomenon in infections with human pathogens. *PLoS One* 5.

Wherry, E.J. (2011). T cell exhaustion. *Nat. Immunol.*

Wherry, E.J., and Kurachi, M. (2015a). Molecular and cellular insights into T cell exhaustion. *Nat. Rev. Immunol.* 15, 486–499.

Wherry, E.J., and Kurachi, M. (2015b). Molecular and cellular insights into T cell exhaustion. *Nat. Rev. Immunol.*

Wherry, E.J., Blattman, J.N., Murali-Krishna, K., van der Most, R., and Ahmed, R. (2003). Viral Persistence Alters CD8 T-Cell Immunodominance and Tissue Distribution and Results in Distinct Stages of Functional Impairment. *J. Virol.*

WHO (2010). Control of the Leishmaniasis. World Health Organization, Geneva. Tech Rep Ser 949, 22–26.

WHO (2012). Recommended treatment regimens for visceral leishmaniasis. Who 5.

WHO (2018). WHO | Obesity and overweight.

Wieland, C.W., Florquin, S., Chan, E.D., Leemans, J.C., Weijer, S., Verbon, A., Fantuzzi, G., and van der Poll, T. (2005). Pulmonary Mycobacterium tuberculosis infection in leptin-deficient ob/ob mice. *Int. Immunol.* *17*, 1399–1408.

Williams, N.C., and O'Neill, L.A.J. (2018). A role for the krebs cycle intermediate citrate in metabolic reprogramming in innate immunity and inflammation. *Front. Immunol.*

Winberg, M.E., Holm, Å., Särndahl, E., Vinet, A.F., Descoteaux, A., Magnusson, K.E., Rasmusson, B., and Lerm, M. (2009). Leishmania donovani lipophosphoglycan inhibits phagosomal maturation via action on membrane rafts. *Microbes Infect.*

Wolfson, R.L., and Sabatini, D.M. (2017). The Dawn of the Age of Amino Acid Sensors for the mTORC1 Pathway. *Cell Metab.* *26*, 301–309.

Woods, A., Johnstone, S.R., Dickerson, K., Leiper, F.C., Fryer, L.G.D., Neumann, D., Schlattner, U., Wallimann, T., Carlson, M., and Carling, D. (2003). LKB1 Is the Upstream Kinase in the AMP-Activated Protein Kinase Cascade. *Curr. Biol.*

Wu, L.-F., Xu, G.-P., Zhao, Q., Zhou, L.-J., Wang, D., and Chen, W.-X. (2019). The association between hypoxia inducible factor 1 subunit alpha gene rs2057482 polymorphism and cancer risk: a meta-analysis. *BMC Cancer* *19*, 1123.

Wu, N., Zheng, B., Shaywitz, A., Dagon, Y., Tower, C., Bellinger, G., Shen, C.H., Wen, J., Asara, J., McGraw, T.E., et al. (2013). AMPK-Dependent Degradation of TXNIP upon Energy Stress Leads to Enhanced Glucose Uptake via GLUT1. *Mol. Cell.*

Xu, X., Grijalva, A., Skowronski, A., Van Eijk, M., Serlie, M.J., and Ferrante, A.W. (2013). Obesity activates a program of lysosomal-dependent lipid metabolism in adipose tissue macrophages independently of classic activation. *Cell Metab.* *18*, 816–830.

Yamaguchi, S., Katahira, H., Ozawa, S., Nakamichi, Y., Tanaka, T., Shimoyama, T., Takahashi, K., Yoshimoto, K., Imaizumi, M.O., Nagamatsu, S., et al. (2005). Activators of AMP-activated protein kinase enhance GLUT4 translocation and its glucose transport activity in 3T3-L1 adipocytes. *Am. J. Physiol. - Endocrinol. Metab.*

Yao, C., and Wilson, M.E. (2016). Dynamics of sterol synthesis during development of Leishmania spp. parasites to their virulent form. *Parasites and Vectors.*

Yao, C.H., Fowle-Grider, R., Mahieu, N.G., Liu, G.Y., Chen, Y.J., Wang, R., Singh, M., Potter, G.S., Gross, R.W., Schaefer, J., et al. (2016). Exogenous Fatty Acids Are the Preferred Source of



Membrane Lipids in Proliferating Fibroblasts. *Cell Chem. Biol.* 23, 483–493.

Zajac, A.J., Blattman, J.N., Murali-Krishna, K., Sourdive, D.J.D., Suresh, M., Altman, J.D., and Ahmed, R. (1998). Viral immune evasion due to persistence of activated T cells without effector function. *J. Exp. Med.*

van Zandbergen, G., Klinger, M., Mueller, A., Dannenberg, S., Gebert, A., Solbach, W., and Laskay, T. (2004). Cutting Edge: Neutrophil Granulocyte Serves as a Vector for Leishmania Entry into Macrophages. *J. Immunol.*

Zhang, L., and Romero, P. (2018). Metabolic Control of CD8+ T Cell Fate Decisions and Antitumor Immunity. *Trends Mol. Med.*

Zhang, L.J., Guerrero-Juarez, C.F., Hata, T., Bapat, S.P., Ramos, R., Plikus, M. V., and Gallo, R.L. (2015). Dermal adipocytes protect against invasive *Staphylococcus aureus* skin infection. *Science* (80- ).

Zhu, Y.P., Brown, J.R., Sag, D., Zhang, L., and Suttles, J. (2015). Adenosine 5'-Monophosphate-Activated Protein Kinase Regulates IL-10-Mediated Anti-Inflammatory Signaling Pathways in Macrophages. *J. Immunol.*

Zoncu, R., Bar-Peled, L., Efeyan, A., Wang, S., Sancak, Y., and Sabatini, D.M. (2011). mTORC1 senses lysosomal amino acids through an inside-out mechanism that requires the vacuolar H<sup>+</sup>-ATPase. *Science* (80- ).

Zuniga, E.I., and Harker, J.A. (2012). T-cell exhaustion due to persistent antigen: Quantity not quality? *Eur. J. Immunol.* 42, 2285–2289.